

INFORMATION TO USERS

This manuscript has been reproduced from the microfilm master. UMI films the text directly from the original or copy submitted. Thus, some thesis and dissertation copies are in typewriter face, while others may be from any type of computer printer.

The quality of this reproduction is dependent upon the quality of the copy submitted. Broken or indistinct print, colored or poor quality illustrations and photographs, print bleedthrough, substandard margins, and improper alignment can adversely affect reproduction.

In the unlikely event that the author did not send UMI a complete manuscript and there are missing pages, these will be noted. Also, if unauthorized copyright material had to be removed, a note will indicate the deletion.

Oversize materials (e.g., maps, drawings, charts) are reproduced by sectioning the original, beginning at the upper left-hand corner and continuing from left to right in equal sections with small overlaps. Each original is also photographed in one exposure and is included in reduced form at the back of the book.

Photographs included in the original manuscript have been reproduced xerographically in this copy. Higher quality 6" x 9" black and white photographic prints are available for any photographs or illustrations appearing in this copy for an additional charge. Contact UMI directly to order.

UMI

A Bell & Howell Information Company
300 North Zeeb Road, Ann Arbor MI 48106-1346 USA
313/761-4700 800/521-0600

NOTE TO USERS

The original manuscript received by UMI contains broken or light print. All efforts were made to acquire the highest quality manuscript from the author or school. Page(s) were microfilmed as received.

This reproduction is the best copy available

UMI



**THE PHOTOCHEMISTRY OF
SUBSTITUTED POLY(ACRYLOPHENONES)**

by

Michelle Marie Delaney-Luu ©

An M. Sc. thesis submitted to the Department of Chemistry in partial fulfillment
of the requirements for admittance to the Degree of Master of Science

Lakehead University

Thunder Bay, Ontario, Canada

June, 1998



National Library
of Canada

Acquisitions and
Bibliographic Services

395 Wellington Street
Ottawa ON K1A 0N4
Canada

Bibliothèque nationale
du Canada

Acquisitions et
services bibliographiques

395, rue Wellington
Ottawa ON K1A 0N4
Canada

Your file Votre référence

Our file Notre référence

The author has granted a non-exclusive licence allowing the National Library of Canada to reproduce, loan, distribute or sell copies of this thesis in microform, paper or electronic formats.

The author retains ownership of the copyright in this thesis. Neither the thesis nor substantial extracts from it may be printed or otherwise reproduced without the author's permission.

L'auteur a accordé une licence non exclusive permettant à la Bibliothèque nationale du Canada de reproduire, prêter, distribuer ou vendre des copies de cette thèse sous la forme de microfiche/film, de reproduction sur papier ou sur format électronique.

L'auteur conserve la propriété du droit d'auteur qui protège cette thèse. Ni la thèse ni des extraits substantiels de celle-ci ne doivent être imprimés ou autrement reproduits sans son autorisation.

0-612-33362-0

Canada

ACKNOWLEDGMENTS

I would like to express my most sincere appreciation to Dr. N.A. Weir for both his support and advice throughout my degree. I would also like to thank my husband, Hao, and my son, Brandon, for their understanding and support during my studies. I would like to thank Dr. J. Arct and Dr. Barabara Arct for synthesizing the polymers and for assistance in the laboratory. I also wish to thank Mr. K. Prignitz for his assistance in the instrument laboratory and the technical staff of the Faculty of Science with special reference to Mr. A. Bharath for his technical assistance.

In addition, I gratefully acknowledge the generous support by the Centres of Excellence (Mechanical and Chemi-Mechanical Pulps Network).

ABSTRACT

Dilute solutions of poly(p-ethoxyacrylophenone) (PEAP) and thin films of poly(p-methoxyacrylophenone) (PMAP), poly(3,4-dimethoxyacrylophenone) (P34DMAP), poly(3,5-dimethoxyacrylophenone) and PEAP were exposed to long-wave UV radiation ($\lambda \geq 300\text{nm}$, degassed). Due to rapid intersystem crossing, photoreactions occurred primarily from the excited triplet state of the carbonyl. The introduction of electron-donating methoxy and ethoxy groups resulted in the formation of low-lying π, π^* triplets, photophysical data being congruent with this. Low molecular weight product evolution of PEAP gave ethane, ethylene and butane, which is consistent with $\text{O-CH}_2\text{CH}_3$ fission. $\text{O-CH}_2\text{CH}_3$ fission results in the formation of phenoxy radicals which are presumed to be the precursors of quinonoid formation whose presence is consistent with spectroscopic data. The principal mode of degradation, random chain scission, is associated with a Norrish type II decomposition. Quenching of PEAP in solution by naphthalene and cis-1,3-pentadiene caused a decrease in chain scission and conformed to Stern-Volmer kinetics. Quenching of PMAP, P34DMAP, P35DMAP and PEAP by naphthalene and cis-1,3-pentadiene (0.34-7.0(w/w) percent) in thin film produced an increase in random chain scission. However, quenching by naphthalene and cis-1,3-pentadiene in the range of 50-100(w/w) percent caused a decrease in random chain scission and the data conformed to the Perrin rate law. Direct triplet quenching of PMAP, P34DMAP, P35DMAP and PEAP at 77K also conformed to Perrin kinetics. The effect on chain scission of PMAP in solution by light absorbers, Tinuvin 327 and Tinuvin 900, showed that these light absorbers also act as quenchers because they conform to Stern-Volmer kinetics.

TABLE OF CONTENTS

A. INTRODUCTION	1
I/ PHOTOCHEMISTRY	1
II/ PHOTOPHYSICAL DEACTIVATION OF AN EXCITED MOLECULE	3
1. INTERMOLECULAR ENERGY TRANSFER	3
2. INTRAMOLECULAR ENERGY TRANSFER	6
(a) INTERNAL CONVERSION (IC)	6
(b) INTERSYSTEM CROSSING (ISC)	7
(c) VIBRATIONAL RELAXATION (VR)	7
3. LUMINESCENCE	7
(a) FLUORESCENCE	8
(b) PHOSPHORESCENCE	8
(c) DELAYED FLUORESCENCE	10
4. PHYSICAL QUENCHING	11
III/ PHOTOCHEMICAL DEACTIVATION OF AN EXCITED MOLECULE	12
1. DISSOCIATION	12
2. INTERMOLECULAR REACTIONS	12
3. INTRAMOLECULAR REACTIONS	12
4. ISOMERIZATION	13
IV/ KINETICS OF PHOTOCHEMISTRY	13
1. PHOTOPHYSICAL PROCESSES	13
2. PHOTOCHEMICAL PROCESSES	14
V/ PHOTOPHYSICS OF KETONE-CONTAINING POLYMERS	16
VI/ PHOTOCHEMISTRY OF KETONE-CONTAINING POLYMERS	19
1. NORRISH TYPE I REACTION	19
(a) THE NATURE AND CHARACTER OF THE CARBONYL GROUP	20
(b) THE NATURE OF THE MEDIUM	21
2. SECONDARY PROCESSES	21
3. NORRISH TYPE II REACTION	21
4. REACTIONS THAT OCCUR IN THE ABSENCE OF γ -HYDROGENS ...	29
VII/ SOLUTION VERSUS SOLID STATE PHOTODEGRADATION	30
VIII/ PREVIOUS STUDIES OF POLY(ACRYLOPHENONES)	31

B. PURPOSE	36
C. EXPERIMENTAL	38
I/ POLYMER PREPARATION	38
II/ POLYMER CHARACTERIZATION	39
1. INFRARED (IR) SPECTRAL CHARACTERISTICS	39
2. NUCLEAR MAGNETIC RESONANCE (NMR) SPECTRAL CHARACTERISTICS	39
3. ULTRAVIOLET (UV) SPECTRAL CHARACTERISTICS	39
4. EMISSION CHARACTERISTICS	40
III/ PHOTOCHEMICAL TECHNIQUES IN SOLUTION	40
IV/ PHOTOCHEMICAL TECHNIQUES IN FILM	42
V/ ANALYTICAL TECHNIQUES	42
VI/ VOLATILE PRODUCT ANALYSIS	44
D. RESULTS	45
I/ POLYMER CHARACTERIZATION	45
1. INFRARED SPECTRAL CHARACTERISTICS	45
2. NUCLEAR MAGNETIC RESONANCE SPECTRAL CHARACTERISTICS	47
3. UV SPECTRAL CHARACTERISTICS OF POLYMERS IN SOLUTION	47
4. UV SPECTRAL CHARACTERISTICS OF POLYMERS IN THIN FILMS	52
5. EMISSION CHARACTERISTICS OF FLUROESCENCE	54
6. EMISSION CHARACTERISTICS OF PHOSPHORESCENCE AT 77K	57
II/ EFFECTS OF UV IRRADIATION ON POLYMER PROPERTIES	67
1. INFRARED SPECTRAL CHANGES	67
2. NMR SPECTRAL CHANGES	67
3. UV SPECTRAL CHANGES	71
4. LOW MOLECULAR WEIGHT PRODUCTS	75
5. MOLECULAR WEIGHT CHANGES IN SOLUTION	77
6. THE EFFECT OF QUENCHERS IN SOLUTION	82
7. MOLECULAR WEIGHT CHANGES IN FILM	89

8. THE EFFECT OF QUENCHERS IN FILM	98
9. CHANGES IN EMISSION SPECTRA	109
10. THE EFFECT OF LIGHT ABSORBERS ON MOLECULAR WEIGHT CHANGES	131
E. DISCUSSION	139
I/ PHOTOPHYSICAL PROCESSES	139
II/ PHOTOCHEMICAL PROCESSES	140
1. QUENCHING IN SOLUTION	148
2. SOLID STATE QUENCHING	149
3. LIGHT ABSORBERS AS INHIBITORS	151
F. REFERENCES	154

LIST OF ILLUSTRATIONS

FIGURES

Figure 1.1. Potential energy diagram displaying excitation and radiative deactivation.

Figure 1.2. Jablonski diagram illustrating photophysical transitions in a photoluminescent system, where straight lines indicate radiative decay and wavy lines indicate radiationless decay.

Figure 1.3. Two electronic states with similar vibrational spacings.

Figure 1.4. Electronic transitions of the carbonyl chromophore.

Figure 1.5. Photoisomerization of phenyl alkyl ketones.

Figure 2.1. Cannon Ubbelohde viscometer for photochemical studies of polymer solutions.

Figure 2.2. Irradiation cell for air free irradiation of polymer films.

Figure 3.1. Infrared spectrum of PEAP.

Figure 3.2. ^1H NMR spectrum of PEAP.

Figure 3.3. ^{13}C NMR spectrum of PEAP.

Figure 3.4. UV absorption spectra of PMAP, P34DMAP, P35DMAP and PEAP (3×10^{-4} M solution in CH_2Cl_2 and instrument sensitive to 0.0001% T).

Figure 3.5. UV absorption spectra of PMAP, P34DMAP, P35DMAP and PEAP (1.5×10^{-4} cm film and instrument sensitive to 0.0001% T).

Figure 3.6. Fluorescence spectra of PMAP, P34DMAP, P35DMAP and PEAP (5×10^{-3} M Solution in CH_2Cl_2) at room temperature.

Figure 3.7. Phosphorescence spectra of PMAP, P34DMAP, P35DMAP and PEAP in glass at 77K.

Figure 3.8. Phosphorescence decay characteristics of PMAP triplet in glass at 77K.

Figure 3.9. Phosphorescence decay characteristics of P34DMAP triplet in glass Wavy line = radiationless decay at 77K.

Figure 3.10. Phosphorescence decay characteristics of P35DMAP triplet in glass at 77K.

- Figure 3.11. Phosphorescence decay characteristics of PEAP triplet in glass at 77K.
- Figure 3.12. Phosphorescence decay characteristics of PMAP triplet in glass at 77K (semi-logarithmic plot).
- Figure 3.13. Phosphorescence decay characteristics of P34DMAP triplet in glass at 77K (semi-logarithmic plot).
- Figure 3.14. Phosphorescence decay characteristics of P35DMAP triplet in glass at 77K (semi-logarithmic plot).
- Figure 3.15. Phosphorescence decay characteristics of PEAP triplet in glass at 77K (semi-logarithmic plot).
- Figure 3.16. Infrared spectral changes of PEAP (6.0×10^{-2} M solution in CH_2Cl_2) after 12 hours of irradiation ($\lambda \geq 300\text{nm}$, degassed).
- Figure 3.17. ^1H NMR spectral changes of PEAP (6.0×10^{-2} M solution in CH_2Cl_2) after 12 hours of irradiation ($\lambda \geq 300\text{nm}$, degassed).
- Figure 3.18. ^{13}C NMR spectrum of PEAP (6.0×10^{-2} M solution in CH_2Cl_2) after 12 hours of irradiation ($\lambda \geq 300\text{nm}$, degassed).
- Figure 3.19. UV absorption spectra of PEAP (3×10^{-4} M solution in CH_2Cl_2) before and after irradiation ($\lambda \geq 300\text{nm}$, degassed and instrument sensitive to 0.0001% T).
- Figure 3.20. UV absorption spectra of PEAP (1.5×10^{-4} cm film) before and after irradiation ($\lambda \geq 300\text{nm}$, degassed and instrument sensitive to 0.0001% T).
- Figure 3.21. Optical density and yellowing characteristics of new broad band absorption at 400nm as a function of irradiation time ($\lambda \geq 300\text{nm}$, degassed).
- Figure 3.22. Low molecular weight gaseous product formation (solid state PEAP) as a function of irradiation time ($\lambda \geq 300\text{nm}$, degassed).
- Figure 3.23. Gel permeation chromatograph of PEAP (1.0×10^{-2} M solution in CH_2Cl_2) before and after 4 hours of irradiation ($\lambda \geq 300\text{nm}$, degassed and run through a $7\mu\text{m}$ pore Ultrastyrage!® linear column at $1.0 \text{ cm}^3 \text{ min}^{-1}$)
- Figure 3.24. Number of chain scissions per original molecule of PEAP (in CH_2Cl_2) as a function of irradiation time ($\lambda \geq 300\text{nm}$, degassed).
- Figure 3.25. Rate of chain scission as a function of PEAP (in CH_2Cl_2) concentration ($\lambda \geq 300\text{nm}$, degassed).

- Figure 3.26. Rate of chain scission as a function of PEAP (in CH_2Cl_2) reciprocal concentration ($\lambda \geq 300\text{nm}$, degassed).
- Figure 3.27. Number of chain scissions per molecule of PEAP (1.0×10^{-2} M solution in CH_2Cl_2) in the presence of naphthalene as a function of irradiation time ($\lambda \geq 300\text{nm}$, degassed).
- Figure 3.28. Number of chain scissions per molecule of PEAP (1.0×10^{-2} M solution in CH_2Cl_2) in the presence of cis-1,3-pentadiene as a function of irradiation time ($\lambda \geq 300\text{nm}$, degassed).
- Figure 3.29. Stern-Volmer plots for quenching of PEAP (1.0×10^{-2} M solution in CH_2Cl_2) triplet ($\lambda \geq 300\text{nm}$, degassed).
- Figure 3.30. Gel permeation chromatograph of PEAP (1.0×10^{-2} M solution in CH_2Cl_2) before and after 4 hours of irradiation in the presence and absence of triplet quenchers ($\lambda \geq 300\text{nm}$, degassed and run through a $7\mu\text{m}$ pore Ultrastyrigel[®] linear column at $1.0 \text{ cm}^3 \text{ min}^{-1}$).
- Figure 3.31. Gel permeation chromatograph of PMAP (1.5×10^{-4} cm film) before and after 4 hours of irradiation ($\lambda \geq 300\text{nm}$, degassed and run through a $7\mu\text{m}$ pore Ultrastyrigel[®] linear column at $1.0 \text{ cm}^3 \text{ min}^{-1}$).
- Figure 3.32. Gel permeation chromatograph of P34DMAP (1.5×10^{-4} cm film) before and after 4 hours of irradiation ($\lambda \geq 300\text{nm}$, degassed and run through a $7\mu\text{m}$ pore Ultrastyrigel[®] linear column at $1.0 \text{ cm}^3 \text{ min}^{-1}$).
- Figure 3.33. Gel permeation chromatograph of P35DMAP (1.5×10^{-4} cm film) before and after 4 hours of irradiation ($\lambda \geq 300\text{nm}$, degassed and run through a $7\mu\text{m}$ pore Ultrastyrigel[®] linear column at $1.0 \text{ cm}^3 \text{ min}^{-1}$).
- Figure 3.34. Gel permeation chromatograph of PEAP (1.5×10^{-4} cm film) before and after 4 hours of irradiation ($\lambda \geq 300\text{nm}$, degassed and run through a $7\mu\text{m}$ pore Ultrastyrigel[®] linear column at $1.0 \text{ cm}^3 \text{ min}^{-1}$).
- Figure 3.35. Number of chain scissions per original molecule of PMAP, P34DMAP, P35DMAP and PEAP (1.5×10^{-4} cm film) as a function of irradiation time ($\lambda \geq 300\text{nm}$, degassed).
- Figure 3.36. Number of chain scissions per molecule of PMAP (1.5×10^{-4} cm film) in the presence of triplet quenchers as a function of irradiation time ($\lambda \geq 300\text{nm}$, degassed).
- Figure 3.37. Number of chain scissions per molecule of P35DMAP (1.5×10^{-4} cm film) in the presence of triplet quenchers as a function of irradiation time ($\lambda \geq 300\text{nm}$, degassed).

- Figure 3.38. Number of chain scissions per molecule of P34DMAP (1.5×10^{-4} cm film) in the presence of triplet quenchers as a function of irradiation time ($\lambda \geq 300\text{nm}$, degassed).
- Figure 3.39. Number of chain scissions per molecule of PEAP (1.5×10^{-4} cm film) in the presence of triplet quenchers as a function of irradiation time ($\lambda \geq 300\text{nm}$, degassed).
- Figure 3.40. Gel permeation chromatograph of PMAP (1.5×10^{-4} cm film) before and after 1 hour of irradiation in the presence and absence of triplet quenchers ($\lambda \geq 300\text{nm}$, degassed and run through a $7\mu\text{m}$ pore Ultrastyrigel[®] linear column at $1.0 \text{ cm}^3\text{min}^{-1}$).
- Figure 3.41. Gel permeation chromatograph of P34DMAP (1.5×10^{-4} cm film) before and after 1 hour of irradiation in the presence and absence of triplet quenchers ($\lambda \geq 300\text{nm}$, degassed and run through a $7\mu\text{m}$ pore Ultrastyrigel[®] linear column at $1.0 \text{ cm}^3\text{min}^{-1}$).
- Figure 3.42. Gel permeation chromatograph of P35DMAP (1.5×10^{-4} cm film) before and after 1 hour of irradiation in the presence and absence of triplet quenchers ($\lambda \geq 300\text{nm}$, degassed and run through a $7\mu\text{m}$ pore Ultrastyrigel[®] linear column at $1.0 \text{ cm}^3\text{min}^{-1}$).
- Figure 3.43. Gel permeation chromatograph of PEAP (1.5×10^{-4} cm film) before and after 1 hour of irradiation in the presence and absence of triplet quenchers ($\lambda \geq 300\text{nm}$, degassed and run through a $7\mu\text{m}$ pore Ultrastyrigel[®] linear column at $1.0 \text{ cm}^3\text{min}^{-1}$).
- Figure 3.44. Stern-Volmer plots for quenching of PMAP, P34DMAP, P35DMAP and PEAP (1.5×10^{-4} cm film) triplets by naphthalene ($\lambda \geq 300\text{nm}$, degassed).
- Figure 3.45. Perrin plots for quenching of PMAP, P34DMAP, P35DMAP and PEAP (1.5×10^{-4} cm film) triplets by naphthalene ($\lambda \geq 300\text{nm}$, degassed).
- Figure 3.46. Phosphorescence spectra indicating the direct quenching of PMAP by 1,3-cyclohexadiene in glass at 77K.
- Figure 3.47. Phosphorescence spectra indicating the direct quenching of PMAP by naphthalene in glass at 77K.
- Figure 3.48. Phosphorescence spectra indicating the direct quenching of PMAP by cis-1,3-pentadiene in glass at 77K.
- Figure 3.49. Phosphorescence spectra indicating the direct quenching of P34DMAP by 1,3-cyclohexadiene in glass at 77K.
- Figure 3.50. Phosphorescence spectra indicating the direct quenching of P34DMAP by naphthalene in glass at 77K.
- Figure 3.51. Phosphorescence spectra indicating the direct quenching of P34DMAP by cis-1,3-pentadiene in glass at 77K.

- Figure 3.52. Phosphorescence spectra indicating the direct quenching of P35DMAP by 1,3-cyclohexadiene in glass at 77K.
- Figure 3.53. Phosphorescence spectra indicating the direct quenching of P35DMAP by naphthalene in glass at 77K.
- Figure 3.54. Phosphorescence spectra indicating the direct quenching of P35DMAP by cis-1,3-pentadiene in glass at 77K.
- Figure 3.55. Phosphorescence spectra indicating the direct quenching of PEAP by 1,3-cyclohexadiene in glass at 77K.
- Figure 3.56. Phosphorescence spectra indicating the direct quenching of PEAP by naphthalene in glass at 77K.
- Figure 3.57. Phosphorescence spectra indicating the direct quenching of PEAP by cis-1,3-pentadiene in glass at 77K.
- Figure 3.58. Stern-Volmer plots for quenching of PMAP (1.0×10^{-2} M solid state solution in CH_2Cl_2) triplet in glass at 77K.
- Figure 3.59. Stern-Volmer plots for quenching of P34DMAP (1.0×10^{-2} M solid state solution in CH_2Cl_2) triplet in glass at 77K.
- Figure 3.60. Stern-Volmer plots for quenching of P35DMAP (1.0×10^{-2} M solid state solution in CH_2Cl_2) triplet in glass at 77K.
- Figure 3.61. Stern-Volmer plots for quenching of PEAP (1.0×10^{-2} M solid state solution in CH_2Cl_2) triplet in glass at 77K.
- Figure 3.62. Perrin plots for quenching of PMAP (1.0×10^{-2} M solid state solution in CH_2Cl_2) triplet in glass at 77K.
- Figure 3.63. Perrin plots for quenching of P34DMAP (1.0×10^{-2} M solid state solution in CH_2Cl_2) triplet in glass at 77K.
- Figure 3.64. Perrin plots for quenching of P35DMAP (1.0×10^{-2} M solid state solution in CH_2Cl_2) triplet in glass at 77K.
- Figure 3.65. Perrin plots for quenching of PEAP (1.0×10^{-2} M solid state solution in CH_2Cl_2) triplet in glass at 77K.
- Figure 3.66. Number of chain scissions per molecule of PMAP (6.0×10^{-2} M solution in CH_2Cl_2) in the presence of Tinuvin 327 as a function of irradiation time ($\lambda \geq 300\text{nm}$, degassed).

- Figure 3.67. Number of chain scissions per molecule of PMAP (6.0×10^{-2} M solution in CH_2Cl_2) in the presence of Tinuvin 900 as a function of irradiation time ($\lambda \geq 300\text{nm}$, degassed).
- Figure 3.68. Quantum yield for chain scission of PMAP (6.0×10^{-2} M solution in CH_2Cl_2) as a function of quencher concentration ($\lambda \geq 300\text{nm}$, degassed).
- Figure 3.69. Stern-Volmer plots for quenching of PMAP (6.0×10^{-2} M solution in CH_2Cl_2) triplet ($\lambda \geq 300\text{nm}$, degassed).
- Figure 3.70. Gel permeation chromatograph of PMAP (6.0×10^{-2} M solution in CH_2Cl_2) before and after 1 hour of irradiation in the presence and absence of Tinuvin 327 ($\lambda \geq 300\text{nm}$, degassed and run through a $7\mu\text{m}$ pore Ultrastyrage[®] linear column at $1.0 \text{ cm}^3 \text{ min}^{-1}$).
- Figure 3.71. Gel permeation chromatograph of PMAP (6.0×10^{-2} M solution in CH_2Cl_2) before and after 1 hour of irradiation in the presence and absence of Tinuvin 900 ($\lambda \geq 300\text{nm}$, degassed and run through a $7\mu\text{m}$ pore Ultrastyrage[®] linear column at $1.0 \text{ cm}^3 \text{ min}^{-1}$).
- Figure 3.72. Reaction scheme summarizing the photoreactions of PEAP.

TABLES

- Table 3.1. GPC Analysis of Methoxy and Ethoxy-Substituted Poly(acrylophenones)
- Table 3.2. UV Absorption Characteristics of Methoxy and Ethoxy-Substituted Poly(acrylophenones) in 3×10^{-4} M Solution in CH_2Cl_2
- Table 3.3. UV Absorption Characteristics of films of Methoxy and Ethoxy-Substituted Poly(acrylophenones) (1.5×10^{-4} cm thick)
- Table 3.4. Fluorescence Characteristics of Methoxy⁷ and Ethoxy-Substituted Poly(acrylophenones) in 5×10^{-3} M Solution in CH_2Cl_2
- Table 3.5. Phosphorescence Characteristics of Methoxy and Ethoxy-Substituted Poly(acrylophenones) in glass at 77K
- Table 3.6. ¹H NMR Characteristics of PEAP in 6.0×10^{-2} M Polymer Solutions in CH_2Cl_2 and 1.5×10^{-4} cm Films After 12 Hours of Irradiation ($\lambda \geq 300\text{nm}$, degassed)
- Table 3.7. ¹³C NMR Characteristics of PEAP in 6.0×10^{-2} M Polymer Solutions in CH_2Cl_2 and 1.5×10^{-4} cm Films After 12 Hours of Irradiation ($\lambda \geq 300\text{nm}$, degassed).
- Table 3.8. Quantum Yields for Gaseous Product Formation from Ethoxy-Substituted Poly(acrylophenone) Film Upon Irradiation ($\lambda \geq 300 \text{ nm}$, vacuum)

Table 3.9. Quantum Yields for Chain Scission ($\lambda \geq 300\text{nm}$) of 6.0×10^{-2} M Polymer Solutions in CH_2Cl_2

Table 3.10. Quenching Constants for the Irradiation of PEAP in 1×10^{-2} M Solution in CH_2Cl_2 ($\lambda \geq 300$ nm)

Table 3.11. Quantum Yields for Chain Scission ($\lambda \geq 300\text{nm}$) Polymers in Thin Film (1.5×10^{-4} cm)

Table 3.12. Analysis of the Quenching of Methoxy and Ethoxy-Substituted Poly(acrylophenone) triplets ($\lambda \geq 300\text{nm}$) in Thin Film (1.5×10^{-4} cm).

Table 3.13. Phosphorescence Analysis of the Direct Quenching of Methoxy and Ethoxy-Substituted Poly(acrylophenones) in glass at 77K in CH_2Cl_2

Table 3.14. Quenching Constants for the Irradiation of PMAP in 6×10^{-2} M Solution in CH_2Cl_2 ($\lambda \geq 300$ nm)

INTRODUCTION

I/ PHOTOCHEMISTRY

Photochemistry is the specific area of chemistry that deals with the interactions of light with matter and includes both the physical and chemical changes that occur after light has been absorbed by an atom or molecule. Photochemistry follows quantum theory which considers electromagnetic radiation to be a stream of particles, or photons. Each photon has a fixed energy equal to $E = hc/\lambda = hv$, where h is Planck's constant, c is the velocity of light *in vacuo*, λ is the photon wavelength and v is the frequency. Thus, light is considered to behave as particles whose energies are quantized.^{1,2,3}

There are two laws of photochemistry, the first is the Grotthus-Draper law which states that the first step of a photochemical reaction is the absorption of light and it is only the absorbed light that is able to induce photochemical change in a molecule.⁴ The second law, the Stark-Einstein law, states that when quanta of light interact with an atom or molecule, the energy that is available is equal to hv because quanta of light can only react with one atom or molecule at a time. The intensity of radiation is proportional to the number of photons per unit time. Thus, if the intensity is increased there will only be an increase in the number of excited molecules, not in the energy that is available to each individual molecule.^{1,3}

Energy levels are quantized, i.e. they can only exist in discrete and separate energy states, which are defined by quantum numbers, and the transition between two given states requires a definite amount of energy (i.e. ΔE). The Bohr condition states that since absorption usually occurs in one step, the energy of the photons of the incident radiation, hv , must equal the energy associated with the transition from the electronic ground to an excited state (i.e. $hv = \Delta E$). Thus, radiation of

only specific energy (or frequency) which brings about an electronic transition within an absorbing species can be absorbed.^{1,3}

An absorption occurs when a photon comes in contact with a molecule and the electric fields associated with both the molecule and the radiation interact making energy transfer from the photon to the molecule possible. This leads to a change in the electronic structure of the molecule, from the ground state to an excited state and it can be visualized in terms of the molecular orbital model as an electron being promoted from an occupied orbital to a vacant orbital of higher energy. Most organic molecules have all electrons paired in the ground state; i.e. the unexcited molecules exist in the ground state as singlets (in terms of spin multiplicity, $2S+1=1$). The promotion of one electron from the singlet ground to an excited state, will generate two singly occupied orbitals. A singlet state will result if the spins of the electrons in these two orbitals are antiparallel. A triplet state occurs when the spins of the electrons in the two orbitals are parallel.⁵ A triplet state has a higher spin multiplicity (i.e. 3) than a singlet state, and according to Hund's rule, this makes it more stable than the singlet state and thus lower in energy.³ The triplet state is more stable because there is a minimum energy of repulsion between electrons when the spins are parallel.⁶

During electronic excitation, a molecule can also become vibrationally excited. This is explained in terms of the Frank-Condon principle, which considers the potential energies of the ground state and the excited singlet and triplet states of a molecule, and transitions between them. For a more complex molecule, this can be considered as a cross-section of the potential energy surface. According to the Frank-Condon principle, electronic transitions occur without a change in nuclear geometry, since the time involved in an electronic transition is very much less than the period of vibration. Electronic transitions can therefore be regarded as vertical transitions between

ground and excited states as shown in Figure 1.1. The transition to the vibrational level will occur at the point of the same nuclear geometry which results in the most efficient energy transfer.^{3,7} For more complex molecules, it is difficult to construct this type of potential energy curve to show the vibrational and electronic energies, so a Jablonski diagram (Figure 1.2) is used instead.³

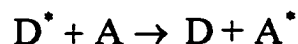
After the photon is absorbed, the excited state that is produced will usually have a short lifetime because there are many ways in which it can be deactivated. These include both physical processes and chemical changes which can compete with each other. The photophysical deactivation of a molecule involves the dissipation of energy, while the photochemical deactivation involves processes that produce chemically different products, in some cases by bond scission.^{1,3,5}

II/ PHOTOPHYSICAL DEACTIVATION OF AN EXCITED MOLECULE

Photophysical deactivation involves the dissipation of energy either through luminescence or by means of transfer of energy to a different form, but there is no chemical change in the molecule.^{1,3,5} There are four main modes of photophysical deactivation for an excited molecule.

1. INTERMOLECULAR ENERGY TRANSFER

An intermolecular energy transfer involves the transfer of energy from the excited molecule, the donor (D), to an acceptor molecule (A) as follows:³



A number of variations exist for transitions from a given excited state to the ground state. For example, the excited donor can go from the first excited triplet state T_1 and deactivate to the singlet

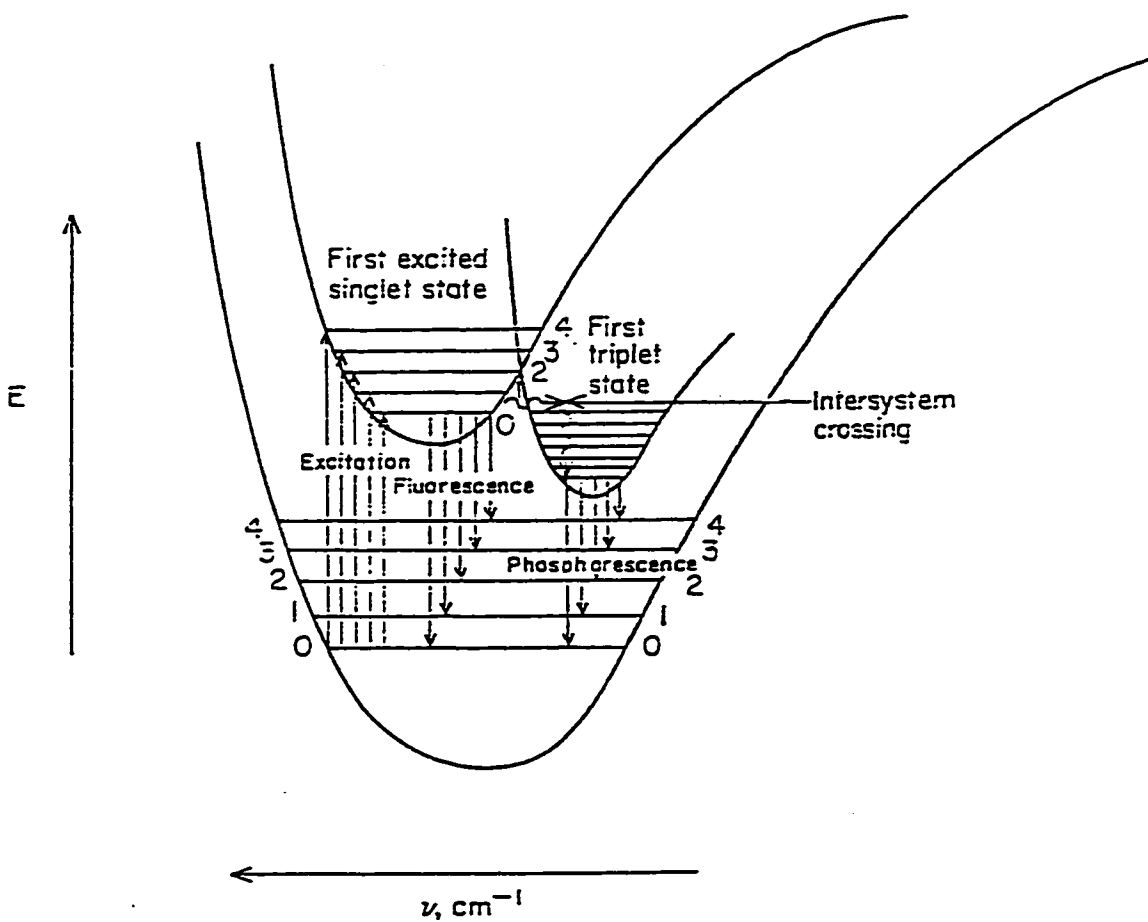


Figure 1.1. Potential energy diagram displaying excitation and radiative deactivation.⁸

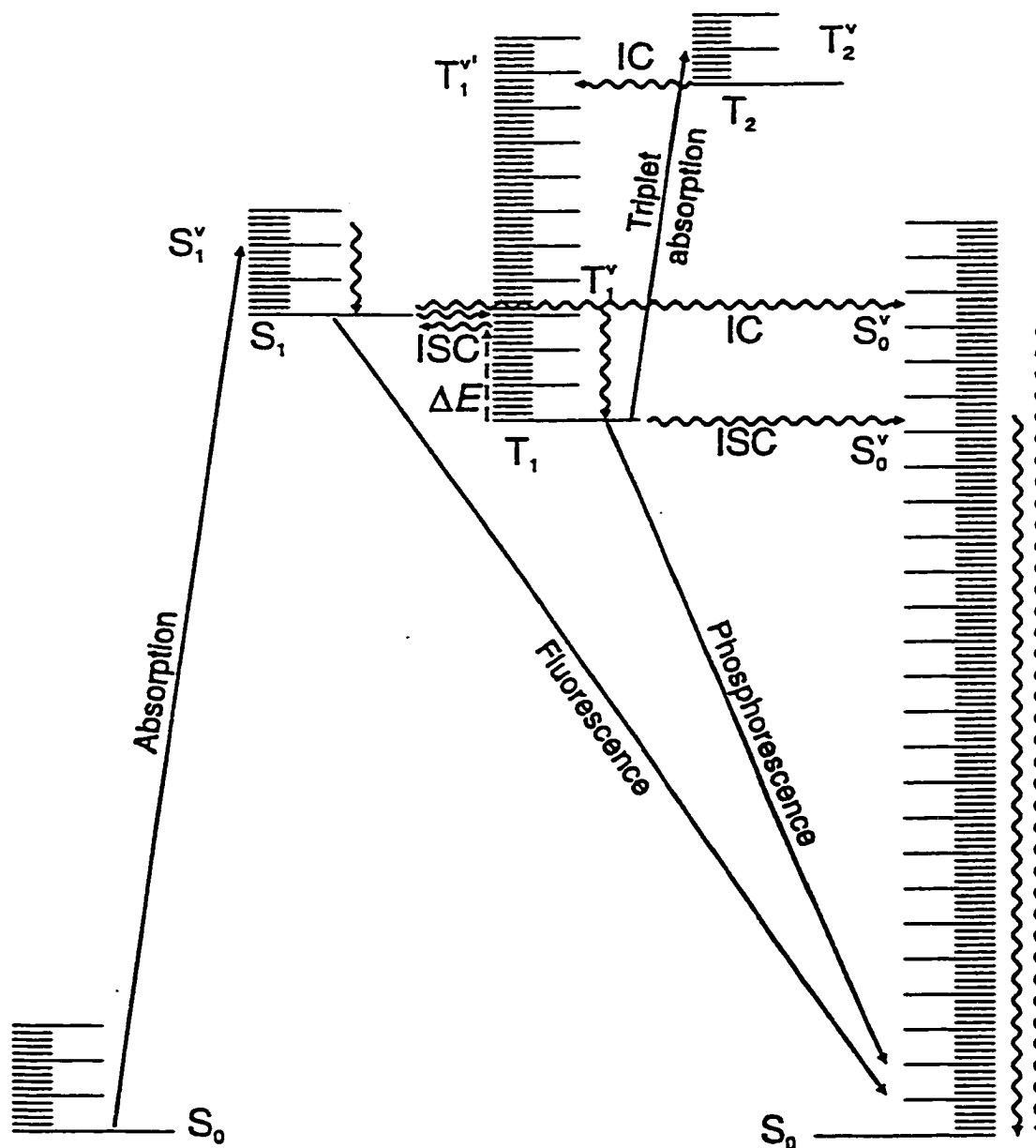


Figure 1.2. Jablonski diagram illustrating photophysical transitions in a photoluminescent system,³ where straight lines indicate radiative decay and wavy lines indicate radiationless decay.

ground state S_0 , while the acceptor will go from ground state S_0 to the excited triplet state T_1 . The energy exchange is viewed as an electronic-electronic transfer but it can be accounted by vibrational, rotational and translational energy transfers. These modes can take up any excess energy that the donor molecule may have so that a complete energy transfer can take place. After the energy exchange, the excited acceptor can then be deactivated photophysically or photochemically.³

2. INTRAMOLECULAR ENERGY TRANSFER

Intramolecular energy transfers occur when a new electronic state is populated in a molecule (M) that differs from the original excited state that occurred from the initial absorption. These types of energy transfers are radiationless transitions because they do not emit a photon and they proceed through the following mechanism:³



These transitions are useful in that they may produce an electronic state that may not have been accessible by the initial absorption. Intramolecular energy transfers can take place between electronic states of both the same and different spin multiplicity. There are three types of intramolecular energy transfer processes which are illustrated as wavy horizontal and vertical lines on the Jablonski diagram (Figure 1.2).

(a) INTERNAL CONVERSION (IC)

This is an electronic conversion between states of the same multiplicity. This can occur because the energies of the lower vibrational levels of higher electronic states and the higher vibrational levels of lower electronic states overlap.⁷ Internal conversions between higher states $S_m \rightarrow S_n$ and $T_m \rightarrow T_n$ are very rapid but internal conversions are slower when they occur from the first

excited singlet state $S_1 \rightarrow S_0$. The rate of internal conversion from the first excited singlet state is slow enough that fluorescence can compete with it.⁵

(b) INTERSYSTEM CROSSING (ISC)

This involves an electronic conversion between states of different multiplicity and occurs by intersection of the singlet and triplet potential energy surfaces.⁷ This process is spin forbidden but is enabled due to spin-orbit coupling.¹ Phosphorescence can compete with the intersystem crossing from the lowest triplet state, $T_1 \rightarrow S_0$, while fluorescence competes with $S_1 \rightarrow T_1$ and $S_1 \rightarrow T_n$ intersystem crossings. The transition of $S_n \rightarrow T_n$ is rare because it is in competition with the very rapid internal conversion to S_1 . A $T_1 \rightarrow S_1$ transition can only occur if T_1 can somehow be thermally activated to a higher vibrational level that has the same energy as S_1 .⁵ Both internal conversion and intersystem crossing convert electronic energy to vibrational energy (heat).

(c) VIBRATIONAL RELAXATION (VR)

Vibrational relaxation is the process that immediately follows both internal conversion and intersystem crossing. Vibrational relaxation occurs in the same electronic state and consists of a rapid relaxation, or decay, to the lowest vibrational level of the lowest excited state.¹

3. LUMINESCENCE

Luminescence is the process by which an excited molecule dissipates its energy by emitting a photon and is thus a radiative loss of energy. Luminescence occurs when the molecule is excited by the absorption of a photon. If a chemical reaction has excited the molecule, then the emission process is called chemiluminescence. Radiative processes are illustrated on the Jablonski diagram

(Figure 1.2) as straight lines and occur when the excited molecule emits a photon. There are two main luminescent processes, fluorescence and phosphorescence.

(a) FLUORESCENCE

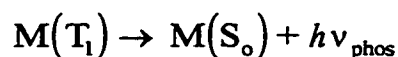
Fluorescence is defined as a radiative transition between states of the same multiplicity (singlets) and can take place in both the solid and liquid state. It can be represented as:



The usual pathway for fluorescence in organic compounds is from the lowest vibrational level of the first excited singlet state to vibrational levels in the ground state, $S_1 \rightarrow S_0$. This emission can occur because rapid vibrational relaxation and internal conversion take place making it a very fast process. A fluorescence spectrum is obtained by measuring the intensity of emission while changing the exciting wavelength. For organic molecules, the absorption band of the greatest intensity is usually the (0,0) vibrational level transition and this corresponds to the longest absorbed and shortest emitted wavelengths. This implies that the higher and lower electronic states must be similar geometrically, and most often similar in terms of spacings between vibrational levels as shown in Figure 1.3. This will lead to mirror image absorption and emission bands. If there are any differences between the two states or if any hydrogen bonding exists, these bands will not be perfectly symmetrical.^{1,3}

(b) PHOSPHORESCENCE

Phosphorescence is the radiative transition between states of different multiplicity. Phosphorescence can be represented by the following:



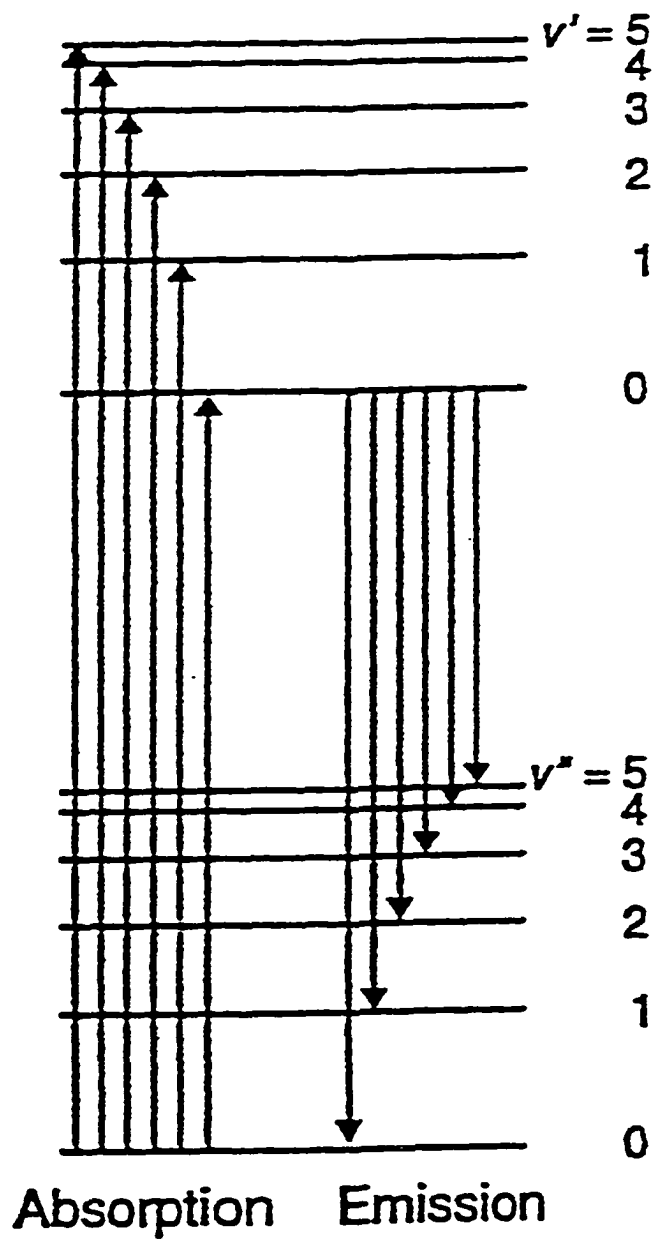


Figure 1.3. Two electronic states with similar vibrational spacings.³

The pathway taken for phosphorescence of organic compounds is from the lowest vibrational level of the first excited triplet state to vibrational levels in the ground singlet state $T_1 \rightarrow S_0$. The population of the excited triplet state T_0 by direct excitation from the singlet ground state S_0 is forbidden. The state is populated via intersystem crossing from the excited singlet state S_1 , thus phosphorescence has a longer lifetime than fluorescence. As a result, many intermolecular and intramolecular energy loss processes become competitive with this type of radiation.³ Most common is the collisional deactivation (quenching) of the triplet by solvent molecules and intersystem crossing to S_0^v . Quenching is minimized by performing phosphorescence studies at 77K (liquid nitrogen). A phosphorescence spectrum is obtained by the same method used for obtaining fluorescence spectra. Phosphorescence spectra can also have mirror image absorption and emission bands, although the (0,0) vibrational level transition usually has a large separation due to conformational differences between the ground and excited states.^{1,3}

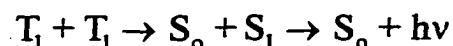
(c) DELAYED FLUORESCENCE

Another, less common mode of luminescence is delayed fluorescence. In delayed fluorescence, the molecules will emit the same fluorescence spectra as normal fluorescence but will differ by a longer lifetime. There are two major types of delayed fluorescence which occur as a result of two different photophysical processes, E-type and P-type. In E-type delayed fluorescence, the emission decays at the same rate as phosphorescence, there is no emission at low temperatures and the process has an activation energy.³ The activation energy is associated with the energy required to repopulate the S_1 state from the T_1 state, with the two energies being close together.



The decay of delayed fluorescence will correspond to the decay of T_1 .^{1,2,3}

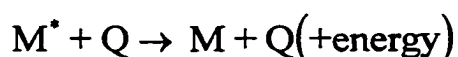
The second type of delayed fluorescence is P-type or triplet-triplet annihilation. This occurs when the lifetimes of two molecules are long enough that an encounter may occur as follows:



The encounter will cause one of the molecules to undergo internal conversion to the ground singlet state. The second molecule will become thermally excited to the lowest excited singlet state and fluorescence will occur from there. The lifetime in P-type delayed fluorescence should be of the same order as phosphorescence. These two types of delayed fluorescence can be distinguished by the fact that P-type is not temperature dependant and also that E-type has a linear relationship between emitted and absorbed intensities while P-type has a squared relationship.^{1,2,3}

4. PHYSICAL QUENCHING

Quenching, also known as deactivation, is the process by which the electronic energy of an excited molecule is transferred to a different atom or molecule called a quencher, Q, as follows:³



In this case though, the excitation in the quencher is not relevant because the electronic energy is unavailable. The energy is converted to vibrational, rotational or translational modes in the quencher eventually becoming dissipated as heat of the surroundings. The presence of a quencher will reduce the intensity of both fluorescence and phosphorescence because quenching competes with emission.⁶ The rate of this process is equal to $k_q[M^*][Q]$, where k_q is the quenching rate constant.^{2,3}

III/ PHOTOCHEMICAL DEACTIVATION OF AN EXCITED MOLECULE

Photochemical deactivation can occur from excited singlet and triplet states and involves processes that invoke chemical change. The lifetimes of these processes range from seconds to picoseconds.⁷ There are four main routes of chemical deactivation of an excited molecule.

1. DISSOCIATION

Dissociation involves the fragmentation of the excited molecule. This process will only occur when the energy of the photon absorbed is greater or equal to the bond dissociation energies within the molecule.

2. INTERMOLECULAR REACTIONS

Intermolecular reactions are chemical reactions that can take place between the excited molecule and a separate molecule, the process being impossible if the molecule was in the ground state. The excited molecule can interact with any unexcited molecules, added reactants or with a solvent if it is in solution. This also includes charge transfer reactions.³

3. INTRAMOLECULAR REACTIONS

Intramolecular reactions occur when one part of the excited molecule reacts with another part of the same molecule. This includes intramolecular additions and reductions which will give structural rearrangements.³

4. ISOMERIZATION

In the isomerization of an excited molecule, the photon must have sufficient energy to produce an internal rearrangement. An example of this type is the isomerization of stilbenes, which involves a cis-trans rotation about single bonds in the singlet and triplet states.³

All of the photophysical and photochemical processes described previously are examples of primary processes because they involve direct reactions of the excited species. Secondary processes, which involve reactions of the species formed in the initial processes, can also occur.⁷

IV/ KINETICS OF PHOTOPROCESSES

1. PHOTOPHYSICAL PROCESSES

The relationship between kinetics and photochemistry is an important one. Kinetics provide insights into many photophysical processes, and can provide information about the mechanisms of photochemical reactions. In photophysical processes, the rate of emission of a radiative process is expressed in terms of lifetime. This term can be used in experiments that use methods similar to flash photolysis, where molecules are irradiated by a brief flash of light after which there is no exciting radiation left. The decay of the excited molecules (M) will proceed via first order kinetics because spontaneous emission is a random process.⁶

$$-\frac{d}{dt}[M^*] = k_r^o[M^*]$$

The natural rate constant k_r^o represents the rate of spontaneous emission where no other photophysical processes are competing. The integrated form of the previous equation,⁶

$$[M^*] = [M^*]_0 e^{-k_r^0 t}$$

can be expressed in terms of emission intensities where $I_r(t)$ is the intensity of emission of the radiative process at time t and $I_r(0)$ is the emission intensity at time 0.

$$I_r(t) = I_r(0) e^{-k_r^0 t}$$

The natural radiative lifetime is defined as the reciprocal of the natural rate constant.⁶

$$\tau_r^0 = \frac{1}{k_r^0}$$

Thus the lifetime can characterize the rate of a given emission process.

2. PHOTOCHEMICAL PROCESSES

The general rate expression for a photo-reaction, $A \xrightarrow{h\nu} \text{products}$, is given as:³

$$-\frac{d(A)}{dt} = \Phi I_A$$

in which Φ is the quantum yield and I_A is the rate of absorption of photons. The quantum yield Φ , which is useful in providing information about photochemical reaction mechanisms, is defined as the number of molecules of reactants consumed per photon of light absorbed,

$$\Phi = \frac{\text{Number of molecules reacting}}{\text{Number of quanta absorbed}}$$

or also by the rate of reaction to the rate of absorption of quanta.¹⁰

$$\Phi = \frac{\text{Rate of reaction}}{\text{Rate of absorption of quanta}}$$

I_A is given by the expression:³

$$I_A = I_0(1 - e^{-\epsilon cl})$$

where ϵ is the molar absorption coefficient, c is the concentration and l is the effective pathlength of the solution. Thus Φ is frequently expressed as:

$$\Phi = \frac{d(x) / dt}{I_0(1 - e^{-\epsilon cl})}$$

which can be approximated as:

$$\Phi = \frac{d(x) / dt}{I_0 \epsilon cl}$$

where ϵ , c and l are small.

The primary quantum yield ϕ expresses the possibility that a molecule will decay through a particular process. Since only one molecule is excited for each photon that is absorbed, the ϕ is given as the number of molecules undergoing the particular process divided by the number of photons absorbed.³ In the case of fluorescence, the quantum yield for fluorescence, i.e. ϕ_{fluor} is given by the expression:⁶

$$\phi_{\text{fluor}} = \frac{\text{Number of molecules fluorescing per unit time per unit volume}}{\text{Number of quanta absorbed per unit time per unit volume}}$$

This can also be expressed in terms of intensities, since the intensity of radiation is proportional to the number of photons emitted per unit time, where I_f is the intensity of fluorescence and I_{abs} is the intensity of the absorbed radiation.⁶

$$\phi_{\text{fluor}} = \frac{I_f}{I_{\text{abs}}}$$

The most useful expression of ϕ_{fluor} is in terms of lifetimes, where τ_f is the measured lifetime of fluorescence and τ_f^0 is the natural radiative lifetime where there are no competing photophysical processes.⁶

$$\phi_{\text{fluor}} = \frac{\tau_f}{\tau_f^0}$$

The primary quantum yields can be used to indicate any photochemical or photophysical process, but the sum of all the primary quantum yields must equal 1.

V/ PHOTOPHYSICS OF KETONE-CONTAINING POLYMERS

Photochemical reactions of the carbonyl chromophore are of much interest and have been intensely investigated.¹ Both simple ketones and ketone-containing polymers having been studied, because the carbonyl chromophore is photochemically labile but thermally stable. In addition, the carbonyl chromophore absorbs in the near ultraviolet region of the spectrum and it can be selectively excited both in a large group of other molecules, and in molecules having more than one chromophore. The UV spectrum of ketone-containing polymers indicates the absorptions of the isolated chromophores.⁹ Absorption by polymers in the near ultraviolet region is of commercial interest because it corresponds to the range of terrestrial sunlight radiation to which polymers are exposed.⁷

Absorption of UV radiation by the carbonyl results in an electron being promoted from an occupied orbital to a vacant orbital of higher energy generating two singly occupied orbitals (Figure 1.4). In the carbonyl chromophore, the non-bonding n orbital is the highest occupied molecular orbital and is localized on the carbonyl oxygen atom. The antibonding π^* orbital is the lowest

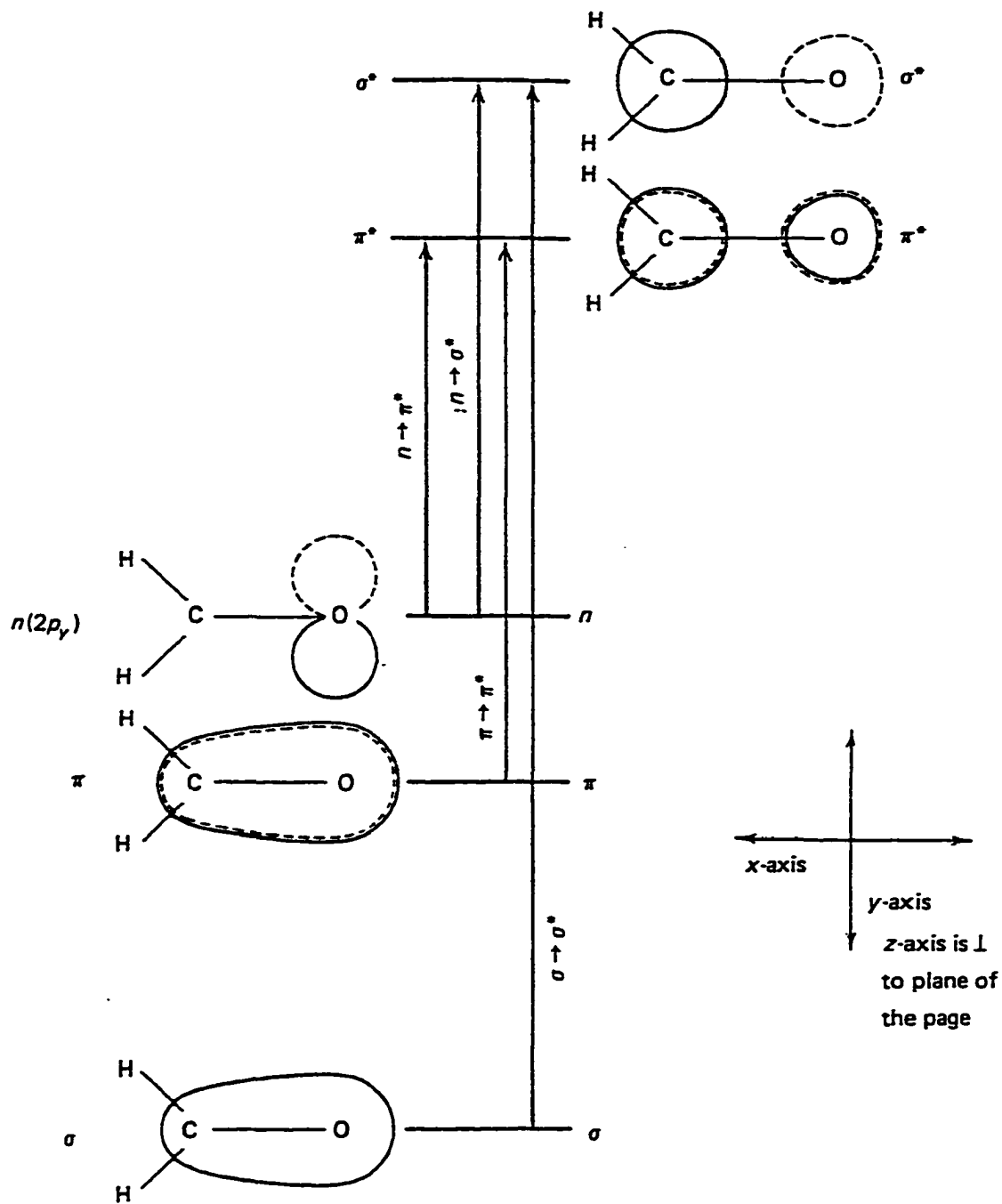


Figure 1.4. Electronic transitions of the carbonyl chromophore.¹

unoccupied molecular orbital and is delocalized over the entire carbonyl group. In aliphatic carbonyl compounds, the excited singlet state is formed by an $n \rightarrow \pi^*$ transition which gives a single absorption at around 280nm. The excited triplet state can be formed from the singlet by intersystem crossing.¹⁰

The intensities of these $n \rightarrow \pi^*$ transitions (at around 280nm) are weak because the transition involves orthogonal orbitals and therefore it is symmetry forbidden. In the (n, π^*) state, the aliphatic carbonyl group will be electrophilic because of the half vacant n orbital (located on the oxygen) in the plane of the carbonyl. The areas above and below the plane of the carbonyl group will be nucleophilic because of the delocalized π^* electron.¹ The energy difference between the singlet and triplet (n, π^*) states is large enough that intersystem crossing is relatively slow. This means that photoreactions can take place from both the excited singlet and triplet states in aliphatic ketones.⁷

In aromatic ketones, the (n, π^*) excited singlet and triplet states have lower energies than those of the aliphatic ketones, and their corresponding absorption bands are shifted bathochromically. These also undergo $\pi \rightarrow \pi^*$ transitions, which are sometimes shifted to such an extent that the (n, π^*) band either becomes a shoulder of the (π, π^*) band or disappears into the (π, π^*) absorption.¹¹ The (π, π^*) band shift is a result of the increasing of the energy of the π orbital and lowering that of the π^* orbital which is caused by the inductive effects of the aromatic ring.¹ The conjugation in aromatic ketones also causes a large increase in the rate of intersystem crossing and the corresponding quantum yield frequently equal to unity.⁶ Thus as far as aromatic ketones are concerned, most of the reactivity is associated with the (n, π^*) triplet.

There are several factors that affect the relative stabilities of the (n, π^*) and the (π, π^*) states of the carbonyl chromophore. In the $n \rightarrow \pi^*$ transition, there is a movement of electron density away from the oxygen, and this state is stabilized by electron-accepting substituents that are in conjugation

with the carbonyl group. In the $\pi \rightarrow \pi^*$ transition, the electron density of the carbonyl group is being increased so that electron-donating substituents will stabilize this state.⁶ If the polarity of the solvent is increased, the (n, π^*) absorption band will undergo a hypsochromic shift and the (π, π^*) band will undergo a bathochromic shift. This stabilizes the (π, π^*) state over the (n, π^*) state and can actually invert their energies.

These factors play a very important role in photoreactions of carbonyl compounds because reactions usually take place from the lowest lying state.⁶ Aromatic ketones can be categorized in terms of the character of the lowest lying state. When the (n, π^*) state is the lowest lying triplet state, the aromatic ketones are reactive, can undergo photoreduction, have high triplet energies (67-74kcal/mol) and have short triplet lifetimes. On the other hand, aromatic carbonyl compounds that are considerably less inclined to undergo photoreduction, have lower triplet energies (55-61kcal/mol), have long triplet lifetimes and have the (π, π^*) state as their lowest lying triplet states.¹²

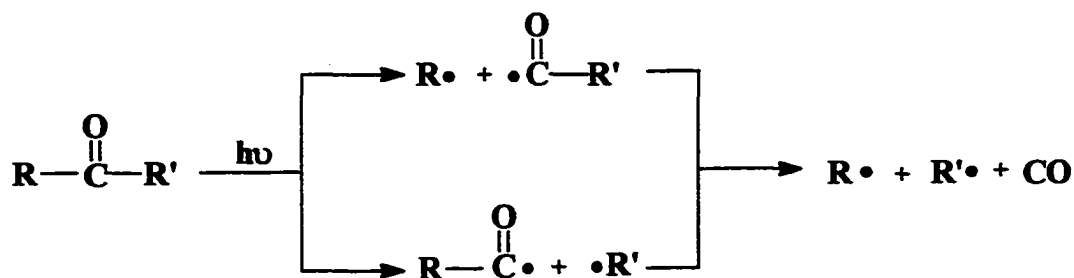
VI/ PHOTOCHEMISTRY OF KETONE-CONTAINING POLYMERS

The photodegradation of polymers involves photoreactions. These are carried out frequently in the absence of oxygen, in order to minimize secondary reactions with oxygen.⁴ There are two principle processes involved in the photodegradation of ketone-containing polymers, i.e. primary and secondary processes. Primary reactions involve two main types of photochemical reactions.

1. NORRISH TYPE I REACTION

The Norrish type I reaction is a type of α -cleavage. This reaction can take place from both the excited singlet and triplet states in aliphatic ketones, but will occur exclusively from the triplet

state in phenyl ketones, where $\phi_{ISC} \approx 1$.¹ The reaction proceeds via cleavage of the carbon σ bond, α to the carbonyl producing two radicals and it can take place in two ways:^{7,13}



The actual pathway depends on the stability of the resulting radicals. The acyl radicals that are produced can further undergo decarbonylation to give another radical (R or R') and carbon monoxide.¹³ In the case of a polymer, R or R' could be at the chain end. This occurs frequently when the compound is vibrationally excited after the initial α -cleavage, but occurs in solution only if the resulting radical (R or R') is very stable.

The efficiency of α -cleavage depends on two main factors, i.e. the nature and character of the carbonyl group and the nature of the medium.

(a) THE NATURE AND CHARACTER OF THE CARBONYL GROUP

The rate of α -cleavage is greater in (n, π^*) triplet states than in (π, π^*) triplet states because the n orbital overlaps with the carbon-carbon σ orbital, weakening the carbon bond α to the carbonyl.¹ If two carbon σ bonds exist in the carbonyl compound, the bond that is the weaker of the two will be cleaved. The quantum yield for the Norrish type I reaction ϕ_1 increases with an increase of substitution on the α -carbon, and cleavage usually occurs on the α -carbon with more substituents because this will produce a more stable radical (inductive effect).¹

(b) THE NATURE OF THE MEDIUM

The quantum yield ϕ_1 is greatest in the vapour phase, i.e. $\phi_{\text{vapour}} > \phi_{\text{liquid}} > \phi_{\text{solid}}$. This can be attributed to the cage effect which exists in concentrated solutions and in the solid state, especially in polymers. The initially formed radical pair are kept in the same vicinity by a cage of solvent molecules in solution and by restricted mobility in the solid state and this can cause recombination, i.e. cage collapse, which decreases the quantum yield.¹⁴ Another reason for the greater ϕ_1 in the vapour phase is that vibrational energy is required for the reaction to take place and vibrational deactivation occurs more readily in solution than in the vapour phase. This vibrational energy requirement would also explain the increase in ϕ_1 with increasing temperature.¹

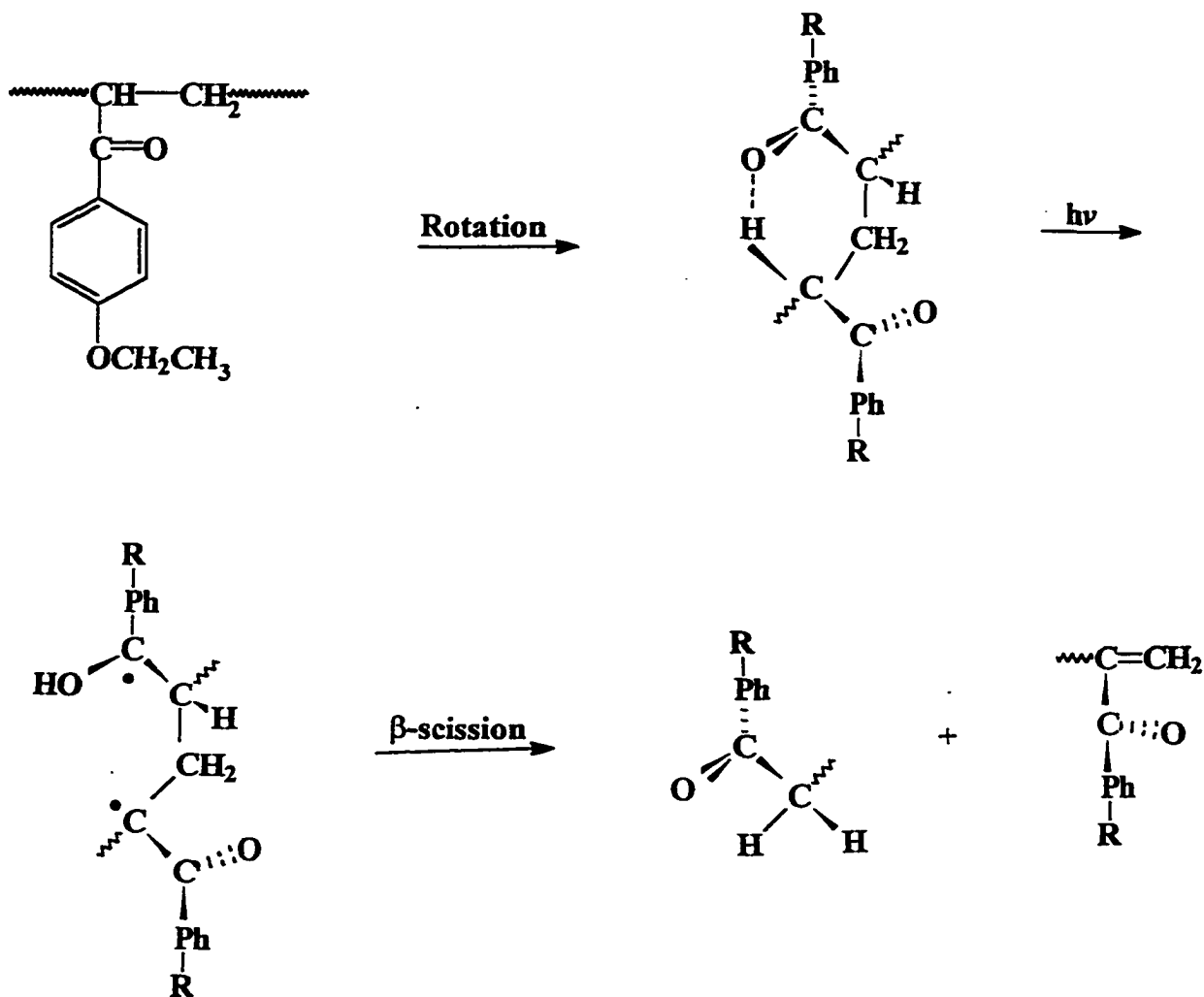
2. SECONDARY PROCESSES

These arise from interactions of the initially formed radicals in the Norrish type I reaction. When the reaction is carried out in a solvent, the small alkyl radicals can interact to give products of disproportionation and combination where it is possible that several radical combinations can lead to crosslinking. The radicals may also participate in abstraction reactions in which the radical may abstract a hydrogen from the solvent, depending on the nature of the solvent.¹ The radicals can also abstract a hydrogen from neighbouring ketones in the solid or liquid phases but this again, depends on the nature of the ketones.⁷

3. NORRISH TYPE II REACTION

The Norrish type II reaction is a non-radical, intramolecular hydrogen abstraction reaction. As in the Norrish type I reaction, it can occur from both the excited singlet and triplet states, but will

occur more probably from the preferred triplet state in aromatic ketones where $\phi_{ISC} \approx 1$.¹ The hydrogen abstraction takes place on the γ -carbon by means of a 6-membered cyclic ring. This leads to cleavage of the α - β carbon-carbon bond giving a terminal olefin and an enol which tautomerizes rapidly to the more stable ketone ($R=CH_2CH_3$):^{7,13}



Yang and Yang¹⁵ showed that, instead of occurring by a concerted process that leads to C-C bond cleavage, the reaction proceeds via an energetically faster 1,4-biradical intermediate. This was confirmed by Wagner¹⁶ by means of biradical trapping experiments.

The efficiency of hydrogen abstraction is affected by the multiplicity and electronic configuration of the excited state of the ketone. The (n, π^*) state is considerably more reactive in γ -hydrogen abstraction than the (π, π^*) triplet state (it is comparable to an alkoxy radical). The geometry of the $n \rightarrow \pi^*$ transition causes a decrease in negative charge on the oxygen atom, making it more electrophilic. The now vacant non-bonding orbital will become involved in reactions in which the electron is replaced.¹⁰ On the other hand, the (π, π^*) triplet state will cause an increase in the negative charge on the oxygen atom making it less electrophilic, and is thus less effective in hydrogen abstraction (than the (n, π^*) triplet). If, however, the (π, π^*) triplet state is the lowest lying state, and it lies sufficiently close to the upper (n, π^*) triplet, vibrational mixing can occur between them and there will be some increased reactivity toward hydrogen abstraction.^{1,10}

The (π, π^*) triplet state is stabilized in a polar solvent, and even more stabilized when there is a relatively small energy difference between the (n, π^*) and (π, π^*) triplet states of the ketone. The formation of the (π, π^*) triplet is also favoured when there are electron-donating substituents on the aromatic ring, thus decreasing the rate of Norrish type II γ -hydrogen abstraction, which requires the (n, π^*) triplet. Electron-withdrawing substituents, however, will favour the formation of the (n, π^*) triplets and cause an increase in the rate of Norrish type II γ -hydrogen abstraction.^{1,6}

Solvent quality and coil density also effect the efficiency of the Norrish type II (and to some extent Norrish type I) reaction in polymers. In order for the two polymer fragments to separate apart, they must diffuse and become disentangled. The rate of disentanglement is determined by the tightness of the coiling and is strongly dependant on the molecular weight of the polymer. If the quality of the solvent is poor, the coil density increases, causing increased entanglement and a decrease in the rate of diffusional separation.

Another factor that becomes important with increased coil density is photoreduction which competes with chain scission.¹⁷ The reason is that a more tightly coiled polymer will make it more likely for previously distant hydrogen atoms to come into contact with an excited carbonyl. This reaction leads to the formation of a new chain radical. An increase in energy transfer and self quenching also become factors in a tightly coiled polymer due to the decrease in the distance between chromophores.^{18,19} This will in turn reduce the rate of random chain scission. On the other hand, as the solvent quality increases, the coil density will decrease, causing an increase in the rate of diffusional separation.²⁰ This is reflected by an increase in the rate of random chain scission.⁷

Several structural factors affect the quantum yields of the Norrish type II reactions in keto-polymers. In small ketones, the efficiency of γ -hydrogen abstraction is independent of ketone concentration, temperature, solution viscosity and the presence of oxygen. However, in polymer molecules, the efficiency of the Norrish type II reaction is very much dependent on the structure of the polymer, for example, the strength of the C-H bond is an important factor in hydrogen abstractability. An increase in chain length of carbonyl compounds causes a reduction in the quantum yield for the Norrish type II reaction ϕ_{II} . This reflects the increasing difficulty in forming the required six-membered cyclic transition state.^{1,21} However, for small methyl and phenyl compounds, ϕ_{II} is independent of chain length.¹⁰ The restricted mobility associated with a decrease in temperature, and in the case of a polymer at sub- T_g temperatures, is particularly important. This results in a decrease in ϕ_{II} because of difficulty attaining the specific conformational requirements for γ -hydrogen abstraction.

An increase in substitution on the γ -carbon will promote the extraction of the proton and increase the efficiency of the Norrish type II reaction, on account of the decrease in bond

dissociation energy of the γ -C-H bond.⁷ Substitution by an electron-donating group on the γ -carbon will also reduce the bond dissociation energy of the γ -C-H bond, and increase the rate of γ -hydrogen abstraction by the electron-deficient oxygen of the (n,π^*) state.¹ On the other hand, electron-withdrawing groups have the opposite effect.

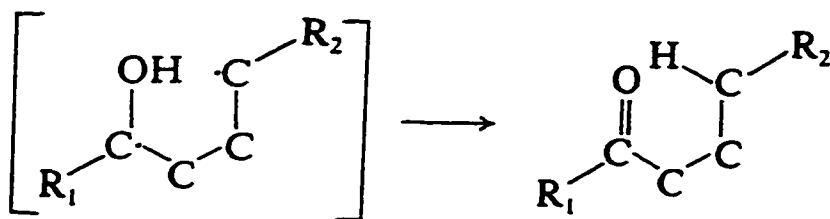
Another structural factor that affects the efficiency of the Norrish type II reaction is the proximity of the ketone chromophore to the γ -hydrogen. The required conformation of the γ -hydrogen relative to the carbonyl is *syn*. This allows the formation of a strain free, 6-membered cyclic transition state in the preferred chair configuration.^{1,17} A γ -hydrogen in the *anti* conformation must rotate to the *syn* conformation before undergoing the Norrish type II reaction.¹⁷ If, however, the triplet lifetime is shorter than the time required for a conformational change (*anti* to *syn*), only the ketones originally in the *syn* configuration will participate in the Norrish type II reaction. This is known as ground state control.^{17,22} In most cases the rate of Norrish type II H-abstraction is about two orders of magnitude greater than the rate of rotation. Thus triplets in the *anti* conformation adopt a passive role in the Norrish type II reaction.

In the ground state, the *anti* and *syn* conformations exist in thermal equilibrium, with the *syn* conformer being more abundant. As a result, both the singlet and triplet (n,π^*) states can exist in two distinct conformations.²³ γ -hydrogen abstraction occurs from the *syn* conformation to give the Z-enol, while α -cleavage can occur from the *anti* conformation. Since both are more rapid than ring inversion, the nature of the products will reflect the relative composition of *anti* and *syn* conformations in the ground state.^{6,24} The rate of γ -hydrogen abstraction can be increased by imposing steric constraints on the rotations of the bonds between the γ -C-H and the carbonyl to

reduce unfavourable conformations. In this case, it is possible that the *anti* conformer can participate in H-abstraction.

Two conformationally distinct enols have been detected following γ -hydrogen abstraction. The *syn*-enol is produced directly by the hydrogen abstraction by both the excited singlet and triplet *syn* conformers, which has been confirmed by triplet quenching studies.²³ Triplet quenching studies also show that only the excited triplet state of the *anti* conformer participates in photoenolization reactions.⁶ Its existence can be explained in terms of the relatively long lifetime of the 1,4-biradical intermediate of the *syn* conformer which allows rotational isomerization (photoisomerization) of the 1,4-biradical intermediate to the *anti* conformation, giving the *anti*-enol.^{23,25,26} A number of *o*-acylstyrenes have been studied and it has been shown that these undergo photoenolization, and a reaction scheme for photoenolization is shown in Figure 1.5.^{23,25,26}

The 1,4-biradical intermediates resulting from the Norrish type II reaction play a very important role in the efficiency of Norrish type II γ -hydrogen abstraction. Spectroscopic properties of the 1,4-biradicals produced in carbonyl-containing polymeric systems show much similarity to analogous mono-radicals. Thus, biradical processes exhibit typical mono-radical behaviour.²⁵ The 1,4-biradical intermediates have been shown to participate in competing processes such as internal disproportionation (reverse hydrogen transfer) which causes rearrangement to the ground state ketone,^{1,27}



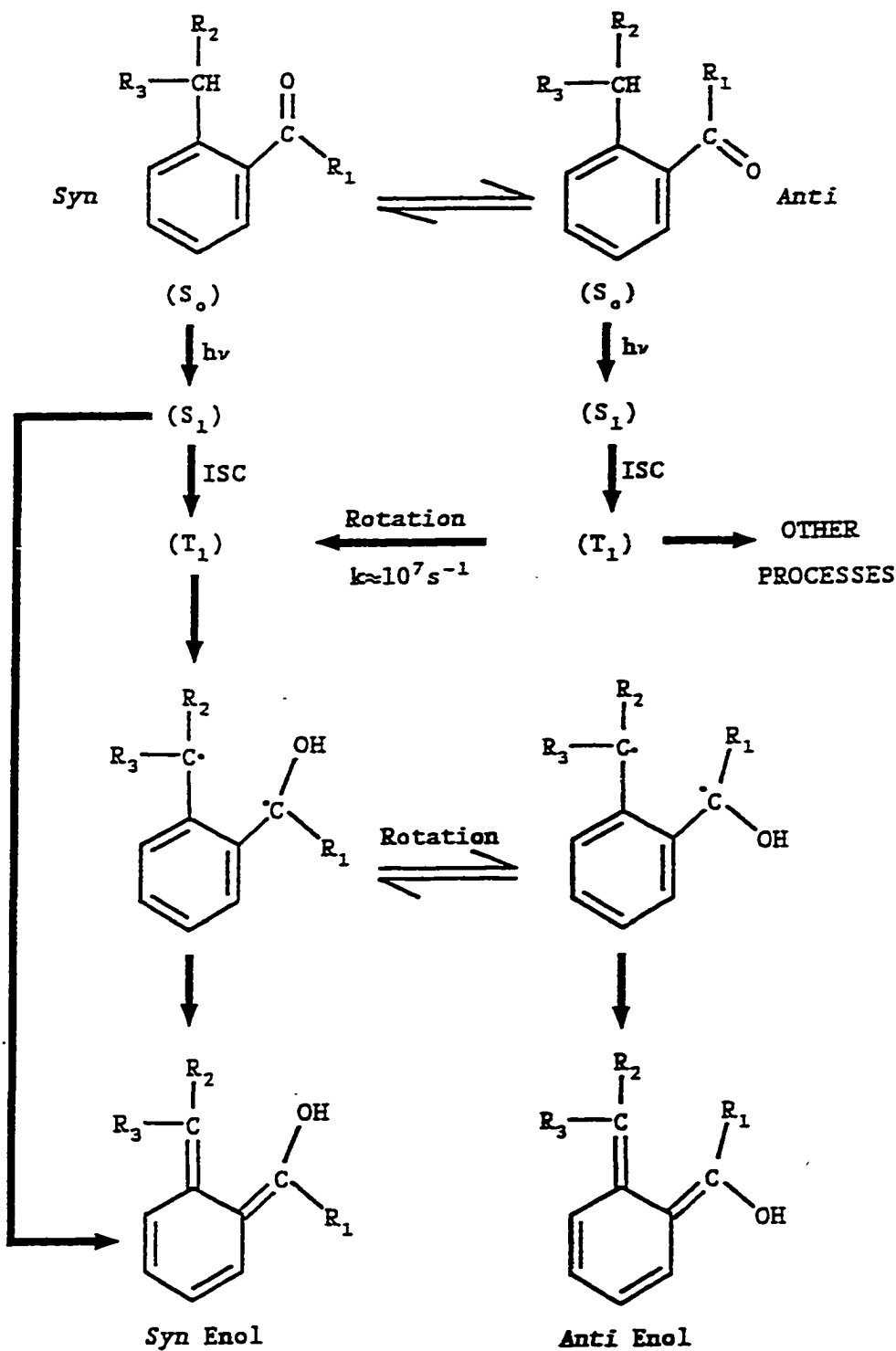
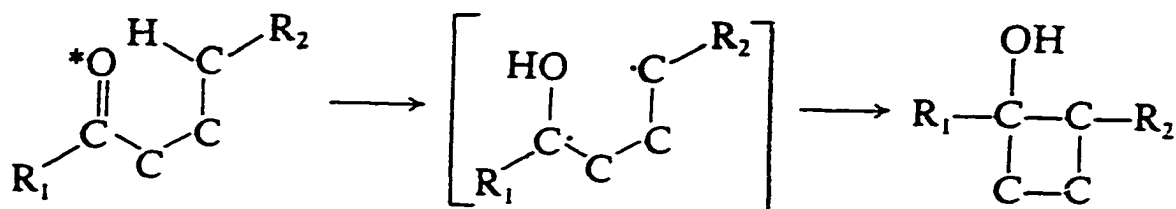


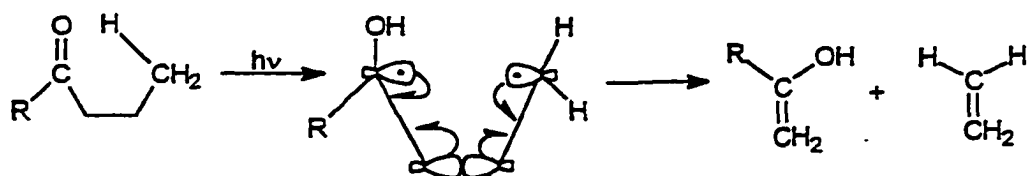
Figure 1.5. Photoisomerization of phenyl alkyl ketones.²⁴

as well as cyclization to form cyclobutanol.^{1,15,24}



The lifetimes of the biradicals are independent of temperature but are dependent on the solvent, lifetimes of the biradicals being enhanced by polar solvents, and this is attributable to the formation of hydrogen bonds, which cause an increase in the distance between the two radical sites. This will ultimately lead to a decrease in the rate of intersystem crossing, preventing reverse hydrogen transfer from occurring. Because cyclization involves only the reaction of the two radical centres, a polar solvent will cause a decrease in the rate of cyclization, resulting in a corresponding considerable increase in ϕ_{II} .²⁴ On the other hand, a polar solvent can sometimes cause contraction of the coils in a polymer which will result in a decreased rate of diffusion and this will ultimately lead to a decrease in the rate of chain scission.²¹

The efficiency of the Norrish type II reaction, in terms of the biradicals, is dependent on the degree that the α - β carbon-carbon and the p-orbital of the biradical are parallel to one another. The more parallel they are, the greater the degree of overlap that can occur between the p-orbitals and the developing π -orbitals of the double bonds.⁶ An example of the conformation that best meets these criteria is as follows:⁶



Any factors that impede the fulfilment of these requirements will cause a reduction in the efficiency of cleavage, ϕ_{II} .

4. REACTIONS THAT OCCUR IN THE ABSENCE OF γ -HYDROGENS

In the absence, or lack of accessibility, of γ -hydrogens, Norrish type I photodegradation, photocyclization, intermolecular hydrogen abstraction (photoreduction) and intramolecular δ -hydrogen abstraction may occur. Studies of poly(vinyl acetophenone) and poly(α -methyl vinyl acetophenone), which lack γ -hydrogens, showed that photodegradation occurred by either a Norrish type I reaction or by photoreduction to give a new polymer radical:^{1,28,29}

PHOTOREDUCTION



New polymer radical

Intermolecular hydrogen abstraction involves the removal of a H atom from a suitable adjacent donor, and occurs most readily when the lowest triplet state of a ketonic species is (n,π^*). The electrophilic (n,π^*) state is stabilized by the relatively high electron density on the oxygen; hence little photoreduction occurs when the (π,π^*) triplet state is the lowest excited state. In compounds capable of undergoing intramolecular hydrogen abstraction, the extent of intermolecular hydrogen abstraction is negligible in terms of rates because of the preferred proximity of the hydrogen in the intramolecular abstraction.¹

Intramolecular δ -hydrogen abstraction involves the formation of a 1,5-biradical which will undergo similar reactions to the 1,4-biradical produced in γ -hydrogen abstraction. The 1,5-biradical will cyclize to form a relatively stable 5-membered ring. However, the cyclic intermediates involved in the intramolecular abstraction of β , δ and even more distant hydrogens, are torsionally strained making them less favourable when γ -hydrogens are present.^{1,30}

VII/ SOLUTION VERSUS SOLID STATE PHOTODEGRADATION

Studies of the photochemistry of ketone-containing polymers in the solid phase have shown that, even at low temperatures, there exists enough molecular motion for photochemical reactions such as the Norrish type II reaction to occur. At 0°K, the constituents of a polymer in thin film possess no motion. As the temperature is increased, the specific volume of the polymer increases. Since bond lengths do not change to a significant extent, the specific volume results from the formation of small holes or voids (free volume) in the polymer matrix, which increase in size and/or number as the temperature increases. This increase in free volume enhances molecular motion, and when the glass transition temperature T_g is reached, segmental motion can occur.³¹

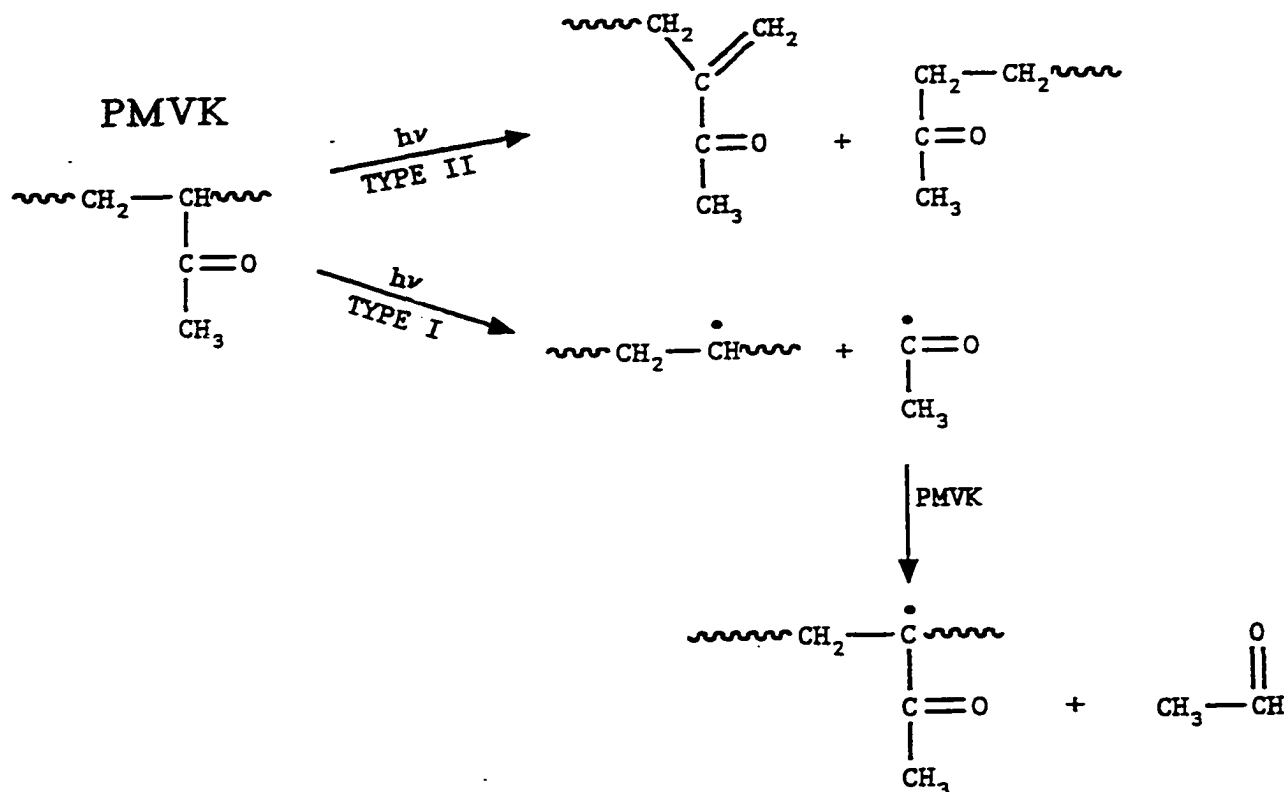
At temperatures above T_g , the free volume increases enough to achieve specific conformational requirements for photoprocesses.³¹ The rate-determining step for reactions in the solid state is defined by the physical state of the polymers, in particular, it is sensitive to the free volume of the polymer.^{31,32} Quantum yields of reactions like the Norrish type II reaction in the solid state decrease considerably at temperatures below T_g , unless the most stable conformation of the polymer is that in which the reaction occurs.³³ The decrease in chain scission can also be associated

with a stronger cage effect in the solid state, which will in turn reduce the rate of diffusive separation of the macro-fragments formed by biradical collapse.

In the crystalline state in which the free volume is much smaller, it has been observed that quantum yields of Norrish type I and II reactions can be both dependent and independent of temperature. For example, in 7-tridecadone, measurements made below its melting point indicated zero quantum yields for Norrish type I and type II reactions.³⁴ At a few degrees above the melting point however, the quantum yield for Norrish type II was comparable to that in solution at the same temperature. This can be explained by a lack of free volume due to the rigidity of the polymer matrix, or possibly also from the delocalization of excitation throughout the crystal.³¹ It is possible for a reaction to take place if the photon releases enough energy to cause local melting in the matrix. There are, however, exceptions to this, for example diacetylene in which the monomer and polymer crystals are almost identical.³¹ In general, quantum yields of reactions of polymers in the solid state are at least two orders of magnitude lower than those in solution, and this reflects the general lack of mobility in the solid state.

VIII/ PREVIOUS STUDIES OF POLY(ACRYLOPHENONES)

Research into the photochemistry of ketone-containing polymers was initiated by Guillet and Norrish^{35,36} who studied the photochemistry of poly(methyl vinyl ketone) (PMVK) in solution and determined that it underwent both Norrish type I and II reactions as follows:^{1,7}

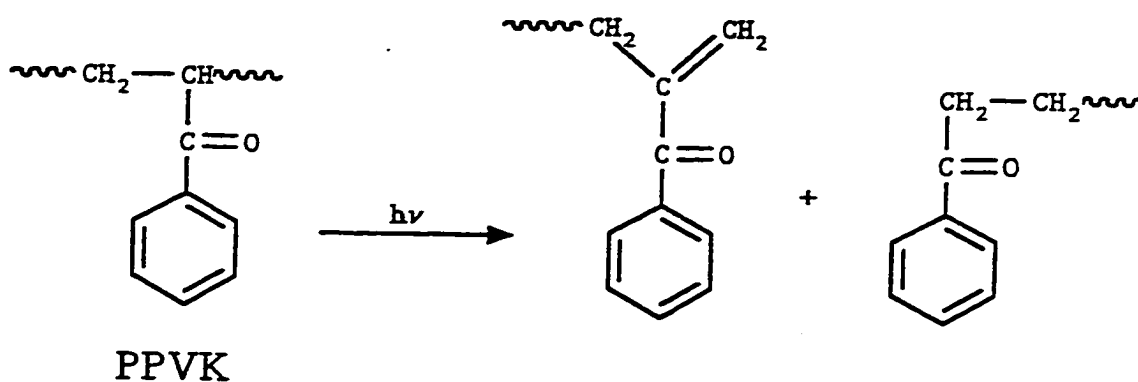


The Norrish type I reaction (α -cleavage) produced an acetyl radical which subsequently abstracted a proton to form acetaldehyde. The Norrish type II reaction is the principle reaction involving random chain scission and occurs via γ -hydrogen abstraction. The quantum yield for the Norrish type II reaction was greater and it was shown that the quantum yield of chain scission decreased with an increase in degradation.¹ This was attributed to the repolymerization by the addition of the radicals formed in the Norrish type I reaction to the terminal olefin produced by the Norrish type II reaction. The efficiency of the type I reaction was dependent upon both the stability of the radical and the rate of diffusion of the radicals (more recent work would suggest that self-quenching was involved).¹

This led to the study of poly(acrylophenone) (PAP), commonly known as poly(phenyl vinyl ketone) (PPVK). Acrylophenone (AP), and derivatives of AP are very sensitive to light and can be

polymerized and copolymerized with ease.¹ PAP has been intensely investigated^{37,38,39,40,41} and is an excellent model of study because aromatic ketones have very rapid intersystem crossing, so all photophysical and photochemical processes occur from the triplet state.^{37,38} Triplet energy transfer in PAP has been investigated^{37,40} and it was shown that very efficient triplet energy transfer occurs along the polymer chains. Thus, the simplest photochemistry was observed by copolymers of AP where the ketone groups are regarded as isolated. Many copolymers of AP have been synthesized^{19,42,43,44,45} and it has been shown that chain scission occurs efficiently.

The main form of degradation of PAP (or PPVK) has been determined to proceed via the Norrish type II reaction to give random chain scission:^{1,7}



Salvin *et al.*⁴⁶ have determined quantum yields of chain scission for oligomers, dimers and trimers of PAP in benzene solutions under nitrogen. It was shown that the quantum yields for the various photoproducts are independent of oligomer configuration.¹

The presence of 1,4-biradicals was confirmed by Small and Scaiano⁴⁷ and they showed that they are very reactive and can undergo intermolecular reactions. The absorbance spectrum of the biradicals was similar to that observed for small aromatic ketones at 450nm. The decay of the biradical was determined to be first order with a lifetime of 76ns in benzene at room temperature.

It was also shown that the rate of decay of the biradicals was increased in the presence of biradical scavengers such as atomic oxygen, NO, SO₂ and tertiary butyl nitrite.

Salvin *et al.*⁴⁶ determined the rate constant for triplet energy transfer for PAP by static quenching of the Norrish type II reaction and found it to be similar to that for valerophenone. This indicates that the rate constant for triplet-triplet energy transfer is independent of the position of the carbonyl when either bound or free. The efficiency of triplet energy transfer from PAP to many common quenchers has been investigated.^{37,43,48,49} Kilp and Guillet showed that the efficiency of triplet energy migration is different for isotactic and atactic forms of PAP, but that the quantum yields for photolysis were almost identical.^{50,51}

Intramolecular triplet energy transfer may also take place after long exposures to UV radiation. The Norrish type II reaction produces an unsaturation on the end of the polymer chain which can act as a triplet quencher for any excited species. The number of unsaturations produced will increase with an increase in exposure time, and eventually self-quenching will become a factor. Self-quenching was confirmed by the non-linearity of S (random chain scission) versus time curves after long irradiation times. These unsaturated groups are efficient quenchers because of the rapid energy transfer that takes place with carbonyl triplets.^{1,37,38}

Substituted AP polymers have been extensively investigated. In all cases the principle reactions are Norrish type II and random chain scission.^{41,52,53,54,55,56,57,58,59,60,61,62,63} The quantum yields for chain scission have been determined and alkyl substituents in the para position on the aromatic ring increases the quantum yield as does halogen substitution (fluorine, chlorine and bromine), but iodine substitution causes the polymer to degrade in a different manner all together. The quantum yield of chain scission is decreased by p-phenyl substitution as well as by the substitution by the

electron-repelling p-methoxy, 3,4 methoxy and 3,5-methoxy groups. Mechanisms for the degradation of methoxy-substituted poly(acrylophenones) have been suggested⁷ and it has been observed that the quantum yields for chain scission are considerably low, and the triplet lifetimes, considerably high. This in turn has been attributed to the increased (π, π^*) character of the carbonyl triplets which leads to a decrease in reactivity in H-abstraction - which is a prerequisite for the Norrish type II reaction.

PURPOSE

The photophysics of a number of methoxy-substituted poly(acrylophenones) have previously been investigated and characterized,⁷ and the photodegradation of these polymers have been studied in solution. The principal degradative reaction is a Norrish type II reaction which leads to random chain scission and to molecular weight decreases. However, coloration also occurs and mass spectroscopy showed that O-CH₃ bond fission was occurring in the methoxy-substituted rings. This, in turn leads to the formation of phenoxy radicals, and the coloration was attributed to the formation of quinonoid species from these radicals. While independent evidence for O-CH₃ fission in the ring was obtained, confirmation data were required. To this end an ethoxy substituted analogue was required.

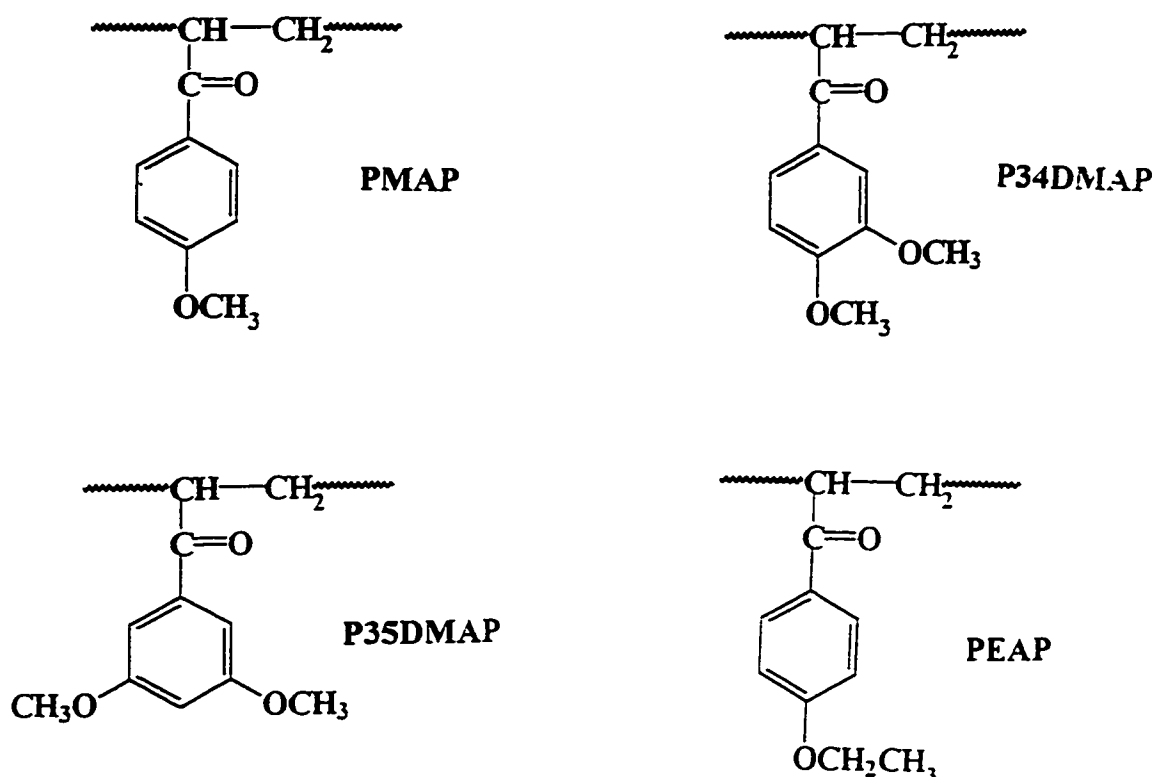
The aims of this work were (a) to study the photophysics and photochemistry of poly(p-ethoxyacrylophenone) (PEAP) in both solid state and solution, a new polymer which had not previously been prepared or characterized, (b) to study the photoreactions of the methoxy poly(acrylophenones), i.e. poly(p-methoxyacrylophenone) (PMAP), poly(3,4-dimethoxyacrylophenone) (P34DMAP) and poly(3,5-dimethoxyacrylophenone) (P35DMAP) in the solid state, little being previously known about their reactions in this medium. The results of these studies have some implications for the photo-yellowing (color reversion) of lignin-rich pulps.

Lignin-rich paper produced by mechanical, semi-mechanical and chemi-mechanical pulping methods experiences yellowing upon exposure to terrestrial sunlight.⁶⁴ The coloration has been associated with UV absorbing components of lignin that undergo photo-reactions.⁶⁵ Lignin is a complex and intractable macromolecular compound, thus studies of photo-yellowing have been done on much simpler model compounds which contain the same chromophores. It has been suggested

that the phenolic hydroxyl group and the aromatic ketone (α -carbonyl) are important in the initial stages of degradation.^{66,67} The yellowing has been attributed to the formation of quinones, which are formed via phenoxy radicals.^{68,69}

Methoxy poly(acrylophenones) are very simple models for lignin, having the advantage that they are macromolecular in nature. Previous work has shown that in solution these compounds undergo O-CH₃ fission upon UV irradiation. The resulting phenoxy radicals are obvious precursors for quinonoid compounds, and the present studies are of more relevance to the actual photochemical degradation of lignin which occurs in the solid state. Another aim is to investigate the photo-yellowing of these compounds in the solid state.

Quenching studies of these polymers were carried out with a number of standard quenchers. However, this work was extended to investigate the possible inhibitory action of two standard light absorbers which are used to retard polymer degradation.



EXPERIMENTAL

I/ POLYMER PREPARATION

The monomer of PMAP was synthesized using previously described methods.^{42,70} The monomer of P34DMAP was prepared in the same manner, but methoxybenzene was replaced with the molar equivalent of 1,2-dimethoxybenzene and the monomer of P35DMAP was prepared similarly, but with methoxybenzene being replaced by the molar equivalent of 3,4-dimethoxybenzene. The monomer of PEAP was synthesized similarly, but methoxybenzene was replaced with the molar equivalent of ethoxybenzene. The polymers of PMAP, P34DMAP, P35DMAP and PEAP were produced by bulk polymerization at 60°C under high vacuum in the absence of an initiator for PMAP and P34DMAP and PEAP, and in the presence of azobisisobutyronitrile (10^{-3} M) for P35DMAP. The polymerization was stopped at approximately 20% conversion to minimize any side reactions by immersing the reaction vessels in liquid N₂. The polymers were isolated by precipitation in methanol. Purification proceeded through repeated dissolution in CH₂Cl₂ followed by precipitation in methanol. The polymers were dried at 70°C at 10^{-5} kPa then stored under vacuum in the dark.

The monomer of P35DMAP was polymerized in the same way, but in the presence of azobisisobutyronitrile to prevent the formation of extremely high molecular weight polymers ($>10^7$) with large polydispersities (>5) which formed in the absence of the initiator.⁷ Because of their limited stability, these high molecular weight polymers readily formed gels and this made characterization by gel permeation chromatography nearly impossible and unreliable. The initiator residues that exist at the chain ends have very low effective concentrations and are not expected to have significant effects on the photochemical reactions of the polymers.⁶²

II/ POLYMER CHARACTERIZATION

The molecular weights of the polymers were determined by gel permeation chromatography (GPC). This was done by combining Waters equipment with a UV detector and a 7.8 x 300 mm Ultrastyrigel® column with 7 μm pores. The polymers were dissolved in CHCl_3 and run through the column at a flow rate of $1.0 \text{ cm}^3 \text{ min}^{-1}$. The column was calibrated against narrow range poly(styrenes).

1. INFRARED (IR) SPECTRAL CHARACTERISTICS

The infrared spectrum of the polymers were recorded in a Brüker IFS66 FTIR Infrared Spectrophotometer. Polymers were dissolved in CH_2Cl_2 and were slowly evaporated onto a NaCl plate to form a layer of polymer film.

2. NUCLEAR MAGNETIC RESONANCE (NMR) SPECTRAL CHARACTERISTICS

Polymers were dissolved in CDCl_3 and the ^1H and ^{13}C assignment were determined using a Brüker AC-E 200 MHz NMR with tetramethylsilane (TMS) used as a standard reference. The identification of the individual carbon atoms were confirmed by spectral editing using Distortionless Enhancement by Polarization Transfer (DEPT) sequence.

3. ULTRAVIOLET (UV) SPECTRAL CHARACTERISTICS

Polymers in both solution (CH_2Cl_2) and film had UV spectra recorded on a Perkin Elmer Lambda 11 UV/VIS Spectrometer. Thin films were prepared by the slow evaporation of a polymer solution (CH_2Cl_2) on the inner wall of a quartz cell.

4. EMISSION CHARACTERISTICS

The fluorescence spectra of polymer solutions in CH_2Cl_2 were determined using a Perkin Elmer LS50B Luminescence Spectrometer. The phosphorescence spectra and phosphorescence lifetimes of the polymers in glass at 77K were also determined using a Perkin Elmer LS50B Luminescence Spectrometer. The analysis of direct phosphorescence quenching was done by obtaining phosphorescence spectra of the polymers with and without quenchers in glass at 77K using a Perkin Elmer LS50B Luminescence Spectrometer.

III/ PHOTOCHEMICAL TECHNIQUES IN SOLUTION

For photochemical studies of the polymers in solution, 6×10^{-2} M dilute polymer solutions were prepared in CH_2Cl_2 . These solutions were placed in a pyrex reaction vessel which was sealed to an Ubbelohde viscometer as shown in Figure 2.1. The solutions were rigorously degassed with N_2 and sealed so that photooxidation could not occur. The apparatus was immersed into a thermostat controlled water bath at $25^\circ\text{C} \pm 1\%$. The apparatus was inverted and the time of flow through the viscometer was determined for the pure solvent (t_0) and for the original polymer solution (t).

The polymer solution was then exposed to long-wave UV radiation ($\lambda \geq 300$ nm) with a Hanovia 200 W medium pressure Hg arc lamp. The solution was kept at a constant distance of 10 cm for all irradiations. The changes in molecular weight were obtained by recording the time of flow of the polymer through the viscometer after several different times of irradiation. Quenching studies were performed in the identical manner as above but by adding either a quencher or light absorber to the original polymer solution prior to degassing.

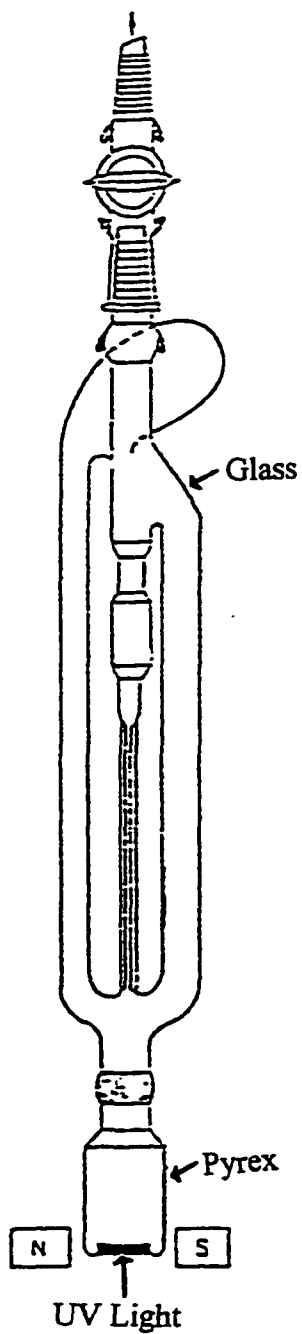


Figure 2.1. Cannon Ubbelohde viscometer for photochemical studies of polymer solutions.⁷

IV/ PHOTOCHEMICAL TECHNIQUES IN FILM

Photochemical studies of polymers in thin film involved the slow evaporation of a polymer solution (CH_2Cl_2) on the inner wall of a specially designed pyrex reaction vessel (Figure 2.2). The vessels were rigorously degassed with N_2 and sealed to prevent photooxidation. These polymer films were exposed to long-wave UV radiation ($\lambda \geq 300 \text{ nm}$) with a Hanovia 200 W medium pressure Hg arc lamp being kept at a constant distance of 10 cm for all irradiations.

The changes in molecular weight were obtained by irradiating samples at different time intervals. The molecular weights of the irradiated polymers were determined by gel permeation chromatography (GPC). This was done by combining Waters equipment with a UV detector and a 7.8 x 300 mm Ultrastyrigel[®] column with 7 μm pores. The polymers were dissolved in CHCl_3 and run through the column at a flow rate of $1.0 \text{ cm}^3 \text{ min}^{-1}$.

V/ ANALYTICAL TECHNIQUES

The analyses of degraded polymeric residues in solution and film took place by examining the polymers at regular intervals of exposure. This was done using a Brüker IFS66 FTIR spectrometer (IR), a Brüker AC-E 200 MHz NMR spectrometer (^1H and ^{13}C NMR spectra, DEPT sequences) and a Perkin Elmer Lambda 11 UV/VIS spectrometer (UV spectra). Changes in molecular weights in both solution and film were determined by gel permeation chromatography (GPC). This was done by combining Waters equipment with a UV detector and a 7.8 x 300 mm Ultrastyrigel[®] column with 7 μm pores. The polymers were dissolved in CHCl_3 and run through the column at a flow rate of $1.0 \text{ cm}^3 \text{ min}^{-1}$.

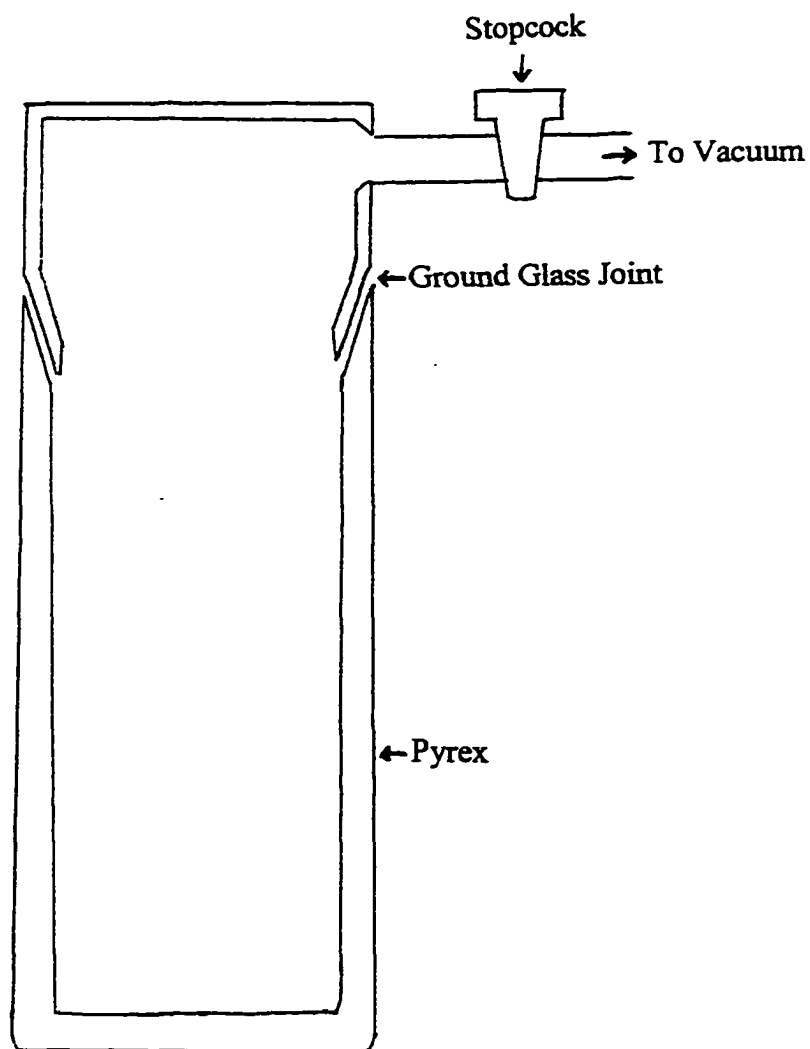


Figure 2.2. Irradiation cell for air free irradiation of polymer films.⁷

VI/ VOLATILE PRODUCT ANALYSIS

Low molecular weight gaseous products were analyzed using an in-line quadrupole mass spectrometer (Spectramass Dataquad 200) which rapidly and repeatedly scanned the range $1 < m/e < 200$ amu. The measurements were made on samples that were withdrawn from the reaction vessel at regular intervals by high vacuum. The equipment was calibrated using authentic samples (Matheson) of the volatile products.

RESULTS

I/ POLYMER CHARACTERIZATION

The number-average and weight-average molecular weights and the polydispersities of PMAP, P34DMAP, P35DMAP and PEAP were determined and are listed in Table 3.1. It can be seen that PMAP, P34DMAP, P35DMAP and PEAP are wide range polymers, and this is perhaps attributable to their ease of polymerization, which, in turn favors gel effects.

Table 3.1. GPC Analysis of Methoxy and Ethoxy-Substituted Poly(acrylophenones).

POLYMER	NUMBER-AVERAGE MOLECULAR WEIGHT (\bar{M}_n)	WEIGHT-AVERAGE MOLECULAR WEIGHT (\bar{M}_w)	POLYDISPERSITY $\left(\gamma = \frac{\bar{M}_w}{\bar{M}_n}\right)$
PMAP	3.2×10^4	7.2×10^5	22.38
P34DMAP	2.2×10^4	3.6×10^5	13.84
P35DMAP	9.6×10^2	1.1×10^3	1.123
PEAP	1.7×10^4	2.0×10^6	17.77

1. INFRARED SPECTRAL CHARACTERISTICS

The infrared absorption characteristics of polymers PMAP, P34DMAP and P35DMAP which have been previously reported,⁷ are typical of aromatic carbonyl polymers having strong absorptions characteristic of carbonyl stretching at 1670 cm^{-1} , 1660 cm^{-1} and 1650 cm^{-1} respectively. Polymer PEAP has similar characteristics with a strong carbonyl absorption at 1670 cm^{-1} . The data is shown in Figure 3.1.

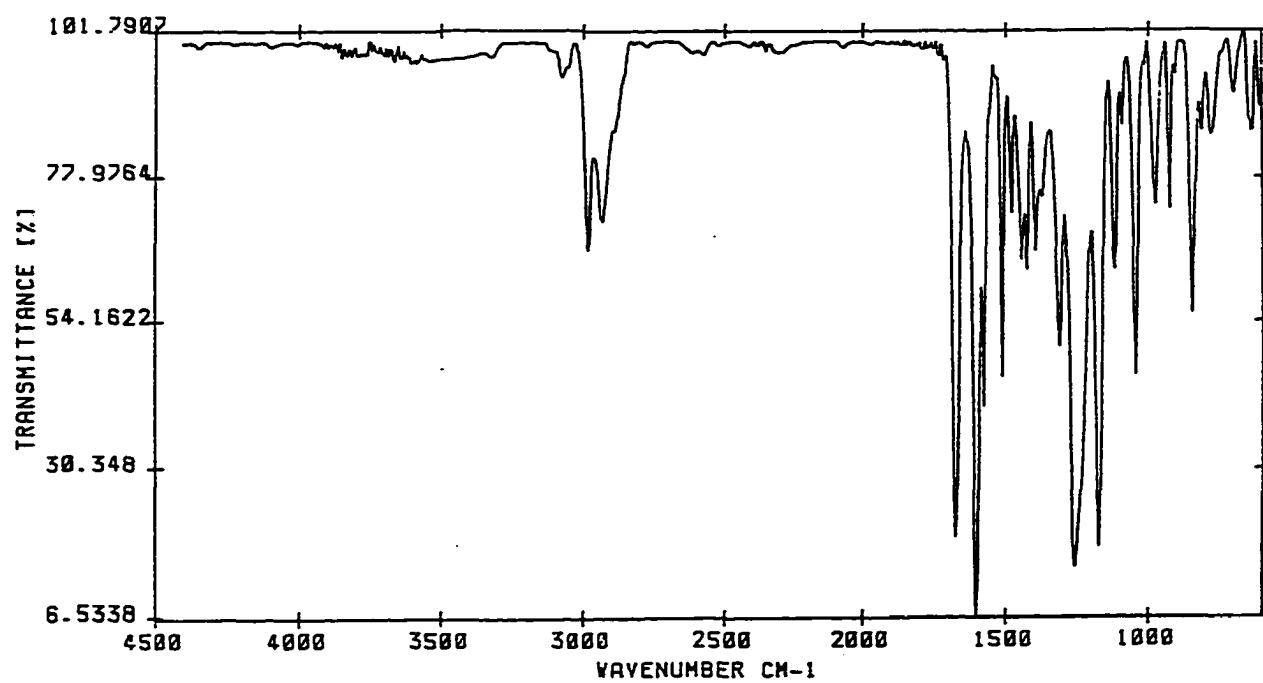
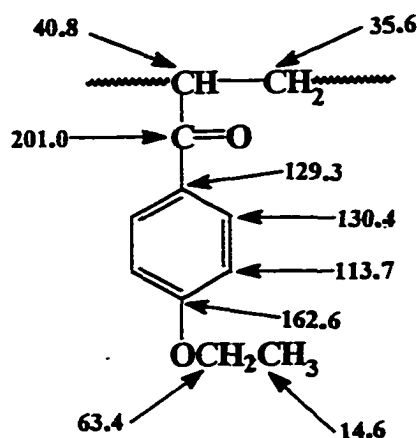


Figure 3.1. Infrared spectrum of PEAP.

2. NUCLEAR MAGNETIC RESONANCE SPECTRAL CHARACTERISTICS

^1H and ^{13}C NMR assignments for polymers PMAP, P34DMAP and P35DMAP have been previously made and the identities of the individual carbon atoms were confirmed using a DEPT sequence.⁷ The ^1H and ^{13}C NMR spectra of PEAP along with the identifications of individual carbon atoms using a DEPT sequence are shown in Figures 3.2 and 3.3 respectively.



3. UV SPECTRAL CHARACTERISTICS OF POLYMERS IN SOLUTION

The UV absorption spectra of PMAP, P34DMAP, P35DMAP and PEAP in solution ($3.0 \times 10^{-4}\text{M}$ in CH_2Cl_2) are shown in Figure 3.4. The major absorbance for all is associated with the $\pi\text{-}\pi^*$ transition of the phenyl group which occurs in the short-wave region around 280nm. The weaker absorption is associated with the symmetry forbidden $n\text{-}\pi^*$ transition of the carbonyl and occurs in the terrestrial solar spectral region ($\lambda \geq 295\text{nm}$) for all four polymers. The $\pi\text{-}\pi^*$ and $n\text{-}\pi^*$ absorption bands overlap in all four polymers and are distinguishable in all polymers except for PEAP where there is a complete overlap of the two absorptions. This complete overlap is caused by a red-shift of the $\pi\text{-}\pi^*$ absorption band. It is well known that electron donating groups (e.g.

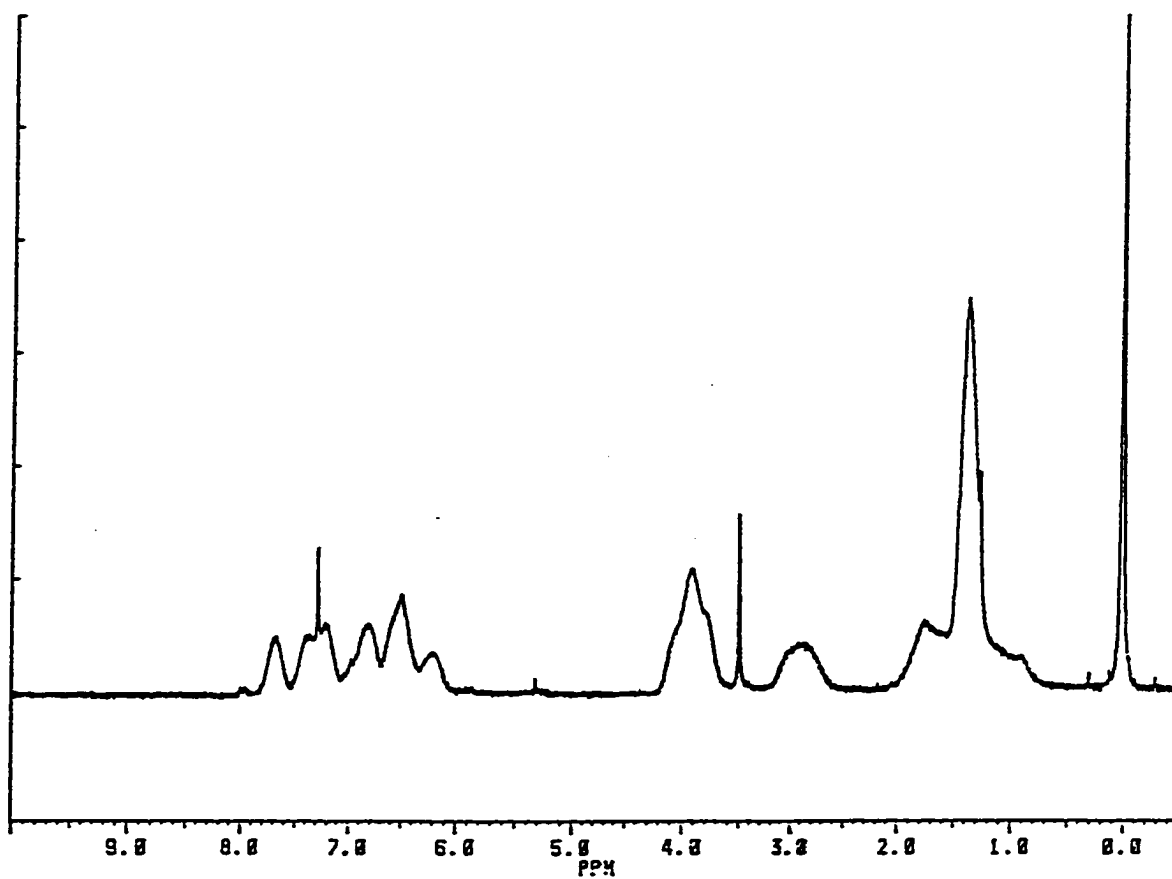


Figure 3.2. ^1H NMR spectrum of PEAP.

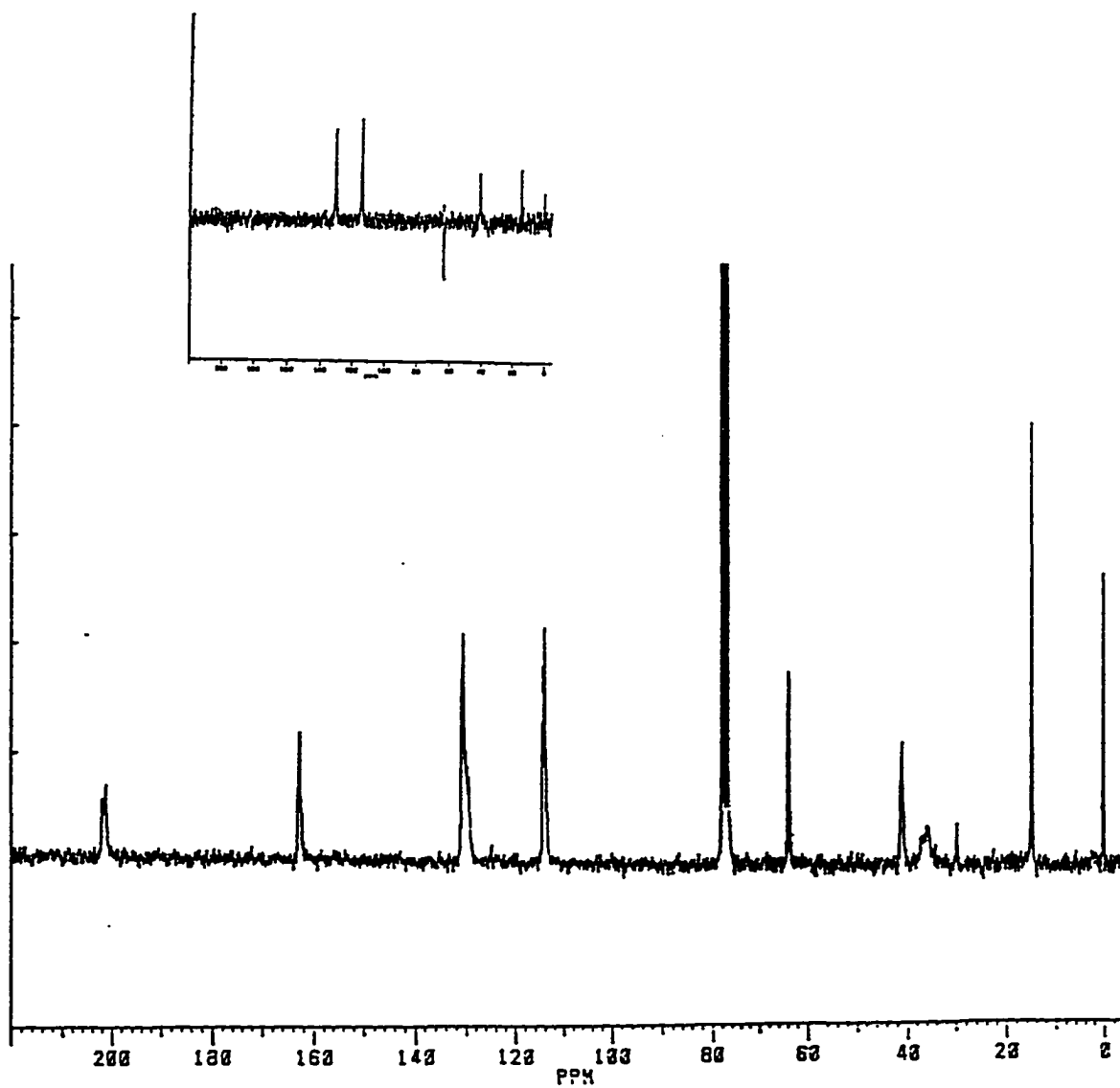


Figure 3.3. ^{13}C NMR spectrum and corresponding DEPT sequence of PEAP.

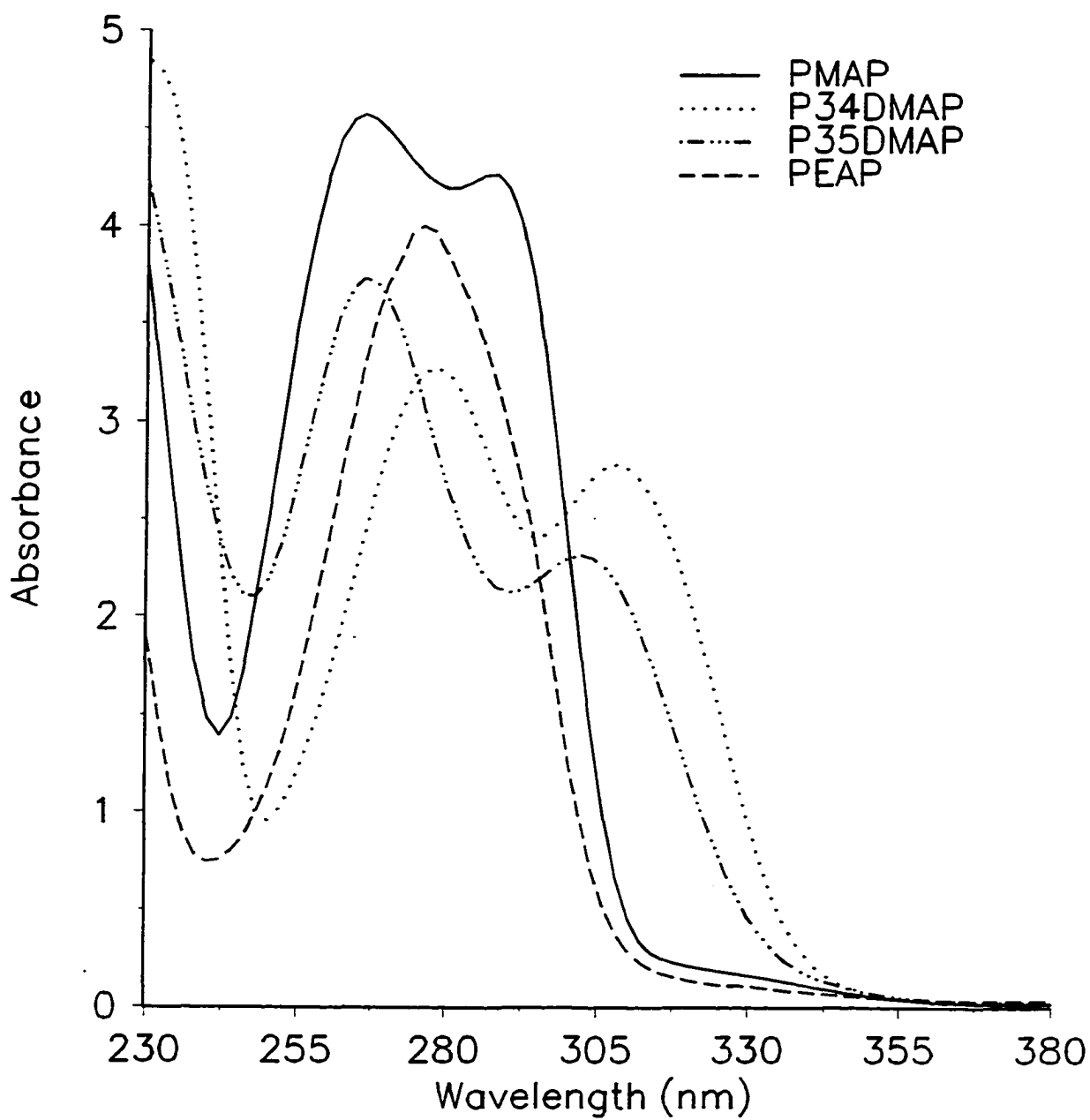


Figure 3.4. UV absorption spectra of PMAP⁷, P34DMAP⁷, P35DMAP⁷ and PEAP (3×10^{-4} M solution in CH_2Cl_2 and instrument sensitive to 0.0001% T).

alkyl) in the ring shift the $\pi \rightarrow \pi^*$ absorption to large wavelengths, and as a consequence more overlap occurs with the $n \rightarrow \pi^*$ absorption.¹

The molar absorption coefficient ϵ , was determined from Figure 3.4 using the relation with absorbance:³

$$\epsilon = \frac{A}{cl}$$

where A is the absorption or optical density, c is the concentration and l is the effective path length. The UV absorption characteristics of PEAP and the previously determined characteristics of PMAP⁷, P34DMAP⁷ and P35DMAP⁷ are summarized in Table 3.2. Because of overlap in PEAP (i.e. the $n \rightarrow \pi^*$ absorption is not resolved), the ϵ value for PEAP was estimated on the basis of A values for the methoxy polymer.

Table 3.2. UV Absorption Characteristics of Methoxy⁷ and Ethoxy-Substituted Poly(acrylophenones) in 3×10^{-4} M Solution in CH_2Cl_2 .

POLYMER	$\lambda_{\text{max}} (n \rightarrow \pi^*)$ (nm)	Molar absorption coefficient, ϵ ($\text{dm}^3 \text{ mol}^{-1} \text{ cm}^{-1}$)
PMAP	305	270
P34DMAP	308	6400
P35DMAP	302	5250
PEAP	305	460

4. UV SPECTRAL CHARACTERISTICS OF POLYMERS IN THIN FILMS

The absorption spectra of these polymers in solution are qualitatively very similar to those of the same polymers in thin films (Figure 3.5), with the absorbances occurring in the same spectral region but intensities different. Polymers P34DMAP and P35DMAP again have distinguishable $\pi \rightarrow \pi^*$ and $n \rightarrow \pi^*$ absorptions, but the $\pi \rightarrow \pi^*$ absorptions of both PMAP and PEAP in thin film undergo bathochromic shifts (red-shifts) causing complete overlap and thus making the resolution of the two transitions impossible. In the case of thin films, UV absorption is better expressed by the Beer-Lambert law:³

$$I_A = I_0(1 - 10^{-\beta l})$$

in which I_A is the absorbed intensity, I_0 is the incident intensity, l is the thickness of the film and β is the absorption coefficient (equivalent to ϵc). In the case of PMAP and PEAP, β values at 305nm are estimated because of the overlap. The absorption coefficient β was determined from the slope of an absorbance versus thickness plot. The UV absorption characteristics of film are summarized in Table 3.3. λ_{\max} values of PMAP and PEAP are estimated at 305nm.

Table 3.3. UV Absorption Characteristics of films of Methoxy and Ethoxy-Substituted Poly(acrylophenones) (1.5×10^{-4} cm thick).

POLYMER	λ_{\max} ($n \rightarrow \pi^*$) (nm)	Absorption coefficient, β (cm^{-1})
PMAP	305	1.9×10^4
P34DMAP	310	4.5×10^5
P35DMAP	304	3.7×10^5
PEAP	305	3.3×10^4

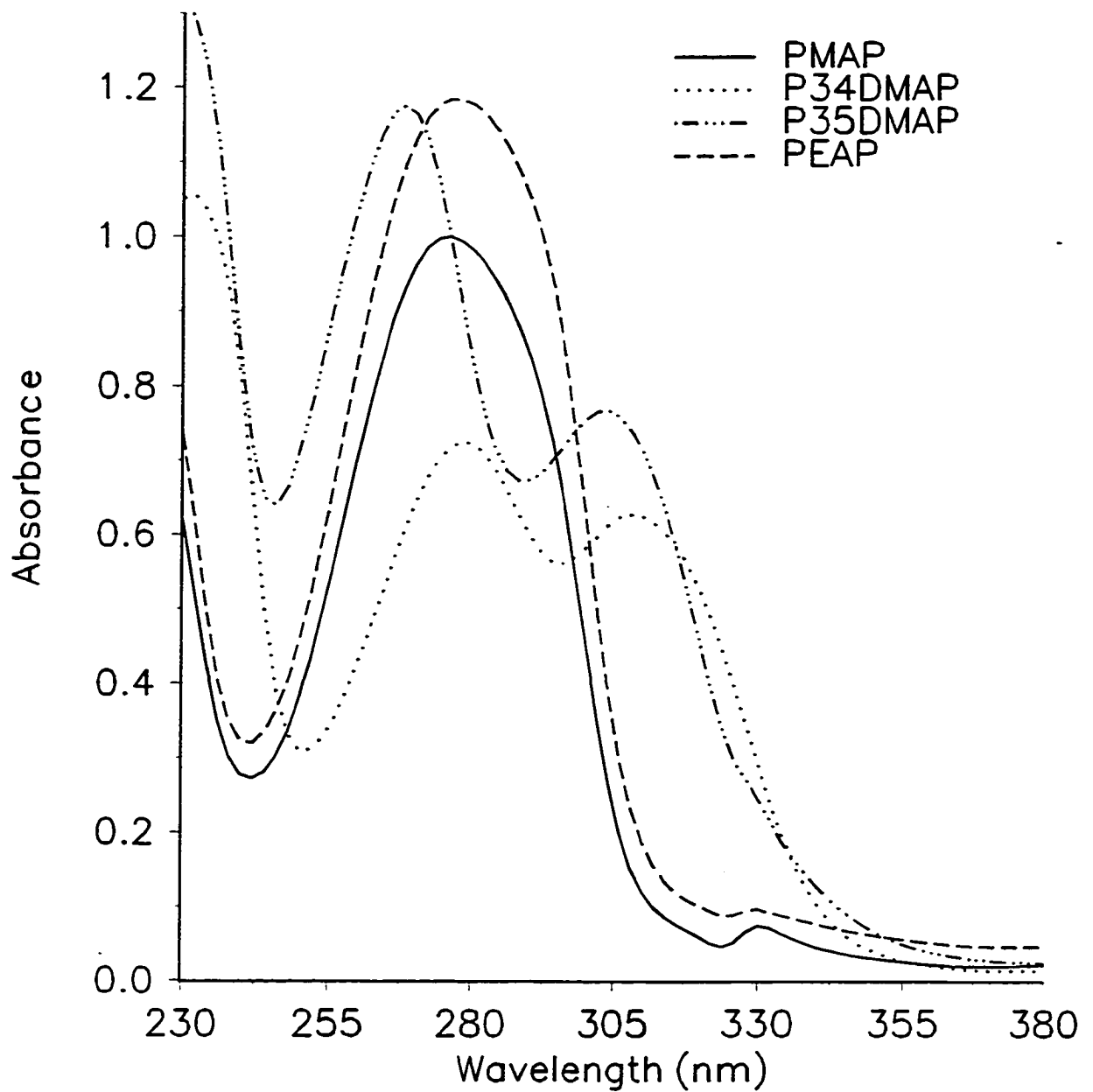


Figure 3.5. UV absorption spectra of PMAP⁷, P34DMAP⁷, P35DMAP⁷ and PEAP (1.5×10^{-4} cm film and instrument sensitive to 0.0001% T).

There is a large difference in the magnitude of ϵ and β values for solution and film and this is most likely due to the overlap of the $\pi \rightarrow \pi^*$ and $n \rightarrow \pi^*$ absorptions.

5. EMISSION CHARACTERISTICS OF FLUROESCENCE

The fluorescence and phosphorescence emission characteristics of PMAP, P34DMAP, P35DMAP and PEAP are shown in Figures 3.6 and 3.7 respectively along with their corresponding excitation spectra. The phosphorescence spectra indicates the existence of $n \rightarrow \pi^*$ triplets and the intensities of phosphorescence are much greater than fluorescence because the quantum yield of intersystem crossing is approximately unity in aromatic carbonyl triplets like these. This explains the very low quantum yields of fluorescence obtained previously for PMAP, P34DMAP and P35DMAP.⁷ The unknown quantum yield of fluorescence of PEAP ϕ_f was estimated by comparison with a compound of known quantum yield of fluorescence ϕ_{fk} , PMAP, using the relation:⁷

$$\phi_f = \frac{I_f \epsilon_k c_k}{I_{fk} \epsilon c} \phi_{fk}$$

where I_f and I_{fk} are the intensities of fluorescence of the unknown and known compounds respectively, ϵ and ϵ_k are the molar absorption coefficients of the unknown and known compounds respectively and c and c_k are the concentrations of the unknown and known solutions respectively.

This can be simplified in the relation:⁷¹

$$\phi_f = \frac{\text{Area under the true fluorescence emission curve for unknown}}{\text{Area under the true fluorescence emission curve for known}} \phi_{fk}$$

The characteristics of fluorescence are summarized in Table 3.4.

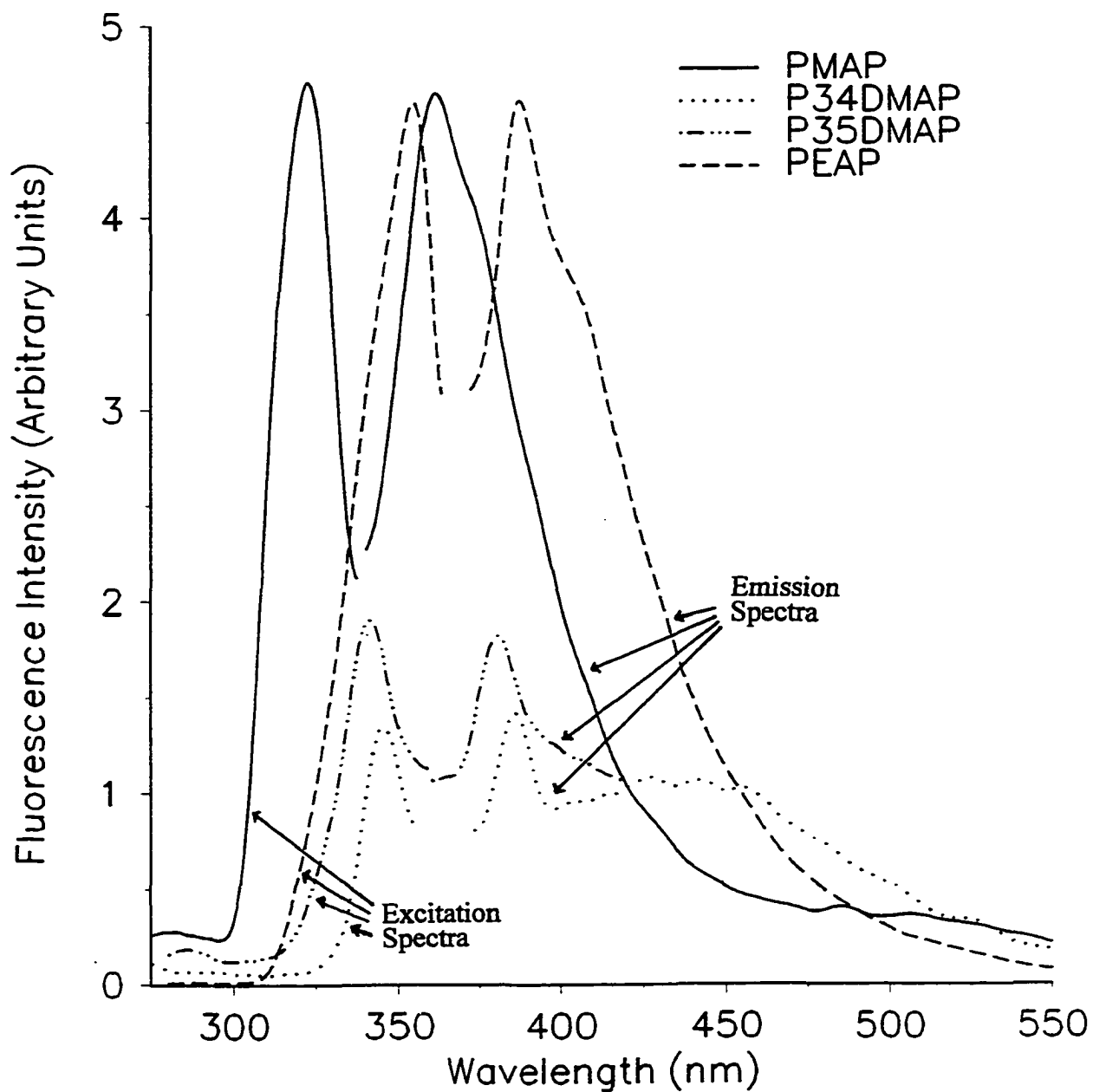


Figure 3.6. Fluorescence spectra of PMAP⁷, P34DMAP⁷, P35DMAP⁷ and PEAP (5×10^{-3} M solution in CH_2Cl_2) at room temperature.

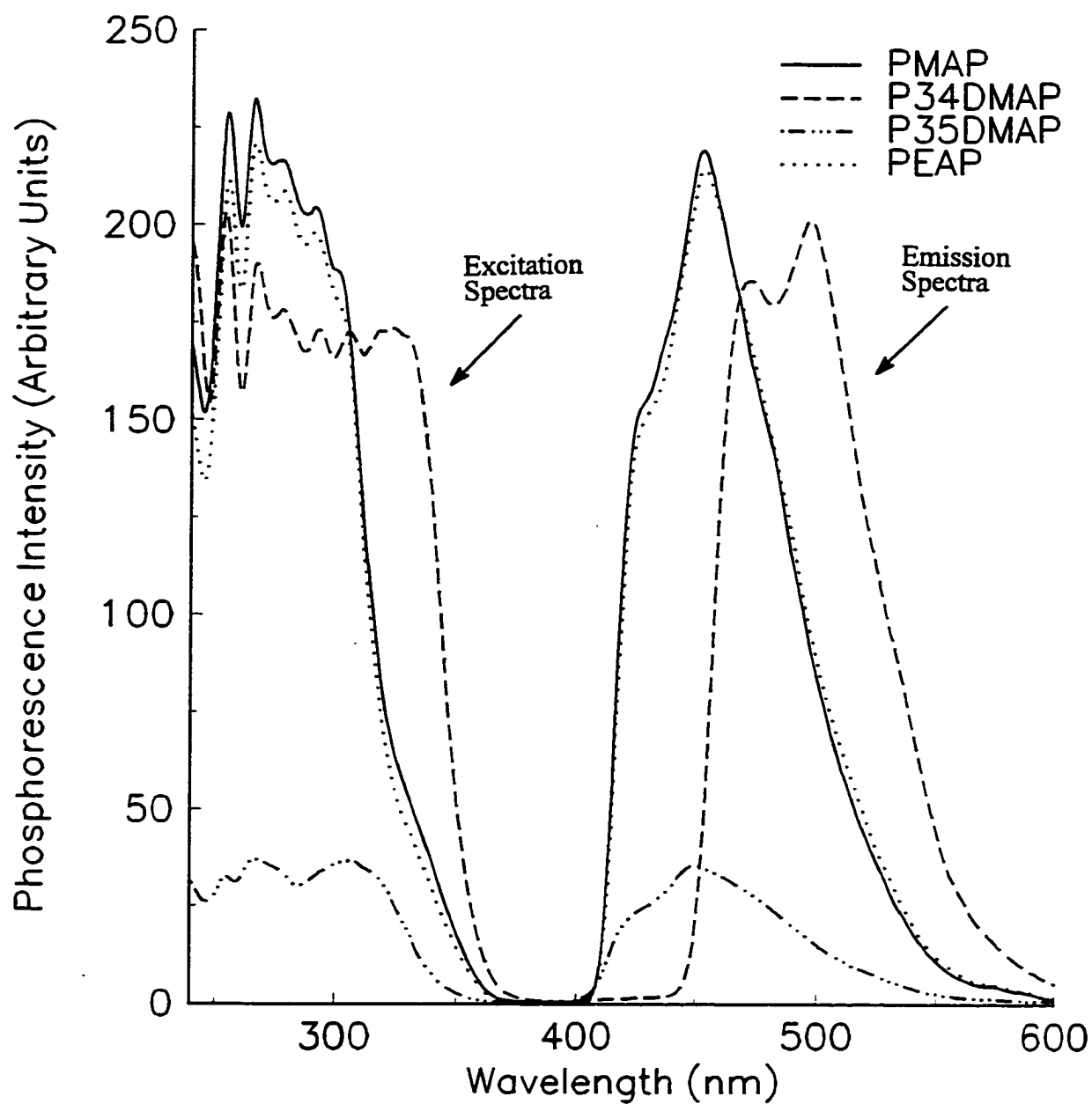


Figure 3.7. Phosphorescence spectra of PMAP⁷, P34DMAP⁷, P35DMAP⁷ and PEAP in glass at 77K.

Table 3.4. Fluorescence Characteristics of Methoxy⁷ and Ethoxy-Substituted Poly(acrylophenones) in 5×10^{-3} M Solution in CH_2Cl_2 .

POLYMER	λ_{max} (excitation) (nm)	λ_{max} (emission) (nm)	$\Phi_{\text{fluorescence}}$ (mol Einstein ⁻¹)
PMAP	323	361	1.35×10^{-4}
P34DMAP	346	385	2.42×10^{-4}
P35DMAP	341	381	3.55×10^{-5}
PEAP	354	388	1.0×10^{-4}

The quantum yield of PEAP is close in magnitude to that of PMAP. The very low fluorescence quantum yields suggest that the singlet state of the carbonyl does not participate in the photochemistry to a measurable extent.⁶²

It can be seen that a mirror image relationship exists between the excitation and fluorescence spectra (Figure 3.6). This symmetry and the relatively small Stokes shift (40nm) implies that the ground and excited electronic singlet states must have similar geometry and perhaps also have similar spacings between vibrational levels.

6. EMISSION CHARACTERISTICS OF PHOSPHORESCENCE AT 77K

The phosphorescence spectra also show reasonable mirror image symmetries along with little vibrational fine structure. This is typical of a triplet which has considerable $\pi-\pi^*$ character.⁷ The triplet energy $E_{\text{T}}(0-0)$ (Table 3.5) is the energy difference between the lowest vibrational levels of the excited triplet (T_1) and ground state (S_0). The absorption band of the greatest intensity is usually that of the (0,0) vibrational level transition and this corresponds to the longest absorbed and shortest

emitted wavelengths. PEAP has a lower triplet energy than the methoxy-substituted poly(acrylophenones). The triplet decay characteristics of PEAP are shown in

Figures 3.8 -3.11. It can be seen that they conform to reasonable exponential decays, ie.

$I_t = I_0 \left(10^{-\frac{t}{\tau}} \right)$, where I_0 is the initial intensity, I_t is the intensity at time t and τ is the triplet lifetime.

Triplet lifetimes were calculated from the slope of the log(phosphorescence intensity) versus time plots shown in Figures 3.12-3.15 using the following relation:

$$\log(I_t) = \frac{-0.434t}{\tau} + \log I_0$$

It can be seen that PEAP has a longer triplet lifetime than both PMAP and P35DMAP and this would confirm that it has substantial $\pi-\pi^*$ character. The phosphorescence characteristics are summarized in Table 3.5.

Table 3.5. Phosphorescence Characteristics of Methoxy and Ethoxy-Substituted Poly(acrylophenones) in glass at 77K.

POLYMER	λ_{\max} (emission) (nm)	E_T (0-0) (KJ mol ⁻¹)	$\tau_{\text{phosphorescence}}$ $\pm 5\%$ (ms)
PMAP	454	263	29
P34DMAP	497	241	47
P35DMAP	452	265	31
PEAP	451	265	37

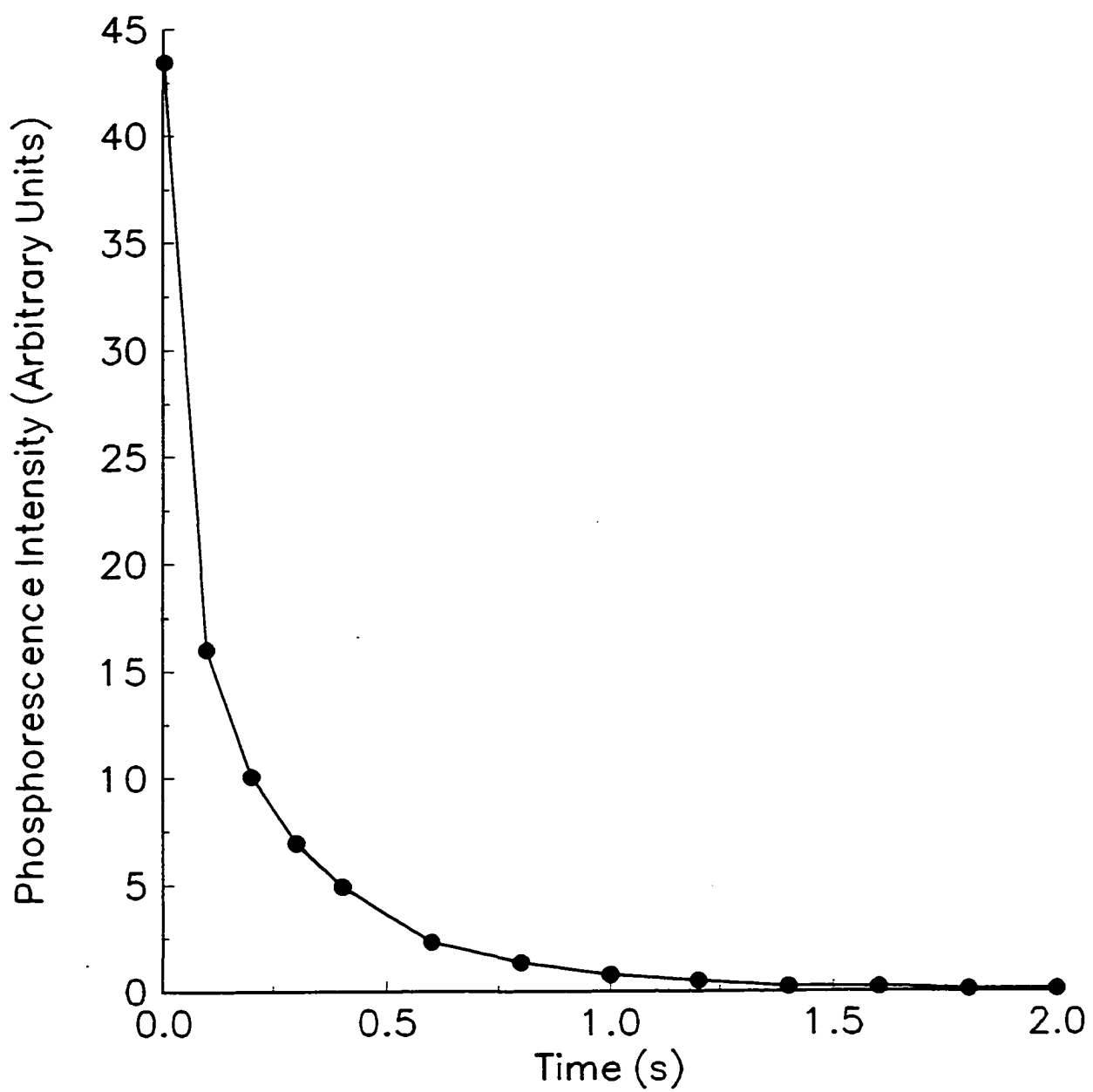


Figure 3.8. Phosphorescence decay characteristics of PMAP triplet in glass at 77K.

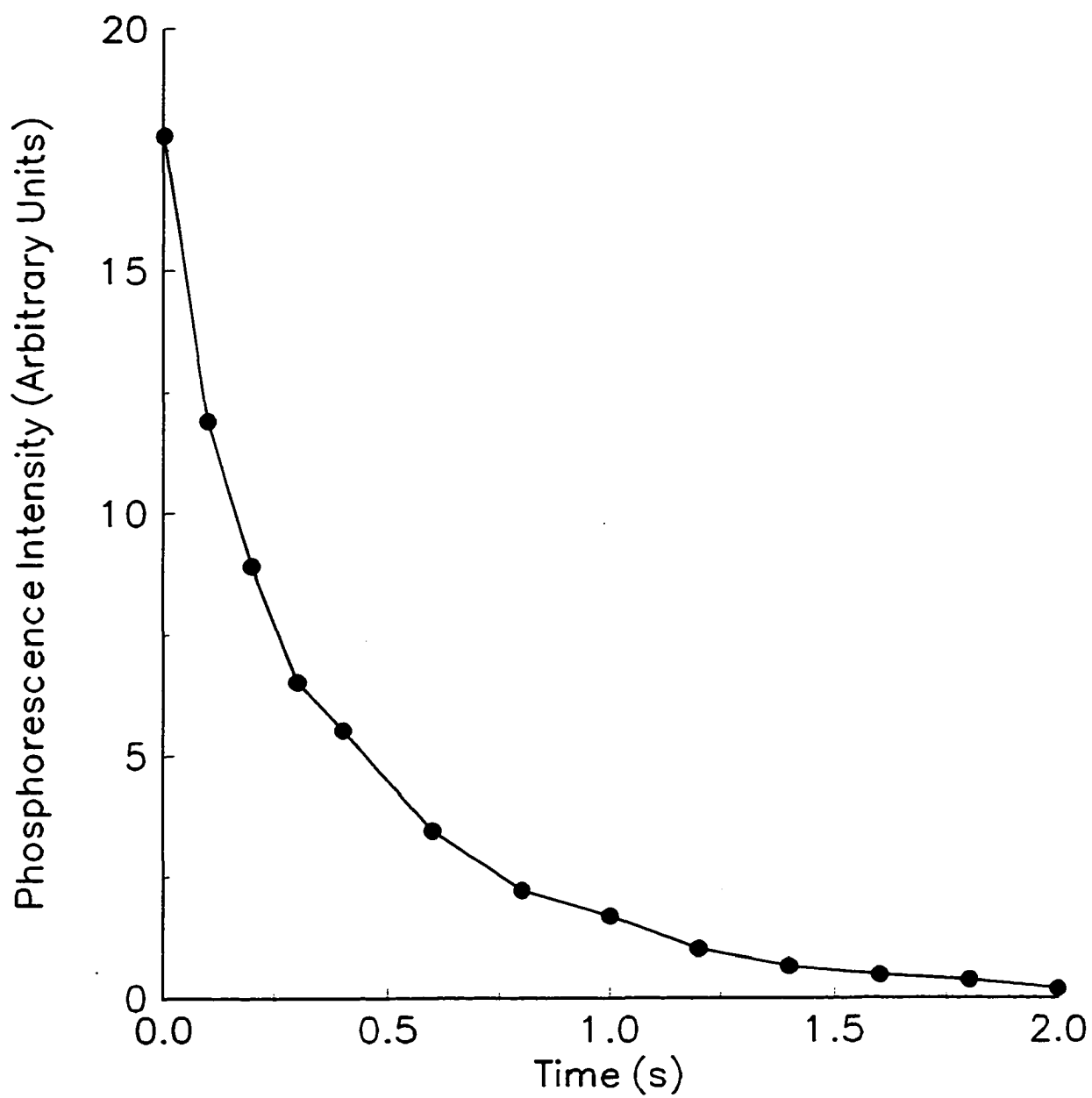


Figure 3.9. Phosphorescence decay characteristics of P34DMAP triplet in glass at 77K.

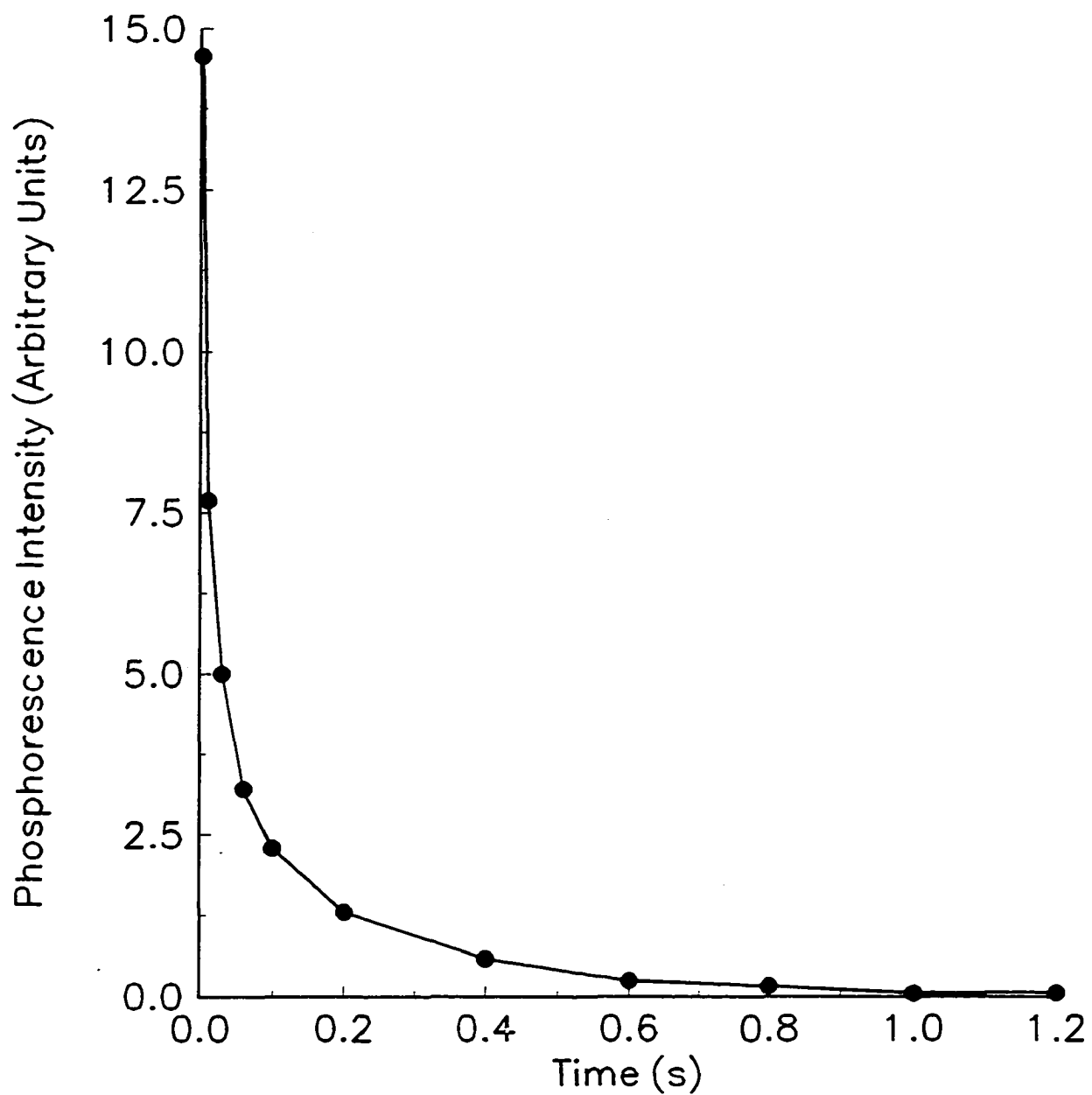


Figure 3.10. Phosphorescence decay characteristics of P35DMAP triplet in glass at 77K.

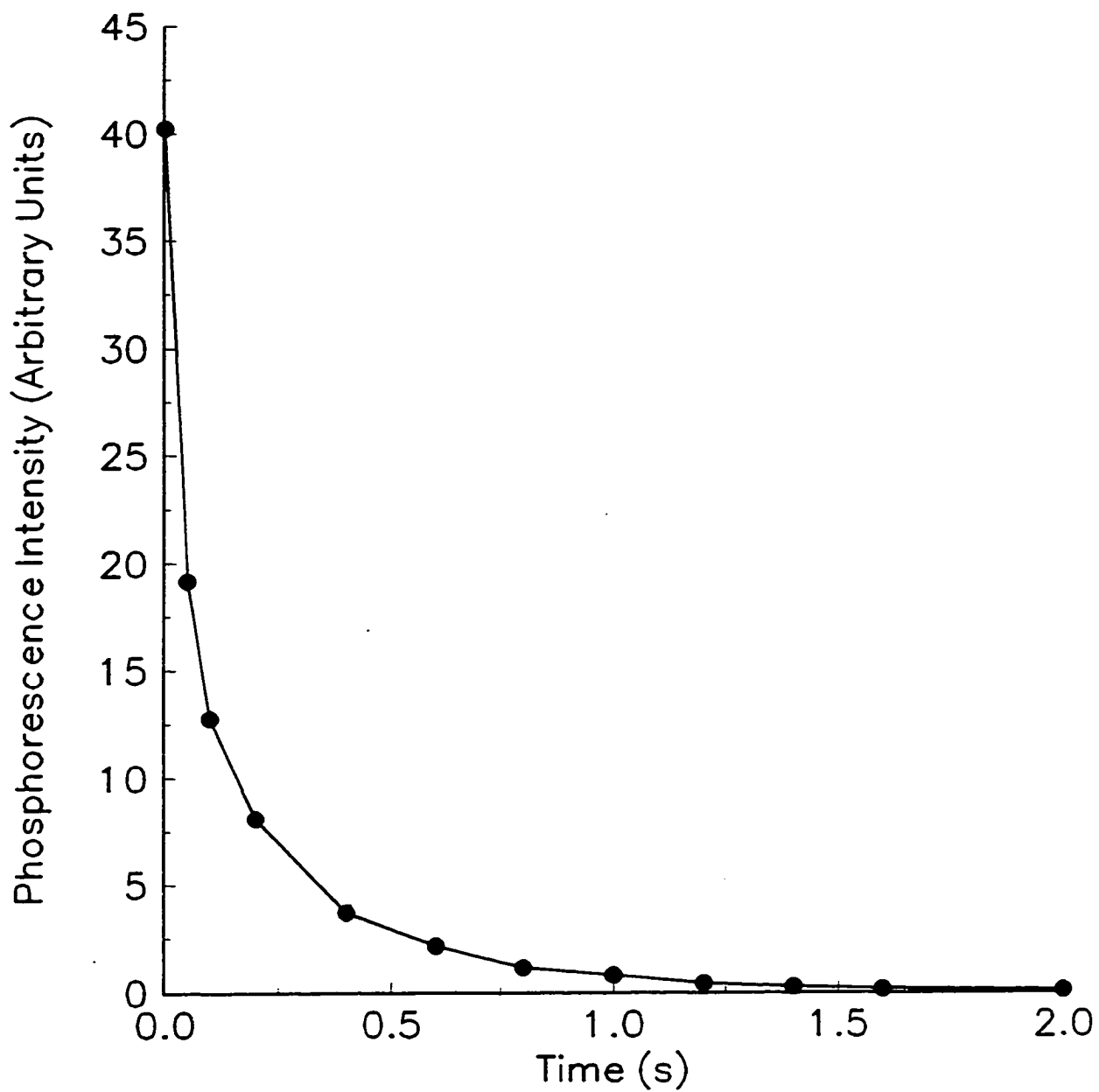


Figure 3.11. Phosphorescence decay characteristics of PEAP triplet in glass at 77K.

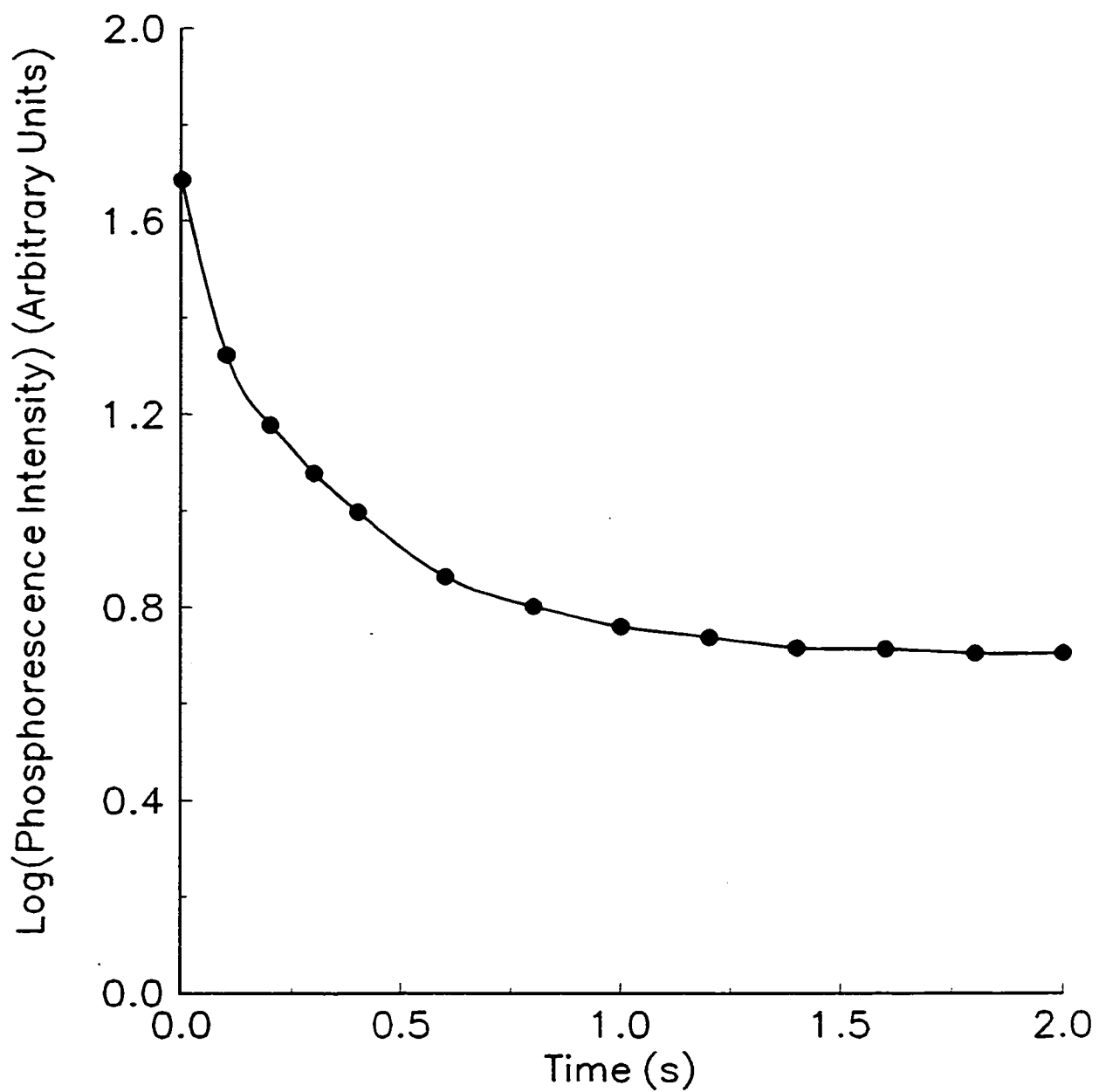


Figure 3.12. Phosphorescence decay characteristics of PMAP triplet in glass at 77K (semi-logarithmic plot).

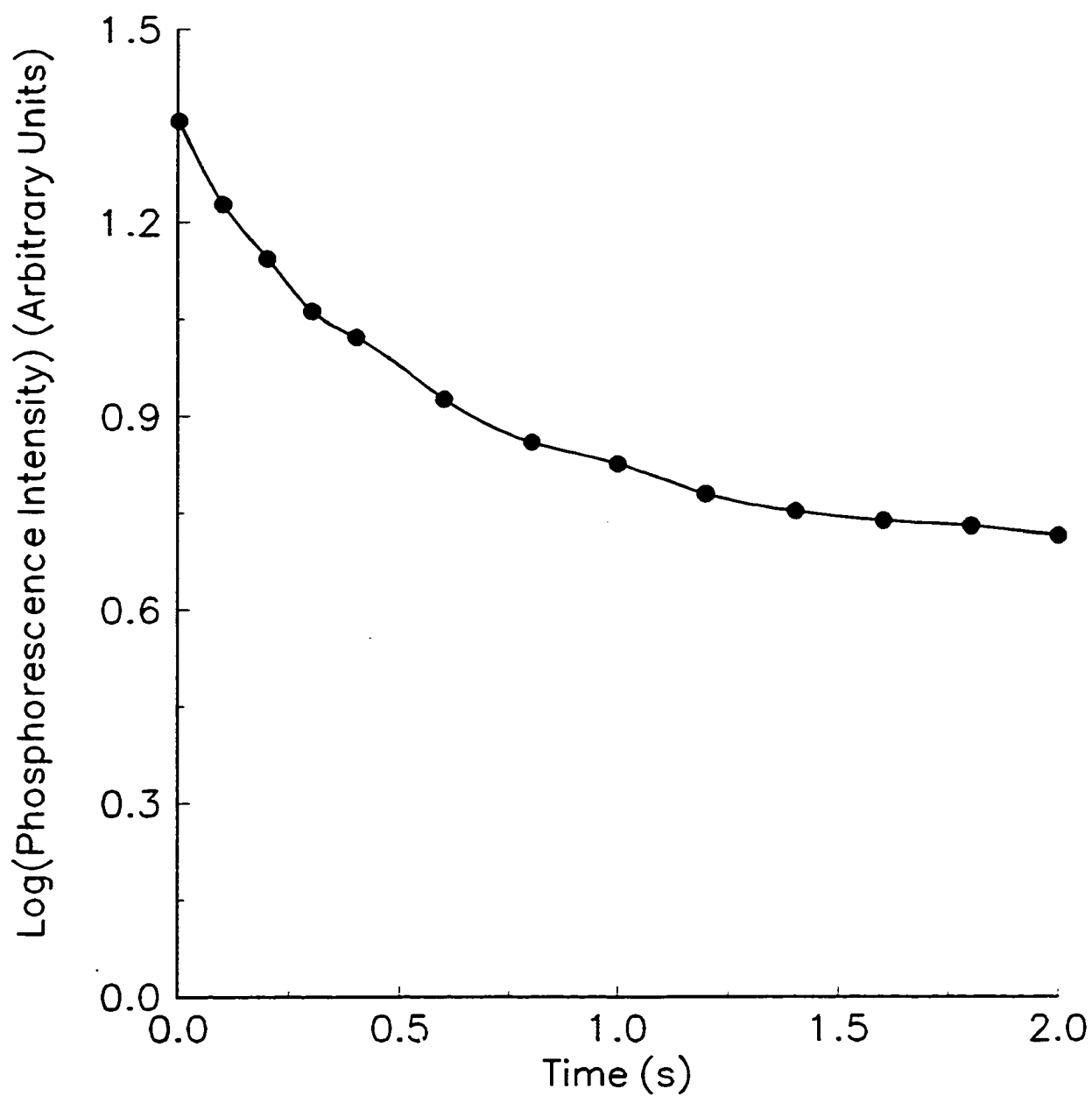


Figure 3.13. Phosphorescence decay characteristics of P34DMAP triplet in glass at 77K (semi-logarithmic plot).

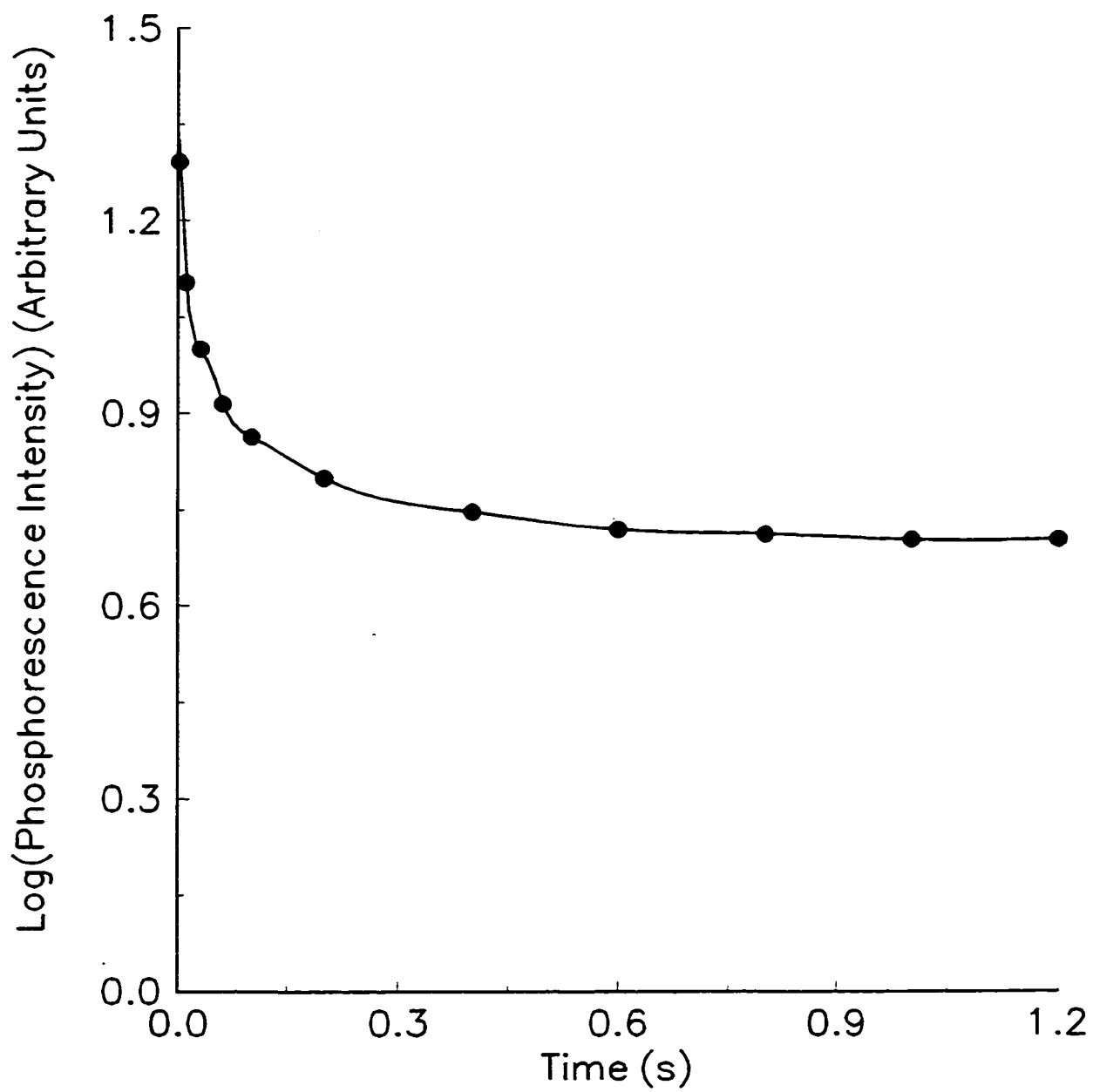


Figure 3.14. Phosphorescence decay characteristics of P35DMAP triplet in glass at 77K (semi-logarithmic plot).

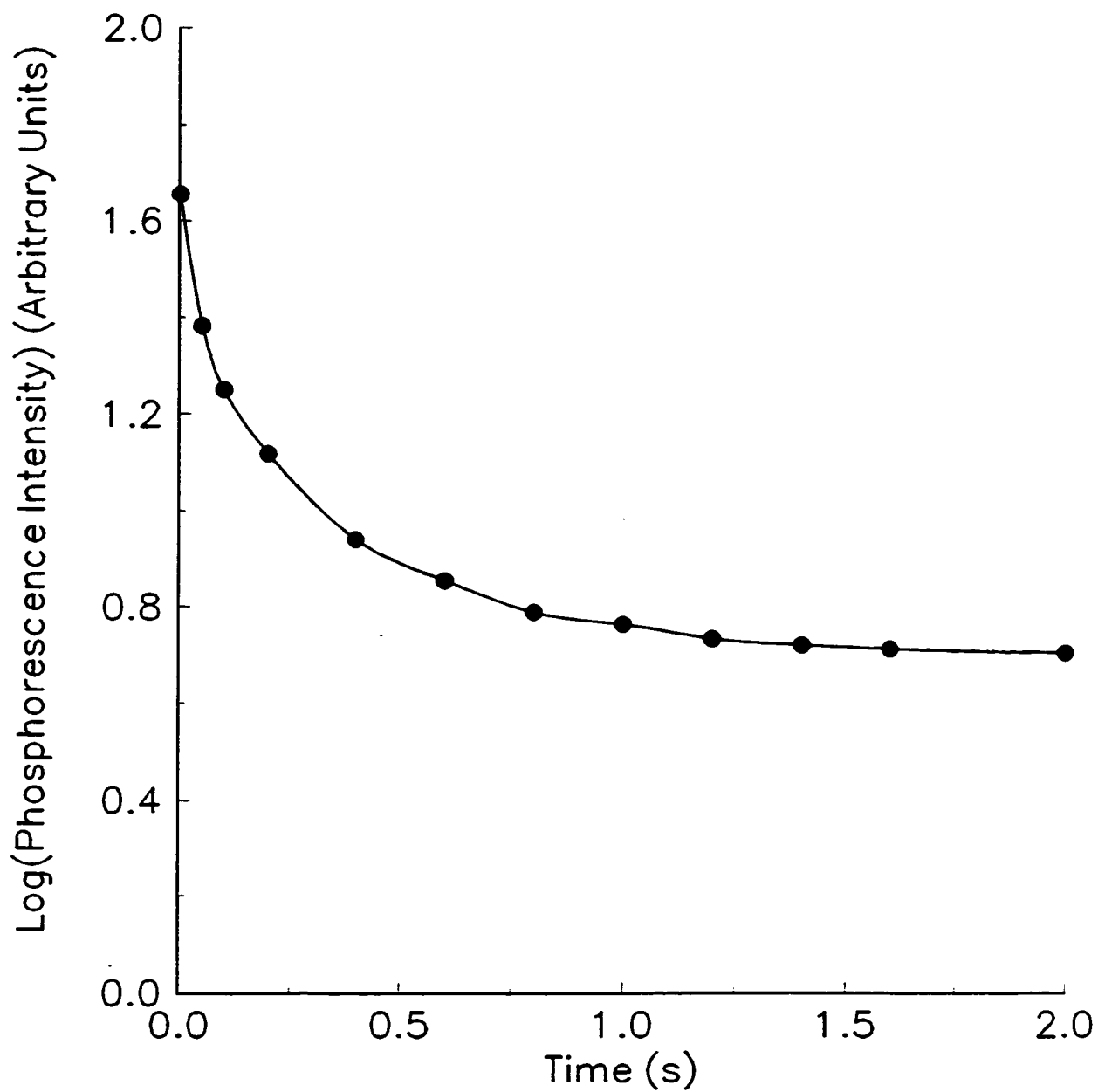


Figure 3.15. Phosphorescence decay characteristics of PEAP triplet in glass at 77K (semi-logarithmic plot).

II/ EFFECTS OF UV IRRADIATION ON POLYMER PROPERTIES

1. INFRARED SPECTRAL CHANGES

The effects of UV irradiation ($\lambda \geq 300\text{nm}$, degassed) on PEAP are shown in Figure 3.16. It can be seen that there is a slight increase in absorbance in the hydroxyl region of $3300\text{-}3500\text{ cm}^{-1}$ for both solution and film and there is a significant increase in the carbonyl region at 1670cm^{-1} for both. There is an increase in absorbance in the $2700\text{-}3000\text{cm}^{-1}$ region for film but no apparent increase for solution.

2. NMR SPECTRAL CHANGES

Changes occur in the ^1H and ^{13}C NMR spectra of PEAP upon long-wave irradiation ($\lambda \geq 300\text{nm}$, degassed) as shown in Figures 3.17 and 3.18. The data are summarized in Tables 3.6 and 3.7.

Table 3.6. ^1H NMR Characteristics of PEAP in 6.0×10^{-2} M Polymer Solutions in CH_2Cl_2 and 1.5×10^{-4} cm Films After 12 Hours of Irradiation ($\lambda \geq 300\text{nm}$, degassed).

FORM OF IRRADIATION	DEPLETION OF CHEMICAL SHIFT	ASSIGNMENT	FORMATION OF CHEMICAL SHIFT	POSSIBLE ASSIGNMENT
Solution & Film	3.68	O-CH ₂ -	5.3	=CH- or =CH ₂
Solution & Film	2.85	-CH-CH ₂	1.25	-CH ₂ -
Solution & Film	1.74	CH-CH ₂ -		
Solution & Film	1.36	CH ₂ -CH ₃		

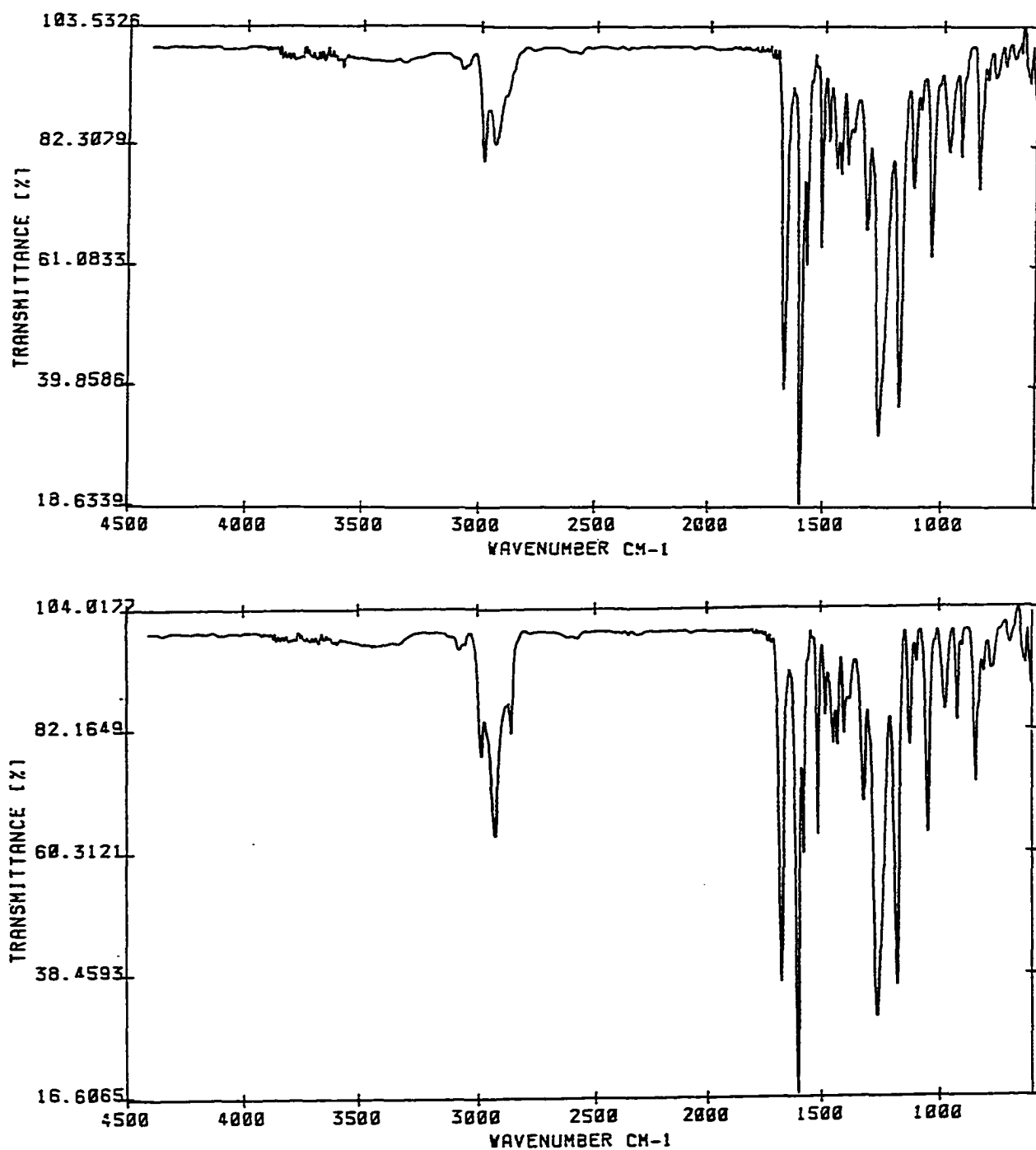


Figure 3.16. Infrared spectral changes of PEAP after 12 hours of irradiation ($\lambda \geq 300\text{nm}$, degassed). Top spectrum = 6.0×10^{-2} M solution in CH_2Cl_2 and Bottom spectrum = 1.5×10^{-4} cm film.

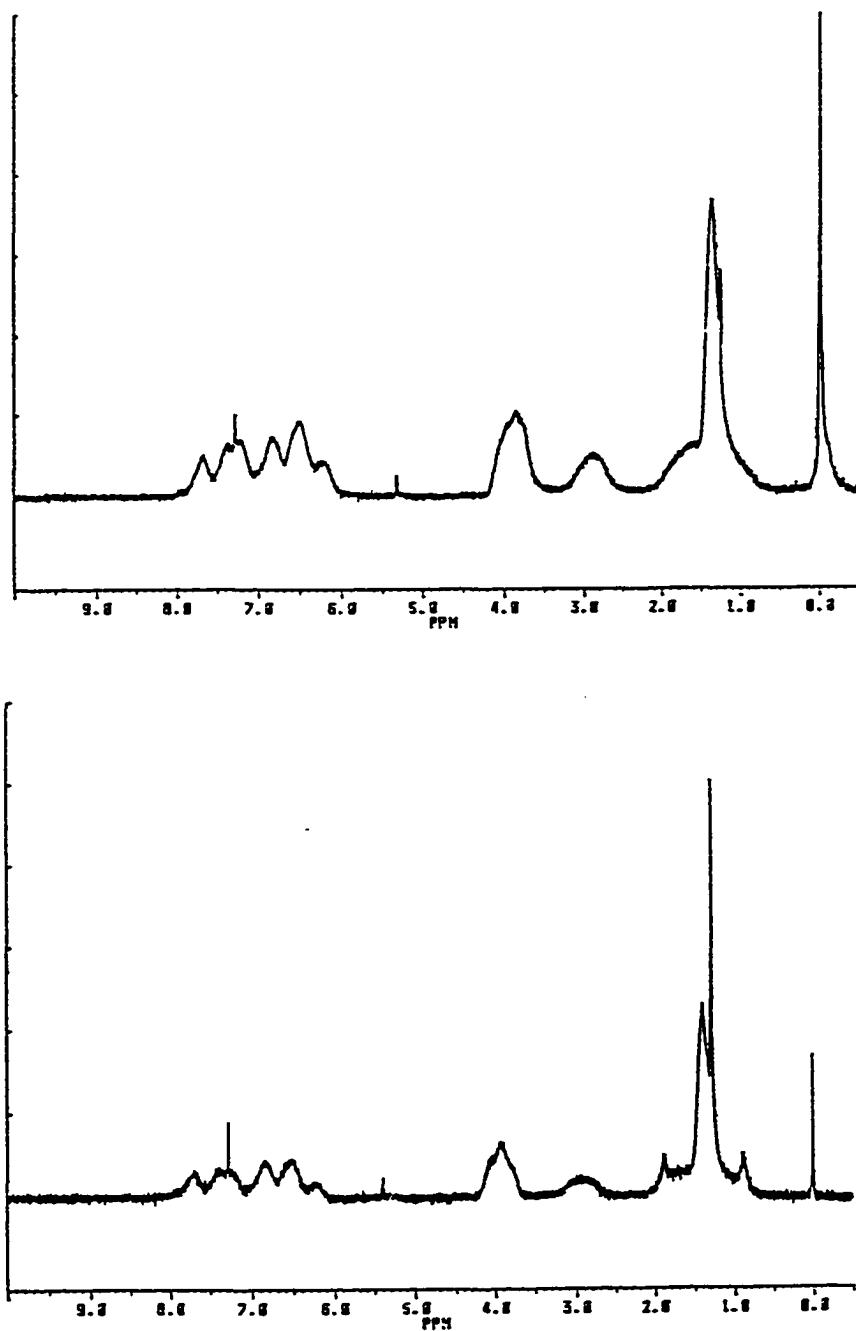


Figure 3.17. ^1H NMR spectral changes of PEAP after 12 hours of irradiation ($\lambda \geq 300\text{nm}$, degassed). Top spectrum = 6.0×10^{-2} M solution in CH_2Cl_2 and Bottom spectrum = 1.5×10^{-4} cm film.

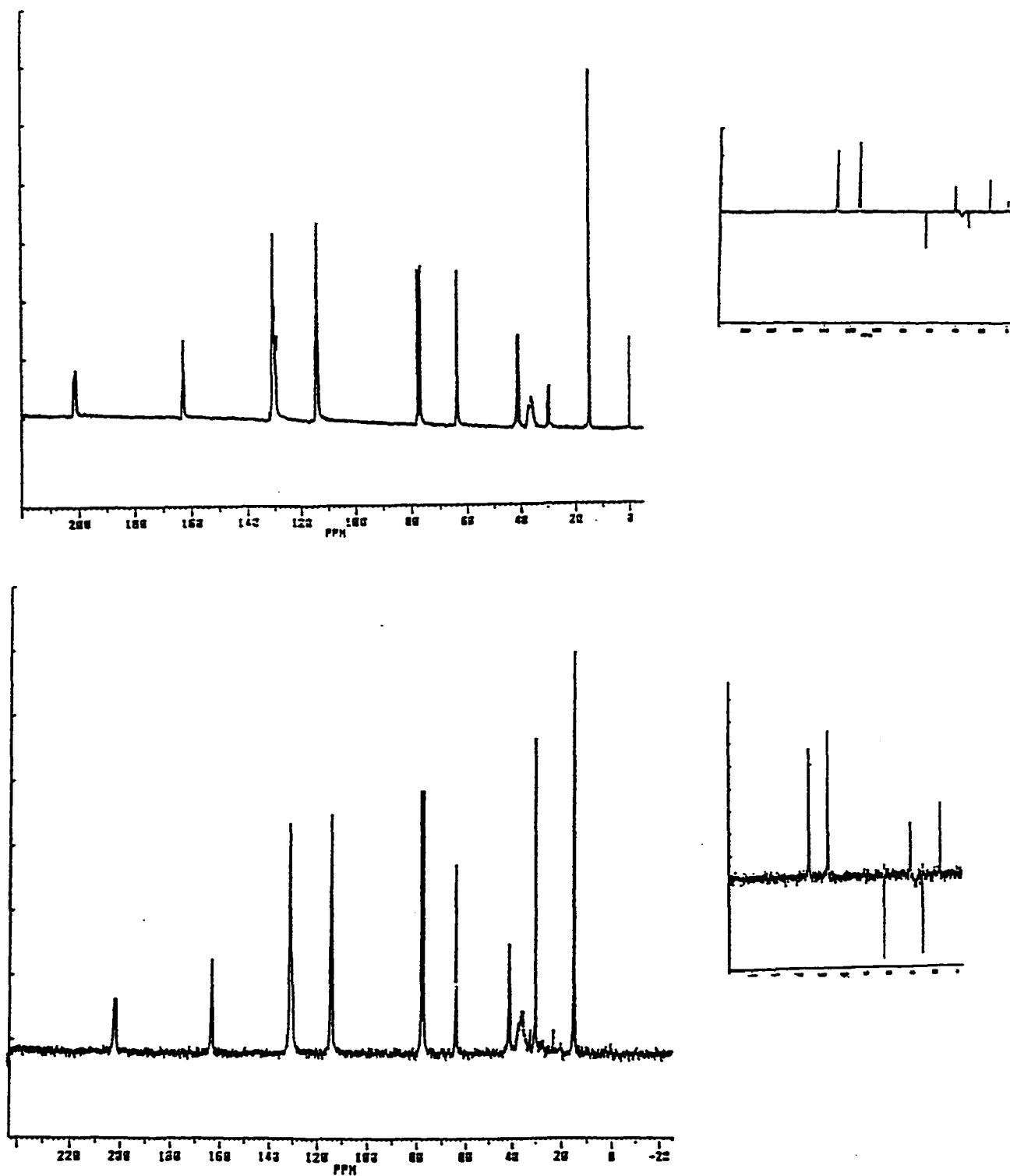


Figure 3.18. ^{13}C NMR spectrum and corresponding DEPT sequence of PEAP after 12 hours of irradiation ($\lambda \geq 300\text{nm}$, degassed). Top spectrum = 6.0×10^{-2} M solution in CH_2Cl_2 and Bottom spectrum = 1.5×10^{-4} cm film.

Table 3.7. ^{13}C NMR Characteristics of PEAP in 6.0×10^{-2} M Polymer Solutions in CH_2Cl_2 and 1.5×10^{-4} cm Films After 12 Hours of Irradiation ($\lambda \geq 300\text{nm}$, degassed).

FORM OF IRRADIATION	DEPLETION OF CHEMICAL SHIFT	ASSIGNMENT	FORMATION OF CHEMICAL SHIFT	POSSIBLE ASSIGNMENT
Solution & Film	63.4	O-CH ₂ -	29.7	-CH ₂ -
Solution & Film	40.8	-CH-CH ₂		
Solution & Film	35.6	CH-CH ₂ -		
Solution & Film	14.6	CH ₂ -CH ₃		

Photolysis leads to changes in the ethoxy peak intensities and these are indications that new carbonyl absorptions occur. However, the data is not sufficiently accurate to use NMR to follow the kinetics of change.

3. UV SPECTRAL CHANGES

The UV spectral changes occurring upon irradiation of PMAP, P34DMAP and P35DMAP in both 3.0×10^{-4} M solution in CH_2Cl_2 and thin film have been previously investigated.⁷ The irradiation of PEAP in both solution (Figure 3.19) and thin film (Figure 3.20) shows similar spectral changes to the methoxy-substituted poly(acrylophenones). The intensities of both the $\pi-\pi^*$ and $n-\pi^*$ absorptions decrease upon irradiation and a new broad, structureless absorption is observed in the long-wave region. As the radiation time increases the absorption of this new band increases in intensity becoming progressively more red-shifted until yellow coloration appears. The time dependant characteristics of the new broad band absorption and coloration in PEAP are shown in Figure 3.21 as increasing optical density at 400 nm. The change in optical density is more prominent

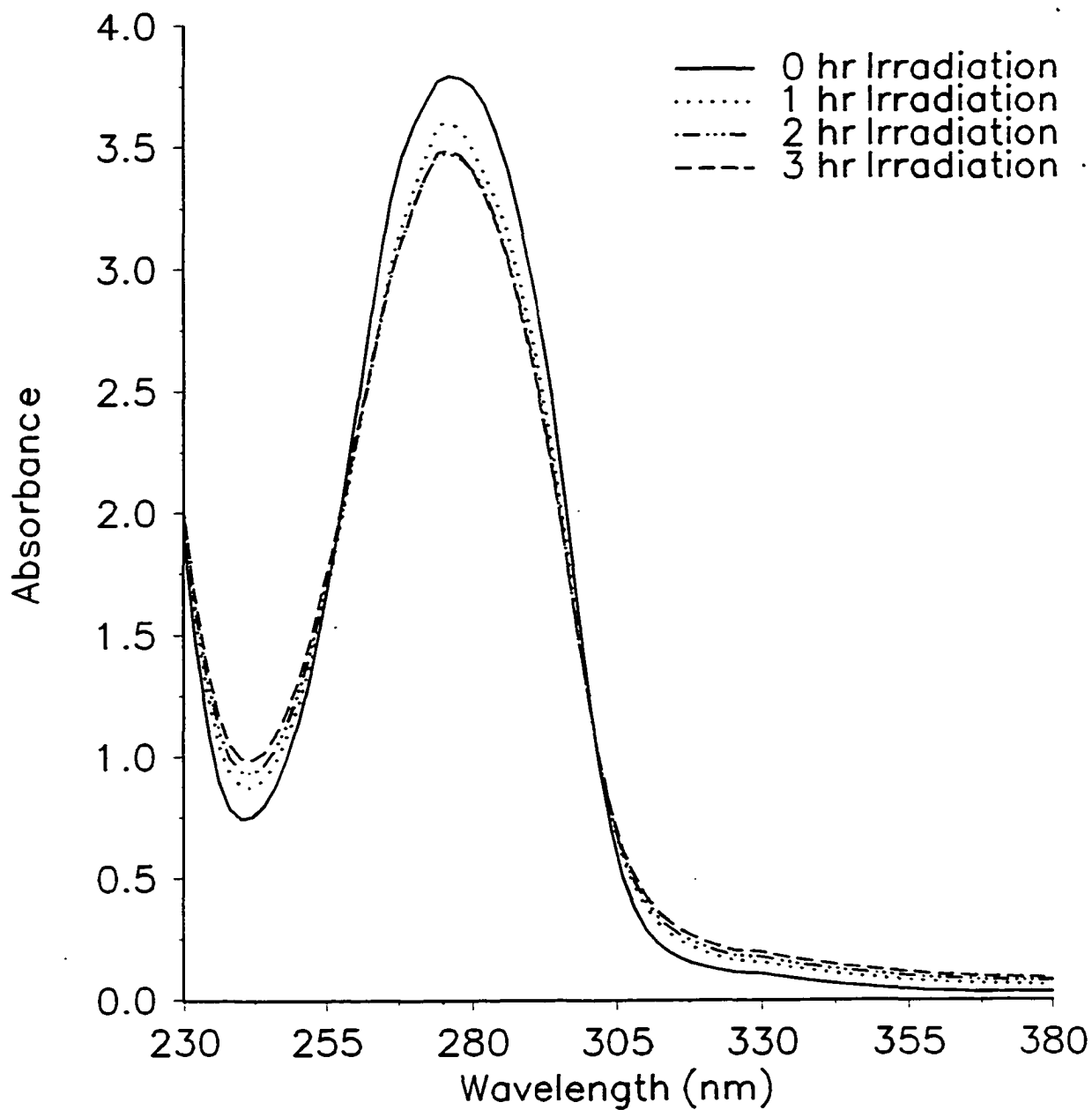


Figure 3.19. UV absorption spectra of PEAP (3×10^{-4} M solution in CH_2Cl_2) before and after irradiation ($\lambda \geq 300\text{nm}$, degassed and instrument sensitive to 0.0001% T).

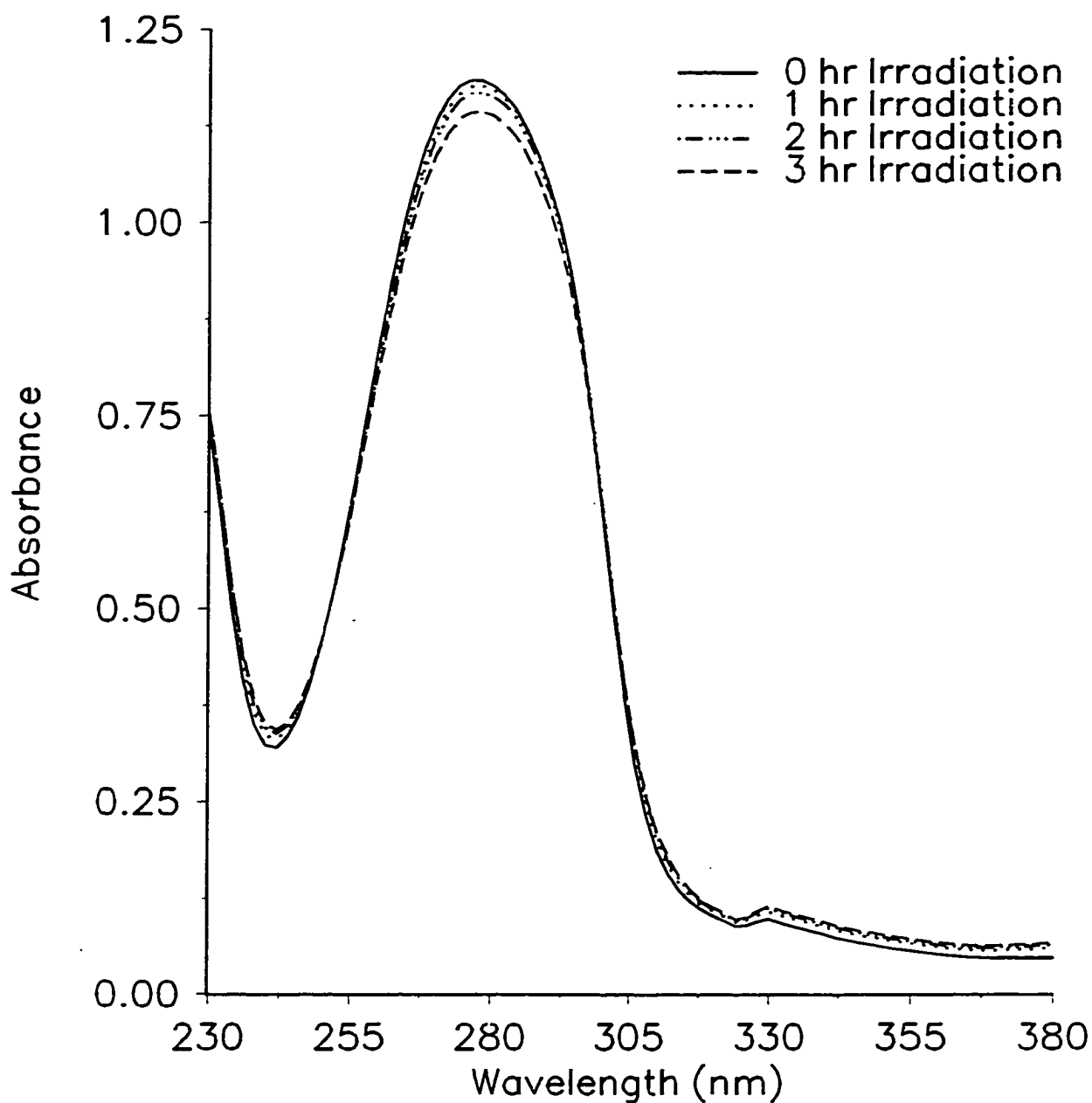


Figure 3.20. UV absorption spectra of PEAP (1.5×10^{-4} cm film) before and after irradiation ($\lambda \geq 300$ nm, degassed and instrument sensitive to 0.0001% T).

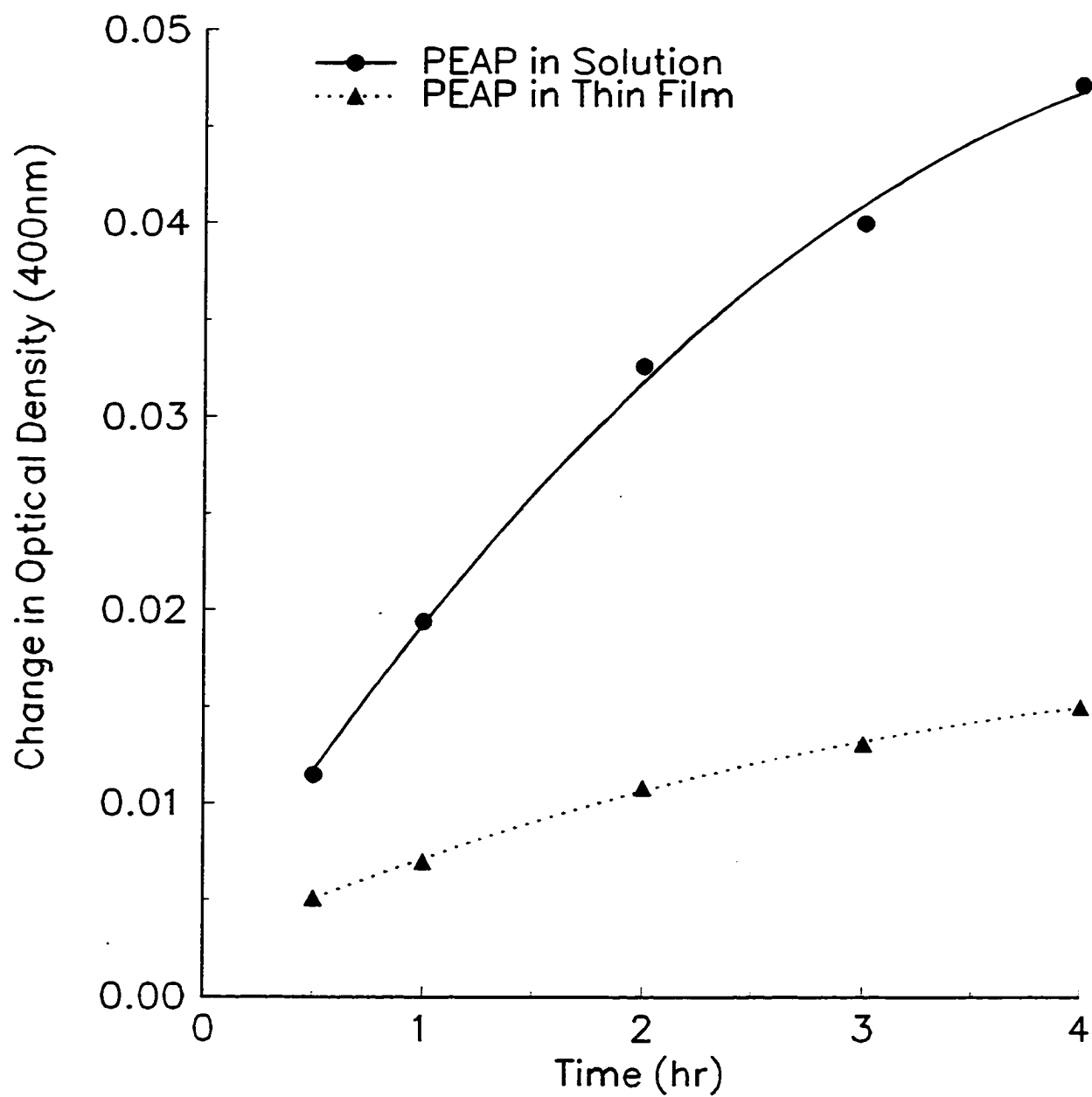


Figure 3.21. Optical density and yellowing characteristics of new broad band absorption at 400nm as a function of irradiation time ($\lambda \geq 300\text{nm}$, degassed).

in solution than in film and the characteristics of coloration are typical of that observed for many polymers, in that it is non-linear in both solution and film.⁶⁰ This behavior has been attributed to formation of new chromophores which absorb in competition with the substrates. This is known as an optical filtering effect.⁶⁰

4. LOW MOLECULAR WEIGHT PRODUCTS

These were determined by quantitative mass spectrometry. The only low molecular weight products previously detected for PMAP, P34DMAP and P35DMAP following irradiation in the solid state were methane and ethane, these being formed from methyl radicals, which were in turn formed by O-CH₃ fission during photolysis. The low molecular weight products detected for PEAP were butane, ethane and ethylene and these can be associated with ethyl radicals presumably formed the same way by photolysis. The time evolution characteristics of butane, ethane and ethylene are shown in Figure 3.22. These results are qualitatively similar to those obtained for PMAP, P34DMAP and P35DMAP in that there exists linearity for only a short time after which the rate falls off.⁷ Since the fall off occurs at only a few percent of degradation, substrate depletion cannot account for it, but it may be a result of the filter effect mentioned above, the new chromophores absorbing the incident UV radiation in competition with the polymer.⁶⁰

The quantum yields for the formation of a product X are determined by:¹⁰

$$\begin{aligned}\phi_x &= \frac{\text{Rate of formation of X in the film}}{\text{Rate of absorption of quanta by film}} \\ &= \frac{d(X)/dt}{I_0(1-10^{-\beta L})A}\end{aligned}$$

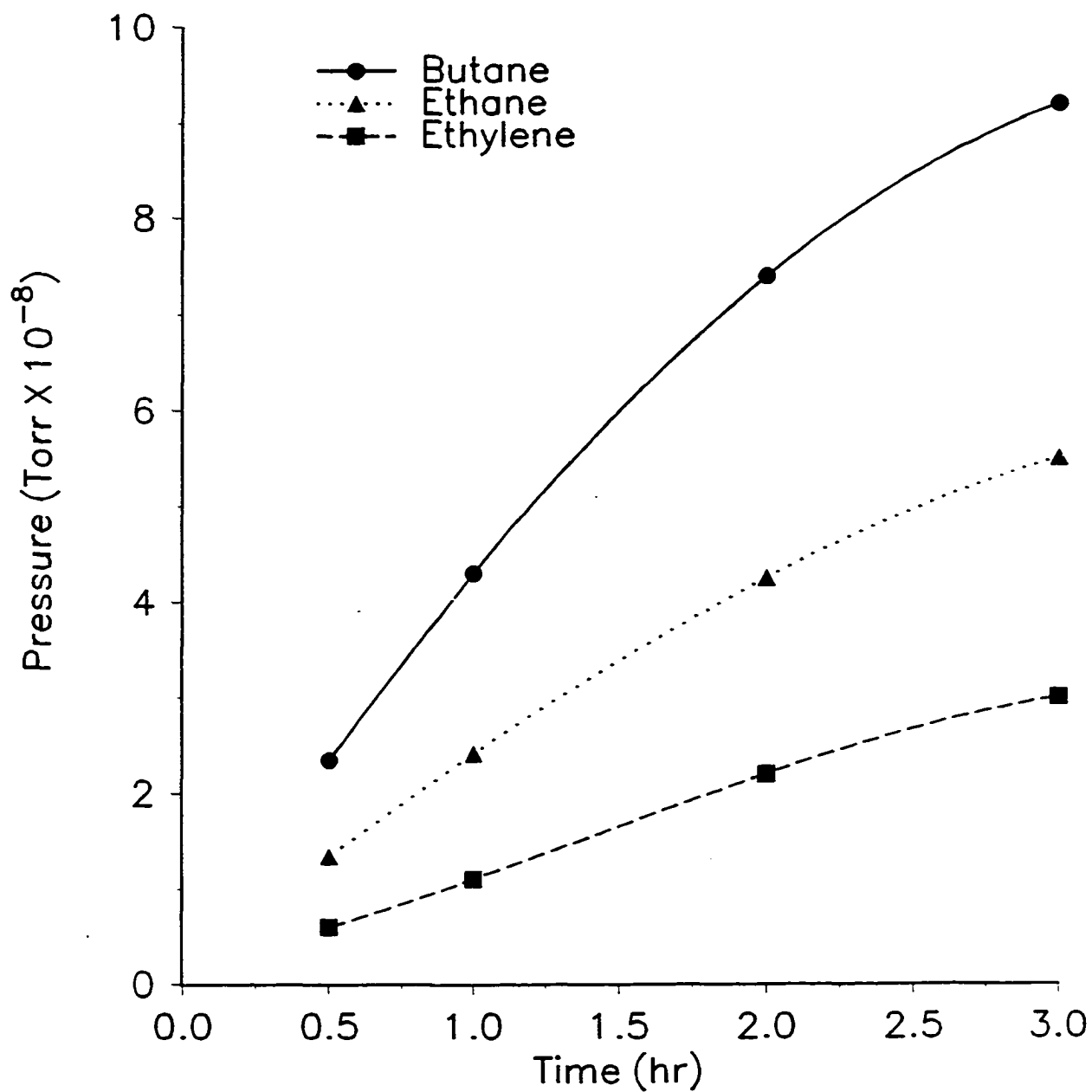


Figure 3.22. Low molecular weight gaseous product formation (solid state PEAP) as a function of irradiation time ($\lambda \geq 300\text{nm}$, degassed).

where I_0 is the UV incident intensity (quanta per unit area per unit time), β is the absorption coefficient, L is the film thickness, and A is the area of the film. When the value of β is small, this can be simplified to:

$$\phi_x = \frac{d(X) / dt}{I_0 \beta LA}$$

The quantum yields for the formation of gaseous products of PEAP are summarized in Table 3.8.

Table 3.8. Quantum Yields for Gaseous Product Formation from Ethoxy-Substituted Poly(acrylophenone) Film Upon Irradiation ($\lambda \geq 300$ nm, vacuum).

POLYMER	$\phi_{C_2H_6}$ ($\pm 10\%$)	$\phi_{C_2H_4}$ ($\pm 10\%$)	$\phi_{C_3H_8}$ ($\pm 10\%$)
PEAP	6.7×10^{-4}	3.1×10^{-4}	1.2×10^{-3}

5. MOLECULAR WEIGHT CHANGES IN SOLUTION

The effect of long-wave UV radiation on the molecular weights of 6×10^{-2} M solutions of PMAP, P34DMAP and P35DMAP in CH_2Cl_2 have been previously investigated and it was observed that irradiation leads to random chain scission.⁷ In the case of PEAP, similar investigations showed that significant changes were in the molecular weights, the results being similar to those observed for the methoxy-substituted poly(acrylophenones). The changes in the distribution of molecular weights for PEAP as indicated by GPC data are shown in Figure 3.23.

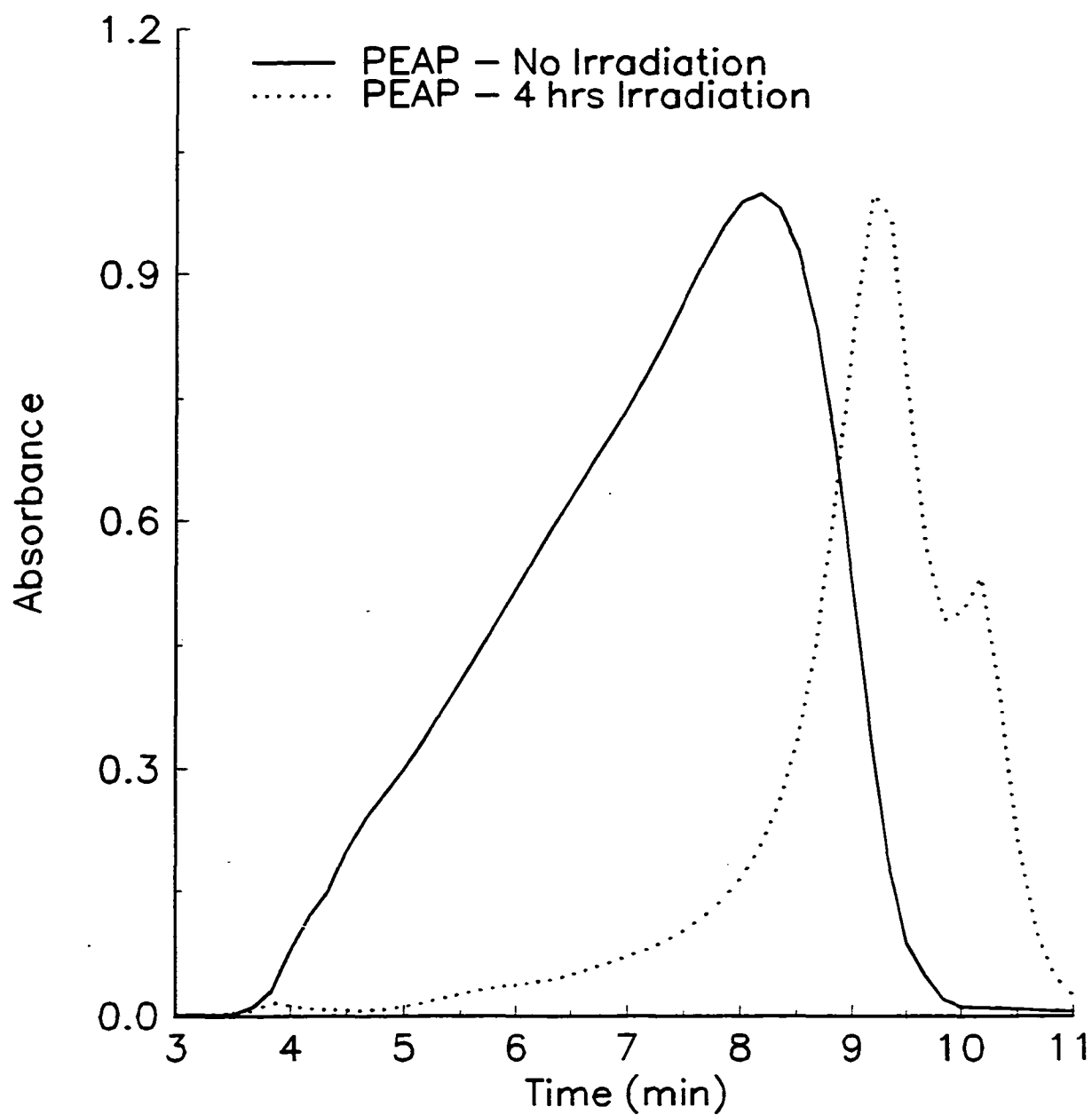


Figure 3.23. Gel permeation chromatograph of PEAP (1.0×10^{-2} M solution in CH_2Cl_2) before and after 4 hours of irradiation ($\lambda \geq 300\text{nm}$, degassed and run through a $7\mu\text{m}$ pore Ultrastyrigel[®] linear column at $1.0 \text{ cm}^3 \text{ min}^{-1}$)

After four hours of irradiation, the distribution becomes narrower and the entire spectrum moves to a higher elution time indicating that new lower molecular weight fragments are formed. Chain scission of the longer molecules results in a shift of the distribution to longer elution times; and at the same time it becomes narrower as the high molecular weight species are degraded.

The changes in molecular weights in solution are measured by viscometry. From these measurements, the relative viscosity η_{rel} can be determined as follows:¹⁰

$$\eta_{rel} = \frac{t}{t_0}$$

where t is the flow time for the polymer solution and t_0 is the flow time of the pure solvent. This is related to the specific viscosity η_{sp} as follows:

$$\eta_{sp} = \eta_{rel} - 1$$

The intrinsic viscosity $[\eta]$ can then be determined by Solomon and Ciuta's equation:¹⁰

$$[\eta] = \frac{\sqrt{2}(\eta_{sp} - \ln \eta_{rel})^{1/2}}{c}$$

where c is the concentration of the polymer solution in g/dl. The number of chain scission per original molecule can then be obtained by:⁹

$$S = \left(\frac{[\eta]_0}{[\eta]_t} \right)^{1/\alpha} - 1$$

where $[\eta]_0$ and $[\eta]_t$ are the intrinsic viscosities before and after irradiation respectively and α is the Mark-Houwink constant and is equal to 0.75.

Figure 3.24 shows the number of chain scissions per original molecule as a function of time of exposure, t , for several concentrations of PEAP. There exists a linearity over the reaction period

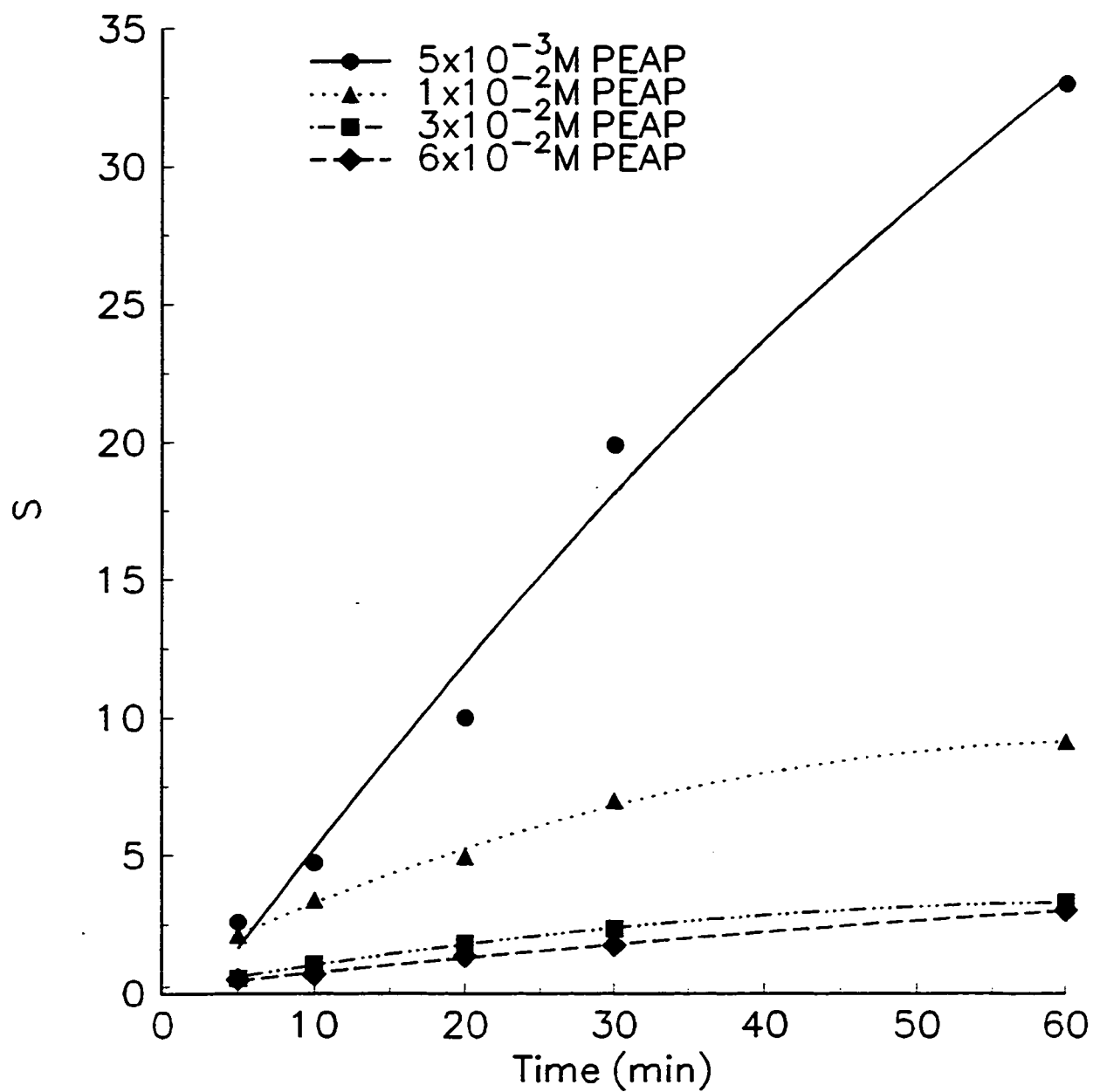


Figure 3.24. Number of chain scissions per original molecule of PEAP (in CH_2Cl_2) as a function of irradiation time ($\lambda \geq 300\text{nm}$, degassed).

which implies that random chain scission is occurring. After prolonged exposure (>12 hours), the rates fall off. This was exhibited by the methoxy-substituted poly(acrylophenones)⁷ and it perhaps implies that competing reactions such as crosslinking or quenching by reaction products are occurring.

The quantum yield for chain scission can be determined by:¹

$$\phi_{cs} = \frac{n}{I_A t}$$

where n is the number of moles of chain scissions, I_A is the number of einsteins of photons absorbed by the polymer solution and t is the irradiation time. The number of moles of chain scissions can be related to the molecular weights and intrinsic viscosities by:¹⁰

$$n = \frac{w}{(\overline{M}_n)_o} \left[\left(\frac{[\eta]_o}{[\eta]_t} \right)^{1/\alpha} - 1 \right]$$

where w is the initial mass of the polymer undergoing irradiation and $(\overline{M}_n)_o$ is the initial number-average molecular weight. The absorbed intensity I_A can be related to the incident intensity I_o by:³

$$I_A = I_o(1 - 10^{-\epsilon c l})$$

where ϵ is the molar absorption coefficient, c is the concentration of the polymer solution and l is the effective path length of the solution.

$$\phi_{cs} = \frac{w \left[\left(\frac{[\eta]_o}{[\eta]_t} \right)^{1/\alpha} - 1 \right]}{(\overline{M}_n)_o I_o [1 - 10^{-\epsilon c l}] t}$$

The quantum yield for chain scission of PEAP was determined from the linear portion of the S versus t plot and is listed in Table 3.9 along with the previously determined values for PMAP, P34DMAP and P35DMAP.⁷

Table 3.9. Quantum Yields for Chain Scission ($\lambda \geq 300\text{nm}$) of 6.0×10^{-2} M Polymer Solutions in CH_2Cl_2 .⁷

POLYMER	ϕ_{cs} ($\pm 10\%$) mol(Einstein ⁻¹)
PMAP	1.0×10^{-1}
P34DMAP	1.1×10^{-4}
P35DMAP	1.0×10^{-4}
PEAP	6.0×10^{-2}

The ϕ_{cs} for PEAP is comparable to that for ϕ_{cs} for PMAP, but is much larger than the values of quantum yield of chain scission for the di-methoxylated poly(acrylophenones).⁷ This no doubt reflects the involvement of triplets with more (n, π^*) character in the case of PEAP. The effect of concentrations of PEAP in solution is again analogous to that for the methoxy-substituted poly(acrylophenones)⁷ in that the rates of chain scission decrease as the polymer concentration increases (Figure 3.24). The rate of chain scission appears to be related inversely to the polymer concentration (Figure 3.26) rather than directly (Figure 3.25).

6. THE EFFECT OF QUENCHERS IN SOLUTION

The effect of quenching on the rate of chain scission of 1×10^{-2} M PEAP in CH_2Cl_2 was investigated using two well known quenchers, naphthalene and cis-1,3-pentadiene. While the

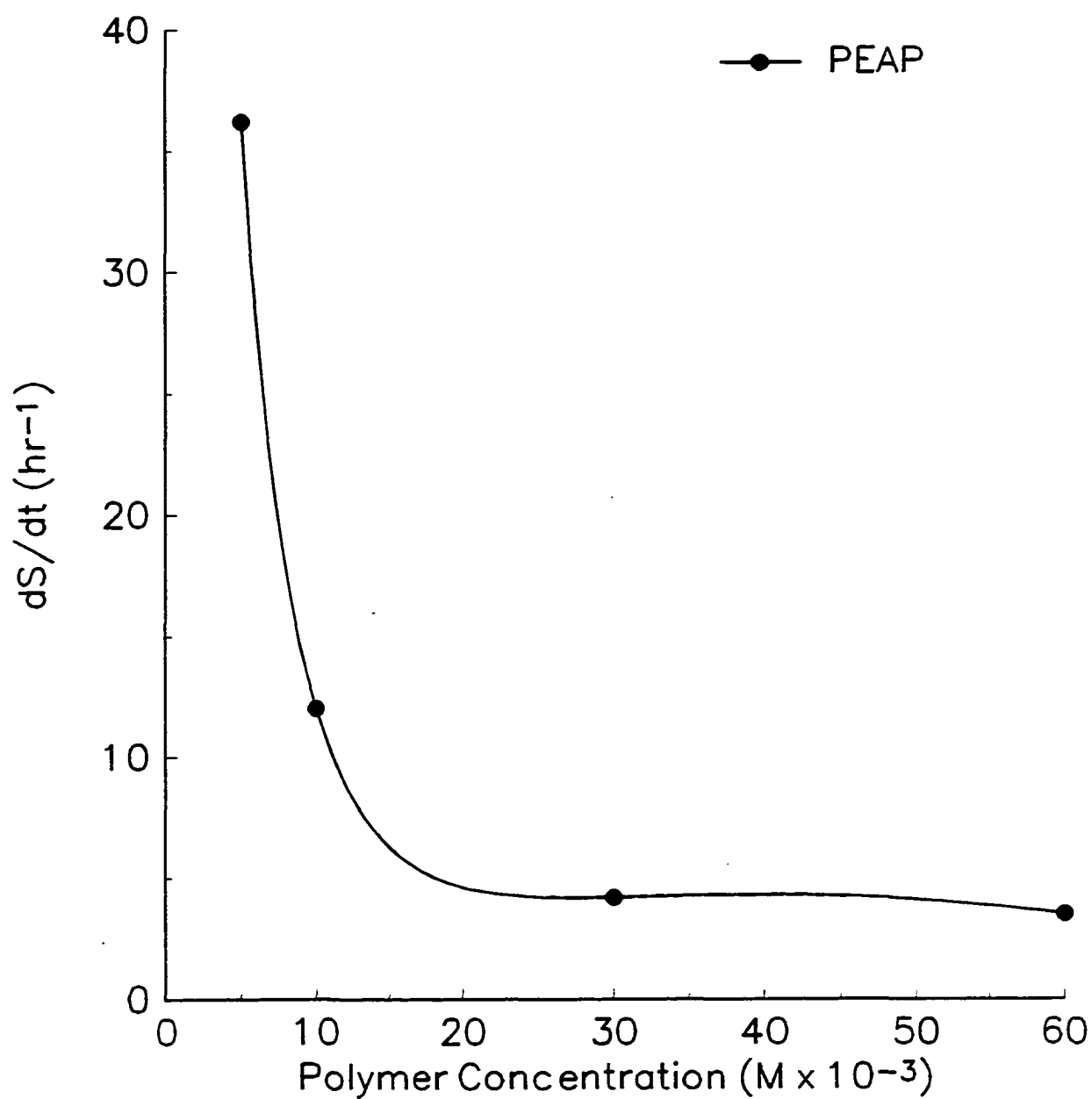


Figure 3.25. Rate of chain scission as a function of PEAP (in CH₂Cl₂) concentration ($\lambda \geq 300\text{nm}$, degassed).

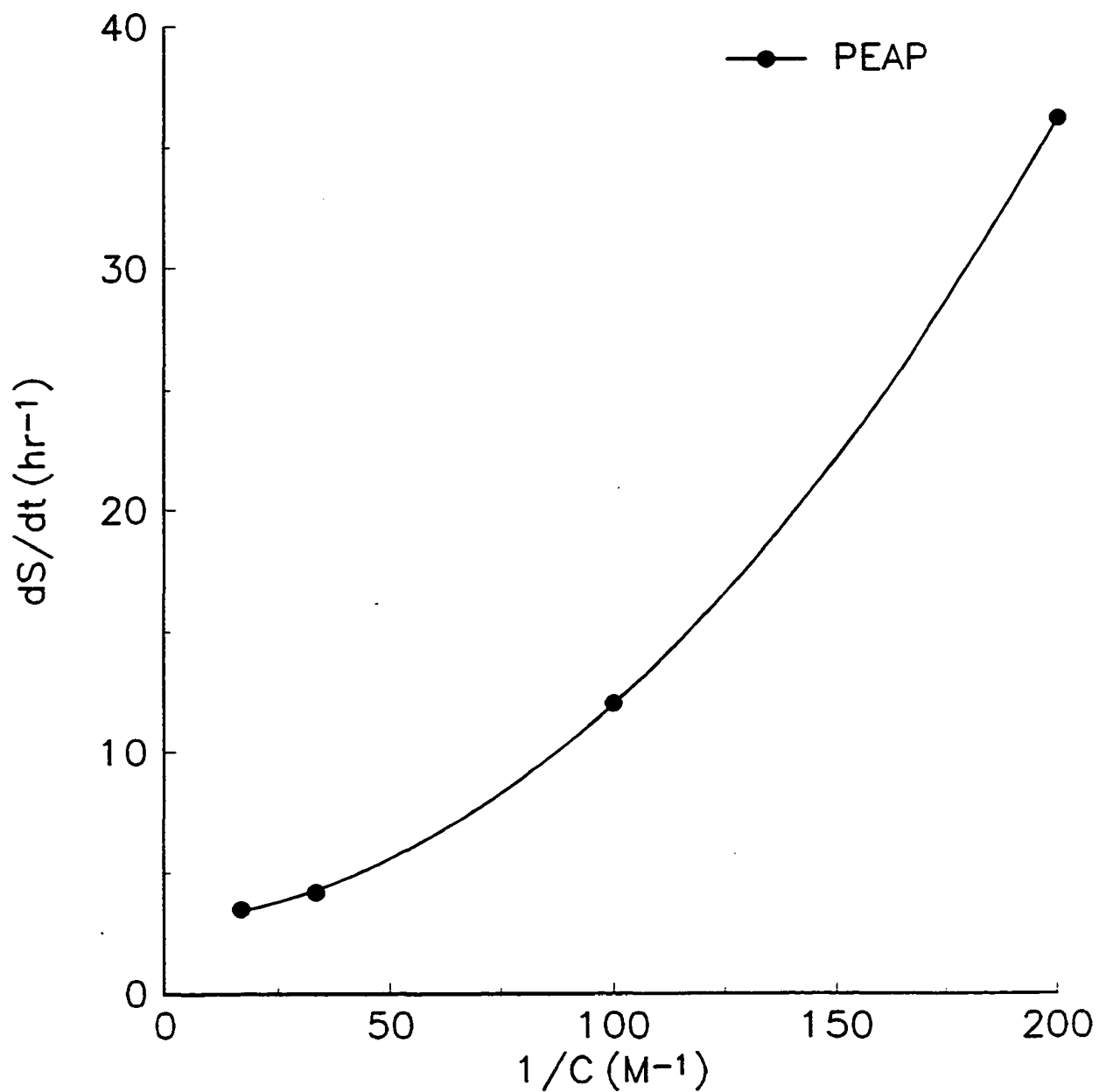


Figure 3.26. Rate of chain scission as a function of PEAP (in CH_2Cl_2) reciprocal concentration ($\lambda \geq 300\text{nm}$, degassed).

addition of both quenchers caused reductions in the rate of chain scission, naphthalene had a more significant effect suggesting that it is a more efficient triplet quencher. The results are shown in Figure 3.27 (naphthalene) and Figure 3.28 (cis-1,3-pentadiene). The results are analogous to those obtained for PMAP, P34DMAP and P35DMAP.⁷ The quantum yield ratios (ϕ_0/ϕ) for chain scission in the absence (ϕ_0) and in the presence (ϕ) of both naphthalene and cis-1,3-pentadiene are plotted as a function of quencher concentration $[Q]$ in Figure 3.29. It can be seen that both sets of data conform well to Stern-Volmer kinetics in which the slope is K_{sv} , the Stern-Volmer constant and the intercept is 1:

$$\frac{\phi_0}{\phi} = K_{sv}[Q] + 1$$

The values of K_{sv} have been determined and are summarized in Table 3.10. The Stern-Volmer constant is related to the triplet lifetime τ_T and the quenching rate constant k_Q by the equation $K_{sv} = \tau_T k_Q$, and the values of k_Q are summarized in Table 3.10. The triplet lifetime of 37ms was obtained from phosphorescence (Table 3.5).

Table 3.10. Quenching Constants for the Irradiation of PEAP in 1×10^{-2} M Solution in CH_2Cl_2 ($\lambda \geq 300$ nm).

POLYMER	K_{sv} (Naphthalene) ($dm^3 mol^{-1}$)	k_Q (Naphthalene) ($dm^3 mol^{-1} s^{-1}$)	K_{sv} (cis-1,3-Pentadiene) ($dm^3 mol^{-1}$)	k_Q (cis-1,3-Pentadiene) ($dm^3 mol^{-1} s^{-1}$)
PEAP	1.28×10^3	3.46×10^7	3.06×10^2	8.27×10^7

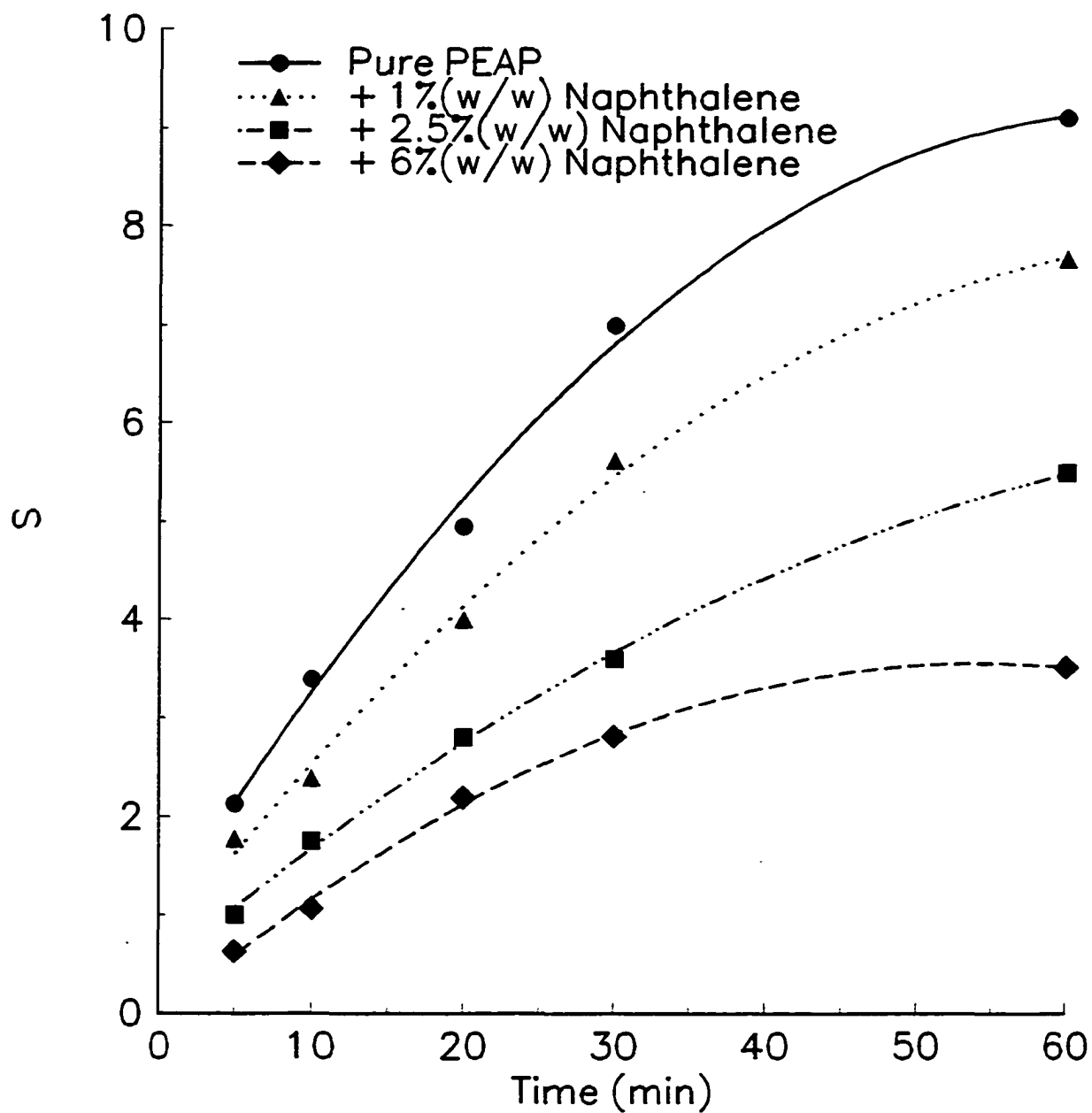


Figure 3.27. Number of chain scissions per molecule of PEAP (1.0×10^{-2} M solution in CH_2Cl_2) in the presence of naphthalene as a function of irradiation time ($\lambda \geq 300\text{nm}$, degassed).

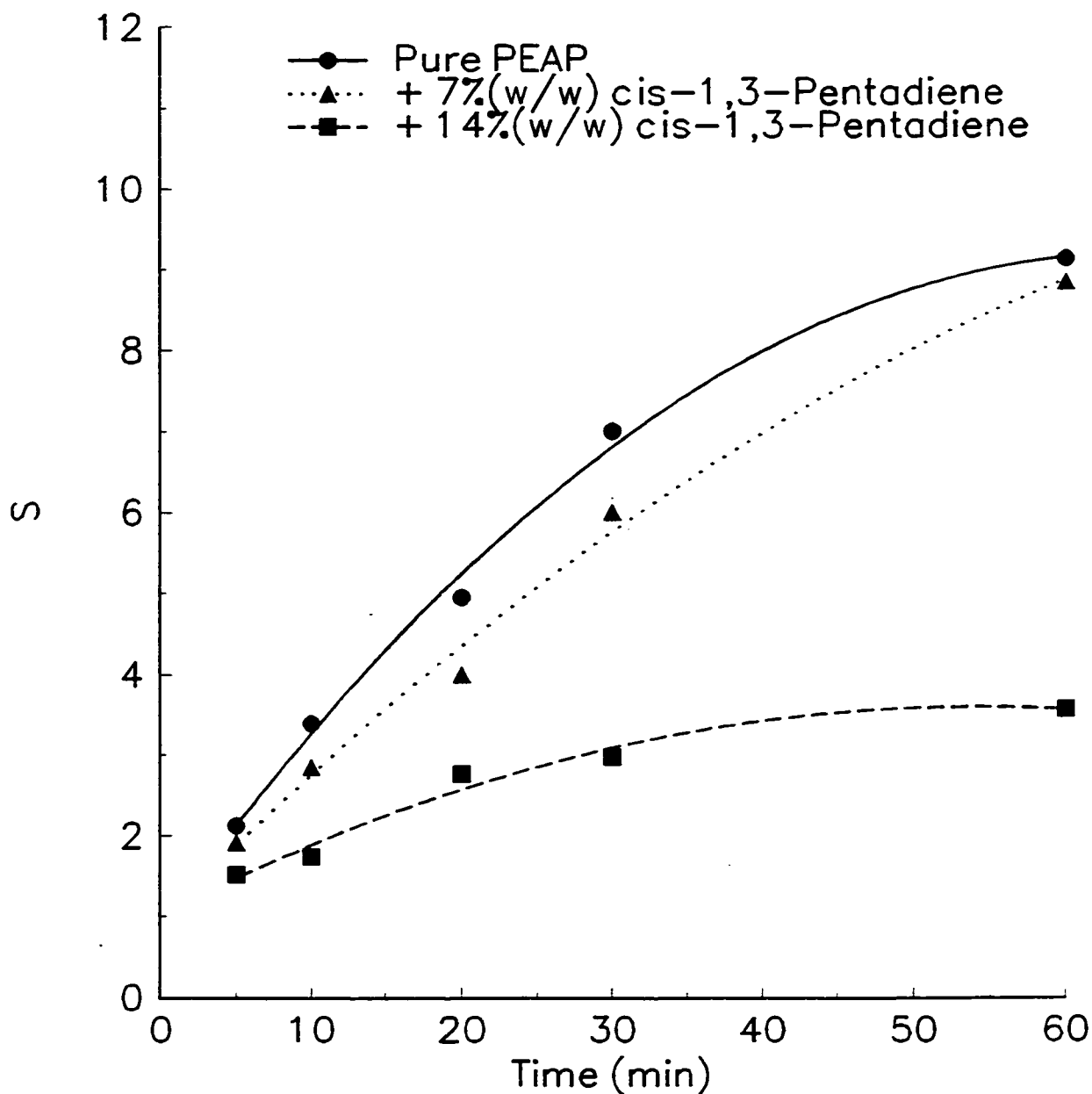


Figure 3.28. Number of chain scissions per molecule of PEAP (1.0×10^{-2} M solution in CH_2Cl_2) in the presence of cis-1,3-pentadiene as a function of irradiation time ($\lambda \geq 300\text{nm}$, degassed).

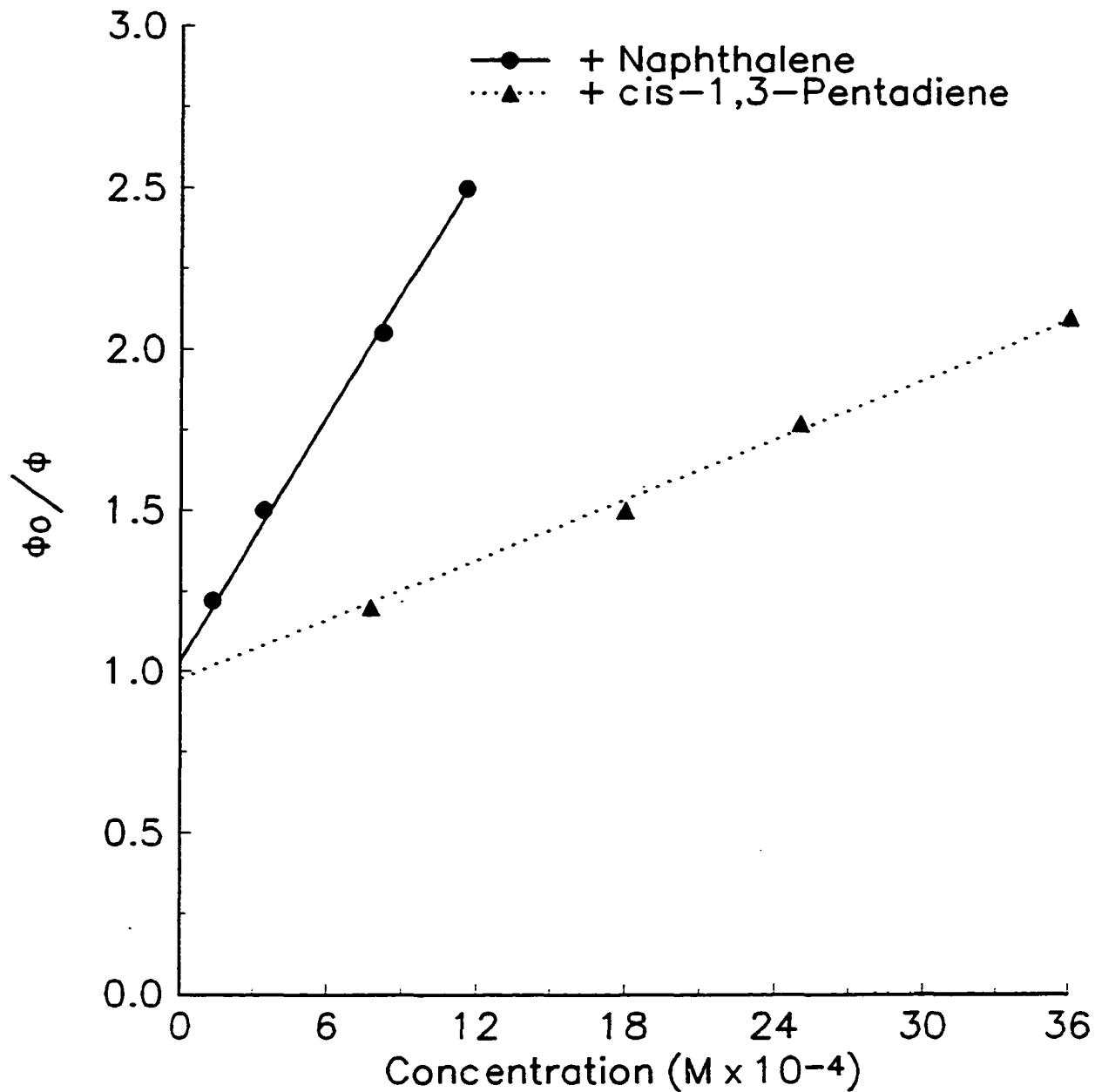


Figure 3.29. Stern-Volmer plots for quenching of PEAP (1.0×10^{-2} M solution in CH_2Cl_2) triplet ($\lambda \geq 300\text{nm}$, degassed).

The values of K_{sv} for PEAP (both naphthalene and cis-1,3-pentadiene) are lower than the corresponding values obtained for PMAP, P34DMAP and P35DMAP. The lower value would suggest that the deactivation process is not diffusion controlled. However, the quenching process may be subject to steric inhibition.

The effects of quenching on the triplet state of PEAP (in solution) by naphthalene and cis-1,3-pentadiene are also reflected by GPC data (Figure 3.30). Both triplet quenchers reduce the rate of photodegradation relative to that in the absence of quenchers and this is reflected by the narrowing of the curves and their movement to shorter elution times relative to the unquenched samples. Naphthalene is slightly more effective, the elution time for naphthalene being shorter than that of cis-1,3-pentadiene.

7. MOLECULAR WEIGHT CHANGES IN FILM

Long-wave UV radiation of PMAP, P34DMAP, P35DMAP and PEAP in thin film (1.5×10^{-4} cm) lead to significant changes in the molecular weights, and the distribution of molecular weights. GPC data for PMAP, P34DMAP, P35DMAP and PEAP are shown in Figures 3.31-34. The distribution curve for PMAP is displaced to a longer elution time while that for P35DMAP is displaced to a shorter elution time upon irradiation. However, while the shape of the distribution for P35DMAP remains relatively unchanged, those for PMAP and P34DMAP broaden. The molecular weight distribution for PEAP is also broadened, indicating the formation of high molecular weight products, presumably by cross-linking, which is favored in the solid state.

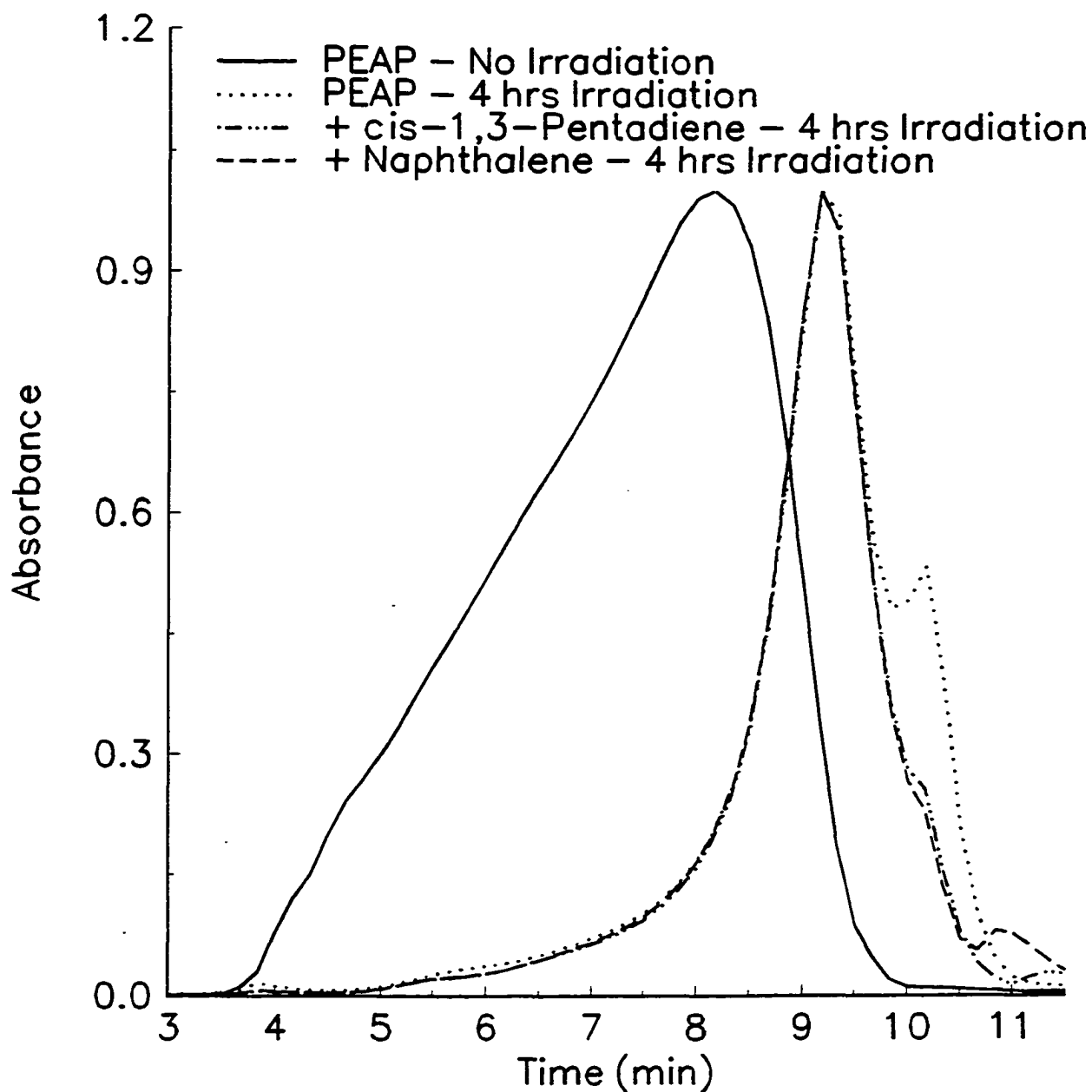


Figure 3.30. Gel permeation chromatograph of PEAP (1.0×10^{-2} M solution in CH_2Cl_2) before and after 4 hours of irradiation in the presence and absence of triplet quenchers ($\lambda \geq 300\text{nm}$, degassed and run through a $7\mu\text{m}$ pore Ultrastyrigel[®] linear column at $1.0 \text{ cm}^3 \text{ min}^{-1}$).

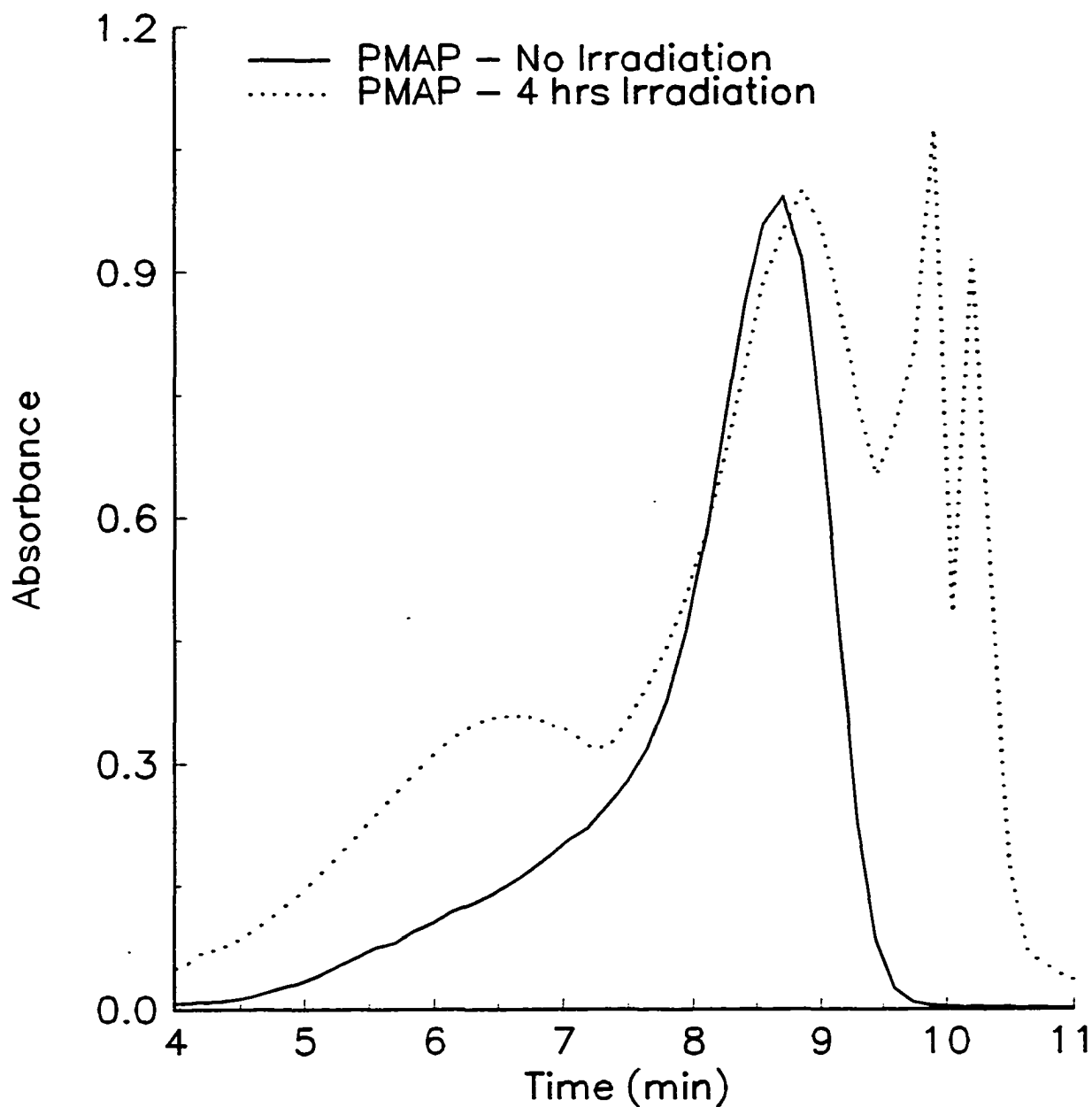


Figure 3.31. Gel permeation chromatograph of PMAP (1.5×10^{-4} cm film) before and after 4 hours of irradiation ($\lambda \geq 300\text{nm}$, degassed and run through a $7\mu\text{m}$ pore Ultrastyrigel[®] linear column at $1.0 \text{ cm}^3 \text{ min}^{-1}$).

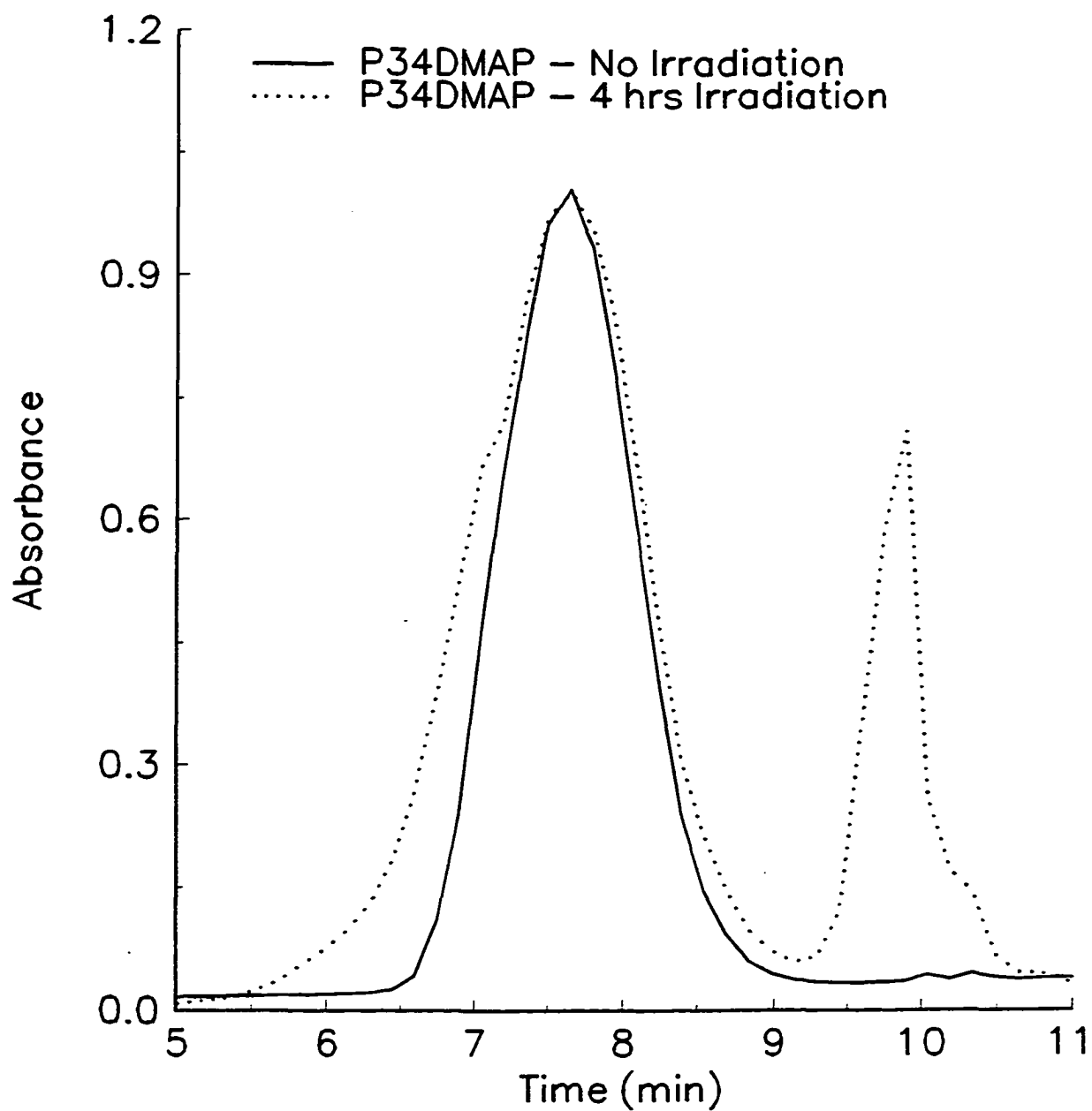


Figure 3.32. Gel permeation chromatograph of P34DMAP (1.5×10^{-4} cm film) before and after 4 hours of irradiation ($\lambda \geq 300\text{nm}$, degassed and run through a $7\mu\text{m}$ pore Ultrastyrigel[®] linear column at $1.0 \text{ cm}^3 \text{ min}^{-1}$).

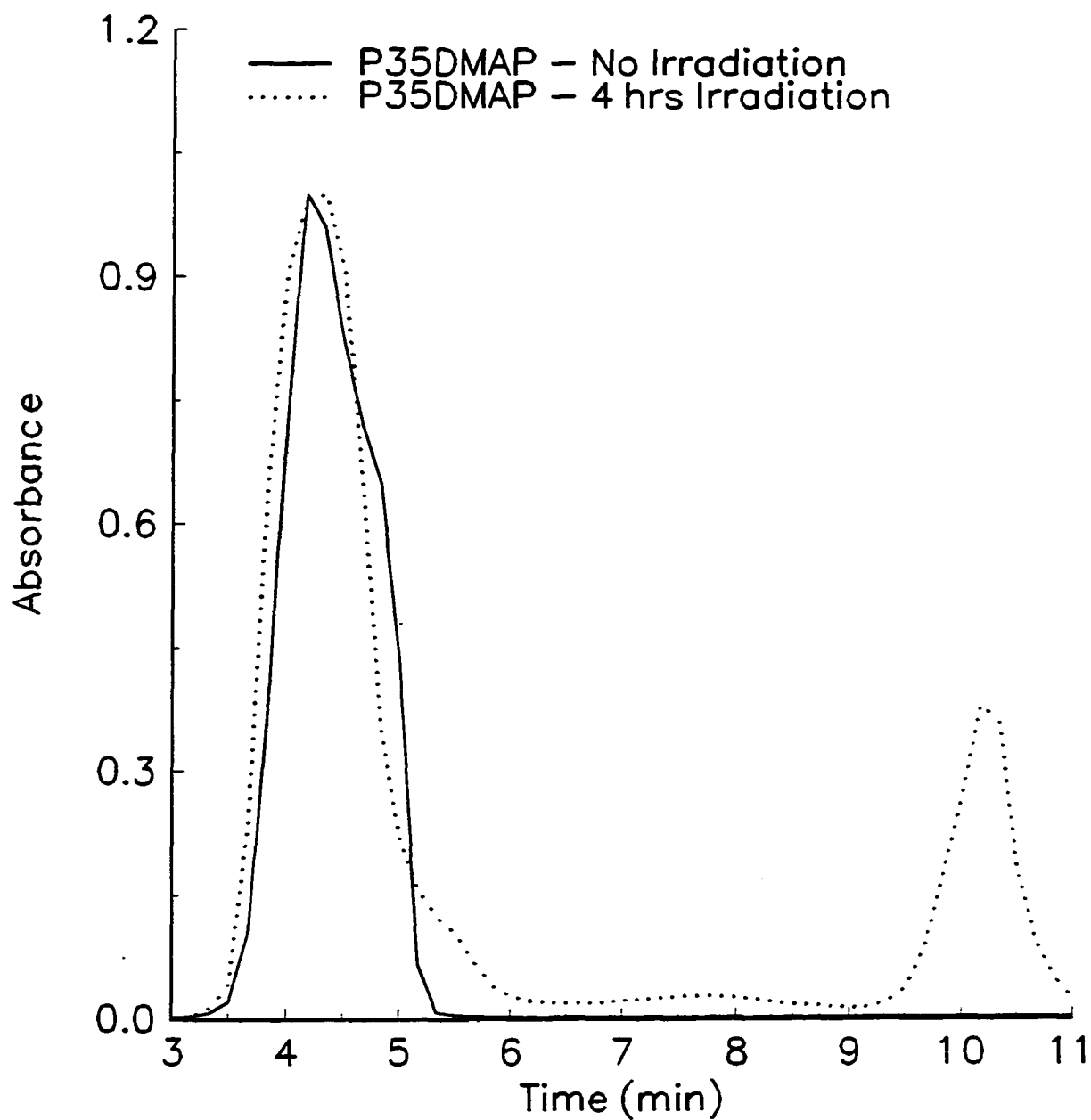


Figure 3.33. Gel permeation chromatograph of P35DMAP (1.5×10^{-4} cm film) before and after 4 hours of irradiation ($\lambda \geq 300\text{nm}$, degassed and run through a $7\mu\text{m}$ pore Ultrastyrigel[®] linear column at $1.0 \text{ cm}^3 \text{ min}^{-1}$).

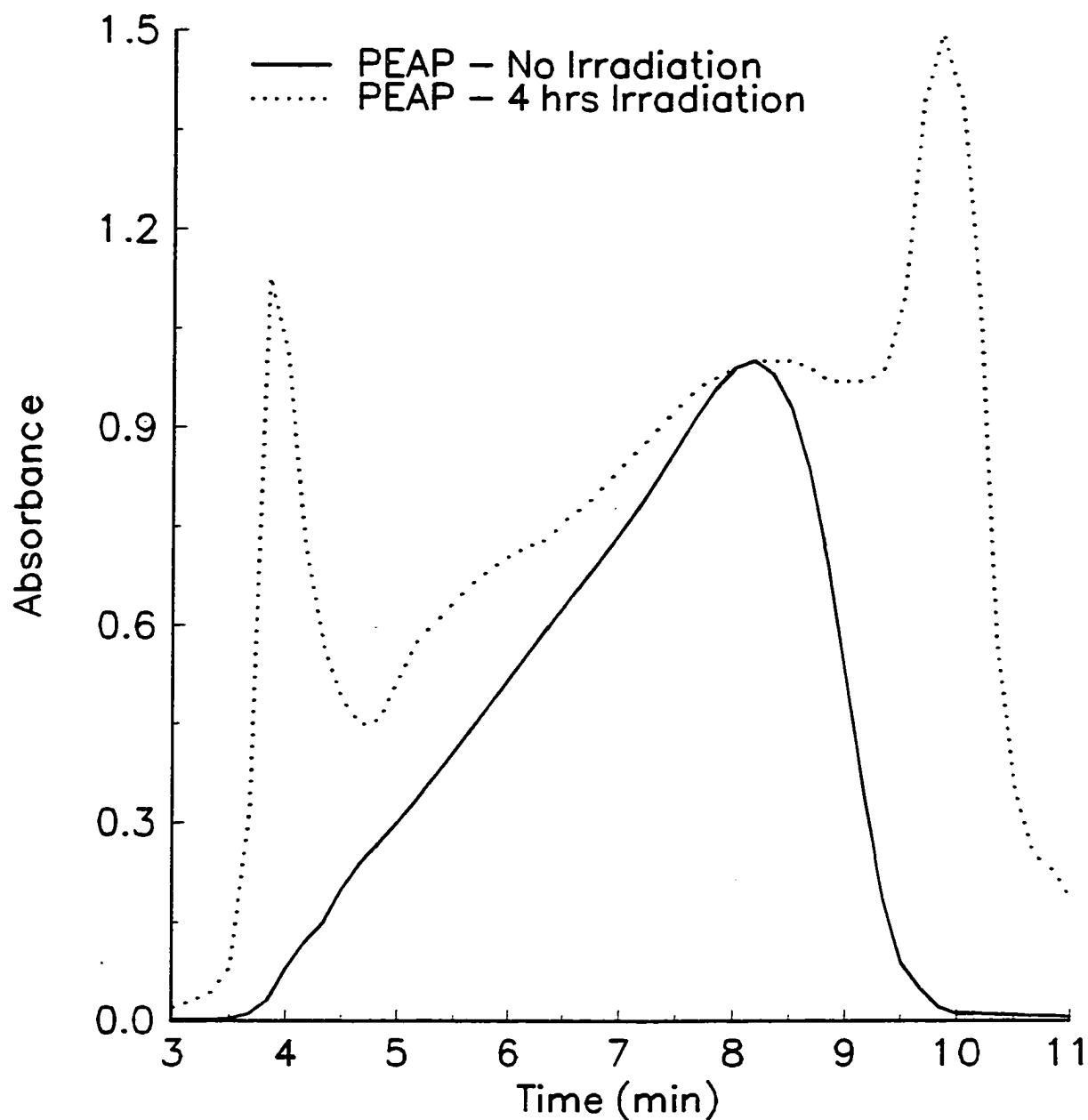


Figure 3.34. Gel permeation chromatograph of PEAP (1.5×10^{-4} cm film) before and after 4 hours of irradiation ($\lambda \geq 300\text{nm}$, degassed and run through a $7\mu\text{m}$ pore Ultrastyrigel[®] linear column at $1.0\text{ cm}^3\text{ min}^{-1}$).

The number of chain scissions per original molecule, S , in film can be determined (as in solution) by the relationship:⁹

$$S = \frac{(\overline{M}_n)_o}{(\overline{M}_n)_t} - 1$$

Figure 3.35 shows the number of chain scissions per original molecule as a function of time of exposure, t , for all four polymers. As in solution, there exists initial linearity which implies that random chain scission occurs. After longer exposures, the rates fall off implying that competing reactions, such as crosslinking or quenching by reaction products are occurring. The extent of chain scission increases upon irradiation for PMAP, P34DMAP and PEAP as in solution, but decreases for P35DMAP, perhaps implying that crosslinking is taking place more rapidly.

The quantum yield for chain scission in film is determined by the relation:⁶

$$\phi_{cs} = \frac{n}{I_A t}$$

where n is the number of moles of chain scissions, I_A is the number of einsteins of photons absorbed by the polymer solution and t is the irradiation time. The number of moles of chain scissions can be related to the molecular weights by:¹⁰

$$n = \frac{w}{(\overline{M}_n)_o} \left(\frac{(\overline{M}_n)_o}{(\overline{M}_n)_t} - 1 \right)$$

where w is the initial mass of the polymer undergoing irradiation, $(\overline{M}_n)_o$ is the initial number-average molecular weight and $(\overline{M}_n)_t$ is the number-average molecular weight after an irradiation time t . The absorbed intensity is related to the incident intensity I_o by:³

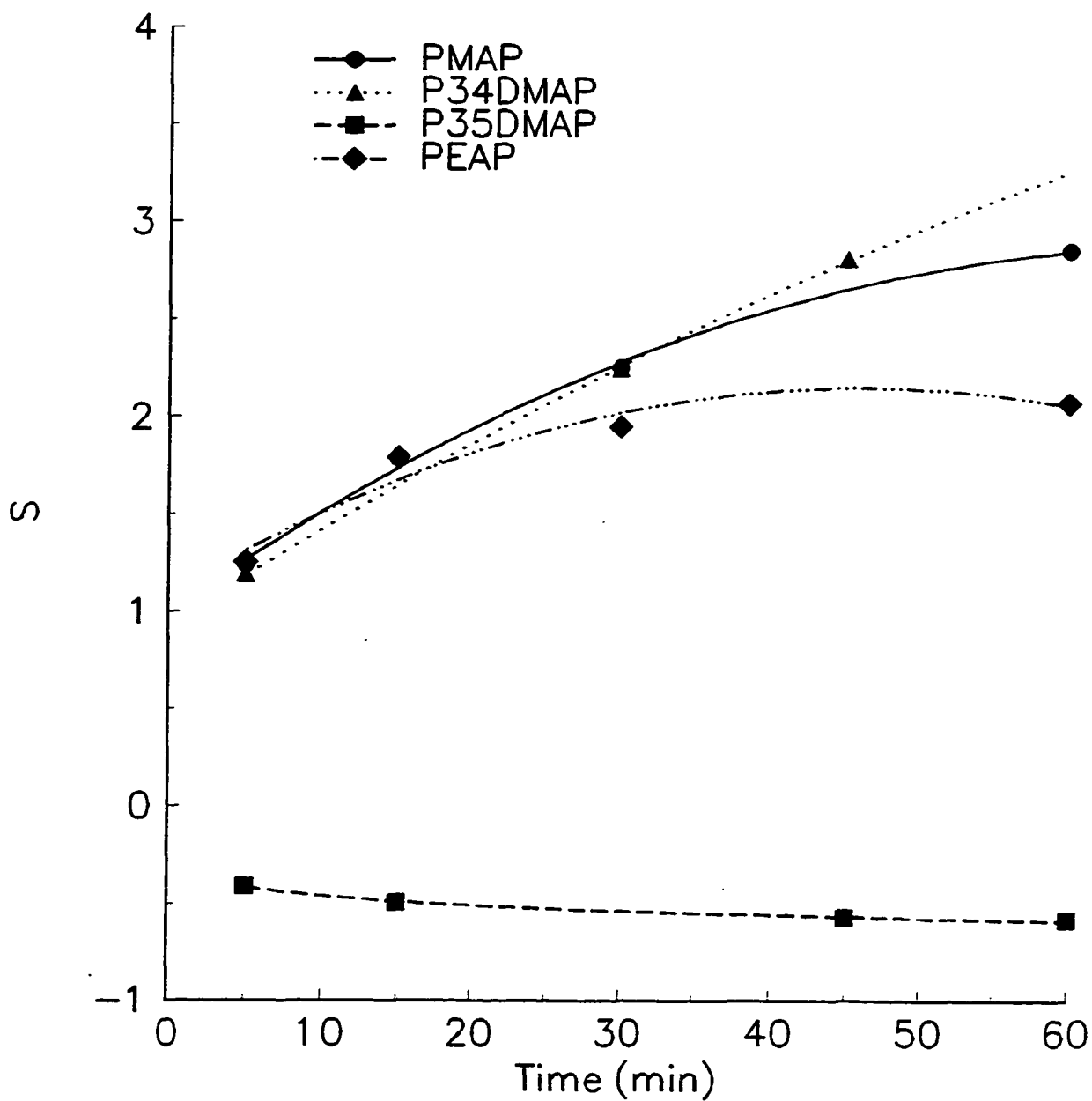


Figure 3.35. Number of chain scissions per original molecule of PMAP, P34DMAP, P35DMAP and PEAP (1.5×10^{-4} cm film) as a function of irradiation time ($\lambda \geq 300\text{nm}$, degassed).

$$I_A = I_0(1 - 10^{-\beta l})$$

where β is the absorption coefficient (equivalent to ϵc) and l is the thickness of the film.

$$\phi_{cs} = \frac{w[(\overline{M}_n)_0 / (\overline{M}_n)_t - 1]}{(\overline{M}_n)_0 I_0 [1 - 10^{-\beta l}] t}$$

The quantum yields for chain scission for all polymers were determined from the linear portion of the S versus t plots and are listed in Table 3.11.

Table 3.11. Quantum Yields for Chain Scission ($\lambda \geq 300\text{nm}$) Polymers in Thin Film ($1.5 \times 10^{-4} \text{ cm}$).

POLYMER	ϕ_{cs} ($\pm 10\%$) mol(Einstein ⁻¹)
PMAP	5.5×10^{-3}
P34DMAP	2.9×10^{-4}
P35DMAP	1.9×10^{-3}
PEAP	7.0×10^{-3}

All values are lower for the solid state reactions and this reflects the difficulty of separation of the macro-fragments in the more viscous medium. The ϕ_{cs} for PEAP is comparable to that for PMAP and both have significantly larger quantum yields of chain scission than the di-methoxylated poly(acrylophenones). This is analogous to the results obtained for solution reactions, and it reflects the character of the triplet.

8. THE EFFECT OF QUENCHERS IN FILM

The effects of naphthalene and cis-1,3-Pentadiene on the rates of chain scission were investigated. The results are shown in Figures 3.36-39. The addition of both quenchers (0.34-7.0(w/w) percent) caused an increase in the rate of chain scission, cis-1,3-pentadiene causing a more significant increase. These results are the complete reversal of what was observed in solution. This increase in chain scission by low concentrations of naphthalene and cis-1,3-pentadiene are also reflected by GPC data (Figures 3.40-43). Both triplet quenchers increase the rate of photodegradation as represented by chain scission, as compared to irradiation in the absence of quenchers and this is also reflected by longer elution times. This could be interpreted in terms of either inefficient quenching because of low effective concentrations of quenchers or that these molecules are acting as sensitizers, although their mechanism of operation is not obvious. It is unlikely on thermodynamical grounds, that they are acting simply as triplet sensitizers.

However, increasing the quencher concentration to a range of 50-100(w/w) percent did produce significant quenching. The addition of both quenchers caused reductions in the rate of chain scission but, as in solution, naphthalene had a more significant effect suggesting that it is a more efficient triplet quencher. The results are shown in Figures 3.36-3.39 (naphthalene). The quantum yield ratios (ϕ_o/ϕ) for chain scission in the absence (ϕ_o) and in the presence (ϕ) of naphthalene are plotted as a function of quencher concentration [Q] in Figure 3.44. It can be seen that the data for PMAP, P34DMAP, P35DMAP and PEAP are near linear but do not conform well to Stern-Volmer kinetics and the intercepts do not equal 1. Quenching in the solid state is better represented by the Perrin equation:¹³

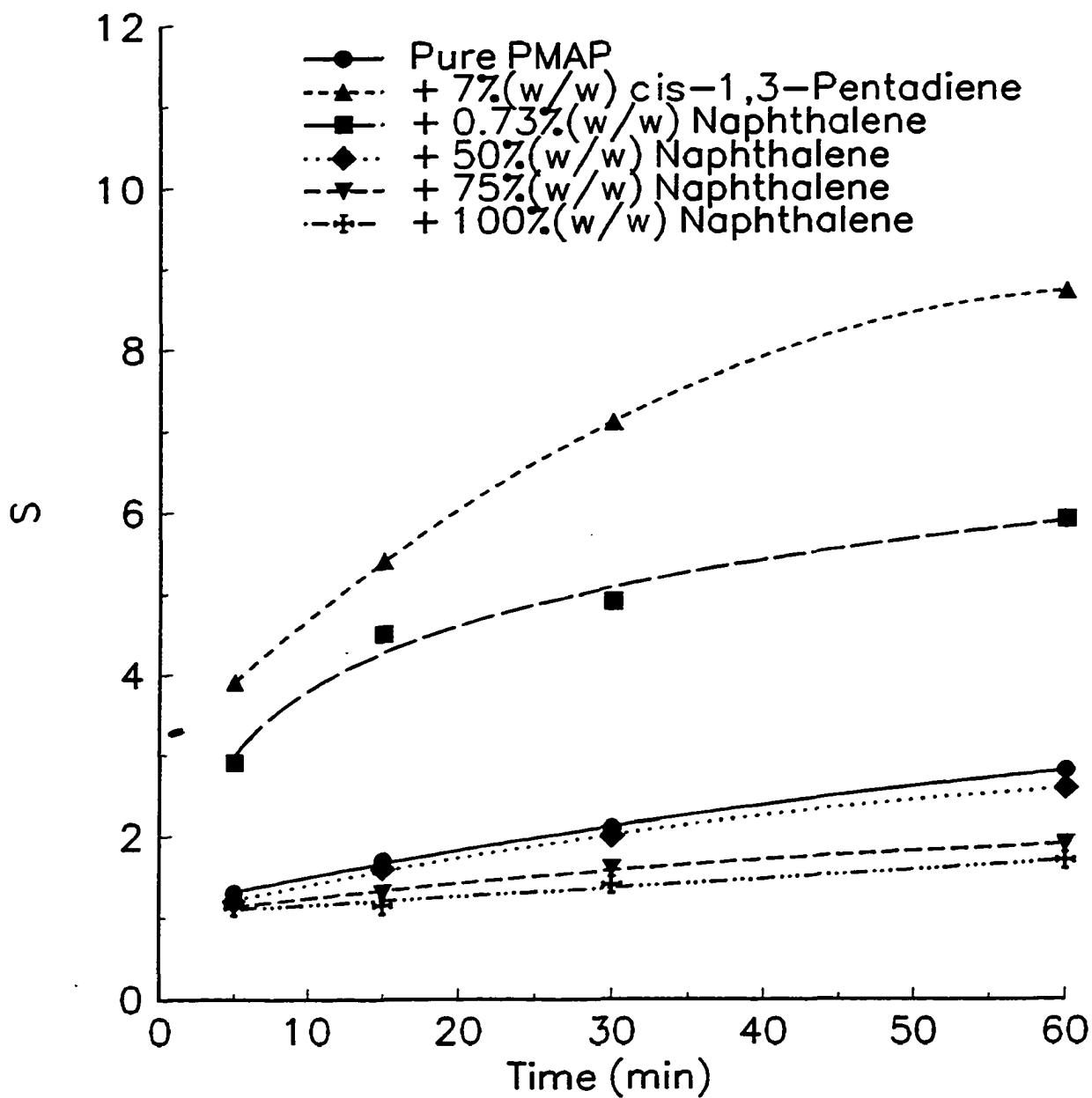


Figure 3.36. Number of chain scissions per molecule of PMAP (1.5×10^{-4} cm film) in the presence of triplet quenchers as a function of irradiation time ($\lambda \geq 300\text{nm}$, degassed).

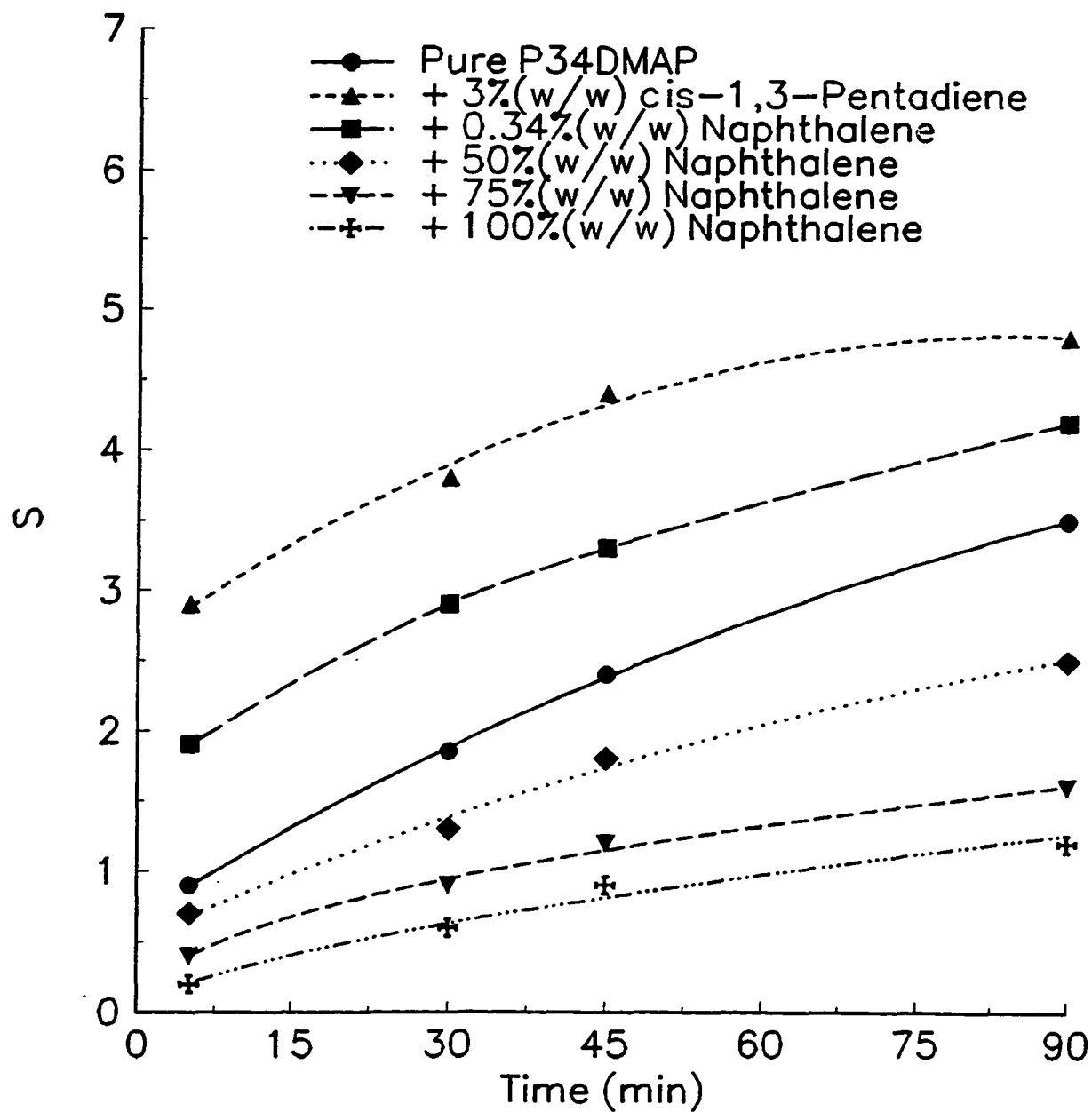


Figure 3.37. Number of chain scissions per molecule of P35DMAP (1.5×10^{-4} cm film) in the presence of triplet quenchers as a function of irradiation time ($\lambda \geq 300\text{nm}$, degassed).

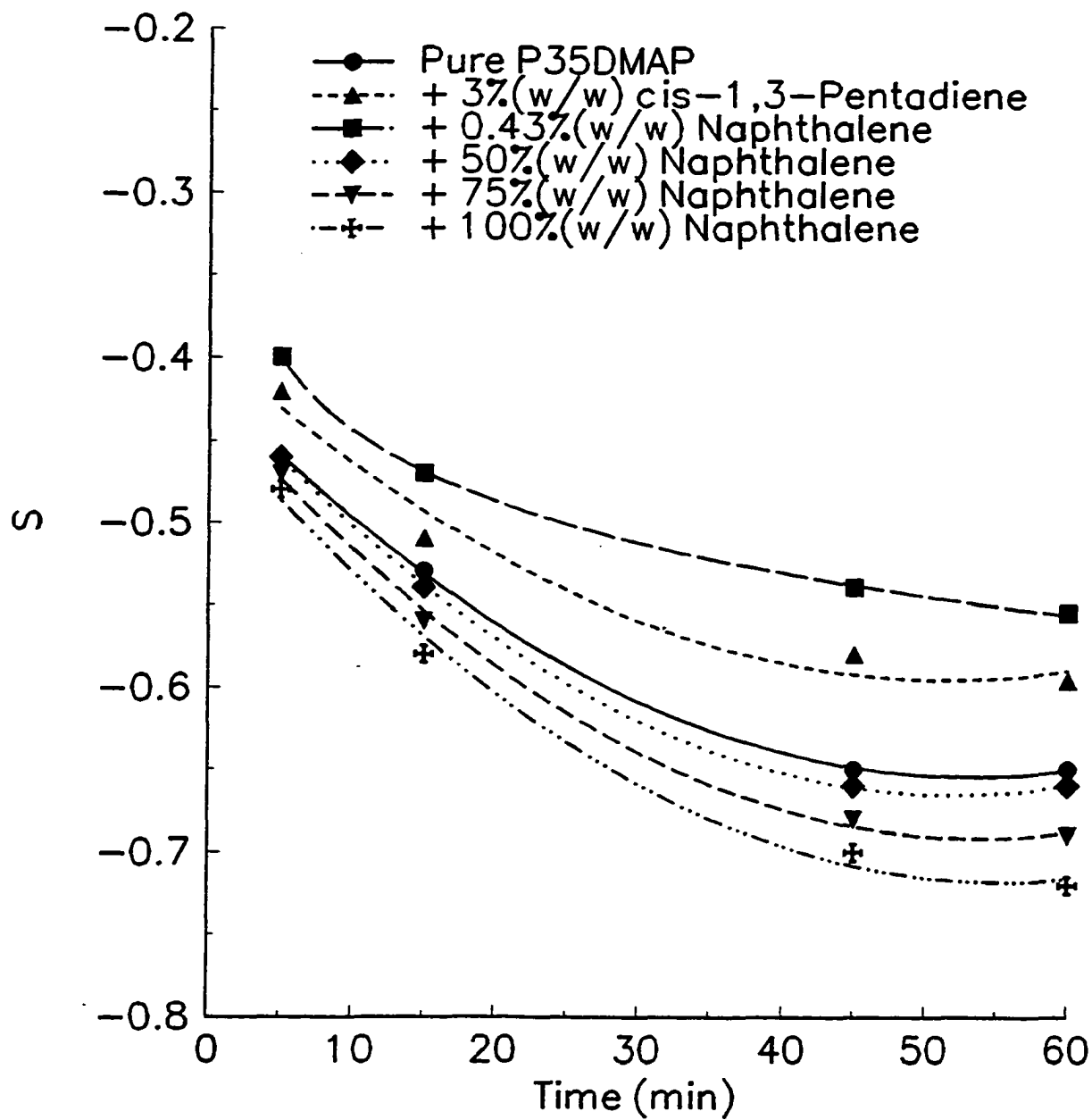


Figure 3.38. Number of chain scissions per molecule of P34DMAP (1.5×10^{-4} cm film) in the presence of triplet quenchers as a function of irradiation time ($\lambda \geq 300\text{nm}$, degassed).

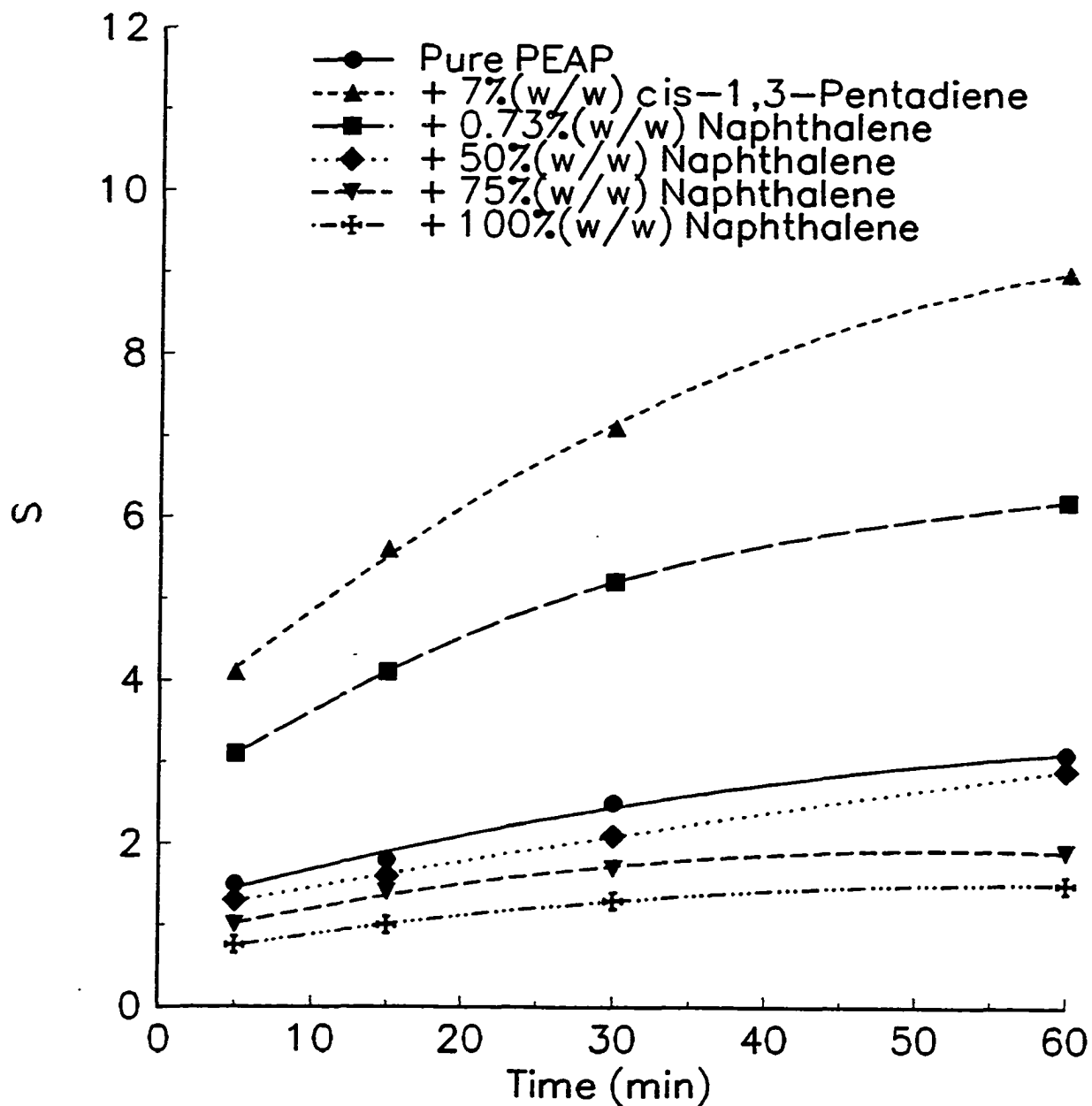


Figure 3.39. Number of chain scissions per molecule of PEAP (1.5×10^{-4} cm film) in the presence of triplet quenchers as a function of irradiation time ($\lambda \geq 300\text{nm}$, degassed).

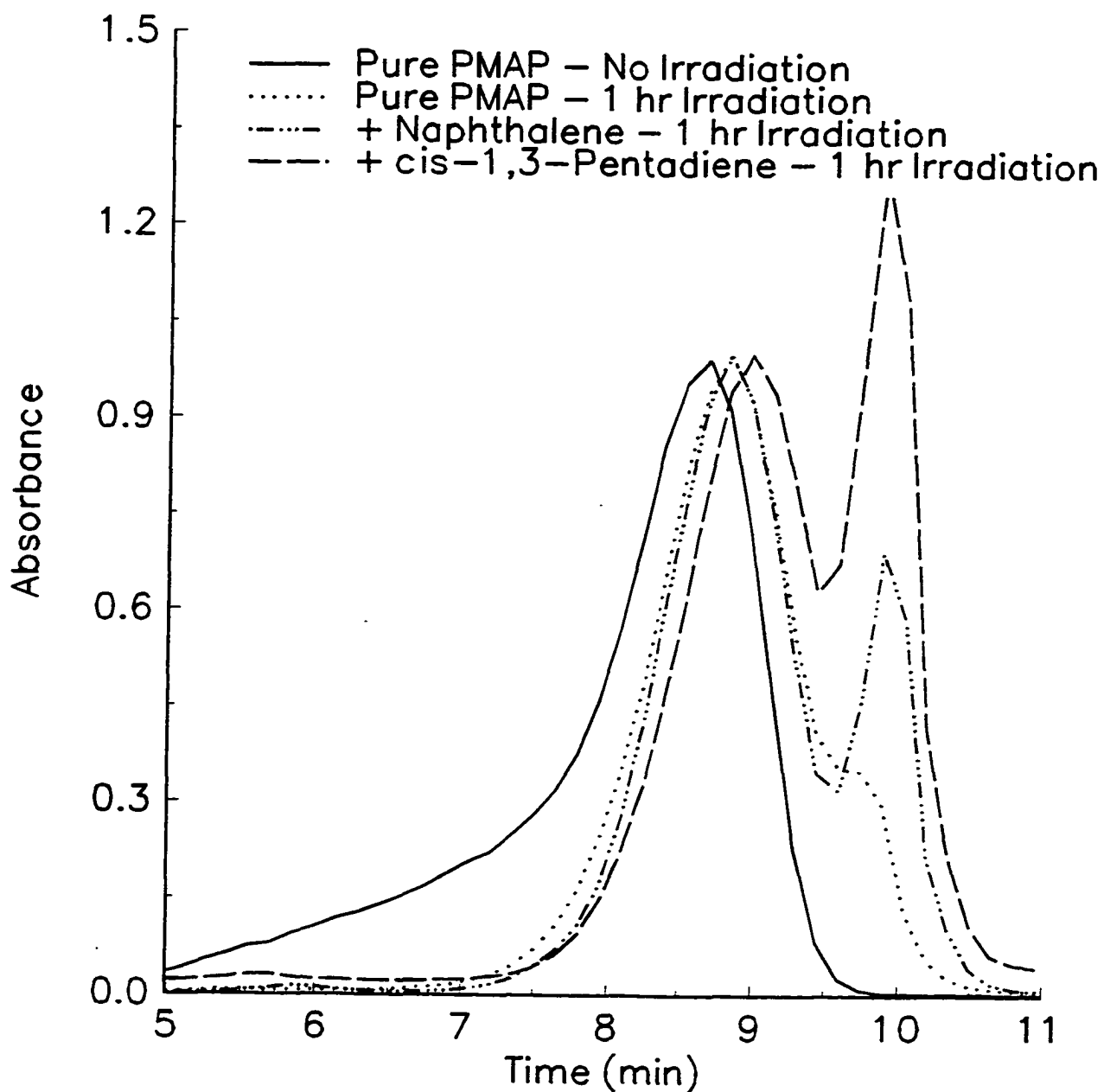


Figure 3.40. Gel permeation chromatograph of PMAP (1.5×10^{-4} cm film) before and after 1 hour of irradiation in the presence and absence of triplet quenchers ($\lambda \geq 300\text{nm}$, degassed and run through a $7\mu\text{m}$ pore Ultrastyrigel[®] linear column at $1.0\text{ cm}^3\text{ min}^{-1}$).

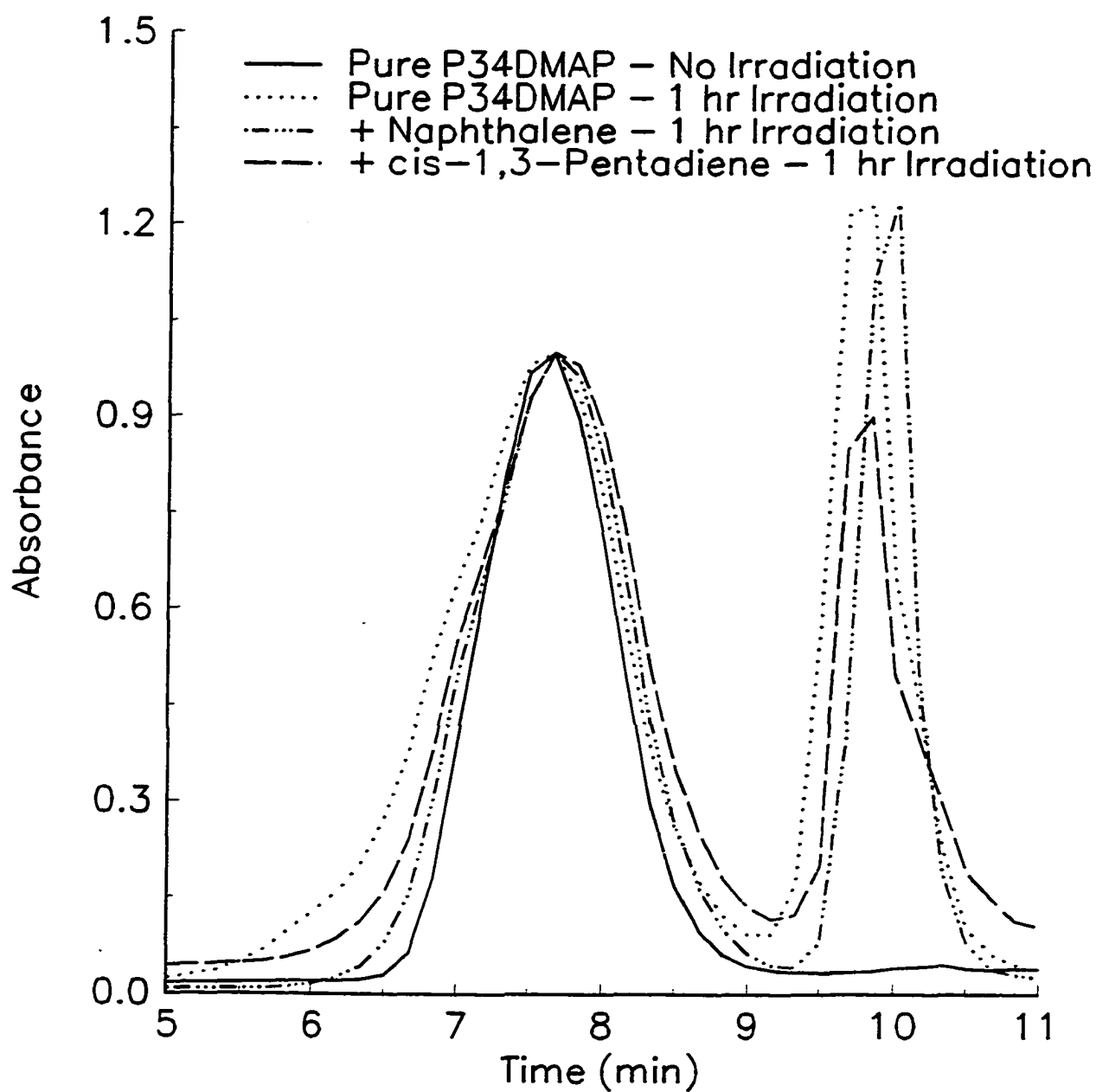


Figure 3.41. Gel permeation chromatograph of P34DMAP (1.5×10^{-4} cm film) before and after 1 hour of irradiation in the presence and absence of triplet quenchers ($\lambda \geq 300$ nm, degassed and run through a $7\mu\text{m}$ pore Ultrastyrigel[®] linear column at $1.0 \text{ cm}^3 \text{ min}^{-1}$).

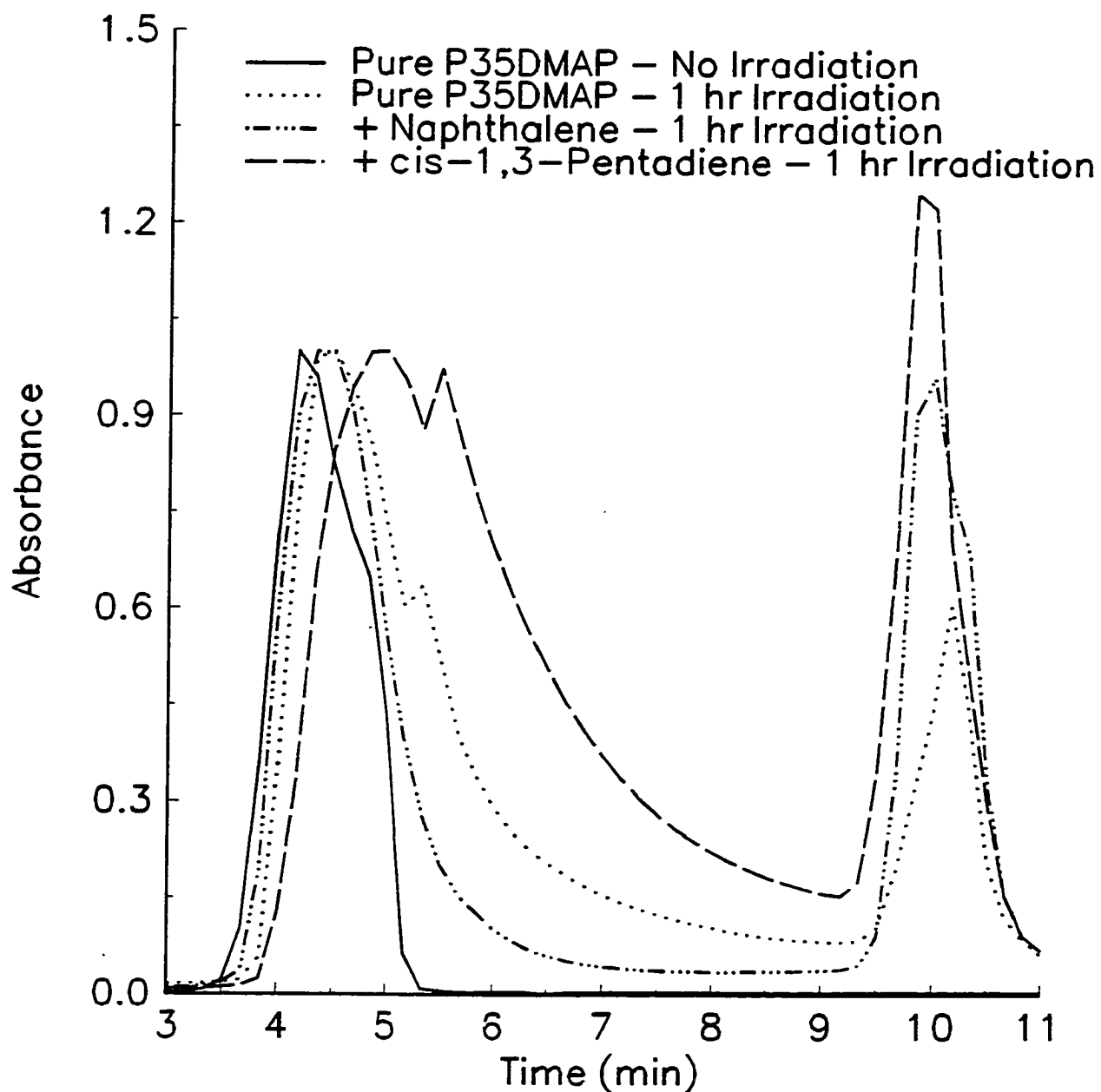


Figure 3.42. Gel permeation chromatograph of P35DMAP (1.5×10^{-4} cm film) before and after 1 hour of irradiation in the presence and absence of triplet quenchers ($\lambda \geq 300$ nm, degassed and run through a $7\mu\text{m}$ pore Ultrastyrigel[®] linear column at $1.0 \text{ cm}^3 \text{ min}^{-1}$).

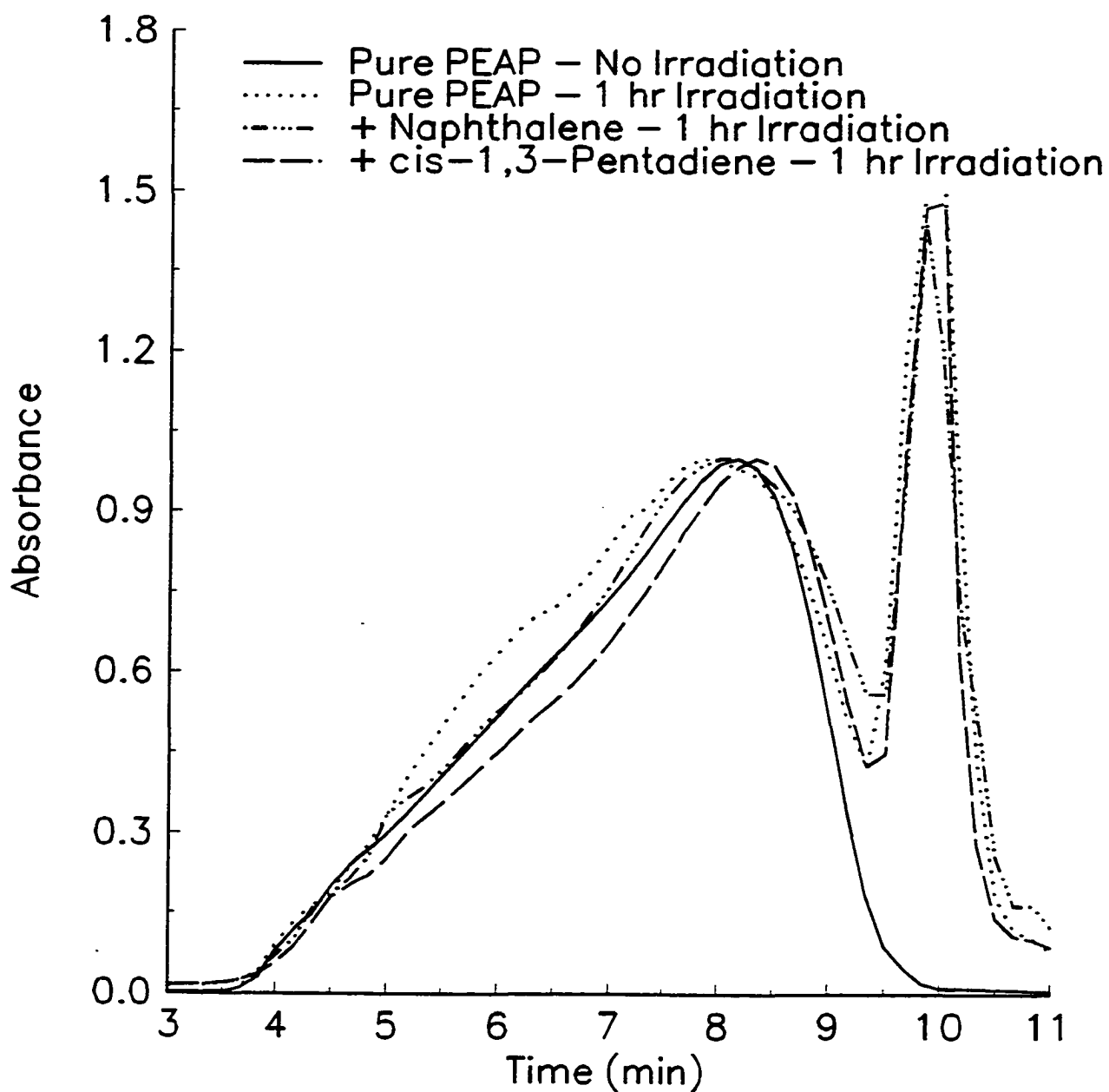


Figure 3.43. Gel permeation chromatograph of PEAP (1.5×10^{-4} cm film) before and after 1 hour of irradiation in the presence and absence of triplet quenchers ($\lambda \geq 300\text{nm}$, degassed and run through a $7\mu\text{m}$ pore Ultrastyrigel[®] linear column at $1.0\text{ cm}^3\text{ min}^{-1}$).

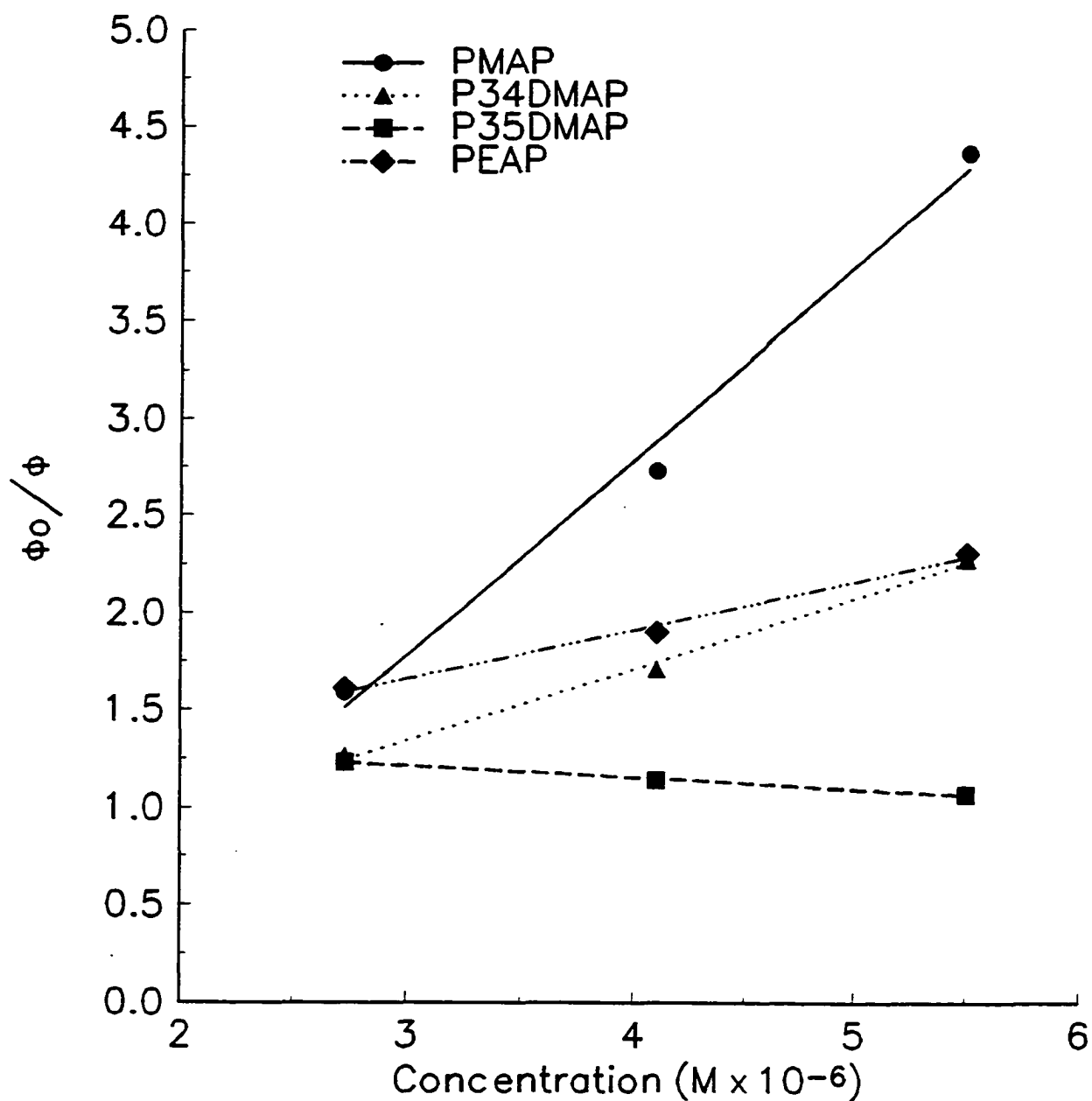


Figure 3.44. Stern-Volmer plots for quenching of PMAP, P34DMAP, P35DMAP and PEAP (1.5×10^{-4} cm film) triplets by naphthalene ($\lambda \geq 300\text{nm}$, degassed).

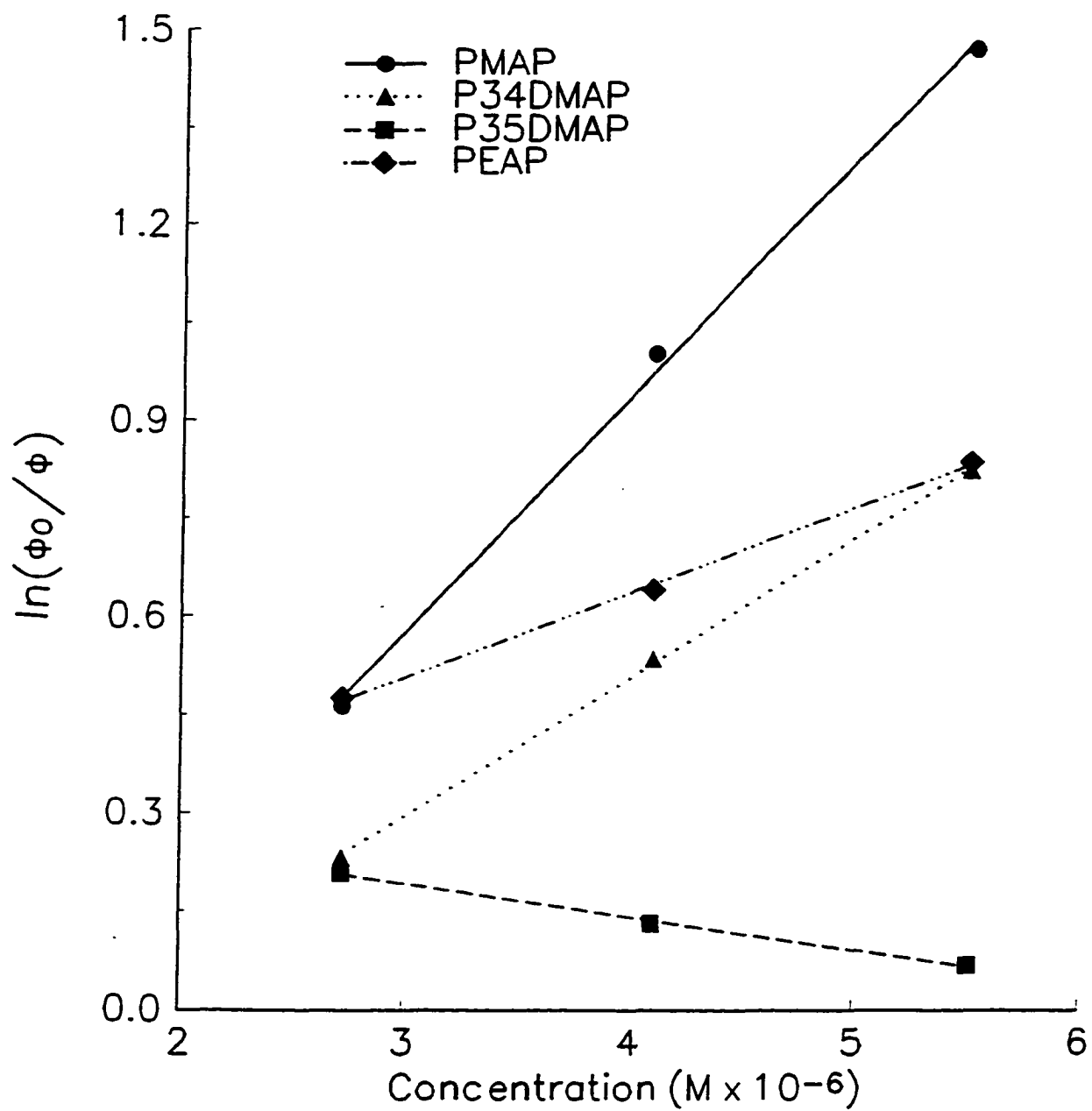


Figure 3.45. Perrin plots for quenching of PMAP, P34DMAP, P35DMAP and PEAP (1.5×10^{-4} cm film) triplets by naphthalene ($\lambda \geq 300\text{nm}$, degassed).

$$\frac{\phi_o}{\phi_x} = e^{N_A[Q]V}$$

where N_A is Avogadro's number, $[Q]$ is the quencher concentration and V is the sphere of action volume. Perrin kinetics can be tested by plotting $\ln(\phi_o/\phi_x)$ versus $[Q]$ for the four polymers. The Perrin data (Figures 3.45) are linear and this suggests that quenching of polymer triplets by naphthalene (50-100(w/w) percent) conforms to the Perrin rate law. The values of the sphere of action volume were obtained from the slopes of the Perrin graphs and are summarized in Table 3.12.

Table 3.12. Analysis of the Quenching of Methoxy and Ethoxy-Substituted Poly(acrylophenone) triplets ($\lambda \geq 300\text{nm}$) in Thin Film ($1.5 \times 10^{-4} \text{ cm}$).

POLYMER	V (Naphthalene) (dm^3)
PMAP	3.44×10^{-19}
P34DMAP	1.90×10^{-19}
P35DMAP	4.32×10^{-20}
PEAP	1.21×10^{-19}

It is clear that the sphere of action volume for naphthalene is the largest for P35DMAP.

9. CHANGES IN EMISSION SPECTRA

Direct quenching of PMAP (Figures 3.46-3.48), P34DMAP (Figures 3.49-51), P35DMAP (Figures 3.52-3.54) and PEAP (Figures 3.55-57) triplets by 1,3-cyclohexadiene, naphthalene and cis-1,3-pentadiene respectively were investigated in glass at 77K in CH_2Cl_2 .

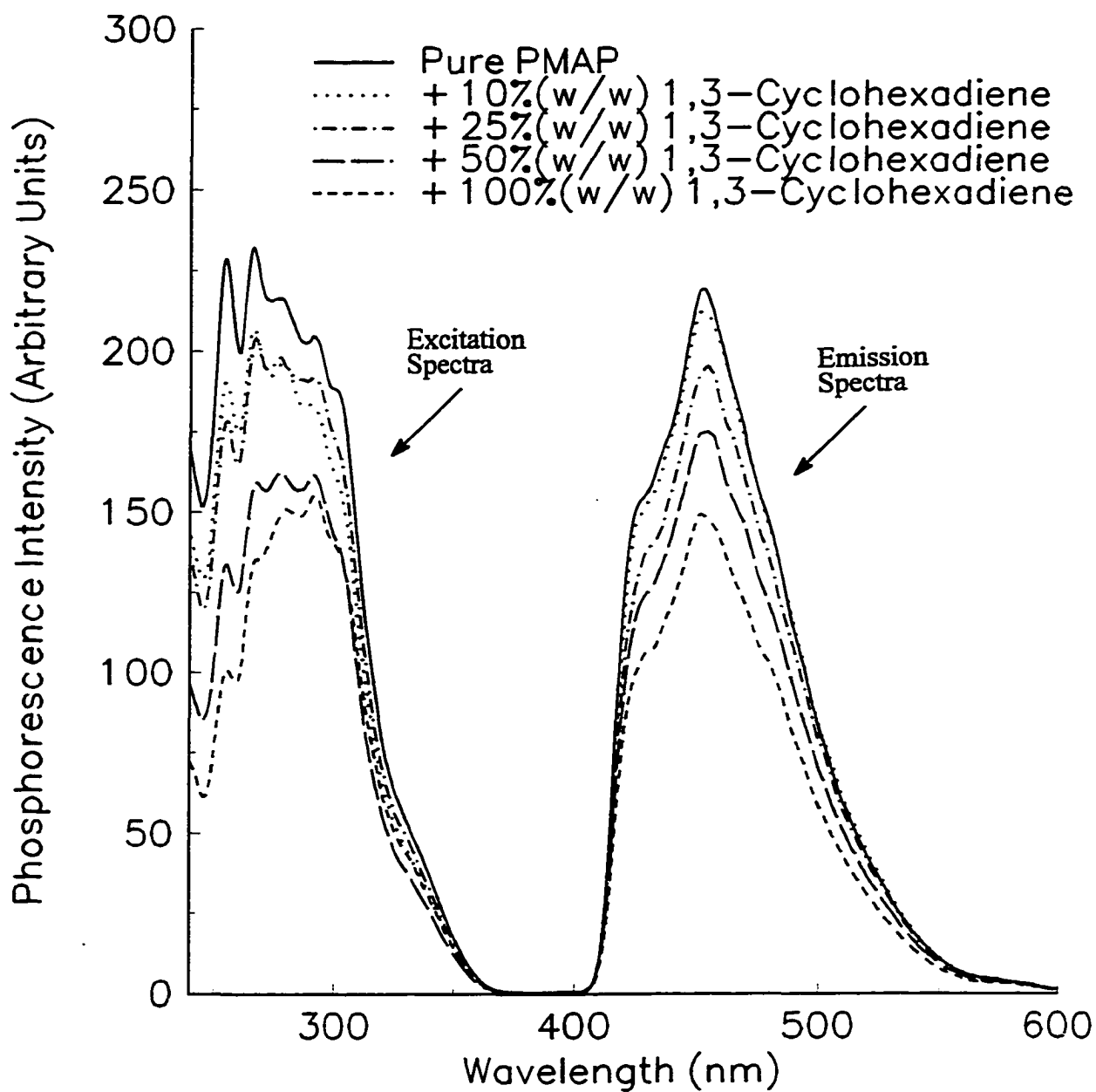


Figure 3.46. Phosphorescence spectra indicating the direct quenching of PMAP by 1,3-cyclohexadiene in glass at 77K.

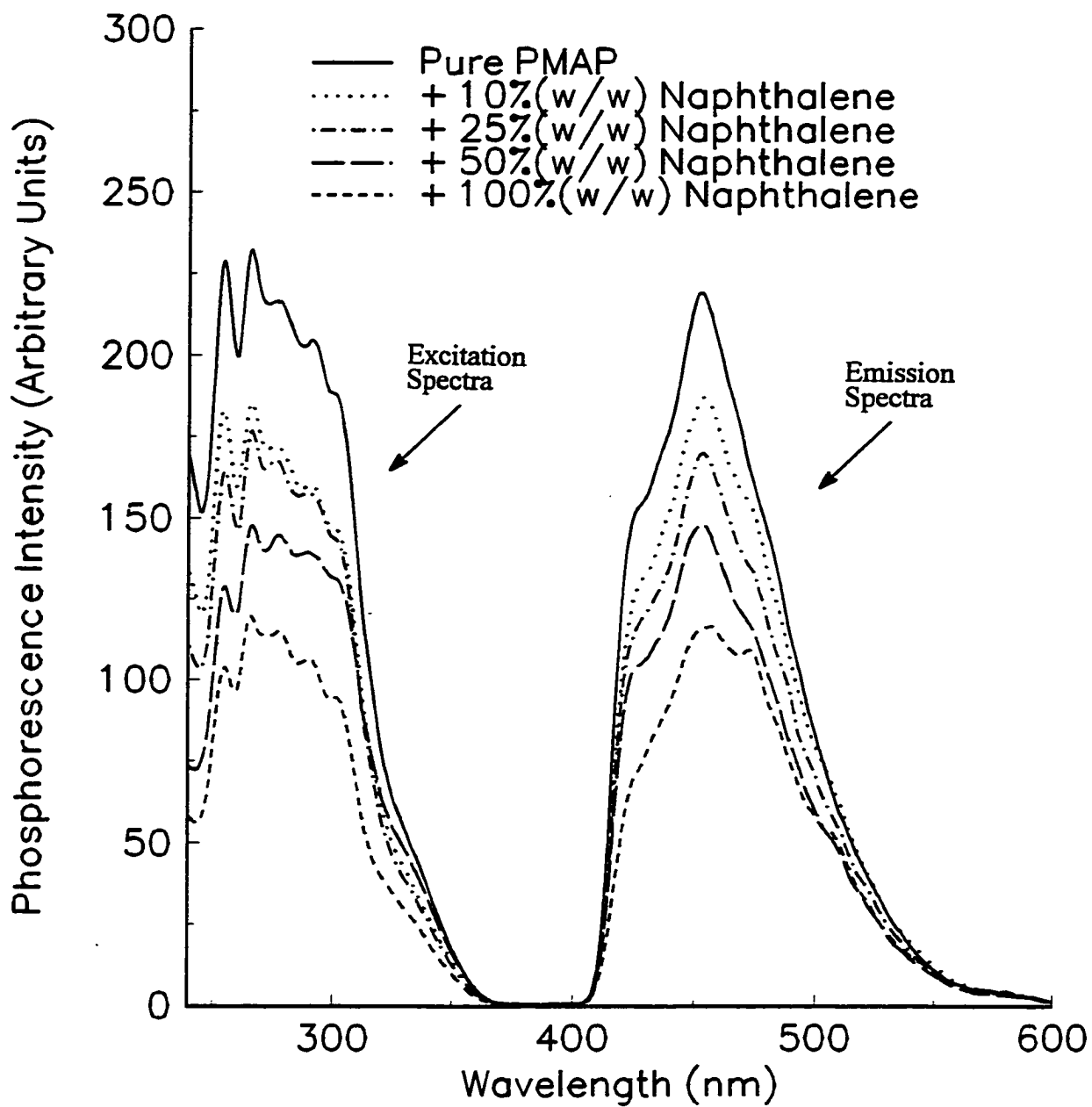


Figure 3.47. Phosphorescence spectra indicating the direct quenching of PMAP by naphthalene in glass at 77K.

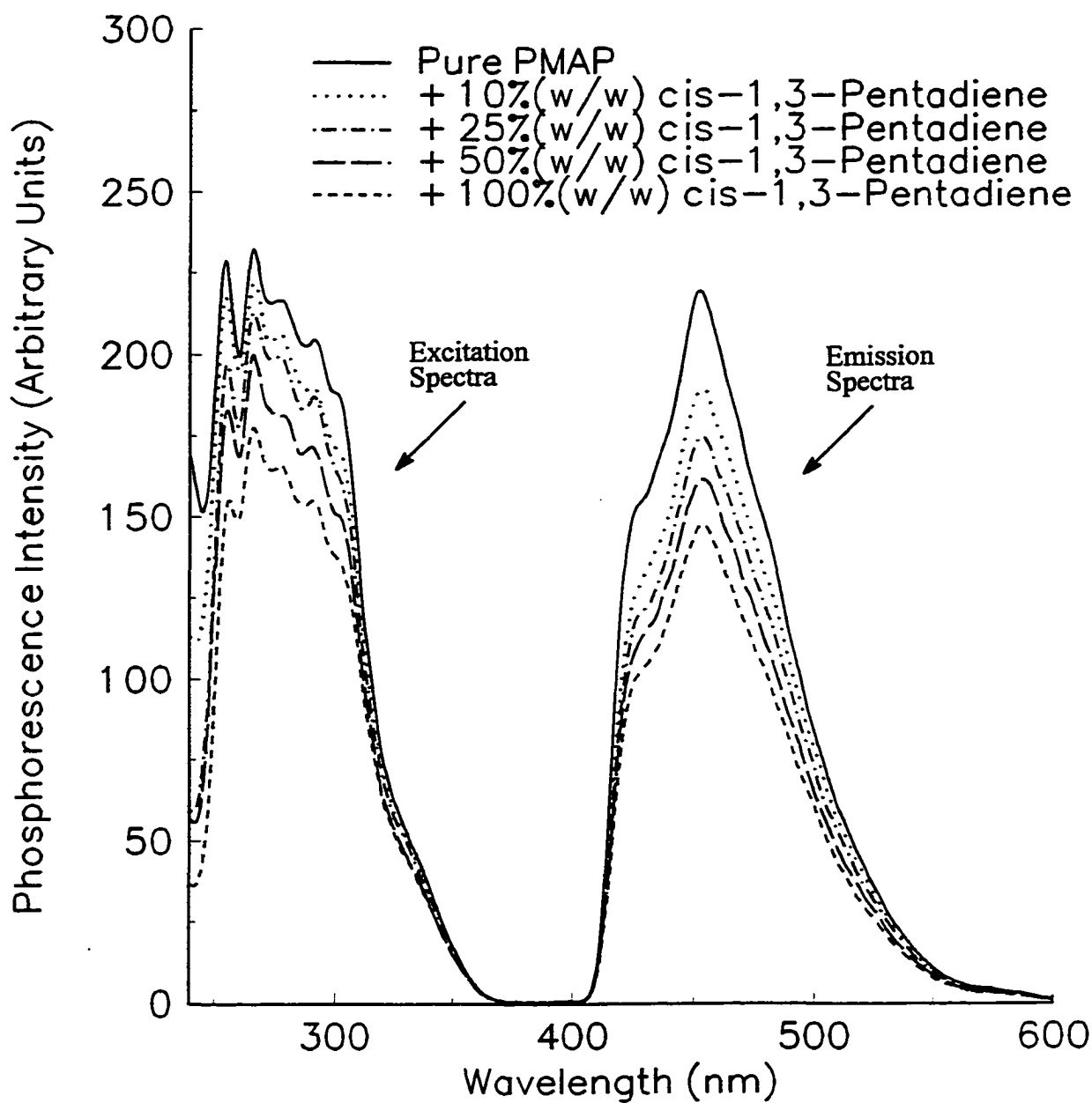


Figure 3.48. Phosphorescence spectra indicating the direct quenching of PMAP by cis-1,3-pentadiene in glass at 77K.

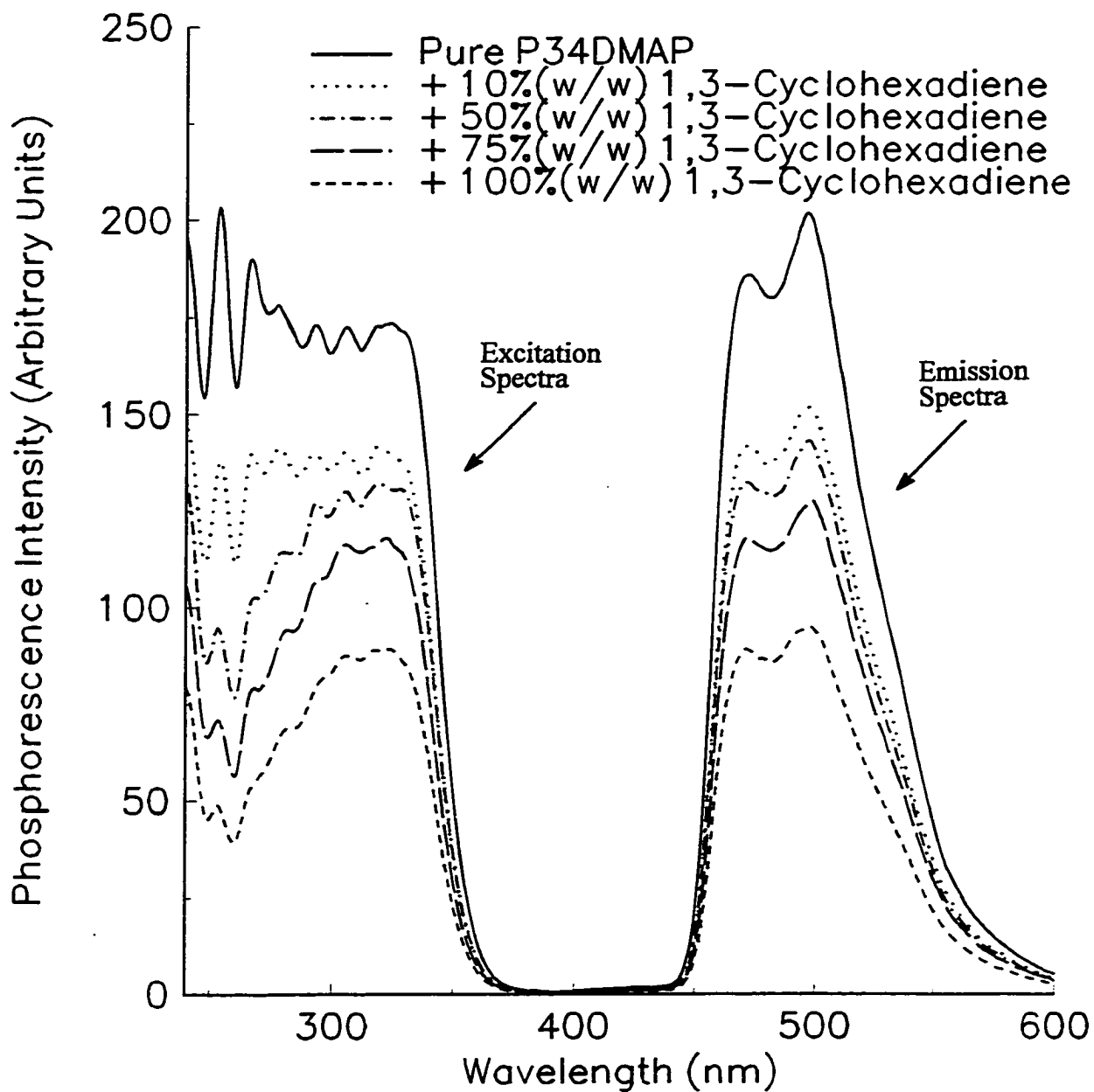


Figure 3.49. Phosphorescence spectra indicating the direct quenching of P34DMAP by 1,3-cyclohexadiene in glass at 77K.

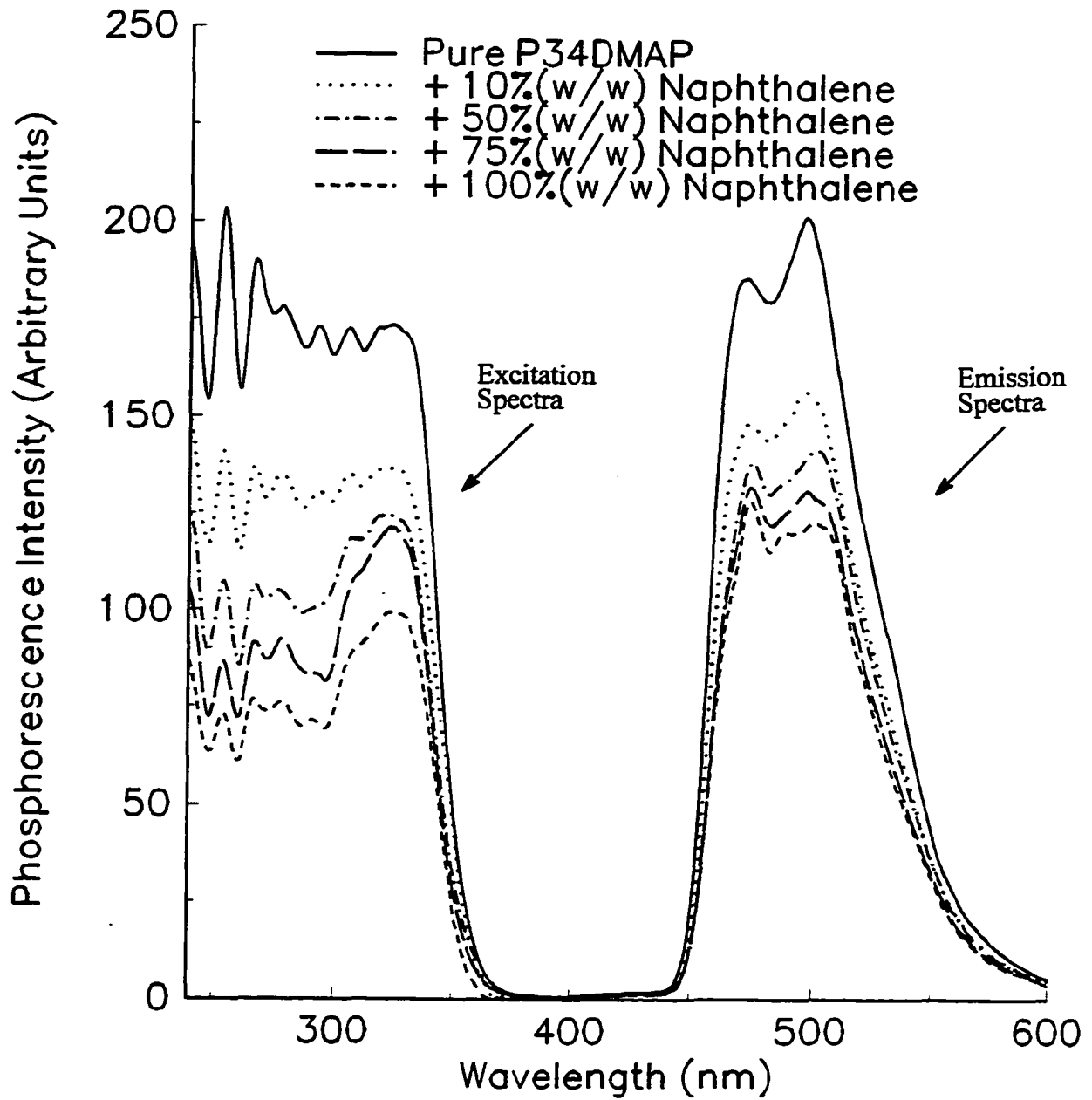


Figure 3.50. Phosphorescence spectra indicating the direct quenching of P34DMAP by naphthalene in glass at 77K.

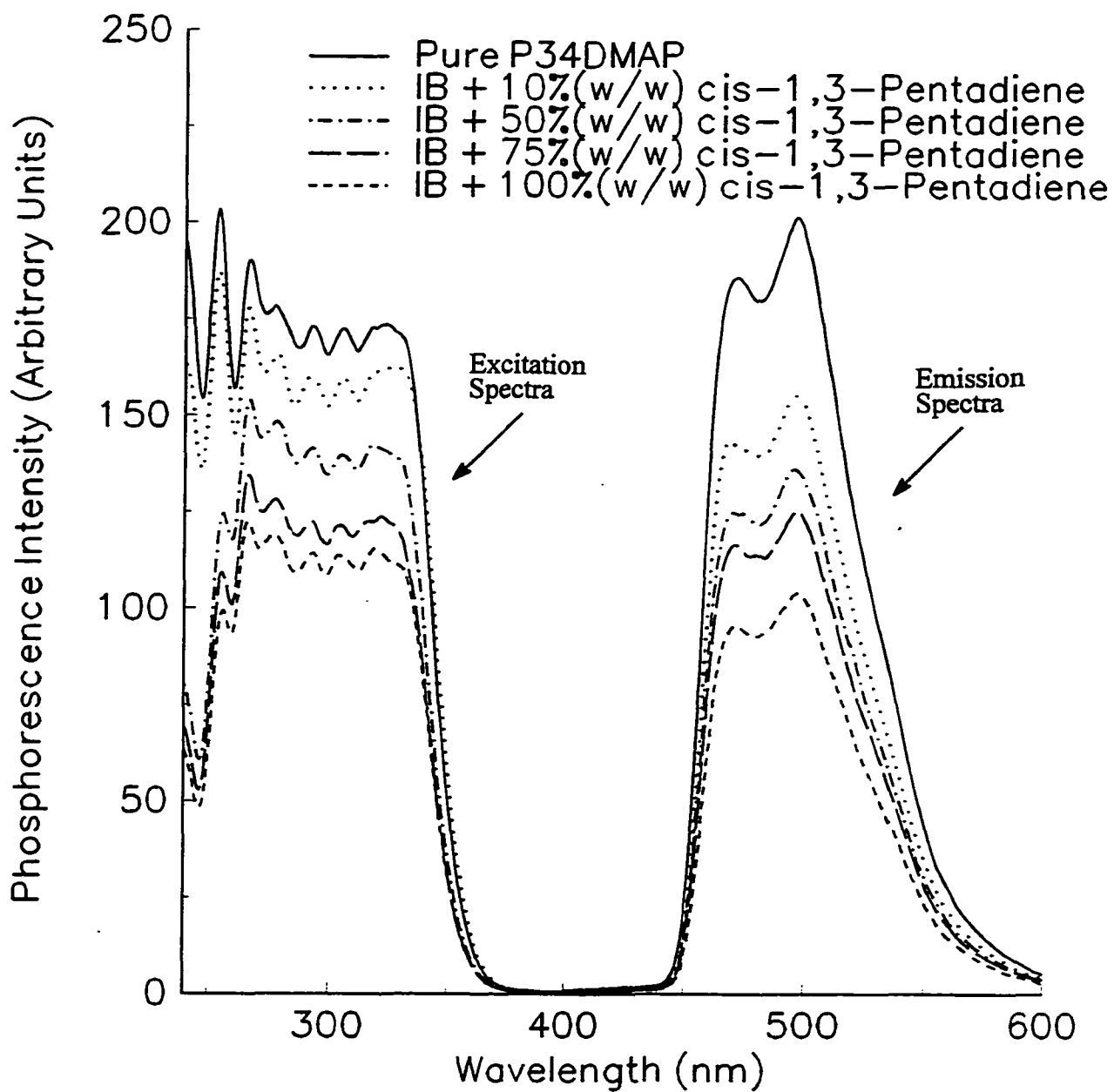


Figure 3.51. Phosphorescence spectra indicating the direct quenching of P34DMAP by cis-1,3-pentadiene in glass at 77K.

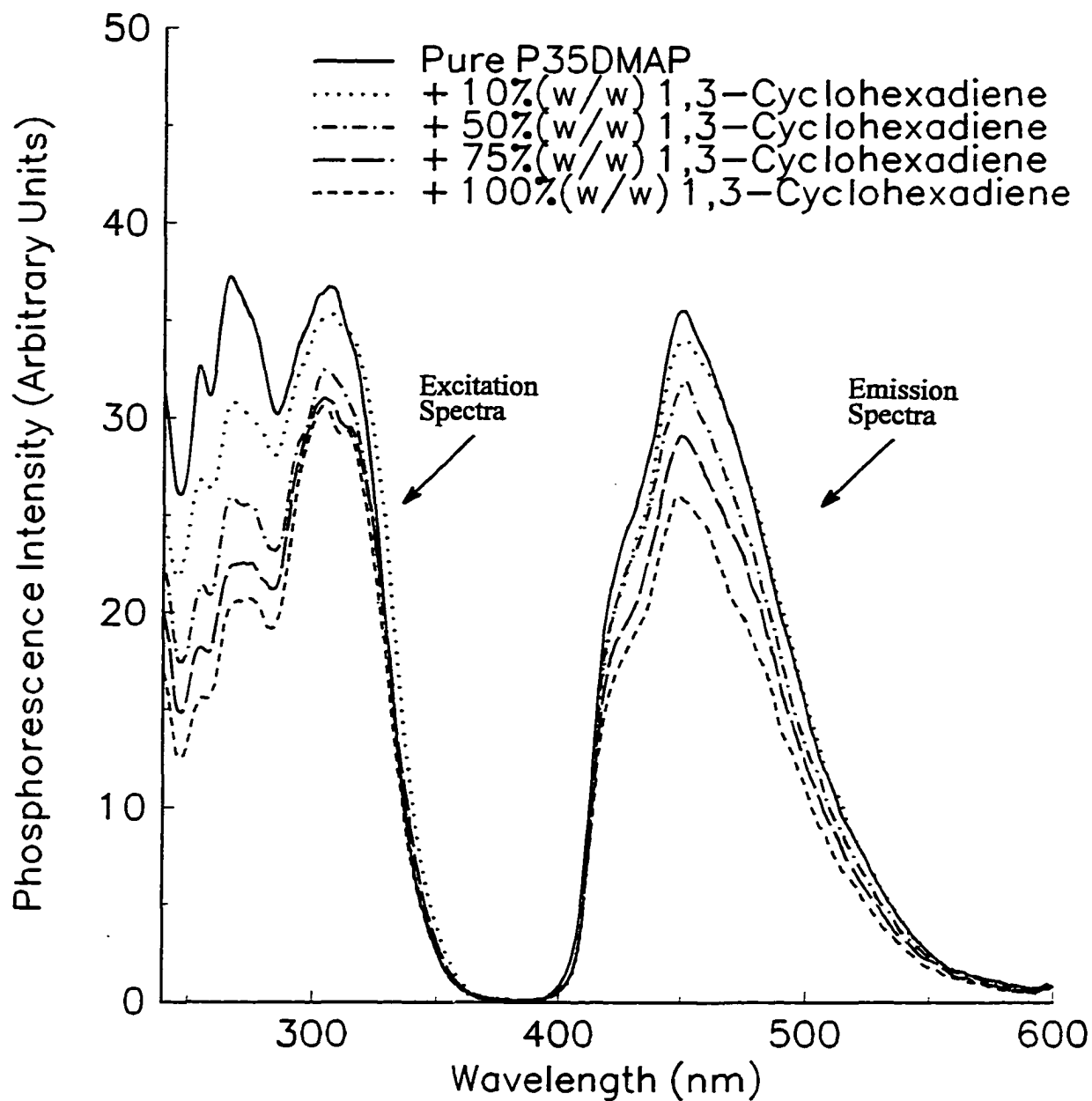


Figure 3.52. Phosphorescence spectra indicating the direct quenching of P35DMAP by 1,3-cyclohexadiene in glass at 77K.

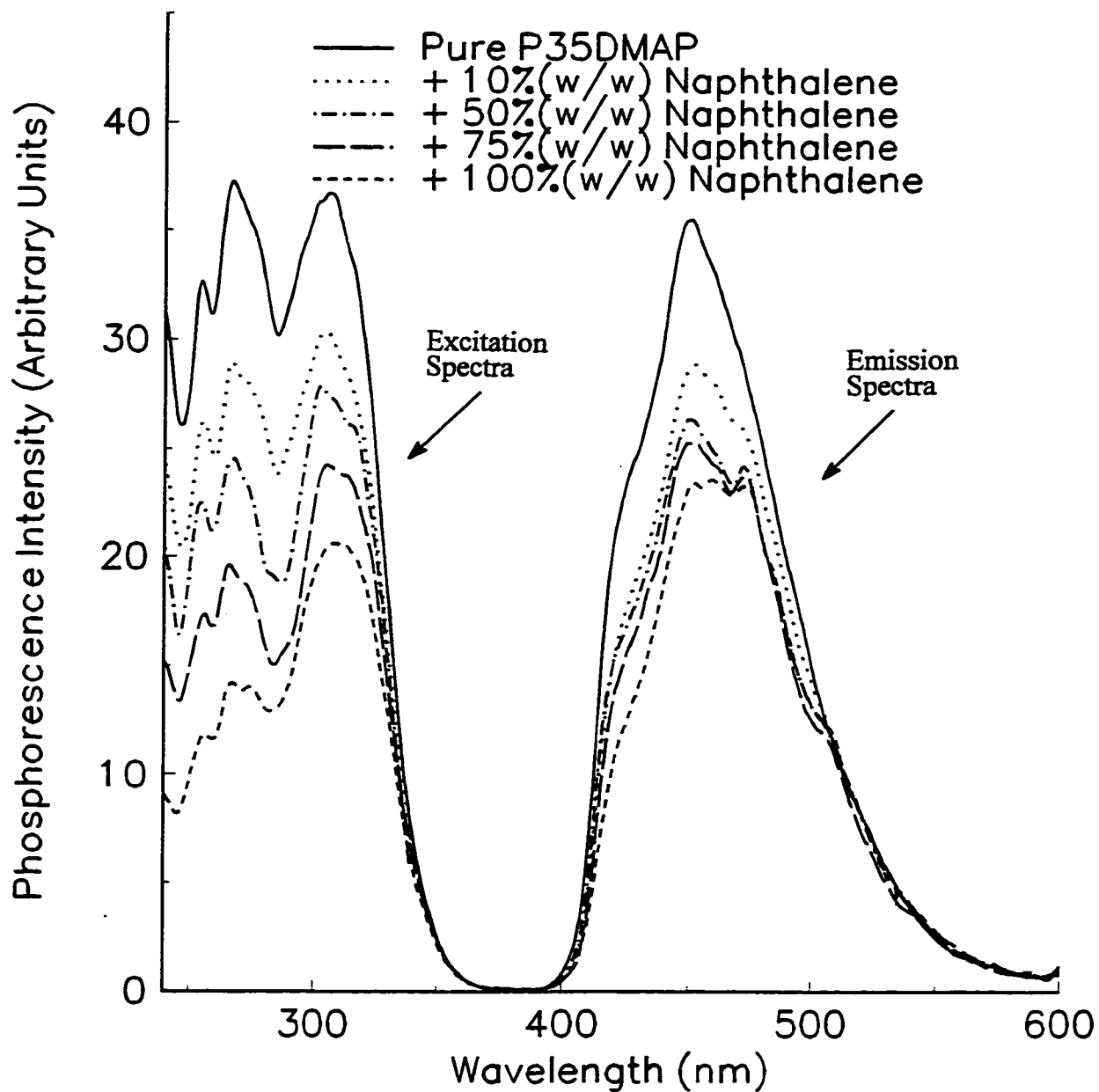


Figure 3.53. Phosphorescence spectra indicating the direct quenching of P35DMAP by naphthalene in glass at 77K.

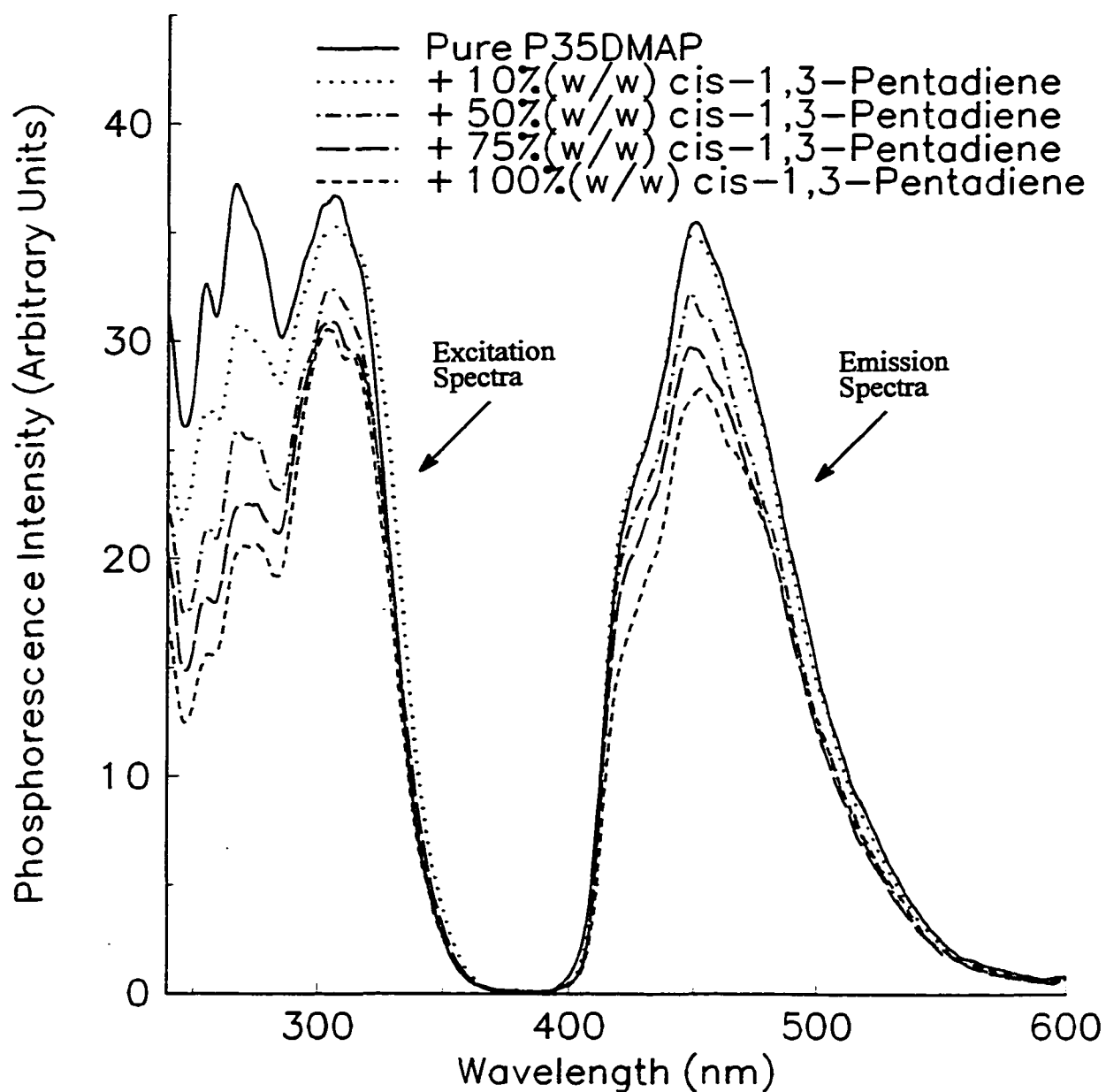


Figure 3.54. Phosphorescence spectra indicating the direct quenching of P35DMAP by cis-1,3-pentadiene in glass at 77K.

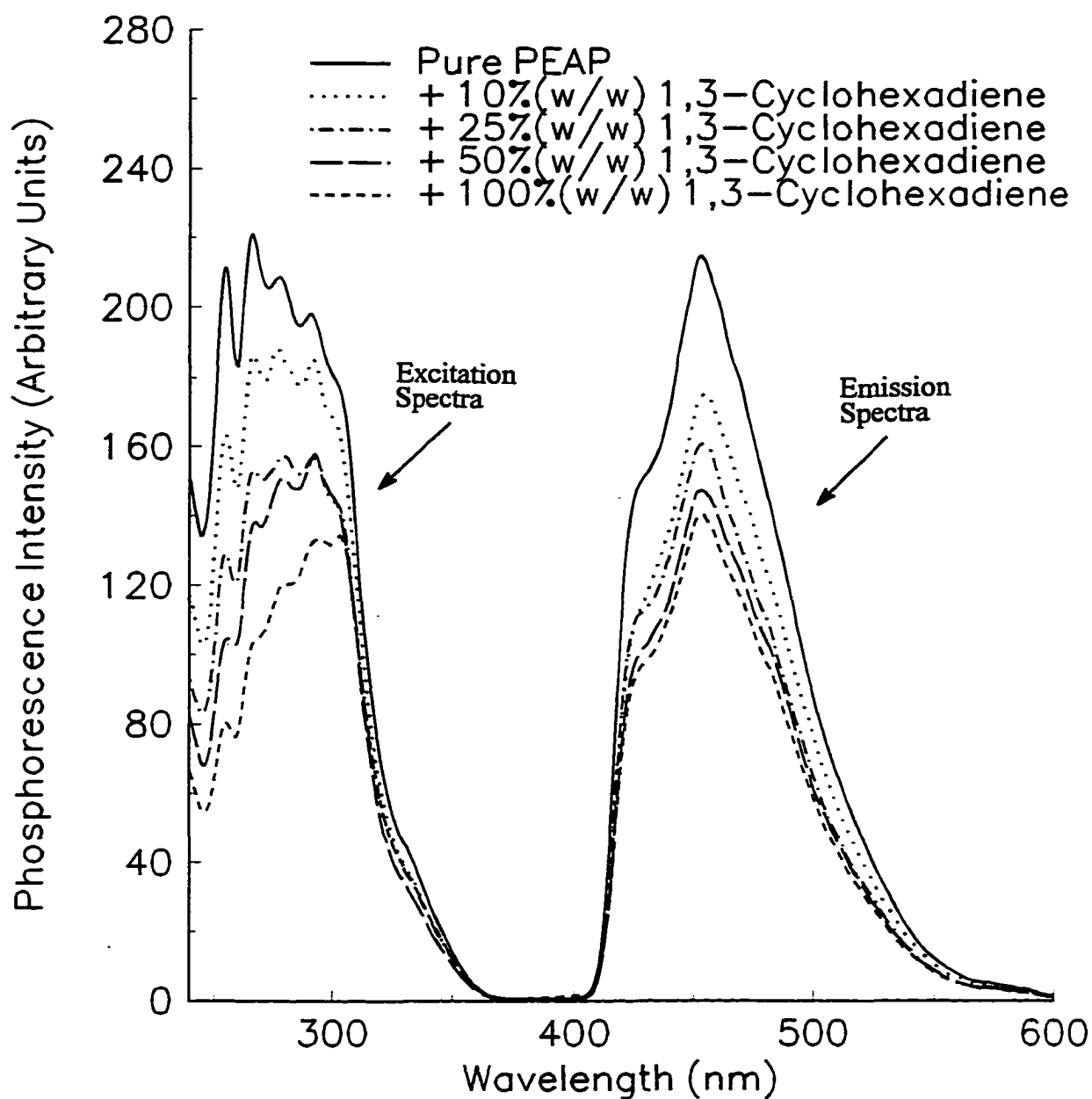


Figure 3.55. Phosphorescence spectra indicating the direct quenching of PEAP by 1,3-cyclohexadiene in glass at 77K.

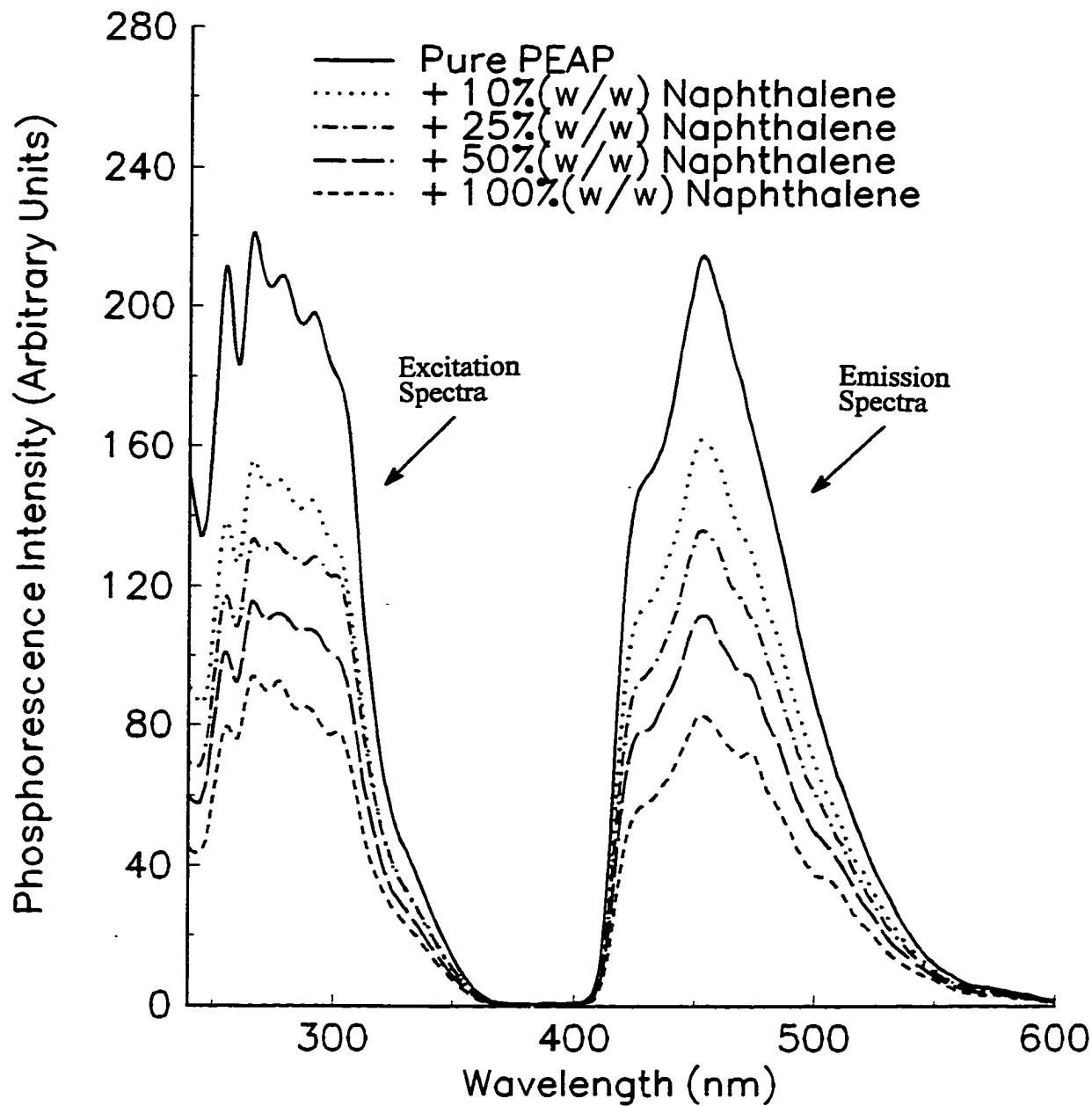


Figure 3.56. Phosphorescence spectra indicating the direct quenching of PEAP by naphthalene in glass at 77K.

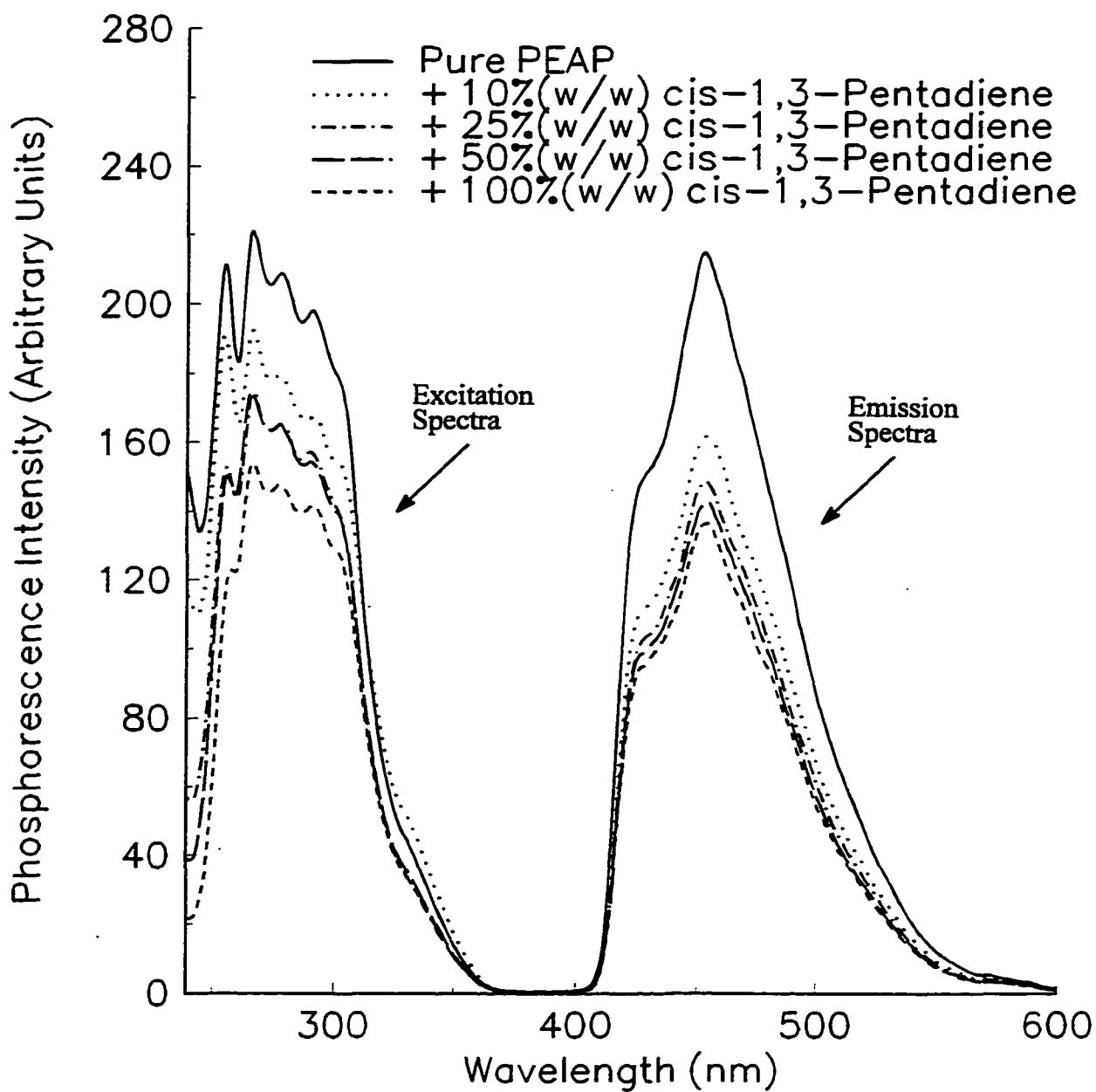


Figure 3.57. Phosphorescence spectra indicating the direct quenching of PEAP by cis-1,3-pentadiene in glass at 77K.

These conditions reflect the polymers in a solid state of immobilization. The phosphorescence intensity ratios (I_0/I_x) in the absence (I_0) and in the presence (I_x) of the quenchers are plotted as a function of quencher concentration $[Q]$ for PMAP (Figure 3.58), P34DMAP (Figure 3.59), P35DMAP (Figure 3.60) and PEAP (Figure 3.61). It can be seen that naphthalene is the most efficient triplet quencher for all four polymers followed by cis-1,3-pentadiene for PMAP and PEAP, and 1,3-cyclohexadiene for P34DMAP and P35DMAP. It can also be seen that all sets of data are near linear but do not conform well to Stern-Volmer kinetics and the intercept is not equal to 1. Quenching in the solid state is better represented by the Perrin equation. Perrin kinetics of direct triplet quenching can be tested by plotting $\ln(I_0/I_x)$ versus $[Q]$ for the four polymers. The Perrin graphs (Figures 3.62-65) are linear and this suggests that quenching of polymer triplets conforms to Perrin kinetics. The values of the sphere of action volume were obtained from the slopes of the Perrin graphs for the four polymers and are summarized in Table 3.13.

Table 3.13. Phosphorescence Analysis of the Direct Quenching of Methoxy and Ethoxy-Substituted Poly(acrylophenones) in glass at 77K in CH_2Cl_2

POLYMER	V (1,3-Cyclohexadiene) (dm^3)	V (Naphthalene) (dm^3)	V(cis-1,3-Pentadiene) (dm^3)
PMAP	4.87×10^{-22}	13.6×10^{-22}	5.25×10^{-22}
P34DMAP	3.94×10^{-22}	6.33×10^{-22}	3.45×10^{-22}
P35DMAP	3.67×10^{-22}	4.82×10^{-22}	2.92×10^{-22}
PEAP	2.59×10^{-22}	15.3×10^{-22}	2.01×10^{-22}

It is clear that the sphere of action volume for naphthalene is the largest for all polymers.

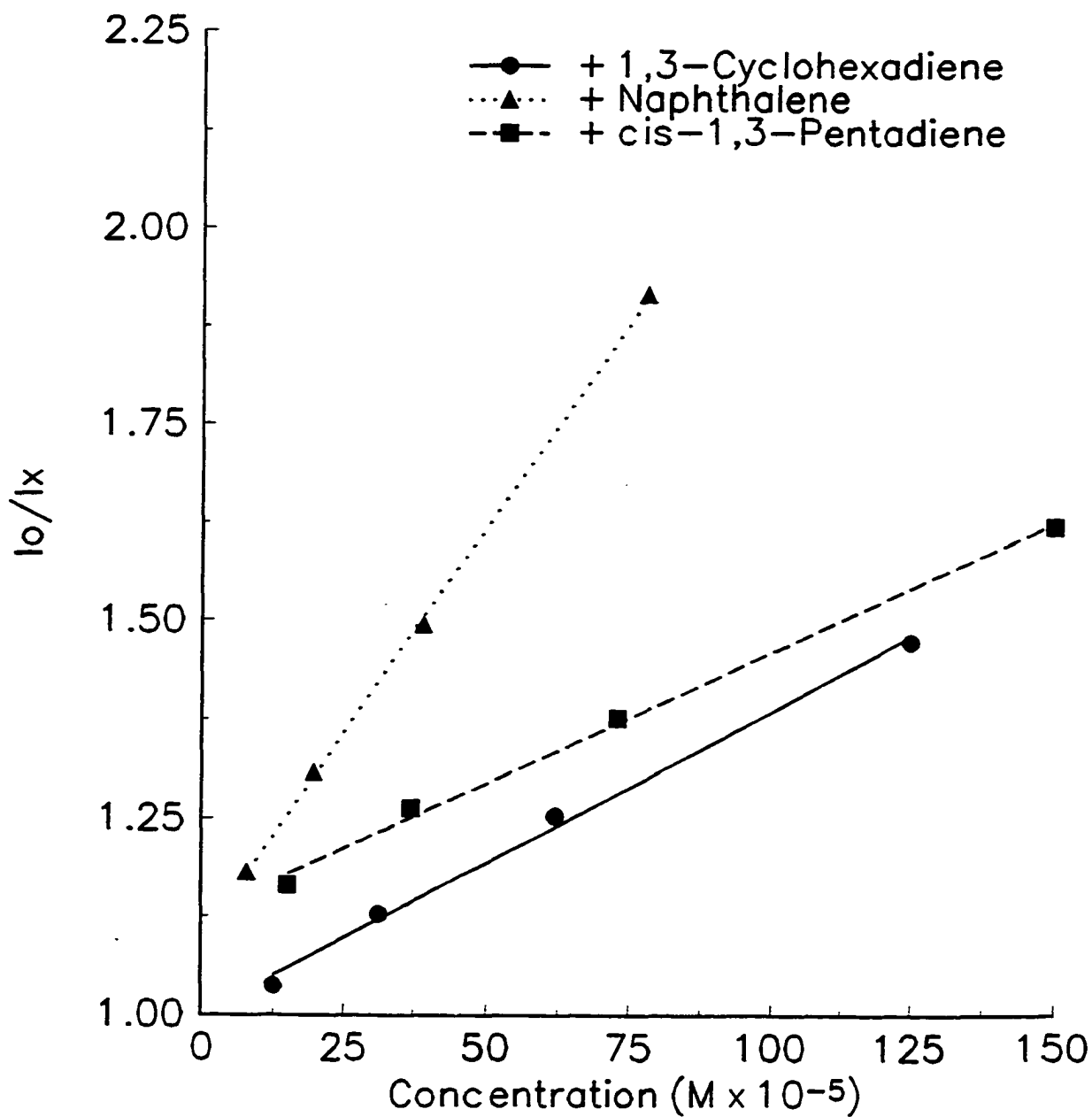


Figure 3.58. Stern-Volmer plots for quenching of PMAP (1.0×10^{-2} M solid state solution in CH_2Cl_2) triplet in glass at 77K.

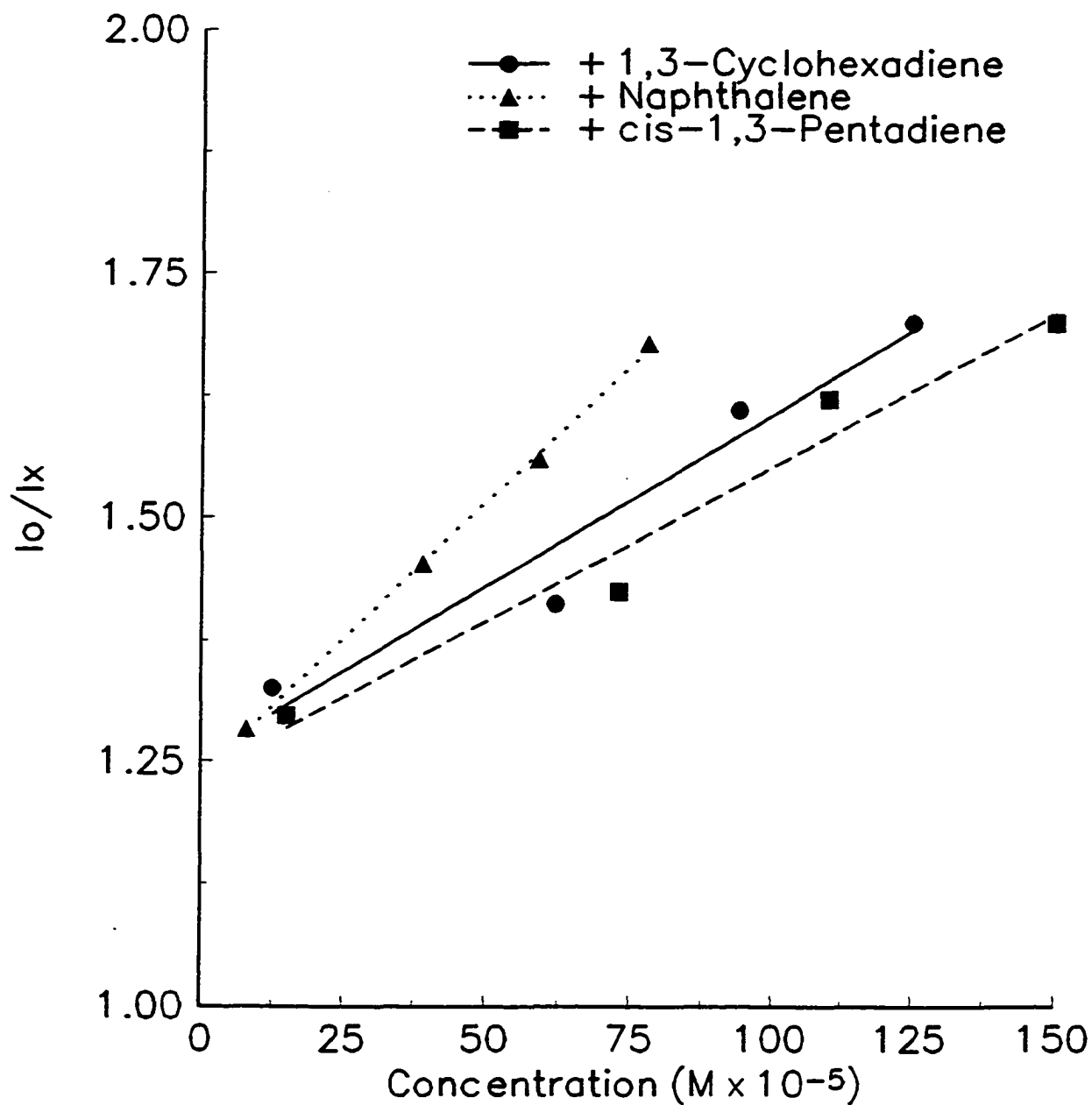


Figure 3.59. Stern-Volmer plots for quenching of P34DMAP (1.0×10^{-2} M solid state solution in CH_2Cl_2) triplet in glass at 77K.

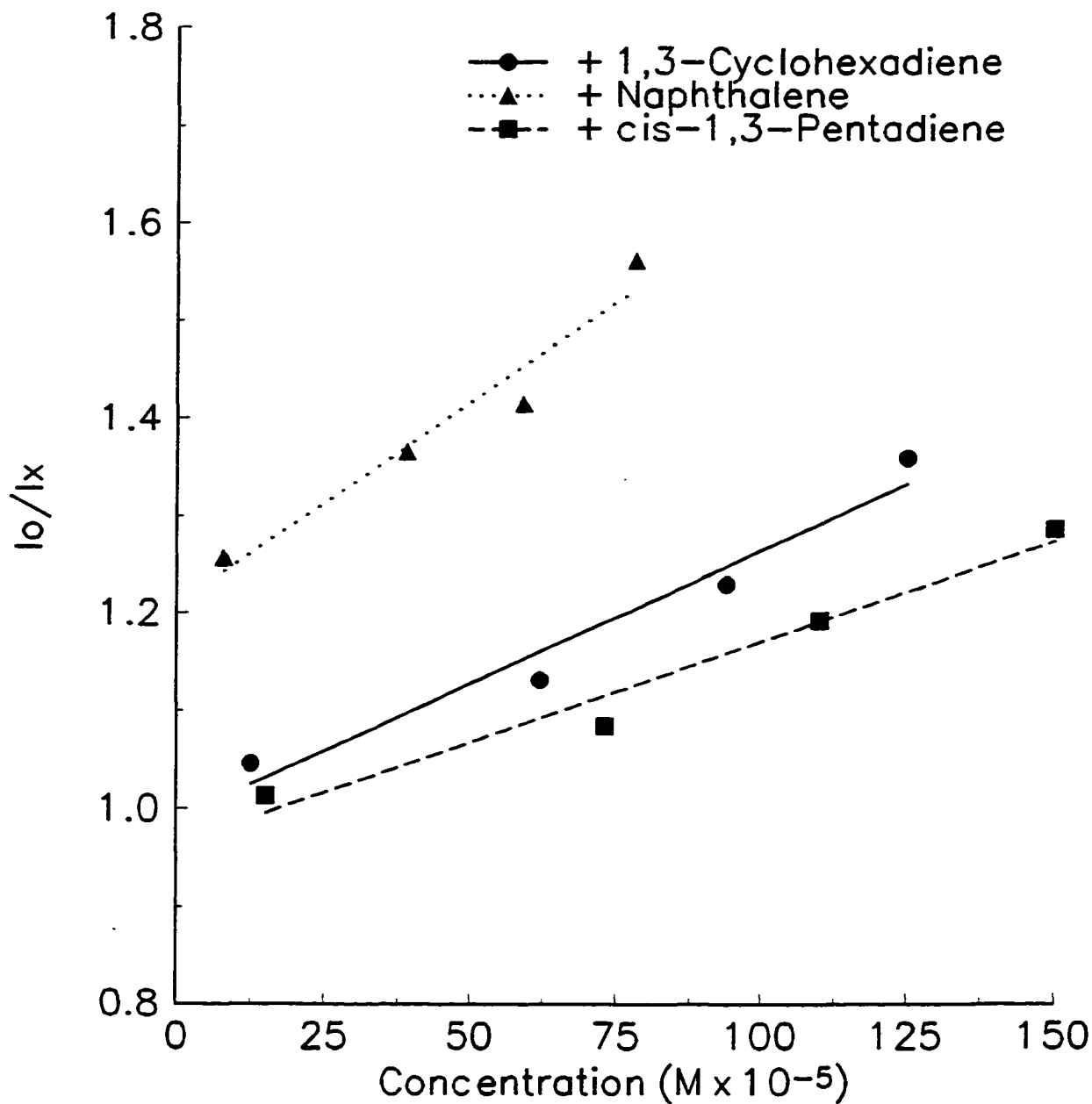


Figure 3.60. Stern-Volmer plots for quenching of P35DMAP (1.0×10^{-2} M solid state solution in CH_2Cl_2) triplet in glass at 77K.

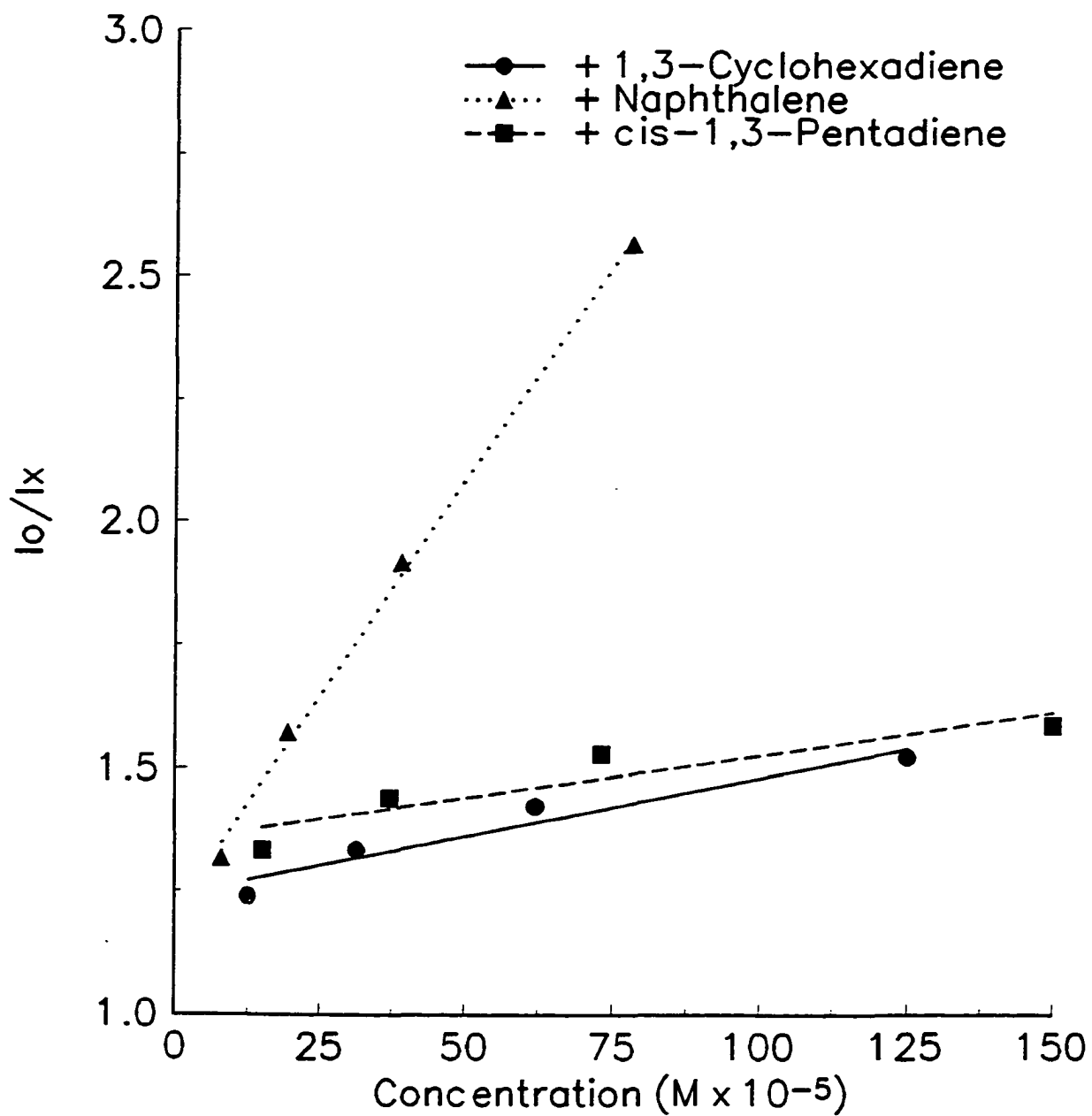


Figure 3.61. Stern-Volmer plots for quenching of PEAP (1.0×10^{-2} M solid state solution in CH_2Cl_2) triplet in glass at 77K.

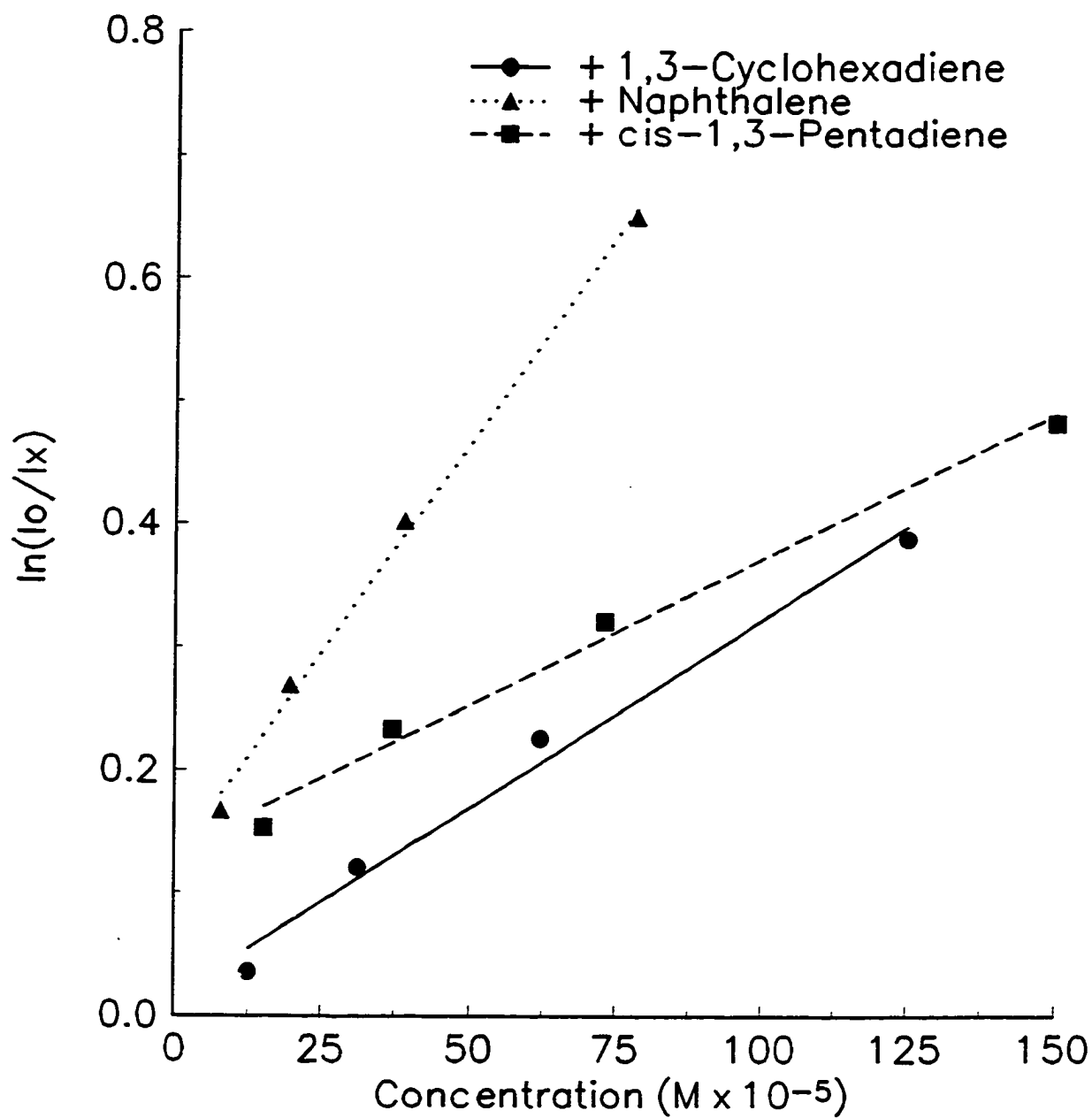


Figure 3.62. Perrin plots for quenching of PMAP (1.0×10^{-2} M solid state solution in CH_2Cl_2) triplet in glass at 77K.

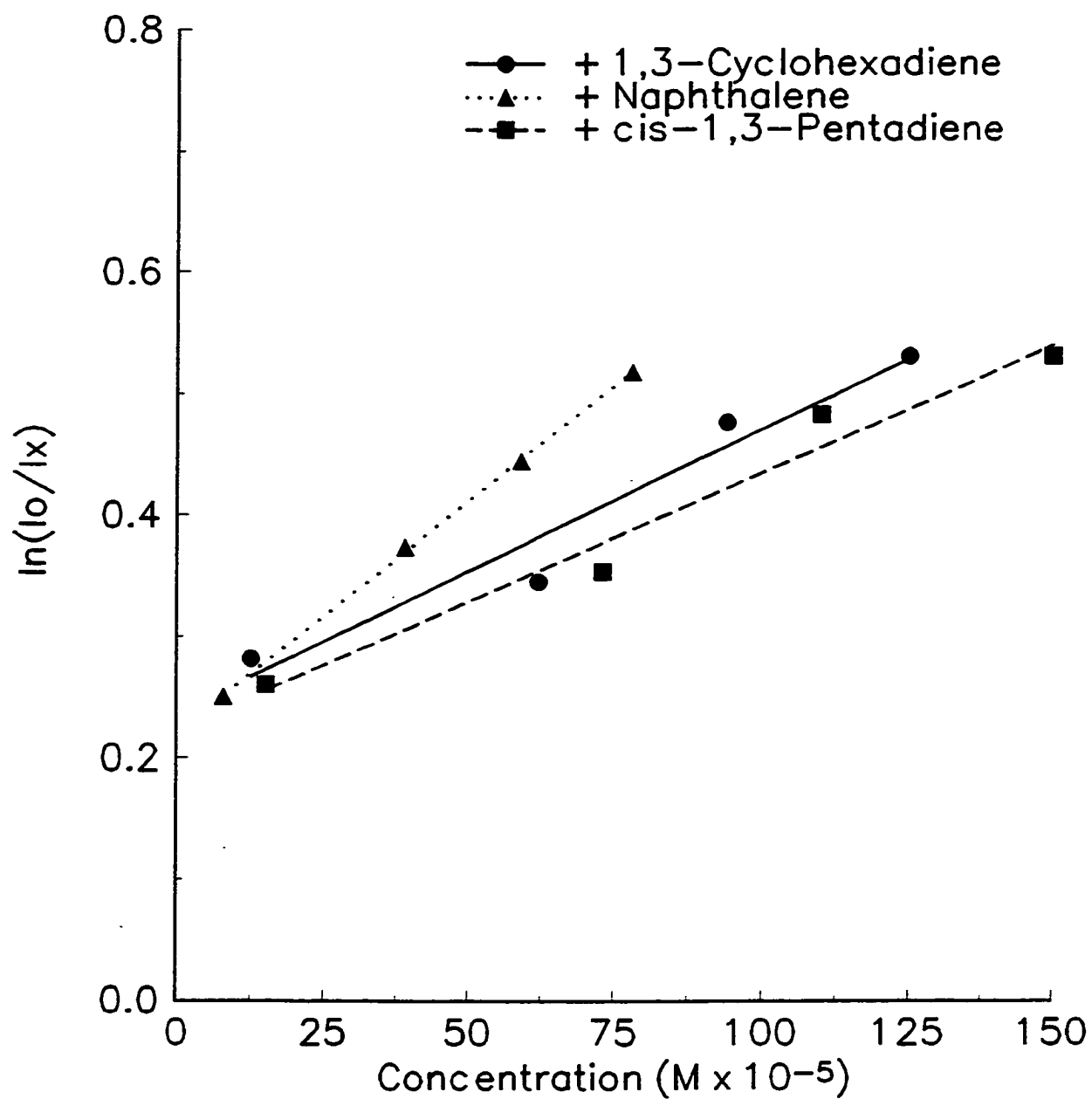


Figure 3.63. Perrin plots for quenching of P34DMAP (1.0×10^{-2} M solid state solution in CH_2Cl_2) triplet in glass at 77K.

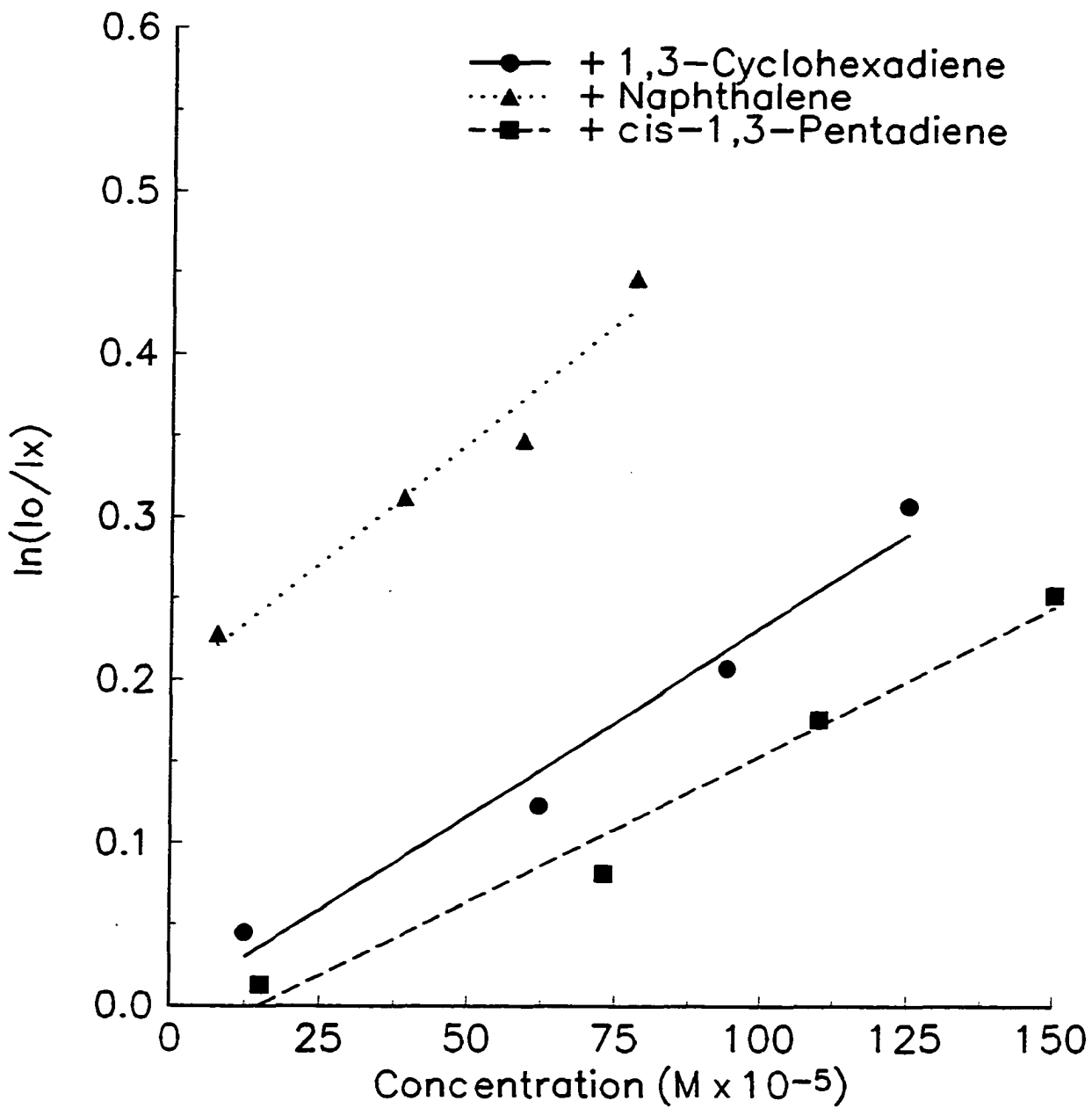


Figure 3.64. Perrin plots for quenching of P35DMAP (1.0×10^{-2} M solid state solution in CH_2Cl_2) triplet in glass at 77K.

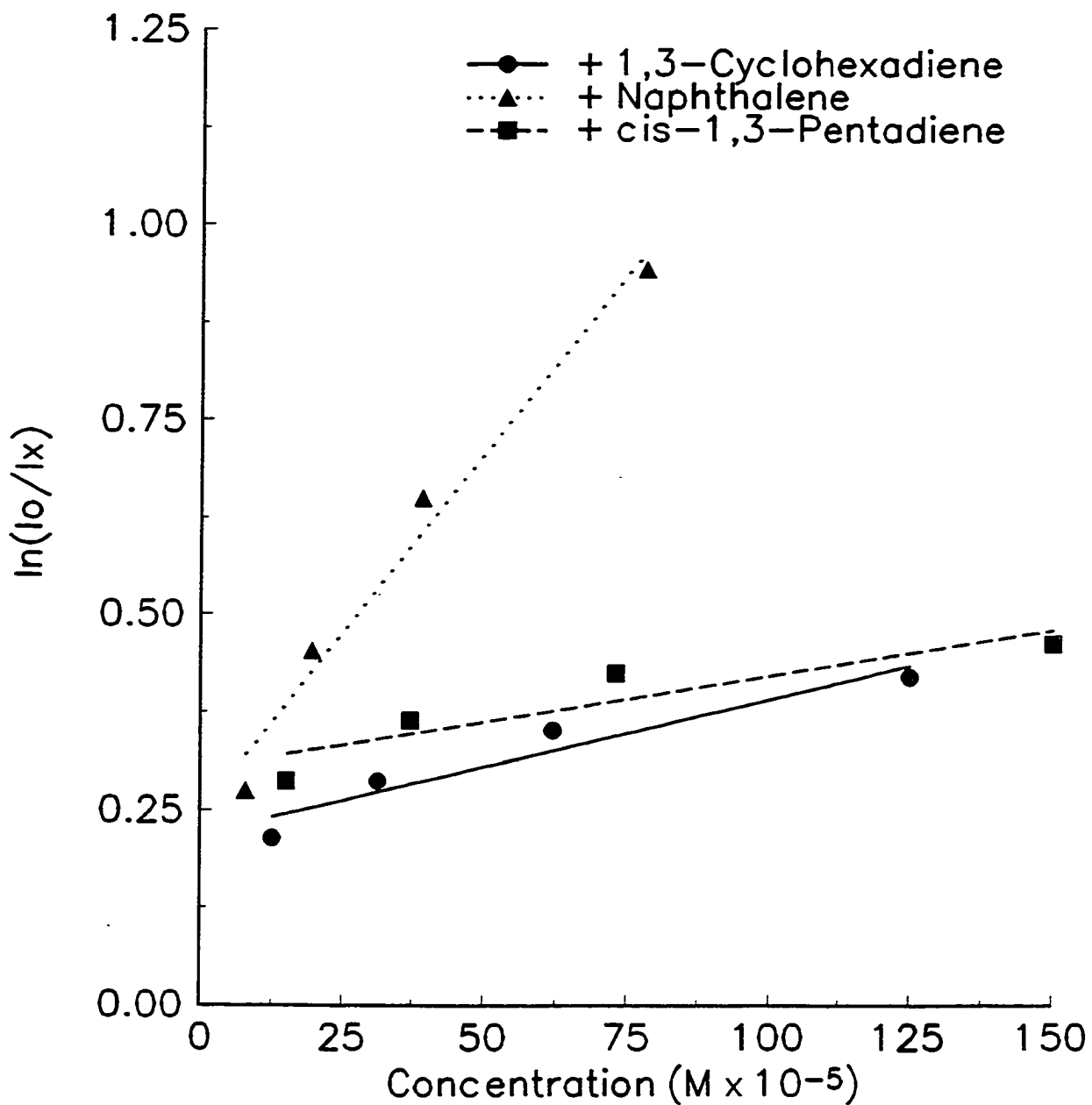


Figure 3.65. Perrin plots for quenching of PEAP (1.0×10^{-2} M solid state solution in CH_2Cl_2) triplet in glass at 77K.

10. THE EFFECT OF LIGHT ABSORBERS ON MOLECULAR WEIGHT CHANGES

The rate of chain scission of 6×10^{-2} M PMAP in CH_2Cl_2 was investigated using two different light absorbers, Tinuvin 327 (Figure 3.66) and Tinuvin 900 (Figure 3.67). The addition of both light absorbers caused a reduction in the rate of chain scission and the rate of chain scission decreased with increasing light absorber concentration. Tinuvin 900 caused a greater reduction in chain scission rate. If these compounds are acting *solely* as light absorbers and filtering out some of the UV incident radiation, the number of chain scissions would be expected to decrease linearly with concentration of light absorber.⁷² In Figure 3.68, quantum yield for chain scission is plotted against the concentration of light absorber. It can be seen that a linear relationship does not exist between these variables. In order to test the possibility that these molecules are also acting as quenchers, the quantum yield ratios (ϕ/ϕ_0) for chain scission in the absence (ϕ_0) and in the presence (ϕ) of both Tinuvin 327 and Tinuvin 900 are plotted as a function of light absorber concentration [Q] in Figure 3.69. Both sets of data conform well to Stern-Volmer kinetics with a slope of K_{sv} and an intercept of 1 which would confirm that they are also functioning as quenchers. The values of K_{sv} have been determined and are summarized in Table 3.14 along with the rate constant k_Q .

Table 3.14. Quenching Constants for the Irradiation of PMAP in 6×10^{-2} M Solution in CH_2Cl_2 ($\lambda \geq 300$ nm).

POLYMER	K_{sv} (Tinuvin 327) ($\text{dm}^3 \text{ mol}^{-1}$)	k_Q (Tinuvin 327) ($\text{dm}^3 \text{ mol}^{-1} \text{ s}^{-1}$)	K_{sv} (Tinuvin 900) ($\text{dm}^3 \text{ mol}^{-1}$)	k_Q (Tinuvin 900) ($\text{dm}^3 \text{ mol}^{-1} \text{ s}^{-1}$)
PMAP	4.3×10^3	1.5×10^8	5.1×10^3	1.8×10^8

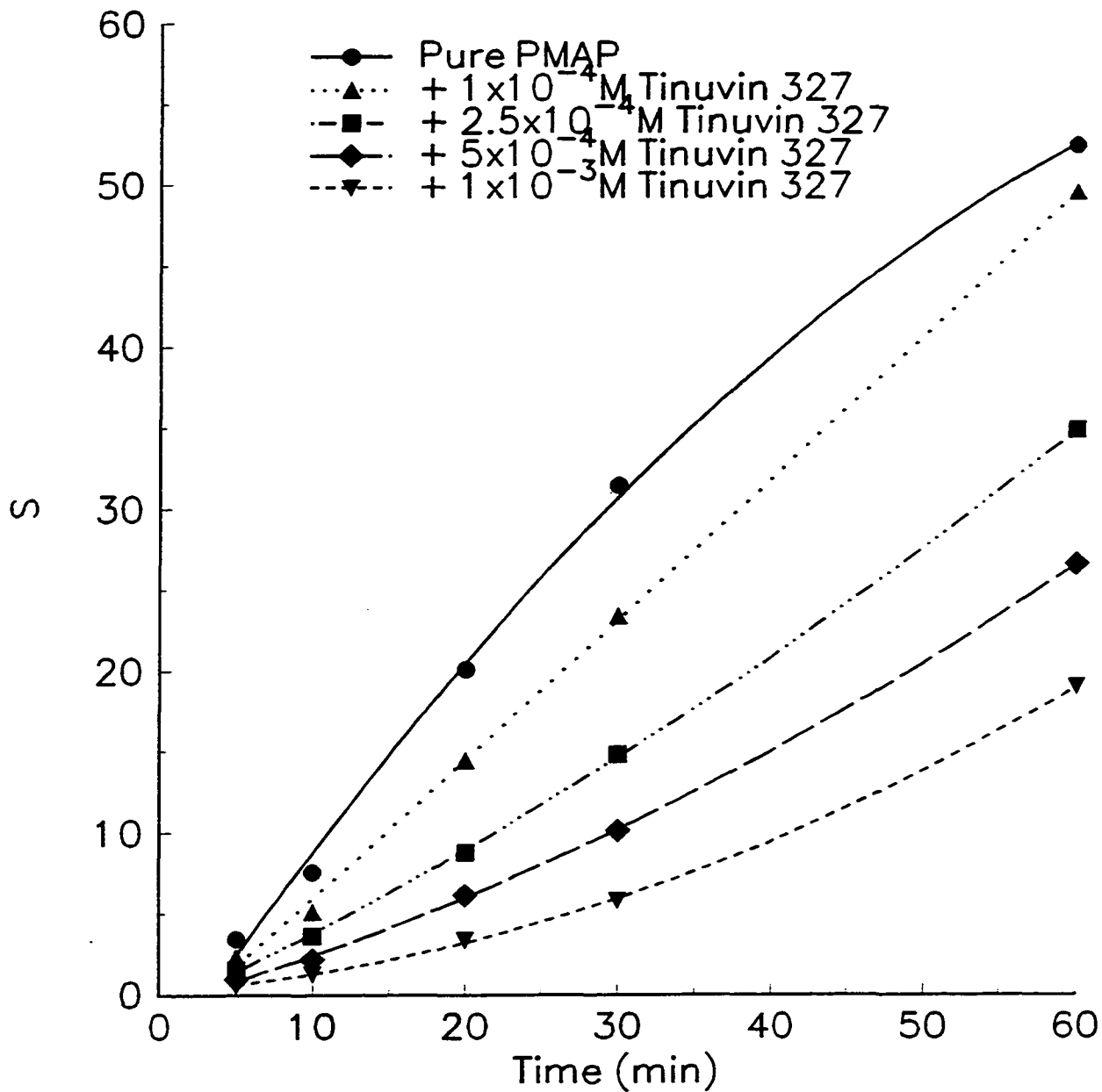


Figure 3.66. Number of chain scissions per molecule of PMAp (6.0×10^{-2} M solution in CH_2Cl_2) in the presence of Tinuvin 327 as a function of irradiation time ($\lambda \geq 300\text{nm}$, degassed).

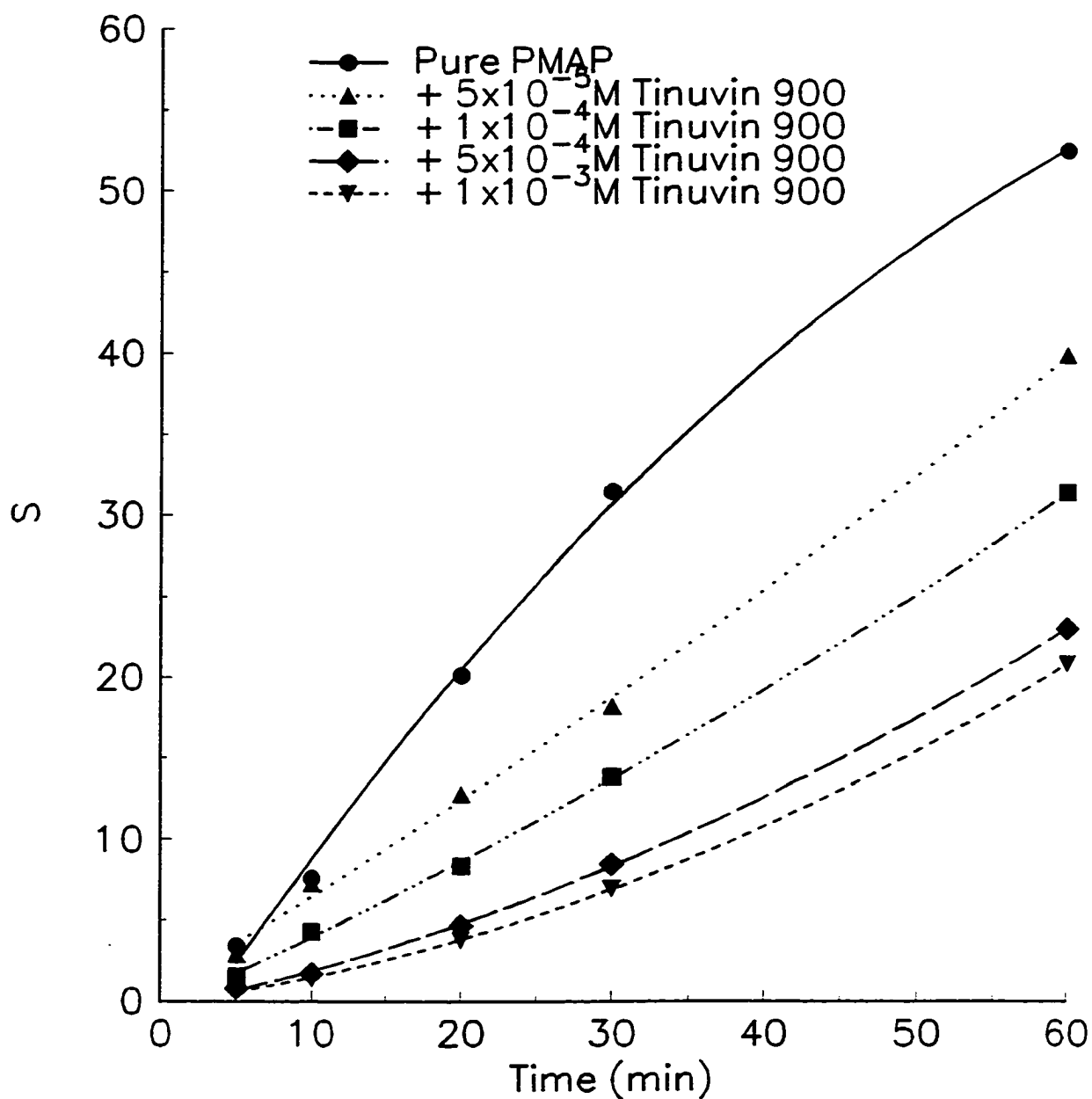


Figure 3.67. Number of chain scissions per molecule of PMAP (6.0×10^{-2} M solution in CH_2Cl_2) in the presence of Tinuvin 900 as a function of irradiation time ($\lambda \geq 300\text{nm}$, degassed).

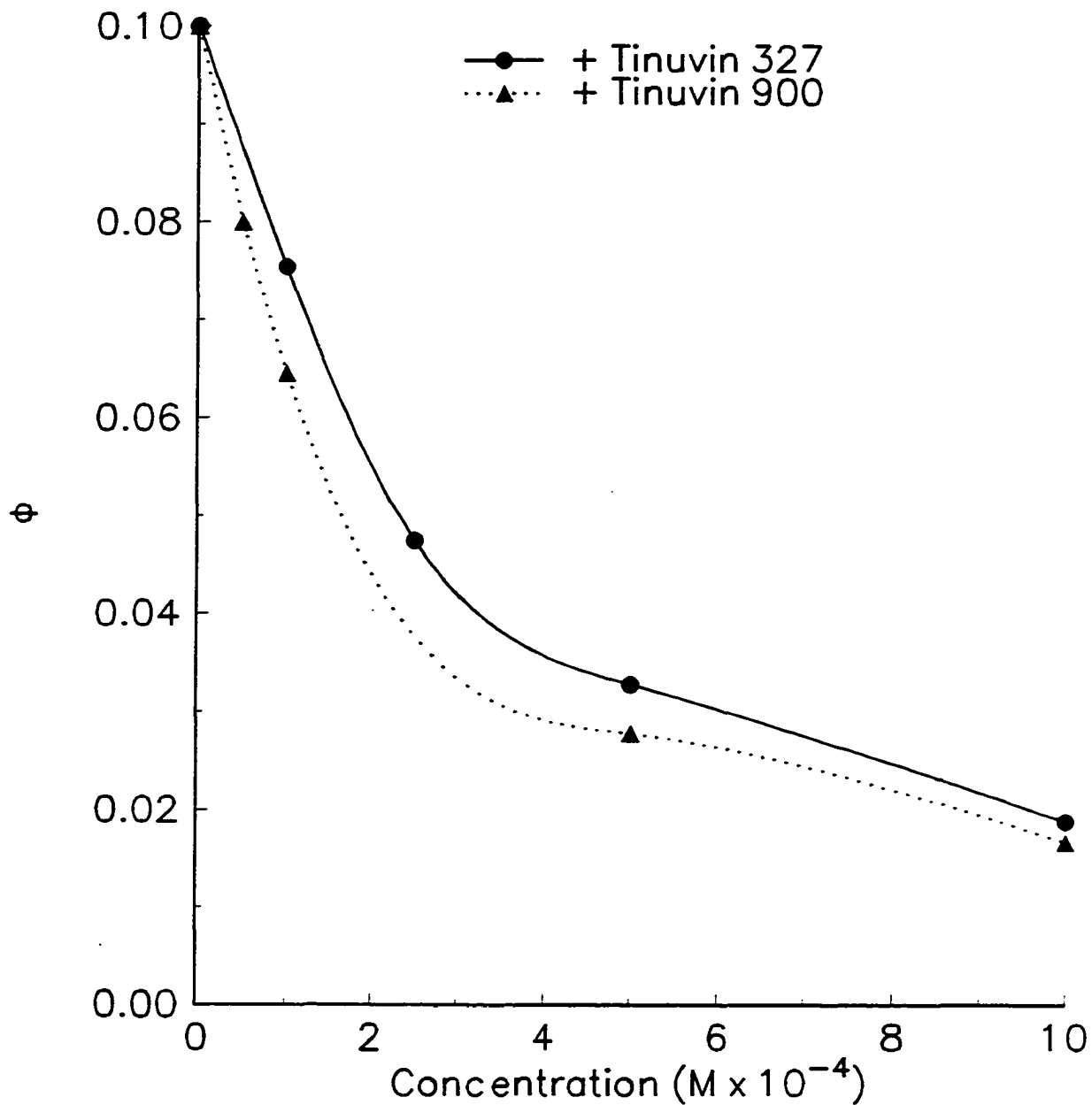


Figure 3.68. Quantum yield for chain scission of PMAP (6.0×10^{-2} M solution in CH_2Cl_2) as a function of quencher concentration ($\lambda \geq 300\text{nm}$, degassed).

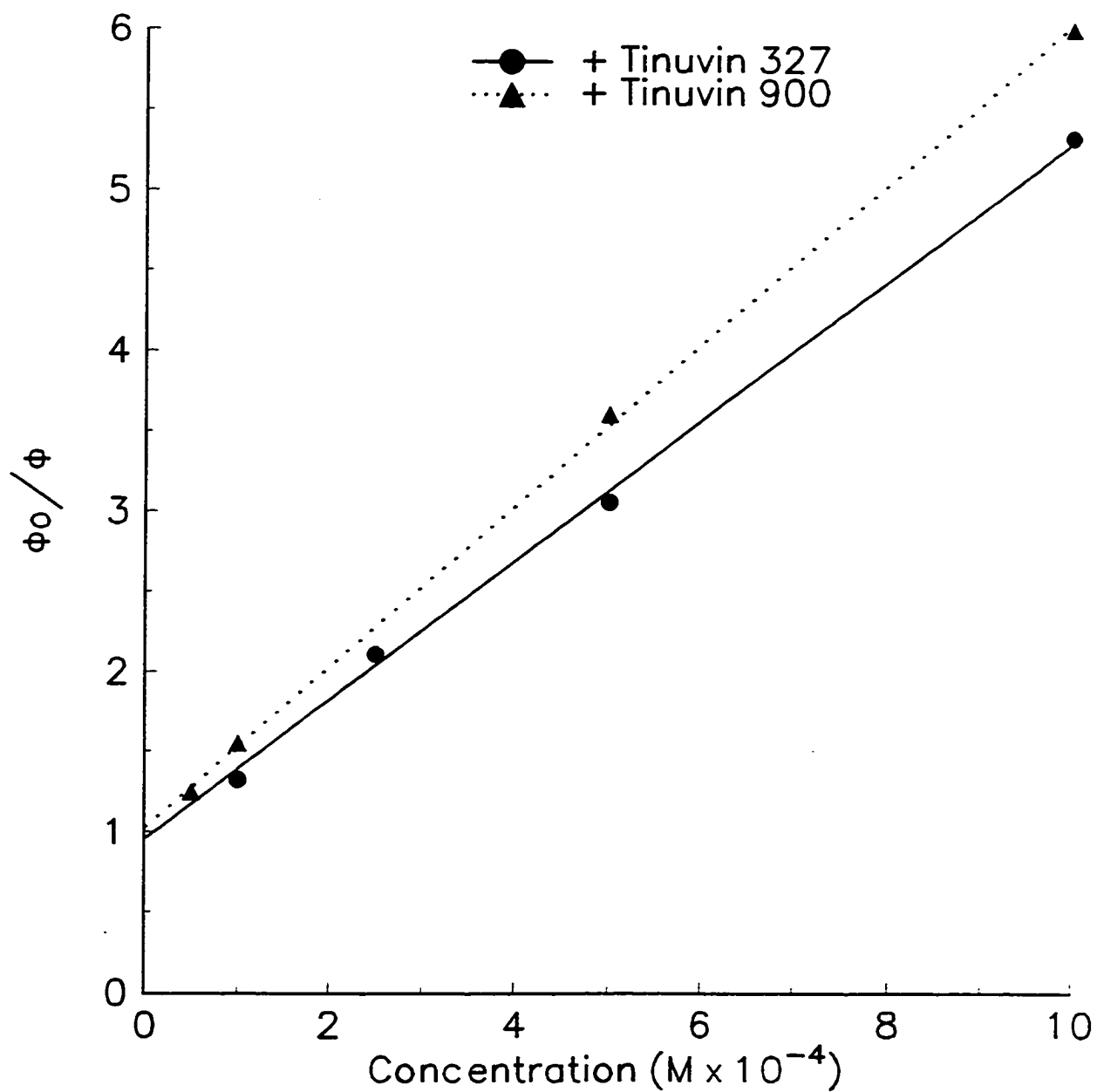


Figure 3.69. Stern-Volmer plots for quenching of PMAP (6.0×10^{-2} M solution in CH_2Cl_2) triplet ($\lambda \geq 300\text{nm}$, degassed).

The value of K_{sv} for PMAP with Tinuvin 327 is larger than the value obtained for naphthalene while K_{sv} for PMAP with Tinuvin 900 is even larger suggesting that these are more efficient quenchers than naphthalene.

The effects of Tinuvin 327 and Tinuvin 900 on PMAP in solution are also demonstrated by GPC data in Figures 3.70 and 3.71 respectively. Both light absorbers reduce the rate of photodegradation compared to irradiation in the absence of quenchers and this is reflected by shorter elution times. Tinuvin 900 appears to be more effective.

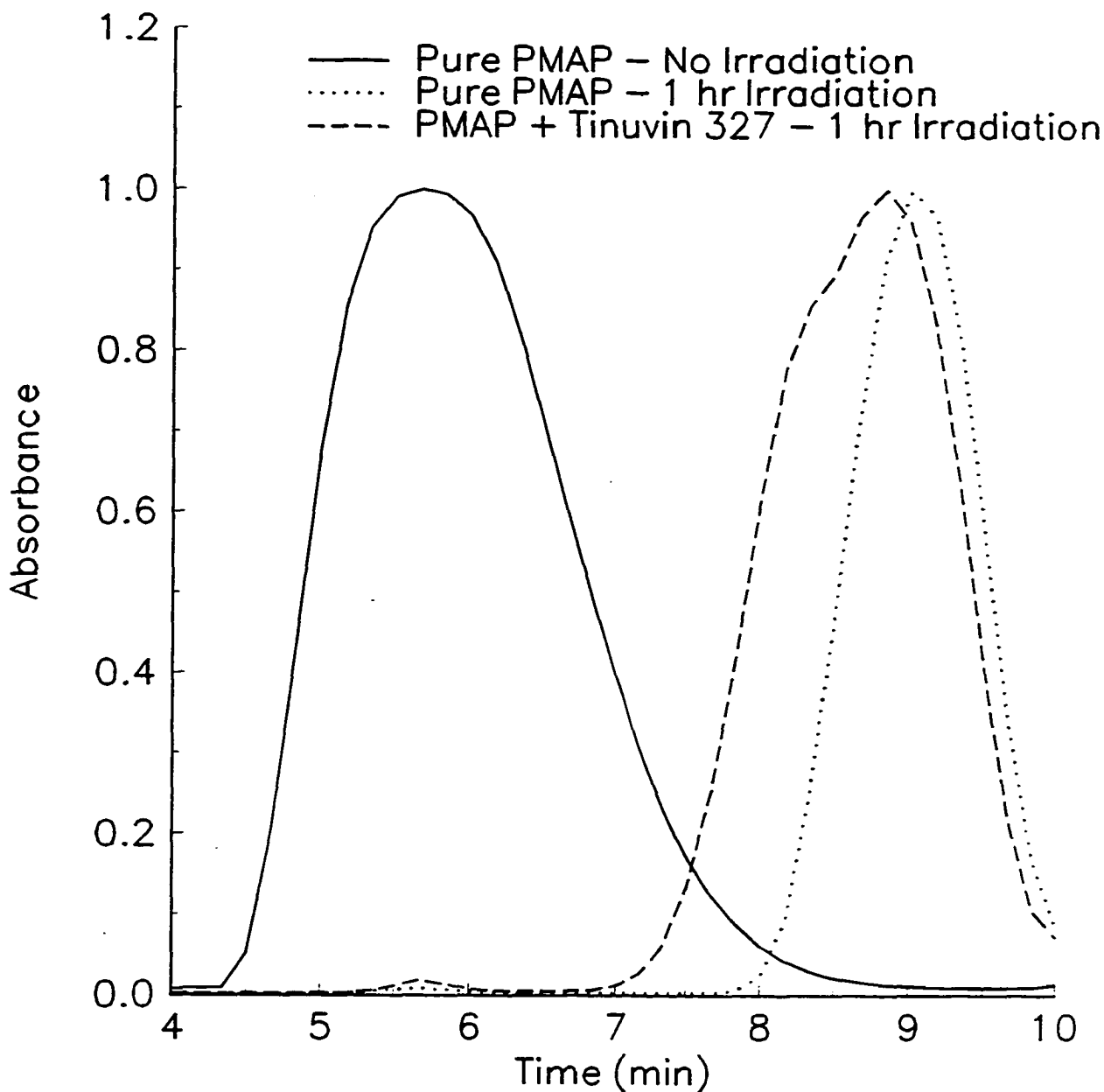


Figure 3.70. Gel permeation chromatograph of PMAP (6.0×10^{-2} M solution in CH_2Cl_2) before and after 1 hour of irradiation in the presence and absence of Tinuvin 327 ($\lambda \geq 300\text{nm}$, degassed and run through a $7\mu\text{m}$ pore Ultrastyrigel[®] linear column at $1.0 \text{ cm}^3 \text{ min}^{-1}$).

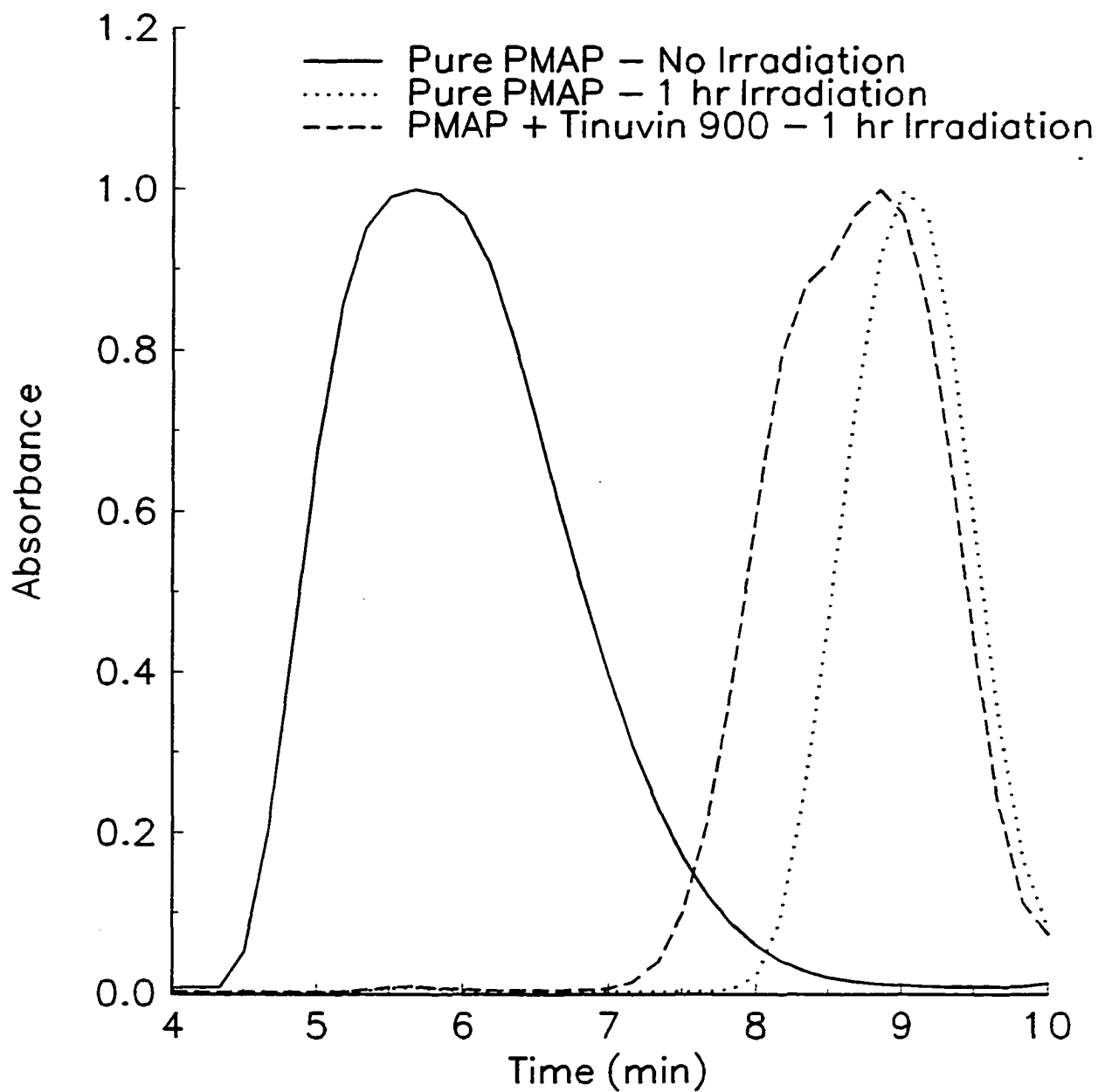


Figure 3.71. Gel permeation chromatograph of PMAP (6.0×10^{-2} M solution in CH_2Cl_2) before and after 1 hour of irradiation in the presence and absence of Tinuvin 900 ($\lambda \geq 300\text{nm}$, degassed and run through a $7\mu\text{m}$ pore Ultrastyrigel[®] linear column at $1.0 \text{ cm}^3 \text{ min}^{-1}$).

DISCUSSION

I/ PHOTOPHYSICAL PROCESSES

Long-wave UV radiation ($\lambda \geq 300$ nm) of poly(acrylophenones) results in the formation of the (n, π^*) excited singlet state (an $n \rightarrow \pi^*$ transition) which gives a single absorption at approximately 305nm. The excited (n, π^*) triplet state is formed by rapid intersystem crossing (ISC) from the excited singlet state with a quantum yield, for aromatic ketones like this, of approximately unity. Phosphorescence spectra (Figure 3.7) confirm the existence of $n \rightarrow \pi^*$ triplets in both methoxy and ethoxy-substituted poly(acrylophenones). The lack of involvement of $n \rightarrow \pi^*$ singlets is confirmed by weak fluorescence intensities (Figure 3.6) and very low (estimated) quantum yields of fluorescence (Table 3.4).

The introduction of electron-donating substituents into the aromatic ring (e.g. OCH_3 or OC_2H_5) causes a perturbation of the energy levels of the bonding and anti-bonding π electrons. This results in a red-shift of the (π, π^*) absorption which is large enough in some cases to cause overlap with the (n, π^*) band.^{54,73} In the case of P34DMAP and P35DMAP in both solution and thin film, and PMAP in solution, the (n, π^*) band becomes merely a shoulder of the (π, π^*) band. For PEAP in both solution and thin film and PMAP in thin film, the (n, π^*) band disappears as a result of complete overlap with the (π, π^*) band (Figures 3.4 and 3.5). The red-shift also leads to increased probability of configurational mixing and vibronic coupling (because of the energetic similarity of the (n, π^*) and (π, π^*) triplets) which causes an increase in the (π, π^*) character of the carbonyl triplets. More importantly, this allows the excitation energy of the carbonyl chromophore to be delocalized into the aromatic π system.¹⁹

Methoxy-substituted poly(acrylophenones) are known to have low lying (π, π^*) triplet states that are less reactive, and consequently, longer lived than the corresponding (n, π^*) states.^{58,62,73} Present data obtained for the ethoxy-substituted poly(acrylophenone) suggest that it behaves similarly. The lifetimes of the di-methoxylated poly(acrylophenones) are longer than PMAP confirming the increase in (π, π^*) character and PEAP has a similar lifetime. The triplet state energies of PMAP, P34DMAP, P35DMAP and PEAP are lower than the corresponding energies of unsubstituted poly(acrylophenones) (Table 3.5). Triplet lifetimes of P34DMAP, P35DMAP and PEAP are longer than those of unsubstituted poly(acrylophenones). This data confirms the increase in (π, π^*) character.⁶² Both di-methoxy substituted poly(acrylophenones) have no apparent vibrational fine structure (Figure 3.7), a characteristic of (π, π^*) triplets. Both PMAP and PEAP, however, have vibronically well resolved emission spectra indicating a higher amount of (n, π^*) character of the triplets.

II/ PHOTOCHEMICAL PROCESSES

Poly(acrylophenones) with increased (π, π^*) character are less reactive in hydrogen abstraction reactions and thus have lower quantum yields for chain scission, since the Norrish type II reaction requires an initial internal H-abstraction.⁶² In both solution and in thin film, PEAP has a comparable quantum yield for chain scission to that for PMAP, which is much larger than di-methoxylated poly(acrylophenones). The increased triplet state reactivity of PEAP means that there is a smaller energy gap between the (n, π^*) and (π, π^*) triplets.⁵³

The excited triplets of the methoxy-substituted poly(acrylophenones) have been shown to undergo two main photochemical processes: random chain scission and O-CH₃ fission.⁷

Experimental data indicate that the ethoxy-substituted poly(acrylophenone) degrades by similar mechanisms, i.e. by ethyl radical formation ($\text{O-C}_2\text{H}_5$ fission) and by random chain scission (a summary of the photoreactions of PEAP is shown in Figure 3.72). The evolution of low molecular weight gaseous products, i.e. ethane, butane and ethylene, from PEAP under solid state irradiation (Figure 3.22) are consistent with $\text{O-C}_2\text{H}_5$ fission and subsequent combination and disproportionation of ethyl radicals. Hydrogen abstraction by ethyl radicals will produce ethane. H-abstraction reactions by the ethyl radicals are most likely to occur at the α -carbon of the backbone of the polymer (Figure 3.72),⁵⁹ this position being favored on energetic grounds.⁷⁴ Reactions of the resultant tertiary radical include crosslinking, cyclization and β -scission (this will be discussed later).⁷

Fission of the $\text{O-C}_2\text{H}_5$ bond is thought to occur through internal conversion, energy being transferred from the excited aromatic ring (in conjunction with the carbonyl group) into the vibrational modes of the C-O bond,⁶³ and this process is made more probable by the overlap and interactions of the energetically similar (n,π^*) and (π,π^*) triplets.⁵⁹ $\text{O-C}_2\text{H}_5$ fission also leads to the formation of phenoxy radicals (Figure 3.72) and will be favored because of the relative stability of the phenoxy radicals (electron delocalization), which increases their lifetimes. This in turn allows the phenoxy radicals to participate in other reactions such as crosslinking and cyclization⁶³ and the formation of quinonoid compounds (Figure 3.72) which are highly colored.⁵⁹ Evidence of this is shown by UV-vis spectral data which show increased long-wave absorbance, and a yellow coloration is also observed (Figures 3.19-20). In terms of the photo-yellowing of lignin, coloration may be attributed to formation of quinones via phenoxy radicals produced from O-CH_3 fission.

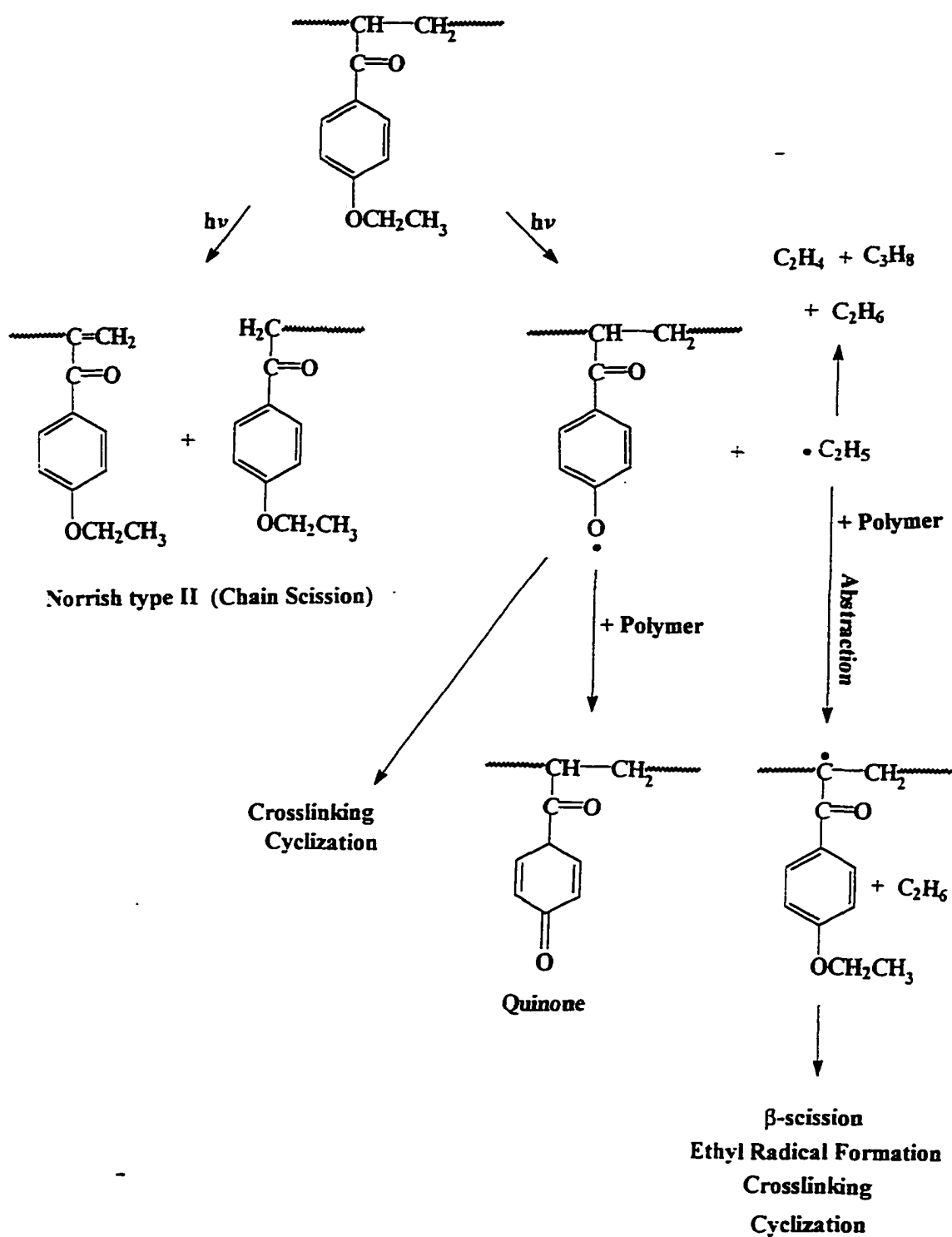


Figure 3.72. Reaction scheme summarizing the photoreactions of PEAP.

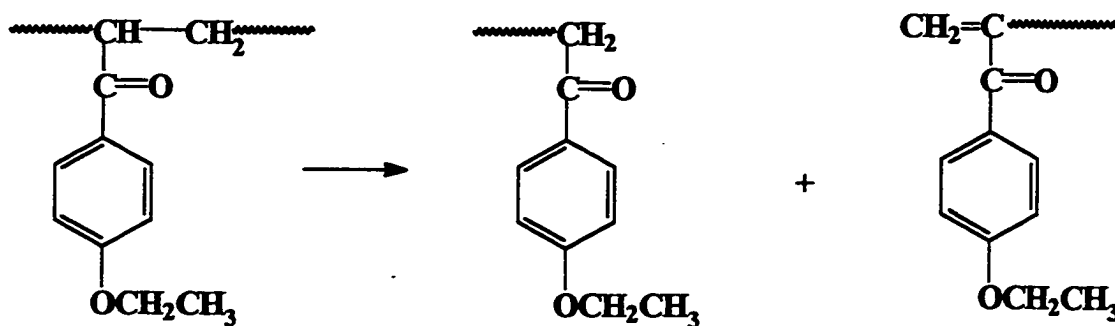
The second main process of photodegradation is random chain scission. This has been observed and extensively investigated for the methoxy-substituted poly(acrylophenones) in solution.⁷ Similar results are observed for the ethoxy-substituted poly(acrylophenone) in solution, as well as for all four substituted poly(acrylophenone) solid state polymers. Random chain scission in the methoxy-substituted poly(acrylophenones) has been attributed to a Norrish type II reaction (γ -H-abstraction) and it is likely that a similar process is involved in PEAP. Decreases in molecular weight of the methoxy⁷ and ethoxy-poly(acrylophenone) (Figure 3.23) in solution is reflected in GPC data which show narrower distributions, which are in turn displaced to longer elution times, i.e. to lower molecular weights.

Random chain scission of PEAP in solution (and previously for PMAP, P34DMAP and P35DMAP)⁷ is indicated by the initial linearity of the S (number of chain scissions per original molecule) versus time of long-wave irradiation plots (Figure 3.24). At longer radiation times, the linearity disappears. The quantum yield of chain scission for PEAP in solution (Table 3.9) is smaller than that of the unsubstituted polymer and comparable to PMAP but much larger than P34DMAP and P35DMAP. The fact that all four substituted polymers have lower quantum yields for chain scission than the unsubstituted one is indicative of less reactivity towards H-abstraction.⁴² PEAP, however, has comparable reactivity toward γ -H-abstraction to PMAP but is more reactive than the di-methoxy substituted poly(acrylophenones) (low photochemical reactivities are characteristic of low lying (π, π^*) triplets).⁵³

Similar results are obtained for random chain scission when the polymers are irradiated in the form of films (1.5×10^{-4} cm thick). The S versus time plots (Figure 3.35) also exhibit linearity; indeed more linear than is observed in solution. This reflects a lower probability of γ -H-abstraction

in film (compared with solution). This, however, is expected since in a more viscous medium there is a decrease in the rate of Norrish type II degradation, the decomposition of the 6-membered transition state being inhibited by the local higher viscosity.

The Norrish type II photoelimination involves a γ -H-abstraction by the CO triplet which leads to a double bond on the end of the chain. For example, the Norrish type II reaction for PEAP is:³⁹

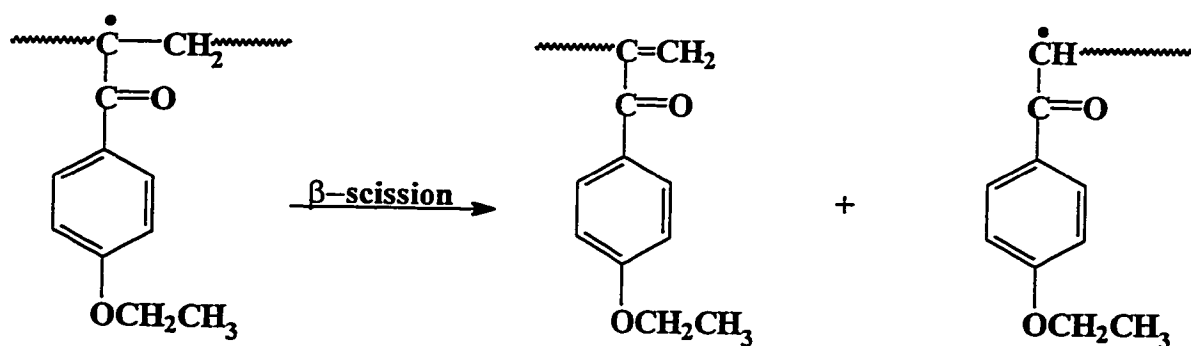


Chain scission is obviously indicated by the GPC data, but the Norrish type II decomposition is confirmed by ¹H NMR (Figure 3.17) in which a new peak appears at 5.30ppm. This is indicative of terminal unsaturation. The newly formed unsaturated carbonyls can act as quenchers for migrating energy (e.g. in the form of triplet energy transfer) and this becomes more important as the degree of degradation increases.¹ Self-quenching is reflected by the non-linearity of S versus time curves at long exposure times and it has been observed for methoxy-substituted poly(acrylophenones) in solution.⁷ Figure 3.24 indicates that it is also involved in PEAP in solution (Figure 3.24) as well as in all four polymers in the solid state (Figure 3.35). Self-quenching is more pronounced in solution than in films for both methoxy⁷ and ethoxy-substituted polymers (Figure 3.19-20), and this is attributable to the smaller extent of rotational freedom of the molecules in the more viscous solid

medium, in which specific conformational requirements for γ -H-abstraction by the triplet cannot necessarily be achieved.⁷

The molecular weight distribution data,⁷ after irradiation in solution and film, for the methoxy-substituted poly(acrylophenones) are different, and this is also observed for PEAP. In solution, the distribution curves for PMAP⁷, P34DMAP⁷, P35DMAP⁷ and PEAP (Figure 3.23), which are displaced to longer elution times as a result of chain scission, become significantly narrower as the high molecular weight species are degraded by chain scission. However, crosslinking is not impossible, and it may also occur in solution. In the films, the molecular weight distribution curves for PMAP, P34DMAP and PEAP are broadened. While the shape and symmetry of the distribution curve for P35DMAP remain unchanged, it is displaced to a shorter elution time, (Figures 3.31-34) indicating the formation of higher molecular weight products, formed presumably by crosslinking. It is interesting also that in the case of an unreactive (π, π^*) triplet in P35DMAP, competition between chain scission and crosslinking is altered in favour of the latter.

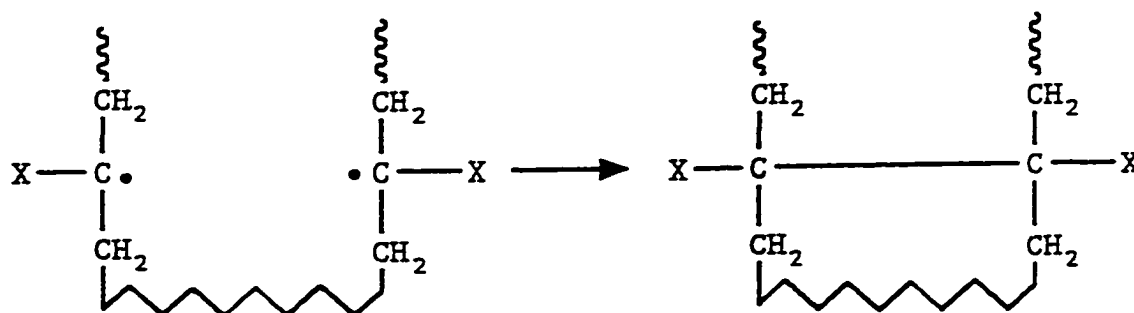
The relative amounts of chain scission and crosslinking are effected by several factors, one of which is β -scission. β -scission follows H-abstraction by ethyl radicals (Figure 3.72) and occurs on the initially formed macroradicals:^{25,28}



β -scission of the macroradicals leads to chain scission and effectively increases the quantum yield for chain scission. The degree of β -scission is greater in solution than in film because the specific conformational requirements for H-abstraction (a precursor for β -scission) are more easily achievable than in the more rigid solid state. This accounts for the narrower molecular weight distribution curves observed for methoxy⁷ and ethoxy-substituted polymers in solution (Figure 3.23) and the broader distribution curves observed in the solid state (Figures 3.31-34).

Another factor that can alter the balance between chain scission and crosslinking is the degree of cyclization, which occurs largely in solution. Cyclization is essentially another type of crosslinking reaction that can occur to a small extent for both methoxy⁷ and ethoxy-substituted poly(acrylophenone). This involves the reaction of two radicals on the chain which are non-adjacent, these radicals being formed by abstraction by ethyl radicals.

CYCLIZATION (INTRAMOLECULAR CROSSLINKING)



(X = methoxy or ethoxy-substituted benzoyl derivative)

Cyclization (intramolecular crosslinking) can take place in solution because of the higher rotational flexibility of the molecules in a lower viscosity medium. Cyclization reactions compete with normal intermolecular crosslinking and essentially shift the balance of the two processes in

favor of chain scission.^{15,24} This accounts for the narrower molecular weight distribution curves observed for methoxy⁷ and ethoxy-substituted polymers in solution. In the viscous solid state, diffusive separation of the macro-radicals formed by collapse of biradical is more difficult and this increases the probability of crosslinking which in turn explains the broader molecular weight distributions observed for degraded films. Another factor which could lead to the broadening of the distribution curves for films is the participation of phenoxy radicals in crosslinking reactions, these reactions being more probable on account of the long lifetimes of these radicals (in some cases hours).⁷⁵

Molecular weight can also affect the balance between chain scission and crosslinking. A polymer with a very high degree of polymerization will experience a large extent of inter-chain entanglement. This in turn restricts the motion, (mainly rotational) and it increases the difficulty of attaining the specific conformational requirements for γ -H-abstraction. In addition, increased entanglement causes a decrease in the rate of diffusive separation of the macro-fragments formed by biradical collapse.²⁰ These factors combine to reduce the degree of chain scission. Inter-chain entanglement may also explain the decrease in the rate of chain scission with an increase in polymer concentration observed for methoxy-substituted poly(acrylophenones)⁷ and for PEAP (Figure 3.25). The higher the polymer concentration, the more likely they are to be entangled, and this will be reflected in a lower rate of macro-radical separation and in the rate of chain scission.

1. QUENCHING IN SOLUTION

The effect of triplet quenching on the rates of chain scission of the methoxy-substituted poly(acrylophenones) (with naphthalene and cis-1,3-pentadiene) in solution have been previously

studied⁷, and similar effects were observed for 1×10^{-2} M PEAP in CH_2Cl_2 . PEAP is readily quenched by both naphthalene and cis-1,3-pentadiene (Figures 3.27 and 3.28 respectively). The data for both quenchers are plotted in an alternative form, and it can be seen that they conform well to Stern-Volmer kinetic (Figure 3.29(reciprocal plot)). The large values of the Stern-Volmer constants (K_{SV}) are comparable with those obtained for the methoxy-substituted poly(acrylophenones)⁷ indicating the involvement of triplets with more $n-\pi^*$ character. The Stern-Volmer constants for PEAP are much larger than those for the unsubstituted poly(acrylophenone) with the same quenchers, confirming that the triplet lifetime is longer than that of the unsubstituted poly(acrylophenone).

In solution, the rate of encounter of the excited species and the quencher is controlled by the rate of mutual diffusion. In the case of aromatic keto-polymers, triplet energy transfer is very efficient, and it is likely that energy transfer will take place on each encounter,¹ i.e. the intermolecular process is diffusion controlled.³ The quenching constants, k_Q , for PEAP in solution are smaller than would be expected for a diffusion-controlled process, for example, k_Q for naphthalene is $3.5 \times 10^7 \text{ dm}^3\text{mol}^{-1}\text{s}^{-1}$ compared with values in the range of $1-9 \times 10^9 \text{ dm}^3\text{mol}^{-1}\text{s}^{-1}$ for typical diffusion controlled reactions.

A small difference in magnitude of k_Q can be explained in terms of diffusional limitations, but the larger differences observed for PEAP cannot be fully accounted for in this manner, since complete immobilization would only reduce the quenching constant by a factor of two.⁶² Other explanations involve the examination of the encounter process between the excited species and the quencher. To obtain optimal energy transfer by the exchange process involved here, specific conformational requirements in terms of the relative orientations of the carbonyl and quencher must

be obtained, and this may be impeded by steric effects associated with the proximities of adjacent polymer chains.⁶²

In addition, stereoelectronic effects, which are independent of the actual diffusion process, may also influence the efficiencies of energy transfer, resulting in significantly reduced values of quenching constants. Stereoelectronic effects involve the twisting of the π -system of either the excited triplet or of the quencher in such a way that the extent of orbital overlap, which is essential for electron exchange, is reduced.⁷⁶ Stereoelectronic effects may also explain the difference in quenching constants for naphthalene and cis-1,3-pentadiene, i.e. the effect is more pronounced in cis-1,3-pentadiene. This difference can also be attributable to reversible energy transfer, which is probable when the quenching rate constants are several magnitudes lower than those of diffusion.⁷⁷ Thus the observed rate of quenching is determined less by the diffusion constant than by energetic and steric factors.

2. SOLID STATE QUENCHING

The effects of quenching of polymers in the solid state have been investigated for PMAP, P34DMAP, P35DMAP and PEAP using naphthalene and cis-1,3-pentadiene. In solution, all four polymers were readily quenched (as indicated by reduced rates of chain scission), but in film, an increase in chain scission rate was observed when quencher concentrations were low (0.34 - 7.0(w/w) percent). Cis-1,3-pentadiene, which was a less efficient quencher than naphthalene in solution, caused a larger apparent increase in chain scission than naphthalene in the solid state. An explanation for this apparent increase in chain scission, could be decreased extents of crosslinking, for example, these molecules are inhibiting cross-linking. In addition, it is conceivable that the

quenchers act as sensitizers in the solid state at low concentrations. However, it is thermodynamically improbable that they are acting simply as triplet sensitizers, and a possible mechanism is not obvious.

The effects of quenching of the polymers in the solid state using quenchers in the range of 50-100(w/w) percent showed a decrease in the rates of chain scission (Figures 3.36-39). Thus at larger effective concentrations of quenchers, the polymer triplets are quenched. The data for quenching did not conform to Stern-Volmer kinetics (data in Figure 3.44 is not linear) as might be expected in solid state quenching. However, the linearity of the $\ln(\phi_0/\phi)$ versus $[Q]$ plots (Figure 3.45) suggests that the quenching of the polymer triplets conforms to, and is better represented by Perrin kinetics. In this model there is a sphere of action. In the solid state, there is no diffusion or migration of molecules, so the transfer of triplet energy from the excited molecule to the quencher can only occur if both species are in close proximity to each other in the rigid polymer matrix.¹³ The proximity in which deactivation of the excited molecule occurs is controlled by a sphere of action. If a quencher exists inside the sphere of action, the excited triplet is immediately deactivated, but if the quencher is outside the sphere of action, no energy transfer will occur.¹³ Naphthalene was found to have the largest sphere of action (Table 3.12) for P35DMAP.

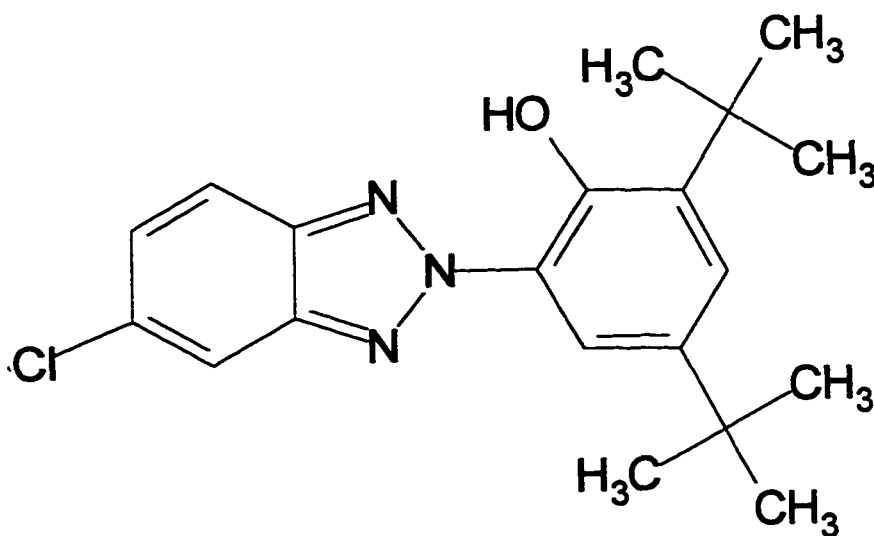
Direct triplet quenching of all four polymers was investigated at 77K with 1,3-cyclohexadiene, naphthalene and 1,3-cis-pentadiene. In direct triplet quenching, no degradation takes place during the measurement, thus self-quenching does not effect the results. The data for quenching did not conform to Stern-Volmer kinetics (Figures 3.58-61 are not linear) as might be expected in solid state quenching. However, the linearity of the $\ln(I_0/I_x)$ versus $[Q]$ plots (Figures 3.62-65) suggests that the quenching of the polymer triplets conforms to, and is better represented

by Perrin kinetics. Naphthalene was found to have the largest sphere of action (Table 3.13) for all four polymers making it the most efficient quencher in the solid state in terms of direct triplet quenching. While there is a good correlation of the data with the Perrin theory, the results indicate that there are probably other factors at play in the solid state degradation reactions of the polymers, which do not appear in simple triplet quenching.

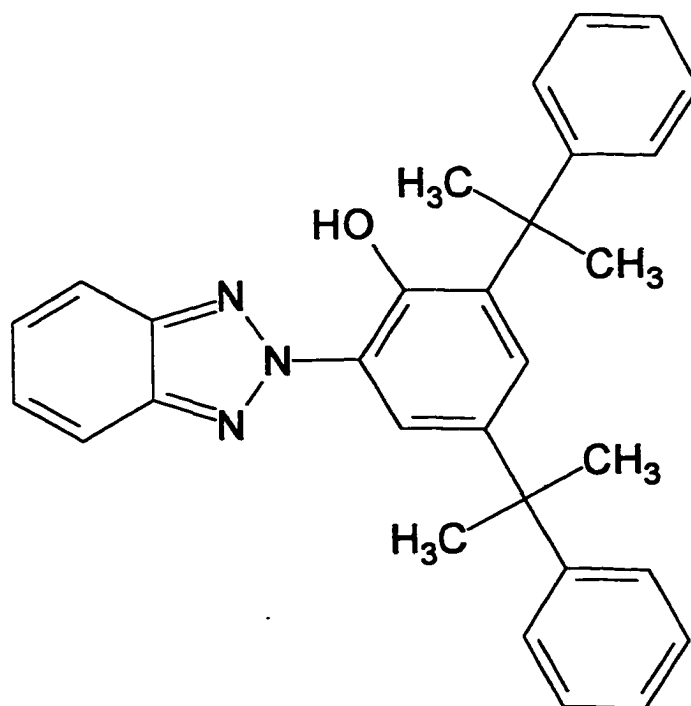
3. LIGHT ABSORBERS AS INHIBITORS

One aspect of the inhibition of photodegradation of polymers, which has considerable commercial interest, is the use of so-called light absorbers to reduce the degradation. The effects of two well known light absorbers, i.e. Tinuvin 327 and Tinuvin 900, on the photodegradation of PMAP in solution was investigated.

TINUVIN 327



TINUVIN 900



If Tinuvin 327 and Tinuvin 900 are acting solely as light absorbers, their effects can be predicted in terms of rates of reactions. The rate of a reaction, R , in the absence of light absorber is given by:⁷²

$$R = \phi I_A$$

where ϕ is the quantum yield and I_A is the rate of absorption of photons by the solution. The absorbed intensity can be related to the incident intensity I_0 by:³

$$I_A = I_0(1 - 10^{-\epsilon cl})$$

where ϵ is the molar absorption coefficient, c is the concentration and l is the effective path length of the solution. If more there exists more than one absorbing molecule in the solution, the total rate of absorption, I_A' :⁷²

$$I_A' = I_0 \sum (1 - e^{-\epsilon_i c_i l})$$

The presence of a light absorber, X, will decrease the effective rate of absorption of the substrate, and the new rate of photo-reaction, I_x , is given by:⁷²

$$I_x = I_A - I_0(1 - 10^{-\epsilon_x c_x l})$$

which, on account of small values of ϵ , c and l , can be approximated as:⁷²

$$I_x = I_0 l (\epsilon c - \epsilon_x c_x)$$

This leads to a new reaction rate represented by:⁷²

$$R_x = \phi I_0 l (\epsilon c - \epsilon_x c_x)$$

This implies that the number of chain scissions should decrease linearly with concentration of light absorber.⁷² However, the plot of quantum yield versus concentration of light absorber in solution (Figure 3.68) is non-linear. This leads to one of two possibilities, either these compounds do not have a large influence on the quantum yields, or they are also acting as quenchers. The latter proposition is supported by the linearity of the Stern-Volmer plot (Figure 3.69) in which the quantum yield ratio for chain scission in the absence and presence of inhibitor (ϕ_0/ϕ respectively) are related to the quencher concentration. The k_Q values for both Tinuvin 327 and Tinuvin 900 (Table 3.14) are smaller than would be expected for diffusion-controlled quenching. The results would suggest however, that these light absorbers are not only reducing the effective intensity of UV radiation incident upon the polymer, but perhaps also acting as quenchers of the triplet state of the carbonyl.

REFERENCES

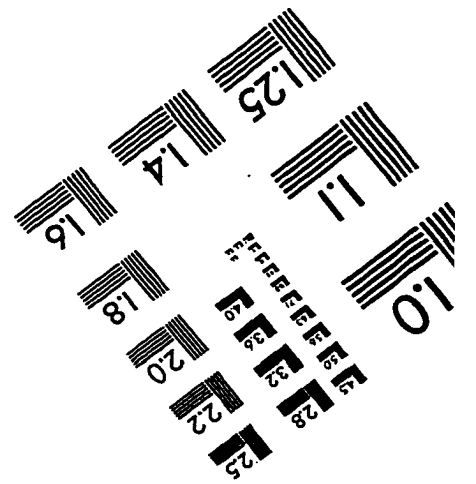
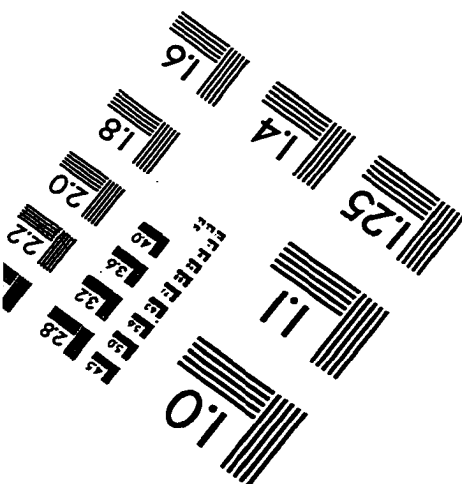
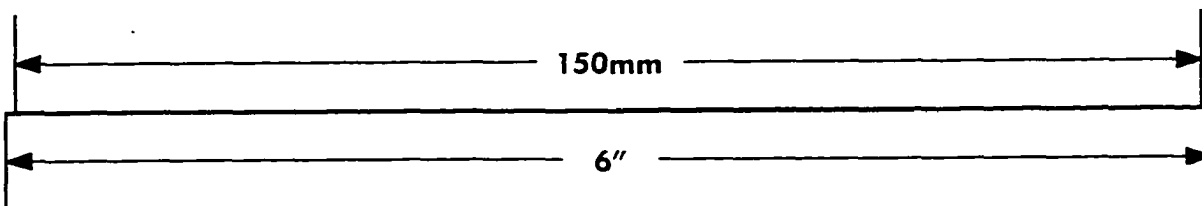
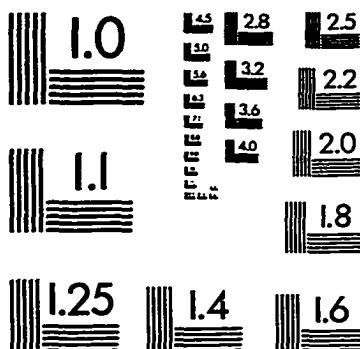
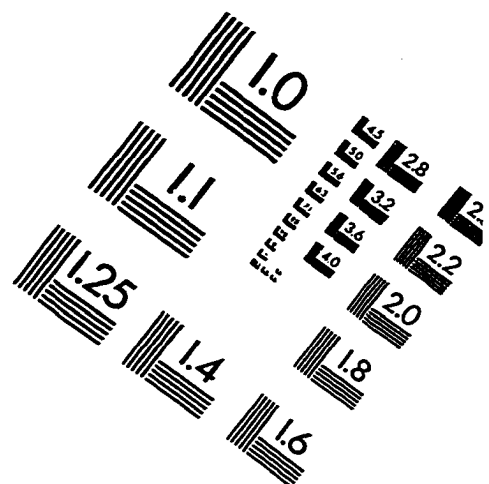
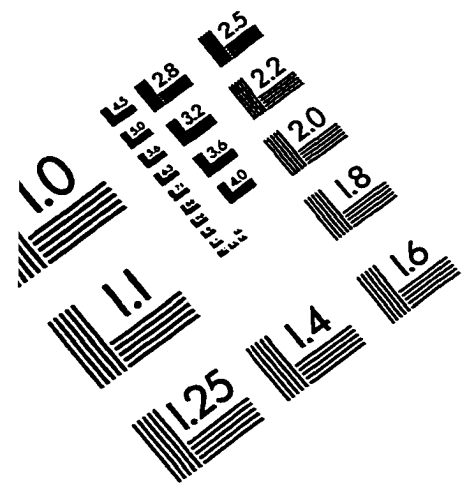
1. J. Guillet. *Polymer Photophysics and Photochemistry*. Cambridge University Press, London (1985).
2. P. Suppan. *Chemistry and Light*. The Royal Society of Chemistry, Cambridge (1994).
3. C.E. Wayne and R.P. Wayne. *Photochemistry*. Oxford University Press, Oxford (1996).
4. J.F. McKellar and N.S. Allen. *Photochemistry of Man-Made Polymers*. Applied Science Publishers Ltd, London (1979).
5. J.A. Baltrop and J.D. Coyle. *Principles of Photochemistry*. John Wiley & Sons, Chichester (1978).
6. A. Gilbert and J. Baggot. *Essentials of Molecular Photochemistry*. Blackwell Scientific Publications, London (1991).
7. A.P. Ceccarelli. *The Photochemistry of Methoxy-Substituted Polyl(acrylophenones)*. Lakehead University, Thunder Bay (1995).
8. W.M. Horspool. *Aspects of Organic Photochemistry*. Academic Press, London (1976).
9. A.V. Patsis. *Advances in the Stabilization and Controlled Degradation of Polymers, Volume II*. Technomic Publishing Co. Inc., Lancaster (1987).
10. J.F. Rabek. *Polymer Photodegradation*. Chapman & Hall, London (1995).
11. S. Patai. *The Chemistry of the Carbonyl Group*. Interscience Publishers, London (1966).
12. J.S. Sweton. *J. Chem. Educ.* **46**(4), 217 (1969).
13. J.F. Rabek. *Photodegradation of Polymers*. Springer, Berlin (1996).
14. W. Albert Noyes Jr., G.S. Hammond and J.N. Pitts Jr. *Advances in Photochemistry, Volume 5*. John Wiley & Sons, New York (1968).
15. N.C. Yang and D.H. Yang. *J. Am. Chem. Soc.* **80**, 2913 (1958).
16. P.J. Wagner, P.A. Kelso and R.G. Zepp. *J. Am. Chem. Soc.* **94**, 7480 (1972).
17. P.J. Wagner. *Acc. Chem. Res.* **16**, 471 (1983).

18. T.J.K.S. Siu and R.D. Burkhart. *Macromolecules* **12**, 336 (1989).
19. W.J. Leigh, J.C. Scaiano, C.I. Paraskevopoulos, G.M. Charette and S.E. Sugamori. *Macromolecules* **18**, 2148 (1985).
20. S. Tagawa and W. Schnabel. *Macromolecules* **12**, 663 (1979).
21. J.E. Guillet and H.C. Ng. *Macromolecules* **18**, 2294 (1985).
22. P.J. Wagner. *Meth. Stereochem. Anal.* **3**, 374 (1983).
23. N.A. Weir, J. Arct and A. Ceccarelli. *J. Photochem. Photobiol. A: Chem.* **72**, 87 (1993).
24. J.C. Scaiano. *Acc. Chem Res.* **15**, 252 (1982).
25. N.A. Weir and K. Whiting. *J. Polym. Sci. Part A: Polym. Chem.* **30**, 1601 (1992).
26. F.D. Lewis, R.W. Johnson and D.E. Johnson. *J. Am. Chem. Soc.* **96**, 6090 (1974).
27. A.J. Kresge. *Chemtracts* **10(4)**, 292 (1997).
28. N.A. Weir and A. Ceccarelli. *Eur. Polym. J.* **26**, 991 (1990).
29. N.A. Weir, A. Ceccarelli and J. Arct. *Eur. Polym. J.* **29**, 737 (1993).
30. W.M. Horspool. *Photochemistry* **27**, 63 (1996).
31. J.E. Guillet, S.K. Li and H.C. Ng. *A.C.S. Symp. Ser.* **266**, 165 (1984).
32. F.W. Deeg, J. Pinsl and C. Brauckle. *J. Phys. Chem.* **90**, 5715 (1986).
33. P. Hrdlovič and J.E. Guillet. *Polym. Photochem.* **7**, 423 (1986).
34. J.C. Scaiano, E.A. Lissi and M.V. Encina. *Rev. Chem. Intermed.* **2(2)**, 139 (1978).
35. J.E. Guillet and R.G.W. Norrish. *Nature* **173**, 625 (1954).
36. J.E. Guillet and R.G.W. Norrish. *Proc. R. Soc. London, Ser. A* **233**, 153 (1955).
37. J.P. Bays, M.V. Encinas and J.C. Scaiano. *Macromolecules* **13**, 815 (1980).
38. M.V. Encinas, K. Fubashi and J.C. Scaiano. *Macromolecules* **12**, 1167 (1979).

39. E. Dan and J.E. Guillet. *Macromolecules* **6**, 230 (1973).
40. C. David, W. Demartean and G. Geuskens. *Polymer* **8(10)**, 497 (1967).
41. C. David, W. Demartean, F. Derom and G. Geuskens. *Polymer* **11(1)**, 61 (1970).
42. I. Lukáč, M. Moravcik and P. Hrdlovič. *J. Polym. Sci.: Polym. Chem. Edn.* **12**, 1913 (1974).
43. P. Hrdlovič, J. Danecek, D. Berek and I. Lukáč. *Eur. Polym. J.* **13**, 123 (1977).
44. I. Lukáč and P. Hrdlovič. *Eur. Polym. J.* **11**, 767 (1975).
45. I. Lukáč and P. Hrdlovič. *Eur. Polym. J.* **15(6)**, 533 (1979).
46. R. Salvin, J. Meybeck and J. Faure. *J. Photochem.* **6**, 9 (1976).
47. R.D. Small and J.C. Scaiano. *Macromolecules* **11(4)**, 840 (1978).
48. I. Lukáč, P. Hrdlovič, Z. Maňásek and D. Belluš. *J. Polym. Sci.: Part A-1* **11**, 767 (1975).
49. C. David, W. Demartean and G. Geuskens. *Eur. Polym. J.* **6(10)**, 1405 (1970).
50. T. Kilp and J.E. Guillet. *Macromolecules* **14(6)**, 1680 (1981).
51. T. Kilp, J.E. Guillet, L. Merle-Aubrey and Y. Merle. *Macromolecules* **15(1)**, 60 (1982).
52. P.J. Wagner, A.E. Kemppainen and H.N. Schott. *J. Am. Chem. Soc.* **95**, 5604 (1973).
53. I. Lukáč and P. Hrdlovič. *Eur. Polym. J.* **14**, 339 (1978).
54. I. Lukáč, S. Chmela and P. Hrdlovič. *J. Photochem.* **11**, 301 (1979).
55. J.C. Selwyn and J.C. Scaiano. *Polymer* **15(6)**, 533 (1979).
56. P. Hrdlovič, J. Trekoval and I. Lukáč. *Eur. Polym. J.* **15**, 229 (1979).
57. J.C. Selwyn and J.C. Scaiano. *Polymer* **21**, 1365 (1980).
58. M.V. Encinas, E.A. Lissi, E. Lemp, A. Zanocco and J.C. Scaiano. *J. Am. Chem. Soc.* **105**, 1865 (1983).
59. N.A. Weir, J. Arct, A. Ceccarelli and A. Siren. *Eur. Polym. J.* **30**, 701 (1994).

60. N.A. Weir, J. Arct, A. Ceccarelli and D. Puumala. *Polym. Degrad. Stab.* **52**, 119 (1996).
61. N.A. Weir, J. Arct and A. Ceccarelli. *Eur. Polym. J.* **32(7)**, 805 (1996).
62. N.A. Weir, J. Arct and A. Ceccarelli. *Polym. Degrad. Stab.* **48**, 333 (1995).
63. N.A. Weir, J. Arct and A. Ceccarelli. *Res. Chem. Intermed.* **21(3-5)**, 353 (1995).
64. S.Y. Lin and K.P. Kringstad. *Tappi* **53**, 658 (1970).
65. N.A. Weir, J. Arct and A. Ceccarelli. *Polym. Degrad. Stab.* **47**, 289 (1995).
66. E. Alder and J. Marton. *A. Chemi. Scan.* **15**, 357 (1961).
67. J. Schmidt and C. Heitner. *J. Wood Chem. Technol.* **13**, 309 (1993).
68. B.J. Zhao, M.C. Depew, N.A. Weir and J.K.S. Wan. *Res. Chem. Intermed.* **19(5)**, 449 (1993).
69. G.J. Leary. *Nature* **217**, 672 (1968).
70. D.J. Casey and C.S. Marvel. *J. Org. Chem.* **24**, 1022 (1959).
71. J.F. Rabek. *Experimental Methods in Photochemistry and Photophysics*. John Wiley & Sons, Chichester (1982).
72. N.A. Weir and D.M. Leach. *J. Photochem. Photobiol. A: Chem.* **114**, 75 (1998).
73. P. Hrdlovič, J.C. Scaiano, I. Lukáč and J.E. Guillet. *Macromolecules* **19**, 1637 (1986).
74. N.A. Weir and M. Rujimethabhas. *Eur. Polym. J.* **18**, 813 (1982).
75. J. Pospisil. *Polym. Degrad. Stab.* **40**, 217 (1993).
76. B. Guerin and L.J. Johnston. *Can. J. Chem.* **67**, 473 (1989).
77. P.J. Wagner. *J. Am. Chem. Soc.* **89**, 2820 (1967).

IMAGE EVALUATION TEST TARGET (QA-3)



APPLIED IMAGE, Inc
1653 East Main Street
Rochester, NY 14609 USA
Phone: 716/482-0300
Fax: 716/288-5989

© 1993, Applied Image, Inc.. All Rights Reserved